Aus der Klinik mit Schwerpunkt Nephrologie und Internistische Intensivmedizin

der Medizinischen Fakultät Charité – Universitätsmedizin Berlin

DISSERTATION

Interleukin-16 in Chronic Kidney Disease – On the Origin, Secretion and Importance

Interleukin-16 in Chronischer Nierenerkrankung – Über Ursprung, Ausschüttung und Bedeutung

zur Erlangung des akademischen Grades

Doctor medicinae (Dr. med.)

vorgelegt der Medizinischen Fakultät

Charité – Universitätsmedizin Berlin

von

Frederic Emanuel Brösecke

Datum der Promotion: 29. November 2024

Vorwort

Teilergebnisse der vorliegenden Arbeit wurden veröffentlicht in:

F. Brösecke, A. Pfau, L. Rubenbauer, T. Ermer, A. B. Dein Terra Mota Ribeiro, S. Burlein, K.-U. Eckardt, M. Reichel, F. Knauf; *Interleukin-16 ist stark erhöht bei Dialysepatient*innen und korreliert mit der Plasmaoxalat Konzentration*, 13. Jahrestagung der Deutschen Gesellschaft für Nephrologie, Rostock, Deutschland, 2021

Table of Contents

List of Figures 5
List of Abbreviations 6
Zusammenfassung 8
Abstract 10
1. Introduction 12
1.1 Inflammation and the Immune System 12
1.1.1 Innate Immune system 13
1.1.2 Adaptive Immune system 17
1.1.3 Cytokines and IL-16 18
1.2 Chronic Kidney disease (CKD) 21
1.3 Immune system properties in CKD patients 23
1.3.1 Uremic retention molecules and Oxalate 23
1.3.2 Cytokines as uremic retention molecules 25
1.3.3 Changes in immune cells 26
1.3.4 Changes in immune mediators 28
1.4 Previous work of my work group 29
1.5 Aims of the study, research questions and hypothesis 38
2. Materials and Methods 41
2.1 Materials 41
2.1.1 Software 41
2.1.2 Laboratory equipment 41
2.1.3 Buffers 42
2.2 Methods 46
2.2.1 Patients/Probands 46
2.2.2 Animals 46
2.2.3 Cell isolation and cell culture techniques 47
2.2.4 Flow cytometry 51
2.2.5 Basal culture of sorted cells 55
2.2.6 ELISA 56
2.2.7 Oxalate Measurement 57
2.2.8 LEGENDplex 58
2.2.9 BMDM Isolation and Differentiation 59
2.2.10 BMDM Stimulation Experiment 60
2.2.11 Protein Concentration Measurement 61
2.2.12 Western Blot 62
2.2.13 LDH Assay 64
2.2.14 PMN Stimulation Experiment 65
2.2.15 Statistical analysis 66

3 Results 67
3.1 Characteristics of healthy controls and dialysis patients 67
3.2 Basal Interleukin-16 secretion of monocyte subsets 68
3.3 Basal Interleukin-16 secretion of PBMCs of healthy control subjects and CKD G5D patients 76
3.4 Intracellular level of IL-16 and caspase-3 activity in patients and healthy control subjects 80
3.5 Monocyte shift in CKD G5D patients 85
3.6 Proportion of Tregs in healthy controls and patients 87
3.7 GSDMD-wt and -ko BMDM 90
3.8 PMN Stimulation 96
4. Discussion 102
4.1 Main findings and interpretation of results 102
4.1.1 IL-16 release of monocyte subsets and monocyte shift 102
4.1.2 IL-16 secretion of PBMCs 105
4.1.3 Intracellular IL-16 level of PBMCs 106
4.1.4 Low-density Neutrophils 108
4.1.5 Regulatory T cells and IL-16 109
4.1.6 IL-16 release by BMDMs 110
4.1.7 PMNs and IL-16 release 111
4.2 Limitations 113
4.2.1 Patients and Control Subjects 113
4.2.2 IL-16 measurement of the supernatant after culture of human cells 115
4.2.3 Sorter-induced cellular stress 116
4.2.4 Isotype controls and FMO 116
4.2.5 BMDM 117
4.2.6 IL-16 Western Blot 117
4.2.7 IL-16 secretion by PMNs 117
4.2.8 Measurement of pro-IL-16 or mature IL-16 117
4.2.9 Causation does not imply causality 118
4.2.10 IL-16 as a retention molecule 118
4.3 Conclusion and future directions 119
References 121
Eidesstattliche Versicherung 136
Anteilserklärung an erfolgten Publikationen 137
Lebenslauf Frederic Emanuel Brösecke 138
Danksagung 139
Bescheinigung Statistik 140

List of Figures

Figure 1: Selected cells of the immune system 13
Figure 2: IL-16 expression in different tissues 19
Figure 3: Oxalate study, New Haven, USA, 2017 30
Figure 4: Oxalate study, New Haven, clinical and laboratory parameters 31
Figure 5: IL-16 study, Berlin, Germany, 2018 32
Figure 6: Impact of HD and HDF on IL-16 concentration in plasma of CKD G5D patients 33
Figure 7: IL-16 secretion of PBMCs after inflammasome activation 34
Figure 8: Gating strategy of monocyte subsets 36
Figure 9: Cytokine secretion of monocyte subsets after basal culture 37
Figure 10: Oxalate and IL-16 concentrations in patients on dialysis and healthy volunteers with normal kidney function 68
Figure 11: Revised FACS Gating strategy for monocyte subsets 69
Figure 12: Morphological characteristics of cultured cells under the light microscope 70
Figure 13: ELISA measurement of IL-16 and TNF-α in the supernatant after culture 71
Figure 14: Cytokine secretion into the supernatant after culture, measured by LEGENDplex 73
Figure 15: Relative cytokine secretion of every monocyte subset 74
Figure 16: Gating strategy for FACS-based isolation of PBMCs 77
Figure 17: Morphological differences of PBMCs after 16 h culture 78
Figure 18: IL-16 secretion of PBMCs 79
Figure 19: Gating strategy of PBMCs for intracellular IL-16 and caspase-3 panel 81
Figure 20: Intracellular level of IL-16 in PBMCs 82
Figure 21: Caspase-3 positive cells 84
Figure 22: Monocyte subtype composition in patients and healthy control subjects 86
Figure 23: Gating strategy of regulatory T cells 88
Figure 24: Comparison of Tregs between patients and control subjects and correlation with IL-16 89
Figure 25: Morphological characteristics of BMDM over the culture period 91
Figure 26: Flow cytometry characterization of BMDM at day 0 and day 7 92
Figure 27: LDH release and IL-16 secretion of GSDMD-wt and -ko BMDM stimulated with LPS, CaOx and ATP 93
Figure 28: Western Blot of BMDM cell lysate after stimulation 95
Figure 29: Assessment of neutrophil purity after PMN isolation 96
Figure 30: PMN culture with CaOx and NaOx and assessment of P.I. positive cells over time . 97
Figure 31: LDH and IL-16 secretion of PMN cultured with CaOx for 5 h, 10 h and 20 h 98
Figure 32: Western Blot analysis of PMN lysate after culture with CaOx or without stimulator 100
Figure 33: Stimulation of PMNs with different stimulators and assessment of LDH and IL-16 release 101

List of Abbreviations

Abbreviation	Explanation
Ab	Antibody
APC	Antigen-presenting cell
API	Ankle-branchial index
ATP	Adenosine triphosphate
BCA	Bicinchoninic acid
BCR	B cell receptor
BMDM	Bone marrow-derived macrophage
BUN	Blood urea nitrogen
CaOx	Calcium oxalate
Casp3	Caspase-3
CD	Cluster of differentiation
CD16+DC	Cluster of differentiation 16 expressing dendritic cell
cDC	Conventional dendritic cell
CKD	Chronic kidney disease
CKD G5D	Chronic kidney disease grade 5 treated by maintenance dialysis
CLR	C-type lectin receptor
CPPD	Calcium pyrophosphate dehydrate
CTLA-4	Cytotoxic T lymphocyte antigen 4
DAMP	Danger-associated molecular pattern
DC	Dendritic cell
ELISA	Enzyme-linked immunosorbent assay
EUTox	European Uremic Toxin
FACS	Fluorescence-activated cell sorting
FMO	Fluorescence minus one
FoxP3	Forkhead-box-protein P3
GFR	Glomerular filtration rate
GSDMD	Gesdermin D
HC	Healthy control
HD	Hemodialysis
HLA-DR	Human Leukocyte Antigen – DR isotype
IL	Interleukin
IL-16	Interleukin-16
kDa	Kilodalton
ko	Knockout
LCF	Lymphocyte chemoattractant factor
LDH	Lactate dehydrogenase
LDN	Low-density neutrophil
LPS	Lipopolysaccharide
LRR	Leucine-rich repeat

MFI	Mean fluorescence intensity
MHC-II	Major histocompatibility complex
mo-DC	Monocyte derived dendritic cell
mRNA	Messenger ribonucleic acid
MSU	Monosodium urate
NaOx	Sodium oxalate
NET	Neutrophil extracellular trap
NK cell	Natural killer cell
NLR	Nucleotide-binding oligomerization domain-like receptor
NLRP3	Nucleotide-binding oligomerization domain-leucine-rich repeat- and pyrin domain-containing protein 3
NOD	Nucleotide-binding oligomerization domain
PAMP	Pathogen-associated molecular pattern
PBMC	Peripheral blood mononuclear cell
PBS	Phosphate-buffered saline
PD	Peritoneal dialysis
pDC	Plasmacytoid dendritic cell
PHA	Phytohaemagglutinin
PMA	Phorbol 12-myristate 13-acetate
PML	Polymorphonuclear leukocyte
PMN	Polymorphonuclear neutrophil
pOx	Plasma oxalate
PRR	Pathogen-recognition receptor
pTreg	Peripherally derived regulatory T cell
RIG-I	Retinoic acid-inducible gene I
RLR	RIG-I-like-receptor
TCR	T cell receptor
TLR	Toll-like receptor
Treg	Regulatory T cell
tTreg	Thymus regulatory T cell
wt	Wild-type

Zusammenfassung

Hintergrund

Chronische, mit Dialyse behandelte Nierenerkrankung des Grades 5 (CKD G5D) geht mit veränderten Eigenschaften des Immunsystems einher, die eine wichtige Rolle bei der erhöhten Mortalität der Patienten*innen spielen. Es ist bekannt, dass Retentionsmoleküle, wie z. B. Oxalat, zu entzündlichen Prozessen beitragen. So weiß man, dass lösliches Oxalat im Plasma (pOx) mit plötzlichem Herztod von CKD-G5D-Patient*innen korreliert und Oxalat zusammen mit Kalzium Kristalle (CaOx-Kristalle) bildet, die Immunzellen aktivieren. Um das Entzündungsmuster von Oxalat zu untersuchen, wurde bei 107 CKD-G5D-Patient*innen in New Haven ein unvoreingenommenes Screening auf 21 Zytokine durchgeführt. Dabei wurde eine Korrelation von pOx mit IL-16 gefunden. Dieser Fund wurde anschließend in einer zweiten Kohorte mit 12 CKD-G5D-Patient*innen in Berlin bestätigt, in der stark erhöhte IL-16 Konzentration bei Patient*innen im Vergleich zu gesunden Kontrollpersonen identifiziert wurden. Man weiß, dass IL-16 von einer Vielzahl verschiedener Zellen sezerniert wird und mit verschiedenen Erkrankungen assoziiert ist. Der Ursprung, der Sekretionsmechanismus und die Bedeutung von IL-16 bei CKD sind unbekannt und sollten in dieser Arbeit untersucht werden.

Methoden

Um den Ursprung von IL-16 bei Patient*innen zu untersuchen, wurden Monozyten-Subtypen und periphere mononukleäre Blutzellen (PBMCs) mittels Durchflusszytometrie (FACS) isoliert und *in vitro* kultiviert. Enzymatic Immunosorbent Assays (ELISAs) wurden verwendet um IL-16 im Überstand zu bestimmen. Die intrazelluläre Konzentration von IL-16 in PBMCs wurde durch FACS bestimmt. Zur Untersuchung eines möglichen Sekretionsmechanismus wurden Neutrophile (PMN) mit CaOx-Kristallen stimuliert. Außerdem wurde Zelltod und IL-16 Ausschüttung von murinen Gasdermin-D-knockout Makrophagen, ausdifferenziert aus Knochenmark, untersucht. Der Anteil von regulatorischen T-Zellen (Tregs) von Patient*innen wurde mit IL-16 korreliert, um eine mögliche Rolle von IL-16 bei CKD zu untersuchen.

Ergebnisse

Es wurde kein Unterschied in der IL-16-Sekretion zwischen Monozyten-Subtypen gefunden. Kein Zelltyp von PBMCs sezernierte mehr IL-16 bei Patient*innen im Vergleich zu gesunden Personen. Es wurde jedoch ein allgemeines Muster der Sekretion zwischen PBMCs identifiziert. Außerdem wurden niedrigere intrazelluläre IL-16 Level in PBMCs bei Patient*innen festgestellt. PMNs sezernierten mehr IL-16 wenn sie in Gegenwart von CaOx-Kristallen kultiviert wurden was mit einer LDH-Freisetzung verbunden war. Es wurde keine Korrelation zwischen dem Treg-Anteil und IL-16 im Plasma der Patient*innen gefunden.

Diskussion

Die Ergebnisse zur IL-16 Ausschüttung von PMNs, die in Gegenwart von CaOx-Kristallen kultiviert wurden, deuten auf einen möglichen Ursprung des erhöhten IL-16 bei CKD-G5D-Patient*innen hin, der mit Zelltod zusammenhängt. Weitere Untersuchungen sind erforderlich, um Ursprung, Sekretion und Bedeutung von IL-16 in CKD zu klären.

Abstract

Background

Chronic kidney disease grade 5 treated with dialysis (CKD G5D) is associated with altered immune system properties that play a major role in the increased mortality of patients. Retention molecules, such as oxalate, are known to contribute to inflammatory processes. Soluble plasma oxalate (pOx) was found to be correlated with the sudden cardiac death of CKD G5D patients. Oxalate combined with calcium forms crystals (CaOx crystals) that activate immune cells. To investigate the immune system pattern of soluble oxalate, an unbiased cytokine screen of 21 inflammatory parameters with oxalate was performed in 107 CKD G5D patients in New Haven, USA. A correlation of pOx with interleukin-(IL)-16 was identified. This finding was subsequently confirmed in a second cohort of 12 CKD-G5D patients in Berlin, Germany. Furthermore, IL-16 was found to be highly elevated in patients compared to healthy control subjects. It is known that IL-16 is secreted by a variety of different cells and is associated with different diseases. The origin, secretion mechanism, and significance of IL-16 in CKD are unknown and were investigated in this work.

Methods

To investigate the origin of IL-16 in patients, monocyte subtypes and peripheral blood mononuclear cells (PBMC) were sorted by fluorescence-activated cell sorting (FACS) and cultured *in vitro*. Enzymatic immunosorbent assays (ELISA) were used to determine IL-16 in the supernatant. The intracellular concentration of IL-16 in PBMCs was determined by flow cytometry. To investigate a possible secretion mechanism, neutrophils (PMNs) were stimulated with CaOx crystals. Additionally, cell death pathways and IL-16 release of bone marrow-derived macrophages lacking gasdermin D were examined. The percentage of regulatory T cells in CKD G5D patients was correlated with IL-16 to investigate a possible role of IL-16 in CKD.

Results

No difference in IL-16 secretion was found between monocyte subsets. No cell type of PBMCs secreted more IL-16 in CKD-G5D patients compared with healthy control individuals. A general pattern of secretion between PBMCs, however, was identified.

Patients were found to have lower intracellular IL-16 levels in PBMCs compared with healthy individuals. Moreover, PMNs secreted more IL-16 when cultured in the presence of CaOx crystals, which was associated with lactate dehydrogenase (LDH) release. No correlation was found between Treg levels and IL-16 in the plasma of patients.

Discussion

Based on these results, it can be considered unlikely that PBMCs are the source of the increased IL-16 concentration in patients. The results on IL-16 secretion from PMNs cultured in the presence of CaOx crystals suggest a possible origin of the increased IL-16 level in CKD-G5D patients related to cell death. Further studies are needed to clarify the origin, secretion, and significance of IL-16 in CKD.

1. Introduction

1.1 Inflammation and the Immune System

Inflammation is a physiological mechanism of the immune system reacting to potentially harmful infections and tissue damage (Medzhitov, 2008; Zhong & Shi, 2019). Inflammatory responses are thought to be beneficial in controlled ways, for example, in terms of protection against pathogens, aiming to restore homeostasis (Medzhitov, 2008).

Chronic low-grade inflammation, however, is considered harmful. As a pathological feature of numerous chronic diseases, it plays an important role in patients' morbidity and mortality (Kotas & Medzhitov, 2015; Minihane et al., 2015).

Furthermore, systemic uncontrolled inflammatory processes with an exaggerated immune response to pathogens, in some cases not even to the pathogen itself, e.g., in the form of a cytokine storm, can lead to devastating disease and death, and this is receiving renewed attention in the wake of the SARS-CoV-2 pandemic (Fajgenbaum & June, 2020; Ragab et al., 2020).

Therefore, a fine balance of necessary and adequate inflammation is required without causing a chronic or excessive immune response. Inflammation can be both friend and foe (Kjekshus, 2015).

The immune system can be fundamentally divided into an innate and an adaptive immune system and into a humoral and cellular part. Cells of the immune system can be further divided by morphological or functional aspects and by their origin. So, for example, peripheral cells in the blood stream with a clear shaped single nucleus are called peripheral blood mononuclear cells (PBMCs). Furthermore, cells that arise from a common myeloid progenitor cell are referred to as myeloid cells, and cells that develop from a lymphoid progenitor cell are referred to as lymphoid cells (Murphy & Weaver, 2016) (Figure 1).

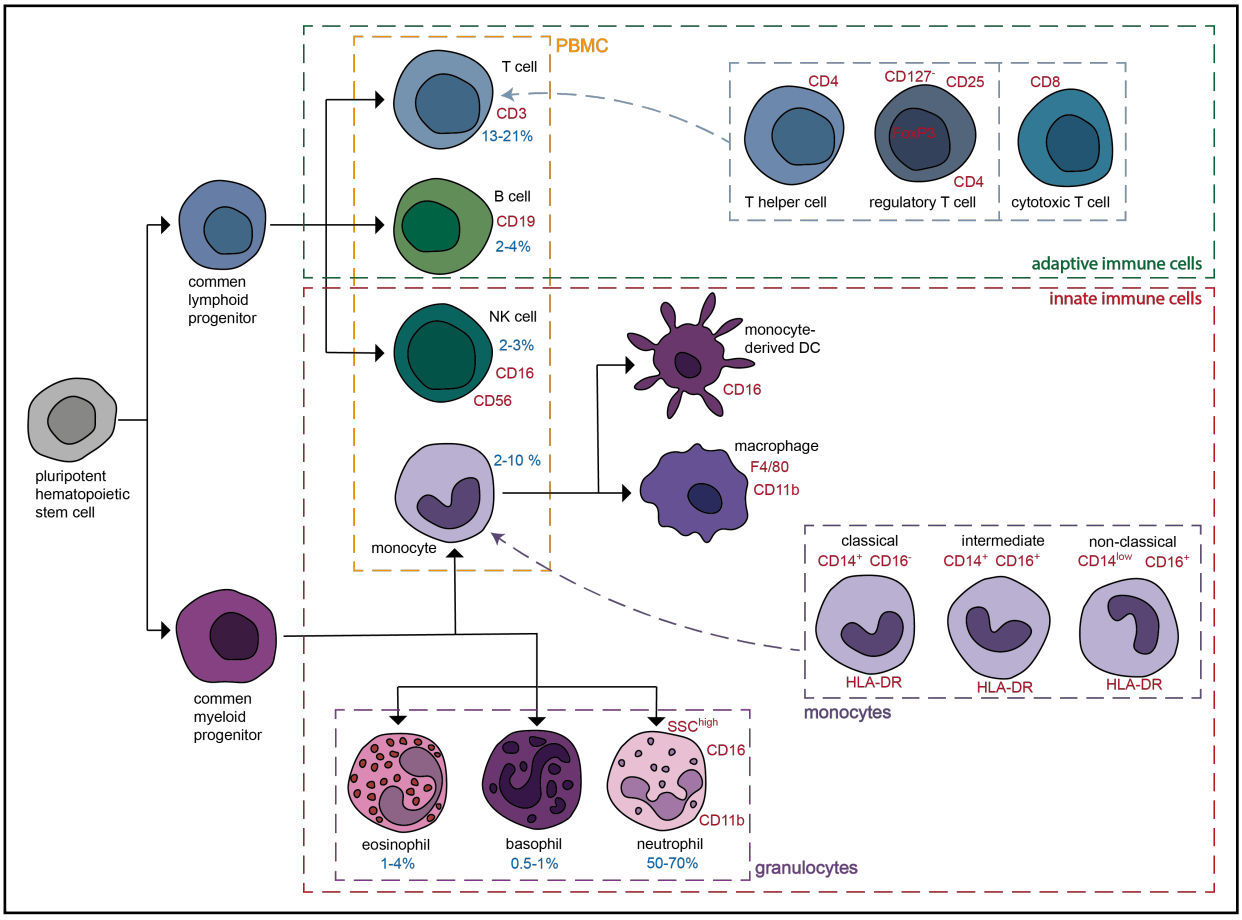

Figure 1: Selected cells of the immune system

Surface- and intracellular markers for flow cytometry (red) and the relative proportion of total leukocytes (blue) shown (Riley & Rupert, 2015). Adapted from: (Murphy & Weaver, 2016).

1.1.1 Innate Immune system

The innate immune system represents the first line of defence against pathogens or immune inducers and provides a non-specific rapid acting immune response (Murphy & Weaver, 2016).

One of the essential properties of the innate immune system is the ability to recognize pathogen-associated molecular patterns (PAMPs), conserved molecular motifs of infectious agents, or danger-associated molecular patterns (DAMPs) released from damaged or dying cells (Gong et al., 2020; Zheng et al., 2020). For this, the innate immune system uses different pathogen-recognition receptors (PRRs), like Toll-like receptors (TLRs), NOD-like receptors (NLRs), C-type lectin receptors (CLRs) and retinoic acid-inducible gene I (RIG-I)-like-receptors (RLRs) (Gong et al., 2020; Zheng et al., 2020).

Additionally, an intracellular protein complex that is often involved in the sensing of PAMPs and DAMPs and triggers a distinct defence mechanism is the inflammasome (Y. Li et al., 2021; Zheng et al., 2020). Depending on the involved proteins, different inflammasome complexes can be distinguished. One of the best studied is the nucleotide-binding oligomerization domain (NOD), leucine-rich repeat (LRR)-, and pyrin domain-containing 3 (NLRP3) inflammasome (Kelley et al., 2019; Y. Li et al., 2021). After activation through a priming signal followed by an activation signal, the protein complex forms, which leads to cleavage of pro-caspase-1 into the active caspase-1, which itself cleaves pro-IL-1β and pro-IL-18 into their biologically active forms. Furthermore, caspase-1 cleaves gasdermin D (GSDMD), which forms pores into the plasma membrane. This loss of cell integrity is part of a pro-inflammatory form of cell death called pyroptosis (Kelley et al., 2019; Shi et al., 2017). Recently, it was shown that in the absence of GSDMD, an activation of the inflammasome does not lead to the classical pyroptosis pathway. Instead, caspase-1 activates caspase-3, which induces apoptotic cell death (Taabazuing et al., 2017; Tsuchiya et al., 2019). There are several protocols to study the NLPR3 inflammasome *in vitro*, and one of the most established is to culture with lipopolysaccharide (LPS) for 3 hours as a priming signal, followed by stimulation with an activation signal for a specific time (H. Guo & Ting, 2020).

The innate immune system consists of an interplay of different immune cells. A summary of the cells essential for this work will be briefly considered here (Figure 1).

Monocytes are mononuclear cells which derive from the bone marrow and circulate in the bloodstream, making up 2-10% of all circulating peripheral leukocytes (Guilliams et al., 2018; Riley & Rupert, 2015). Despite possessing functional properties themselves, they also migrate to inflamed tissue where they differentiate into monocyte-derived macrophages or monocyte-derived dendritic cells (Coillard & Segura, 2019). Since 1989, we have known about a different subpopulation of monocytes, which were identified by morphology and flow cytometry (Passlick et al., 1989). Based on differences in the expression of lipopolysaccharide receptor antigen CD14 and immunoglobulin Fcγ receptor type III CD16 in combination with HLA-DR (MHC-II), three distinct monocyte subsets can be distinguished: 80-90% consist of $CD14^+$ $CD16^-$ "classical monocytes", while the remaining 10-20% are shared by $CD14^+$ $CD16^+$ “intermediate monocytes” and $CD14^{low}$ $CD16^+$ “non-classical” monocytes. (Guilliams et al., 2018; Passlick et al., 1989). Some observations argue that the classical monocytes may be the precursor for both

$CD16^+$ monocyte subsets (Coillard & Segura, 2019); however, the differences between these human monocyte subsets *in vitro* and *in vivo* are still under debate (Boyette et al., 2017).

Dendritic cells (DCs) are important for the initiation of an immune response and present a link between innate and adaptive immunity (Collin & Bigley, 2018). Developing in the bone marrow, DCs derive from the common myeloid progenitor, which develops from the pluripotent hematopoietic precursor (Patente et al., 2019). DCs are heterogeneous (Boltjes & Van Wijk, 2014), however, and show high expression of HLA-DR and no expression of the lineage markers CD3, CD19, and CD56 (Collin et al., 2013). Based on their surface markers and functionality, different DCs subsets can be distinguished. Conventional DCs (cDCs), which can be further subdivided into types 1 and 2, can be distinguished from plasmacytoid DCs (pDCs) and monocyte-derived DCs (mo-DCs) (Patente et al., 2019). For the latter population, exact markers and characteristics are still partly under discussion. CD14, which is not expressed by DCs, can be used to differentiate DCs from human monocytes in the bloodstream (Boltjes & Van Wijk, 2014). Some of the monocyte-related DCs also express CD16 and are referred to as CD16+DCs (Collin et al., 2013; Rhodes et al., 2019). Although sharing many similar genes, these mo-DC subsets form distinct clusters in single-cell RNA sequencing (Villani et al., 2017).

Resident and recruited macrophages are present in almost all tissues (Murphy & Weaver, 2016) and are involved in tissue regeneration, phagocytosis of cellular debris, and secretion of inflammatory mediators and growth factors (Wynn & Vannella, 2016). A variety of different macrophage subtypes has been described based on the tissues in which they are found and the phenotype that characterizes them. Generally, activated macrophages are divided into a rather pro-inflammatory M1 phenotype and a rather anti-inflammatory M2 phenotype (Yunna et al., 2020). To study their functions *in vitro*, macrophages can also be generated by differentiation from bone marrow hematopoietic precursor cells of mice using growth factors, such as M-CSF (Rios et al., 2017). This results in a homogeneous population of $F4/80^+$ $CD11b^+$ cells (Assouvie et al., 2018). These surface markers are well established and commonly used to characterize macrophages by flow cytometry (Austyn & Gordon, 1981; Lai et al., 1998). The resulting cells are referred to as bone marrow-derived macrophages (BMDMs). In addition to the relative convenience of cell generation and handling, it must also be considered as an

advantage that genetically modified mice can be used, allowing the influence of individual genes on macrophage function to be studied (Assouvie et al., 2018).

Granulocytes, or polymorphonuclear leukocytes (PMLs), are an abundant myeloid cell type that stands out due to densely staining granules and irregularly shaped nuclei. Polymorphonuclear neutrophils (PMNs), or neutrophils, are by far the most numerous granulocyte subtype, which makes them the most abundant circulating leukocyte in humans, making up 50-70% of all leukocytes (Summers et al., 2010). Neutrophils develop in the bone marrow and are released into the bloodstream, where they briefly circulate for a half-time of 6-8 hours and subsequently migrate to the tissues, where they spend another 6 days before being renewed (Quinn & DeLeo, 2020; Summers et al., 2010). The lifetime of neutrophils in blood is still under debate; however, it is generally expected to be less than one day (Lahoz-Beneytez et al., 2016; Lawrence et al., 2020). In the case of infection or tissue damage, neutrophils can sense PAMPs or DAMPs and become activated (J. Wang, 2018), which leads to the execution of effector mechanisms including phagocytosis, the generation of reactive oxygen species, and neutrophil extracellular traps (NETs) (Castanheira & Kubes, 2019). The high importance of neutrophils for the defence against pathogens can be seen in the heterogeneous bone marrow failure syndrome “Congenital Neutropenia”, with the absence of neutrophils and with recurrent severe infections in patients (Zeidler et al., 2009). In sterile tissue injuries and the sensing of DAMPs, neutrophils are essential in clearing cellular debris for tissue repair and homeostasis (Castanheira & Kubes, 2019; J. Wang, 2018). Neutrophils can be identified in flow cytometry by their high granularity, resulting in high side scatter (SSC), and the surface markers CD11b, CD14, CD15, CD16 and CD62L (Lakschevitz et al., 2016).

Additionally, innate lymphoid cells can be seen as an essential component of the innate immune system (Spits et al., 2013), with the largest subgroup compromised of natural killer cells (NK cells) (S. Ong et al., 2017), which exhibit their effector function without further pre-stimulation (Mandal & Viswanathan, 2015). After development in the bone marrow from a common lymphoid progenitor cell, NK cells circulate in the blood and reside in many tissues (Grégoire et al., 2007). When a virally infected or neoplastic cell is recognized (Herberman et al., 1975), NK cells demonstrate a cytotoxic and immunomodulatory property by death receptor interaction, secretion of cytotoxic granules (Prager et al., 2019), and secretion of cytokines (Cooper et al., 2001). Making up approximately 10% of all PBMC, NK cells can be identified by flow cytometry by the

absence of CD3 as well as the expression of CD16 and CD56 (Cooper et al., 2001; Valipour et al., 2019).

1.1.2 Adaptive Immune system

The adaptive immune system forms the specific immune defence against pathogens by recognizing specific short peptides called antigens. In a complex combination system of gene segments, humans evolve a vast repertoire of antigen recognition molecules that can recognize a wide range of antigens derived from pathogens (Murphy & Weaver, 2016). Different antigen-recognition molecules make up the core of the adaptive immune system. First, there are B cell receptors (BCRs) and soluble immunoglobulins or antibodies produced by B cells (Justiz Vaillant et al., 2021), which consist of a heavy and a light chain and can directly bind antigens (Minervina et al., 2019). Second, T cell receptors (TCRs) present on T cells, and consisting of a α/β or γ/δ chain, can recognize short peptides, which are processed and presented by antigen-presenting cells (APCs), namely DC, or macrophages (Alcover et al., 2018). The interaction of APC and TCR represents a linkage of the innate and adaptive immune system.

As various adaptive immune cells will be further considered in the course of this work, the essential ones will be described here (Figure 1).

T cells are mononuclear lymphoid cells that derive from a common lymphoid progenitor and migrate from the bone marrow to the thymus, where development into mature T cells occurs (Murphy & Weaver, 2016). Several subsets of T cells with unique functions in the immune system can be identified by assessing surface markers and intracellular markers, e.g., by flow cytometry (Mousset et al., 2019). As the main linage marker, all T cells express CD3, which is a protein complex that is part of the TCR. As mentioned earlier, T-γδ- and T-αβ-cells can be subdivided based on different TCRs, although the latter account for the much larger proportion in PBMCs (Kalyan & Kabelitz, 2013). Furthermore, two main groups of T-αβ cells, namely T helper CD4+ cells and cytotoxic CD8+ T cells, can be found. Orchestrating the immune response through the production of linage-specific cytokines, different CD4+ T helper cells were identified (Zhu, 2018).

Of all CD4+ T cells, regulatory T cells (Tregs) account for approximately 5-10% (Georgiev et al., 2019). Two different Treg populations with distinct functions are distinguished. First, thymus regulatory T cells (tTregs) develop from immature T cells in the thymus and are

of great importance in the development of T cell self-tolerance (Shevach & Thornton, 2014). Second, there are Tregs that develop extrathymically from naïve T cells in the periphery and are called peripherally derived Tregs (pTregs) (Shevach & Thornton, 2014). Overall, Tregs play an essential role in the suppression of the immune response. The immunosuppressive properties of Tregs are mediated by different pathways (Georgiev et al., 2019; Togashi et al., 2019). In this context, the consumption of IL-2 (Thornton & Shevach, 1998), the expression of cytotoxic T lymphocyte antigen 4 (CTLA-4) (Qureshi et al., 2011), and the secretion of immunosuppressive cytokines such as IL-10, IL-35, and TGF- β (Collison et al., 2007; Steinbrink et al., 1997) play important roles. In flow cytometry, Tregs can be identified based on their high expression of IL-2 receptor alpha chain (CD25) and their low expression of IL-7 receptor alpha chain (CD127) (W. Liu et al., 2006). FoxP3 is a very characteristic intracellular marker of Tregs (Hori et al., 2003).

B cells, which also belong to the mononuclear lymphoid cells, also derive from the common lymphoid progenitor cell (Murphy & Weaver, 2016). Unlike T cells, however, B cell development takes place entirely in the bone marrow. After mature B cells have migrated to secondary lymphoid organs, they can encounter antigens presented to them by other immune cells such as macrophages or DCs. Subsequently, they differentiate into short lived plasma cells, or they may become high affinity antibody-producing plasma and memory B cells (Vazquez et al., 2015). Several characteristic surface markers have been identified to define B cells, such as CD19, which is known as the pan-B cell marker, and CD20, which is found on mature B cells (LeBien & Tedder, 2008).

1.1.3 Cytokines and IL-16

Cytokines are small polypeptides (15-20 kDa) that play an important role in communication between cells through autocrine, paracrine, and endocrine signalling (Rose-John, 2018), and act on the migration, differentiation, and activation of immune cells. They can be divided based on their biologic functions into growth factors, interleukins, interferons, and chemokines (Heinrich et al., 2014). Furthermore, pro-, and anti-inflammatory cytokines can be distinguished, even though many cytokines exhibit various context-dependent effects.

Interleukin-16 (IL-16) was first discovered by Center and Cruikshank in 1982 (W. Cruikshank & Center, 1982; W. W. Cruikshank et al., 2000) and has been detected to varying degrees in several tissues and cell types since then.

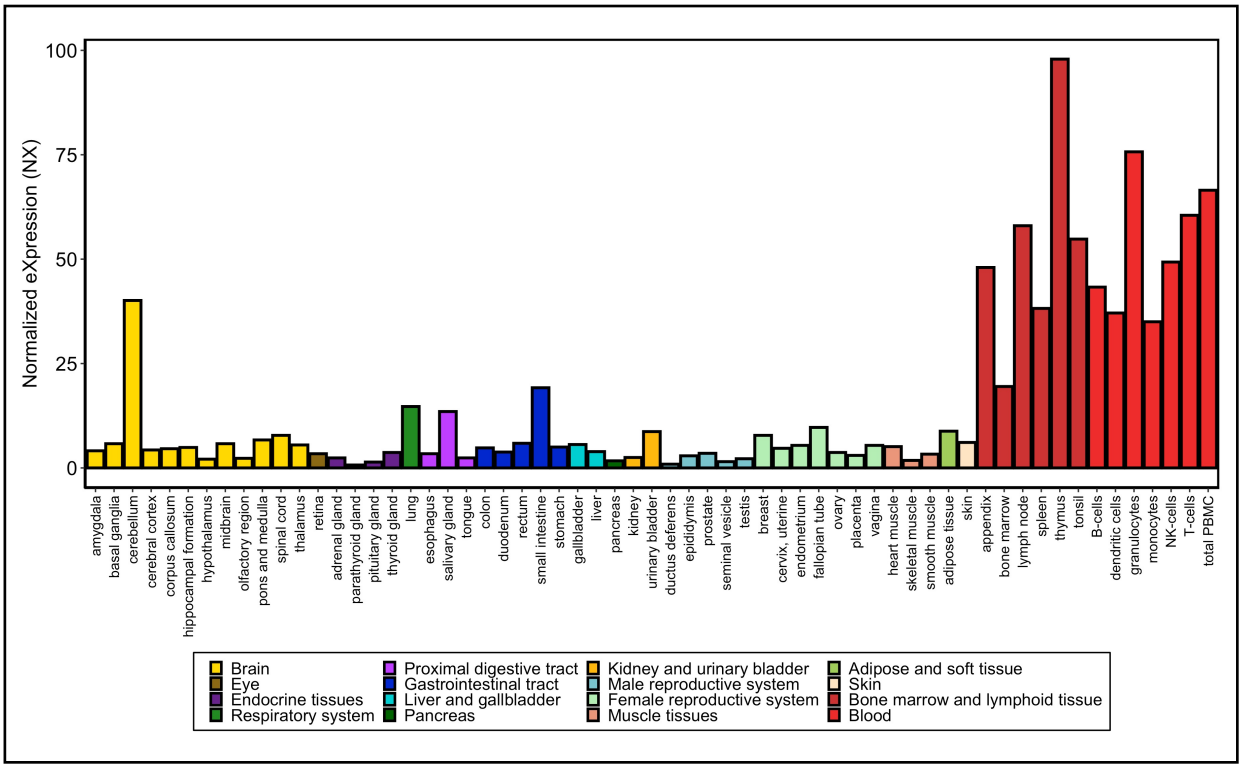

Figure 2: IL-16 expression in different tissues

Normalized IL-16 mRNA expression in different tissues and cell types. Adapted from: (The Human Protein Atlas, 2021).

While the level of IL-16 mRNA in certain tissues like brain, pancreas, small bowel, or colon was hardly detectable, in spleen, thymus and peripheral blood leukocytes, high IL-16 mRNA concentrations were found (Chupp et al., 1998).

The Human Protein Atlas (http://www.proteinatlas.org) calculates a consensus transcript expression level of IL-16 (NX) based on three transcriptomics datasets (HPA, GTEx and FANTOM5) for a range of tissues with multiple sub-tissues (Robinson & Oshlack, 2010; The Human Protein Atlas, 2021). In line with the consensus IL-16 expression data of the Human Protein Atlas (Figure 2), IL-16 is known to be synthesized and secreted by a variety of immune cells, including T cells (Zhang et al., 1998), B cells (Kaser et al., 2000), NK cells (Andersson et al., 2016), neutrophils (Roth et al., 2015), monocytes (Elssner et al., 2004), eosinophils (Lim et al., 1996), DCs (Kaser et al., 1999), mast cells (Rumsaeng

et al., 1997), and non-immune cells, as fibroblasts (Sciaky et al., 2000), epithelial (Arima et al., 1999), and neuronal cells (Kurschner & Yuzaki, 1999).

Human IL-16 is produced as a precursor form found in many tissues with a molecular weight of 80 kDa (Baier et al., 1998; Chupp et al., 1998). Active caspase-3 cleaves the precursor IL-16 molecule into a N-terminal pro-IL-16 and a C-terminal secreted/mature IL-16 (Richmond et al., 2014; Zhang et al., 1998). Mature IL-16 with a molecular mass of 17 kDa (Keane et al., 1998) is secreted following cell activation and is stored upon subsequent stimulation. While the exact mechanism of secretion or release is not yet fully understood, the process is thought to be associated with lytic cell death (Elssner et al., 2004; Richmond et al., 2014; Roth et al., 2015). In this regard, IL-16 has already been named as an alarmin (Rider et al., 2017). Extracellularly, IL-16 is described to aggregate and form homo-tetramer with approx. 60 kDa in size (Keane et al., 1998; Mühlhahn et al., 1998).

Originally, IL-16 was referred to as "lymphocyte chemoattractant factor" (LCF) because it was primarily considered a chemoattractant for T cells (W. Cruikshank & Center, 1982). Subsequent studies demonstrated that IL-16 exerts pleiotropic immunomodulatory functions associated with both pro- and anti-inflammatory properties.

Pro-inflammatory effects of IL-16 were detected in *in vitro* experiments, which showed that IL-16 induced the upregulation and secretion of pro-inflammatory cytokines from PBMCs (Mathy et al., 2000). Furthermore, murine experiments examining the absence of IL-16 using knockout mice or blocking antibody described reduced inflammation in models for asthma (C. Li et al., 2019), inflammatory bowel disease (Keates et al., 2000; P. Wang et al., 2013), delayed hypersensitivity reaction (Yoshimoto et al., 2000), and experimental autoimmune encephalomyelitis (Skundric et al., 2005), suggesting a pro-inflammatory property of IL-16.

Meanwhile, an anti-inflammatory effect was observed when T cells were pre-incubated with IL-16, which has been shown to strongly inhibit T cell activation (W. W. Cruikshank et al., 1996), and furthermore, by adding IL-16 to a lymphocyte culture which reduced the proliferation rate as measured by [^{3}H] Thymidine (Matsumoto et al., 2009). In an *in vivo* model of antigen-induced allergic asthma, the administration of recombinant IL-16 showed potent immunosuppressive effects (Bie et al., 2002).

Furthermore, it was described that T cell cultures with recombinant IL-16 induce FoxP3 expression in T cells *in vitro*, which argues for the ability of IL-16 to induce Tregs (McFadden et al., 2007). The relevance of this finding needs to be further determined.

In healthy humans, serum levels of IL-16 were measured in different cohorts and by different methods and were found to be 187 pg/ml (Purzycka-Bohdan et al., 2016), 101 pg/ml (Alexandrakis et al., 2004), and 88 pg/ml (Long et al., 2015). In several diseases, IL-16 was elevated, for example in psychiatric (Stelzhammer et al., 2014), orthopaedic (Chen et al., 2019; S.-X. Luo et al., 2015), inflammatory (Kawabata et al., 2020; Lee et al., 1998; Purzycka-Bohdan et al., 2016; X. Wang et al., 2019), metabolic (Lichtenauer et al., 2015), and oncologic diseases (Alexandrakis et al., 2004; Tang et al., 2016; H. Yang et al., 2017). Furthermore, IL-16 gene polymorphisms were associated with oncologic (Kashfi et al., 2016; Q.-S. Luo et al., 2014; M.-F. Wu et al., 2020), orthopedic (S.-X. Luo et al., 2015), inflammatory (Glas et al., 2003; Xue et al., 2009), and cardiovascular (X. Liu et al., 2013; J. Wu et al., 2011) diseases.

Overall, it must be stated that the exact role of IL-16 in the physiological homeostasis, as well as in the pathogenesis of many diseases, remains to be defined.

1.2 Chronic Kidney disease (CKD)

The kidneys play a central role in maintaining human health by excreting waste products and regulating numerous homeostatic mechanisms throughout the body (Pape et al., 2014).

As a result of various diseases, patients can lose kidney function, with far-reaching consequences.

A reduction in kidney function is a common condition and affects approximately 13.4% of the population worldwide (Hill et al., 2016). Disease stages are distinguished based on the severity of kidney function reduction, measured either by the presence of damage, determined by albuminuria, or the remaining kidney function, as determined by glomerular filtration rate (GFR). Kidney disease persisting longer than three months is referred to as *chronic* kidney disease, and complete loss of function as *kidney failure* or CKD grade 5 (CKD G5) (Levey et al., 2005, 2020; Levey & Coresh, 2012).

According to the USRDS annual data report of 2019, the most common causes of chronic kidney failure (also termed end-stage renal disease) in the USA were diabetes, hypertension, glomerulonephritis, cystic kidneys, and other/unknown reasons (Saran et al., 2020; USRDS, 2019).

Due to chronic kidney failure, patients receive maintenance kidney replacement therapy consisting of dialysis or organ transplantation. Patients receiving regular dialysis are also referred to as CKD G5D patients (Levey et al., 2020). Generally, two dialysis methods are distinguished, namely hemodialysis (HD), which is mainly performed on specialized dialysis units, and peritoneal dialysis (PD), which is conducted mainly at home. The most established method in Germany is HD, with a proportion of 94% (Gemeinsamer Bundesausschuss, 2020), and it is usually performed three times a week.

Regular dialysis can be seen as a high burden for patients in regards to quality of life due to extensive and intensive treatment (Gadaen et al., 2021), and for health care systems due to the high economic costs associated with dialysis (Couser et al., 2011). A recent calculation showed that the annual costs for patients with CKD G5D were 15 times higher than those of a reference group of the same age in Germany (Gandjour et al., 2020).

For almost 50 years (Lindner et al., 1974), research has established that cardiovascular incidences are more frequent in patients suffering from CKD, leading to increased cardiovascular mortality (Navaneethan et al., 2015; Thompson et al., 2015). In a large European cohort, the cardiovascular morality rate of patients starting dialysis was 8.8 times higher than in the general population. Additionally, non-cardiovascular diseases - e.g., oncologic and infection related - were highly elevated (de Jager, 2009). Overall, 40-50% of all CKD patients die from cardiovascular events (Jankowski et al., 2021).

Several vascular changes in chronic kidney failure patients on maintenance dialysis were also independently associated with increased mortality, including an increase in the ankle-branchial index (API) (Gu et al., 2019), abdominal aortic calcification (Okuno et al., 2007), peripheral arterial disease (Y. Yang et al., 2016), and coronary artery calcification (X.-R. Wang et al., 2019).

The connection between CKD and vascular changes as well as increased cardiovascular events is in many cases a pro-inflammatory activity state, which, together with dyslipidemia and uremic toxins (Alani et al., 2014; Rapp et al., 2020), can lead to vascular

changes including atherosclerosis and vascular calcifications (Cozzolino et al., 2018; Gisterå & Hansson, 2017).

Another main cause of the morbidity and health care costs of CKD G5D patients are infections (Ishigami & Matsushita, 2019), which are associated with an increased risk of mortality (Saran et al., 2020; Sarnak & Jaber, 2000). This is also amplified by the reduced responsiveness to vaccination, which puts the CKD G5D patients at increased risk (Ghadiani et al., 2012; Mathew et al., 2014).

Furthermore, an increase in neoplastic diseases can be seen, especially in virus-associated cancers in patients suffering from CKD (Maisonneuve et al., 1999; Stewart et al., 2009), which can clearly - at least partly - be explained by changes in the immune system.

Therefore, the altered characteristics of the immune system in CKD require considerable attention and will therefore be addressed further.

1.3 Immune system properties in CKD patients

Fundamental changes in the immune system of CKD patients have been described in several review articles (Betjes, 2013; Ebert et al., 2020; Kato et al., 2008; Zoccali et al., 2017), including elevated inflammatory mediators, and differences in the immune cell number, composition, as well as functionality. Overall, a persistent low-grade inflammatory activity can be found if kidney function is reduced or lost.

With the aim of systematically addressing these changes, some of the key contributors and alterations are discussed separately.

1.3.1 Uremic retention molecules and Oxalate

With progressive loss of kidney function, retention molecules are excreted less in the urine and hence accumulate in the plasma, where their concentration increases (Vanholder et al., 2003). While most molecules originate endogenously from the metabolism, some are also absorbed through food consumption or are produced by the intestinal microbiota (Meijers et al., 2014). Some of these uremic solutes have toxic effects on various organs, which can lead to a so-called uremic syndrome with many symptoms, including neurological complications (Hamed, 2019). Uremic *toxins* are

therefore defined based on two criteria: First, these molecules are normally excreted by the kidneys and accumulate in CKD, and second, they "interact negatively with biological functions" (Castillo-Rodríguez et al., 2017; Vanholder et al., 2003).

Uremic retention molecules and toxins are an extremely heterogenous group of substances with a molecular mass between 500 Dalton and 58 kDa, enabling them to cross the glomerular filtration barrier under normal conditions (Vanholder et al., 2018). Based on the definitions of the European Uremic Toxin work group (EUTox, 2021), which characterizes and captures all known uremic retention molecules, those molecules can be divided into (1) small free water-soluble low molecular weight compounds, (2) protein bound compounds and (3) middle molecules. The uremic toxins categories show differences in the removal characteristics during dialysis (Vanholder et al., 2018).

The effect of the different uremic toxins on immune cells can be inhibitory and/or pro-apoptotic, contributing to infections. The effect can also be activating, priming and/or anti-inflammatory, leading to increased inflammation (G. Cohen, 2020).

Oxalate, a uremic toxin which belongs to small water-soluble compounds (Marangella et al., 1992; Mydlík & Derzsiová, 2008), is an end-product of metabolism (Crivelli et al., 2021) and is absorbed through food as well as being generated endogenously. Overall, however, the predominant part of plasma oxalate (pOx) originates from the liver (Brzica et al., 2013; Ermer et al., 2016), where it is produced in the metabolism of glyoxylate (Holmes & Assimos, 1998; Lange et al., 2012). As the excretion of oxalate is mainly conducted through the urine (Osswald & Hautmann, 1979), a reduction in kidney function leads to increased pOx levels (Prenen et al., 1985). Elevated pOx levels can lead to the formation of calcium oxalate (CaOx) crystals, which can be deposited in many sites of the body, especially in the kidneys, and thereby damage the kidneys (Cochat et al., 2012).

CaOx crystals can form CaOx stones, which are the most common type of kidney stone, accounting for approx. 70-80% of all stones in humans (Lieske et al., 2014; Thongprayoon et al., 2020), and can lead to kidney stone disease (also known as nephrolithiasis or urolithiasis), which is a common condition in the general population, affecting approximately 9% of the US American population (Scales et al., 2012), and which is also a risk factor for the development of CKD (Rule et al., 2011).

Elevated levels of plasma oxalate can also be found in the genetic disease primary hyperoxaluria, in which liver enzyme deficiencies are responsible for increased oxalate

production; this disease also leads to kidney damage (Pierre & Gill, 2013). High levels of pOx were found to be associated with decreased estimated GFR (Milliner et al., 2021). The effect of oxalate on kidney disease progression was also studied using a murine model with a high oxalate diet, which resulted in a decrease in GFR and an increase in plasma blood urea nitrogen (BUN) and creatinine, indicative of kidney injury (Mulay et al., 2016). Interestingly, the link between oxalate and kidney damage goes both ways, with high levels of oxalate leading to kidney damage and kidney damage also leading to increasing levels of oxalate in the bloodstream.

In recent years, significant progress has been made in the understanding of oxalate-induced inflammation. In particular, the effect of CaOx crystals was investigated. In an animal model of oxalate induced nephropathy, the NLRP3 inflammasome of innate immune cells was identified to be the main contributor to the progression of kidney failure (Knauf et al., 2013). Furthermore, *in vitro* experiments confirmed this direct effect of CaOx crystals on dendritic cells, which become activated and secrete IL-1β (Mulay et al., 2013). CaOx crystals were further found to induce neutrophil necrosis, measured by LDH release and loss of cell integrity, as determined by live cell imaging (Desai et al., 2017; Elferink & Riemersma, 1980).

High levels of plasma oxalate were recently identified to be associated with higher overall mortality and the sudden cardiac death of CKD G5D patients (Pfau et al., 2021). The effect of plasma oxalate on inflammatory cells and immune responses in patients with CKD is still the subject of further research.

1.3.2 Cytokines as uremic retention molecules

Elevated cytokine levels in patients with impaired kidney function may occur for several reasons. As already mentioned, pro-inflammatory triggers, such as uremic toxins and the increased secretion of cytokines by immune and non-immune cells, play a fundamental role. It must also be considered, however, that the excretion or degradation of cytokines is reduced if kidney function is impaired (Castillo-Rodríguez et al., 2017; Schindler, 2004).

Over the last few years, the number of cytokines considered by the EUTox work group to be uremic toxins has increased (Castillo-Rodríguez et al., 2017). Currently, IL-1β, IL-6, IL-18, TNF-α, IL-8 and IL-10 are counted among them, even though some of the cytokines on the list are controversial (Duranton et al., 2012; EUTox, 2021).

Various approaches have been used to study human clearance or degradation of cytokines. Radioactively labeled rIL-10, for example, was injected into rats and rapidly disappeared from the bloodstream, with the kidney being primarily responsible for this excretion (Rachmawati et al., 2004). Similarly, IL-1α (Poole et al., 1990) and IL-1β (Asumendi et al., 1996) were identified to be mainly degraded by the kidneys in rats.

Urinary cytokine concentrations are studied in several pathologies. As such, elevated concentrations have been identified as a predictor of the severity of urinary tract infections (Armbruster et al., 2018), as a biomarker for intestinal bladder pain syndrome (Jiang et al., 2020), and were found elevated in hyperfiltration of type 1 diabetes (T1D) (Har et al., 2014), as well as acute tubular damage (Fellström et al., 2021). In diabetic nephropathy, elevated levels of urinary IL-1, IL-6, and IL-8 were detected (Donate-Correa et al., 2020). When associating plasma concentrations of cytokines in low-grade inflammation with urinary cytokine excretion no correlation was found, suggesting a modulatory role of the functioning kidney (Nobles et al., 2015).

Methods to remove cytokines from circulation by extracorporeal blood purification in the treatment of sepsis have recently been proposed and are currently under investigation (Monard et al., 2019; Seeliger et al., 2020). While successful clearance of cytokines was found (Schädler et al., 2017), evidence of a favorable outcome for patients is still pending (Seeliger et al., 2020; Snow et al., 2021). TNF-α, which is present in the blood as a homotrimer with a molecular mass of 51 kDa, showed the lowest clearance rate compared with smaller cytokines (Harm et al., 2020), which illustrates the importance of the molecular mass on the clearance, at least by extracorporeal blood purification.

1.3.3 Changes in immune cells

In CKD patients, a variety of changes in a broad spectrum of immune cells are described. In the following, changes in the cell number, composition, activation state, and functionality of immune cells are discussed for a selection of cell types.

Compared to healthy controls, neutrophils of CKD patients exhibit a higher basal activation state measured by superoxide release (J. W. Yoon et al., 2007), hydrogen peroxide (J. W. Yoon et al., 2007), or radical oxygen species (ROS) (Kim et al., 2017). The basal formation of neutrophil extracellular traps (NET) was also significantly higher (Kim et al., 2017). In studies of neutrophil functionality, decreased migratory capacity

(Rossaint et al., 2016) and an impaired phagocytosis were noted (Mahajan et al., 2005). Different possible mechanisms for the increased priming (Betjes, 2013) and impaired functionality (Chonchol, 2006) have been proposed. The percentage of spontaneous apoptotic neutrophils from HD patients was found to be increased compared to healthy controls (Majewska et al., 2003), which was further enhanced after dialysis treatment (Fukushi et al., 2020). Furthermore, *in vitro* and *in vivo* experiments showed that a uremic environment increases the apoptosis of neutrophils (Cendoroglo et al., 1999; Jaber et al., 1998) and enhances the susceptibility for apoptosis (Jaber et al., 2001). It is remarkable that neutrophils of CKD patients show an increase in cell death *in vitro*, as the total number of neutrophils is not decreased in patients. The number of PML even increases with decreasing kidney function (Sela et al., 2005). This suggests that an increased generation of neutrophils is occurring in patients.

TLRs play a key role in innate immunity by recognizing DAMPs and PAMPs (Zindel & Kubes, 2020). In neutrophils, TLR4, and in monocytes TLR2 and TLR4 were found upregulated in CKD G5D patients (Gollapudi et al., 2010; Grabulosa et al., 2018; Koc et al., 2011), also suggesting an increased activation state.

It is widely accepted that the composition of monocytes in CKD patients differs from healthy individuals and a higher proportion of $CD14^+$ $CD16^+$ intermediate and $CD14^{low}$ $CD16^+$ non-classical monocytes can be found, respectively (Nockher & Scherberich, 1998; Schepers et al., 2015). In particular, a subgroup of intermediate monocytes was found elevated in CKD (Naicker et al., 2018); however, the exact mechanism leading to this change in monocyte composition is not known (Betjes, 2013). Considered pro-inflammatory, these intermediate and non-classical monocytes are getting a high level of attention as they are suspected to play a major role in the development of atherosclerosis (Betjes, 2013; Hénaut et al., 2019) and are independently associated with increased mortality in CKD patients and cardiovascular events (Heine et al., 2008, 2012; Rogacev et al., 2011).

Lymphoid cells, namely T and B cells, were found to be reduced in CKD patients (Xiang et al., 2016; J.-W. Yoon et al., 2006). In particular, naïve T cells are diminished (Litjens et al., 2006; J.-W. Yoon et al., 2006). The $CD4^+/CD8^+$ T cell ratio was found decreased in CKD patients (Xiong et al., 2021). In *ex vivo* analysis of different T cell subsets, an increase of apoptosis was identified (Moser et al., 2003; Saad et al., 2014) and a

susceptibility towards activated apoptosis (Meier et al., 2002), which might explain the reduction of cells (J.-W. Yoon et al., 2006).

Both lymphocytes and monocytes were found to exhibit pro-apoptotic changes (Dounousi et al., 2012).

1.3.4 Changes in immune mediators

In a study of 3430 patients from the Chronic Renal Insufficiency Cohort (CRIC) study, several inflammatory mediators were found elevated in patients with reduced kidney function (Gupta et al., 2012). Furthermore, increased fibrinogen, TNF-α, and IL-6, and decreased serum albumin were independent predictors of estimated GFR loss, and each independently represented a risk factor for the progression of kidney disease after correction for cofactors (Amdur et al., 2016). This study clearly showed the relevance of inflammation processes, measured by humoral markers, in the progression of CKD.

Generally, a large variety of different cytokines and acute phase proteins are described to be elevated in CKD. Many of those inflammatory markers have been independently identified as predictors of cardiovascular disease events and/or survival in CKD patients, namely CRP (Iseki et al., 1999; Zimmermann et al., 1999), PTX3 (Krzanowski et al., 2017; Sjöberg et al., 2016; Suliman et al., 2008; Tong et al., 2007), Fibrinogen (Goicoechea et al., 2008; Weiner et al., 2008; Zoccali et al., 2003), serum amyloid A (Dieter et al., 2016) GDF-15 (Tuegel et al., 2018), IL-1β (S. D. Cohen et al., 2010), IL-6 (S. D. Cohen et al., 2010; do Sameiro-Faria et al., 2013; Meuwese et al., 2011; Panichi et al., 2004), IL-10 (Yilmaz et al., 2014), IL-18 (Chang et al., 2015; S. D. Cohen et al., 2010), TNF-α (Meuwese et al., 2011), sTWEAK (Fernández-Laso et al., 2016), TNFR1/2 (Gohda et al., 2017), DcR3 (Hung et al., 2012), MCP-1 (Gregg et al., 2018), VEGF (Q. Guo et al., 2009; Mallamaci et al., 2008).

Both the impact of inflammatory responses on cardiovascular events and survival, and the opportunity for treatment by strategies to influence inflammation, have been demonstrated (Lorenzatti, 2021). The treatment with canakinumab, a specific IL-1β antibody in the Canakinumab Anti-Inflammatory Thrombosis Outcomes (CANTOS) study, reduced cardiovascular events in CKD patients in this study of 10,061 patients (Ridker et al., 2018). Ongoing studies are investigating the potential of IL-6 antibodies for the treatment of inflammation in CKD patients on maintenance HD (Pergola et al., 2021).

Thus, considering the extensive role of inflammatory mediators in the bloodstream of CKD patients and the therapeutic opportunities that are currently beginning to be explored, comprehensive knowledge of all the inflammatory mediators involved is essential for our understanding of disease and the development of novel treatment possibilities.

1.4 Previous work of my work group

To investigate the systematic oxalate-associated immune pattern of CKD G5D patients, Theresa Ermer, a predoctoral fellow who has been in our working group, conducted a study in New Haven, CT, USA in 2016. Cytokine and oxalate concentrations were determined, and clinical data were collected in a cohort of 24 PD and 83 tri-weekly HD patients (107 patients in total) who had given written informed consent to participate in the study, were over 18 years of age, had been treated for at least 3 months, were medically stable, and had no evidence of acute infection. Further characteristics of the study population have already been published (Pfau et al., 2021).

Overall, 21 cytokines were measured using an unbiased cytokine screen, namely a V-PLEX Proinflammatory Panel 1 and a V-PLEX Cytokine Panel 1 Human (both Meso Scale Diagnostics, Rockville, USA) as well as an IL-33-Quantikine enzyme-linked immunosorbent assay (ELISA, R&D Systems, Minneapolis, USA). Additionally, pOx was determined through enzymatic assay with oxalate oxidase (Trinity Biotech, Bray, Ireland).

To verify that the measurements were relatively consistent over time, in 25 patients (11 HD, 14 PD) blood was collected at four subsequent sessions, weekly after the long interval in HD patients and monthly at clinical appointments in PD patients. The median coefficient of variation (CV) for cytokine measurements of 25 patients at four consecutive sessions was calculated. IL-16 showed a median CV of 8.97% (IQR 2.3) in the HD group and 10.06% (IQR 10.1) in the PD group. POx showed a median CV of 9.41% (IQR 9.69) in the HD group and 16.74% (IQR 25.2) in the PD group.

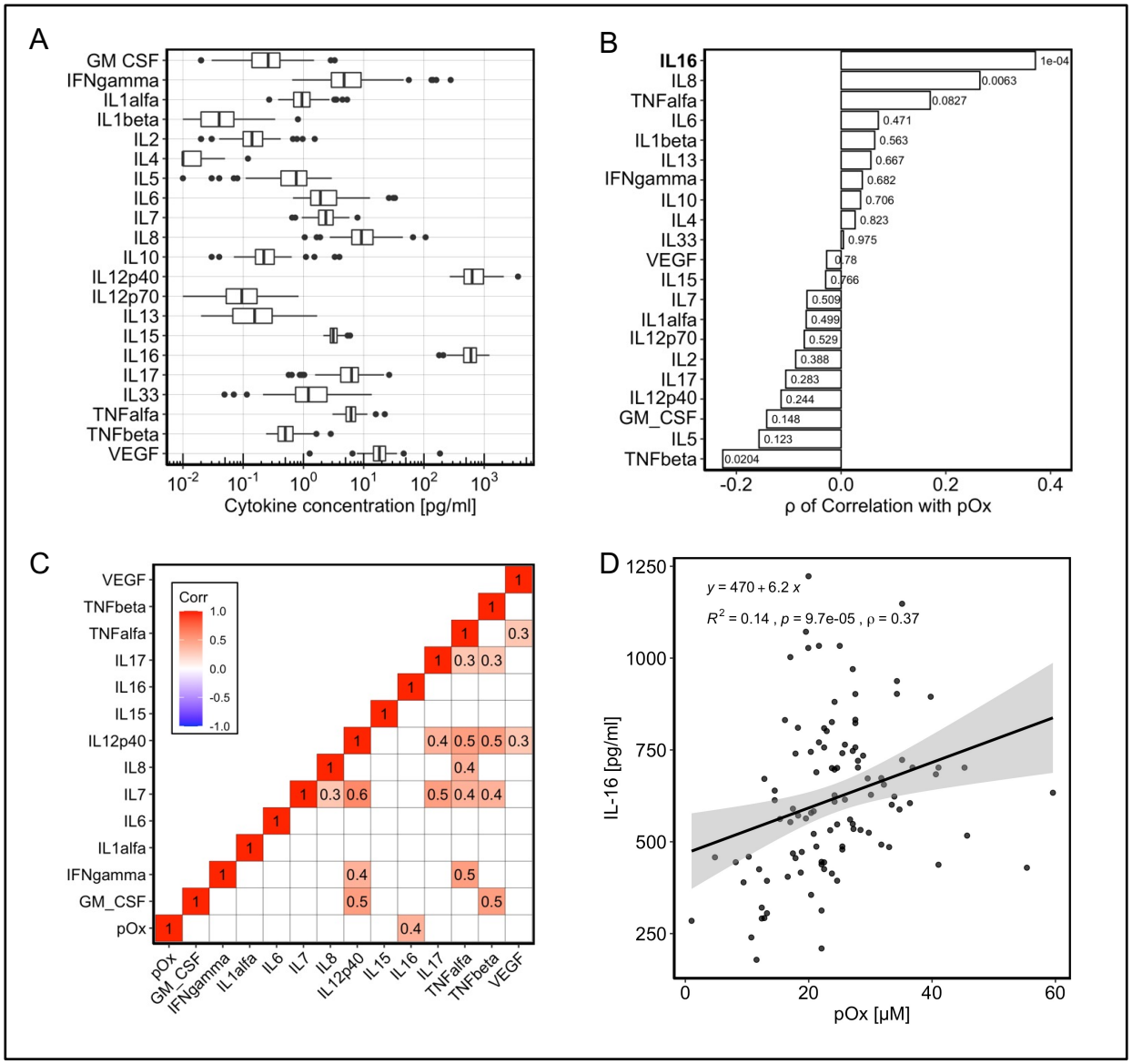

Figure 3: Oxalate study, New Haven, USA, 2017

Study conducted by Theresa Ermer. In total, 107 CKD G5D patients were included. (A) Absolute concentration of 21 cytokines. (B) Correlation coefficient of pOx with cytokines, Spearman's ρ on x-axis and p-value behind the respective bar. (C) Correlation matrix of selected cytokines. (D) Correlation of pOx and IL-16, n=105.

Figure 3A shows the measured absolute cytokine concentrations in the cohort. Large differences in the concentrations were evident, with the highest cytokine abundance for IL-12p40 followed by IL-16 in the plasma of the patients. The correlation of each cytokine with pOx was calculated. For visualization, the correlation coefficient of the Spearman correlation (Spearman's ρ) was plotted on the x-axis, with the p-value printed small behind the respective bar (Figure 3B). It becomes clear that IL-16 represents the strongest correlation with pOx of all measured cytokines, with the highest Spearman's ρ of 0.37.

Since correction for multiple testing is required, a strict p-value of 0.0024 is considered statistically significant (Bonferroni Correction for multiple comparisons 0.05/21). IL-16 is found to be the only cytokine to show a significant correlation with pOx. Figure 3C presents a correlation matrix for selected cytokines. Since only complete cases could be included in the analysis, some cytokines with many missing values had to be excluded. IL-16 shows no further correlation with any of the selected cytokines. Figure 3D shows the correlation of pOx and IL-16 (ρ = 0.37, p = <0.001).

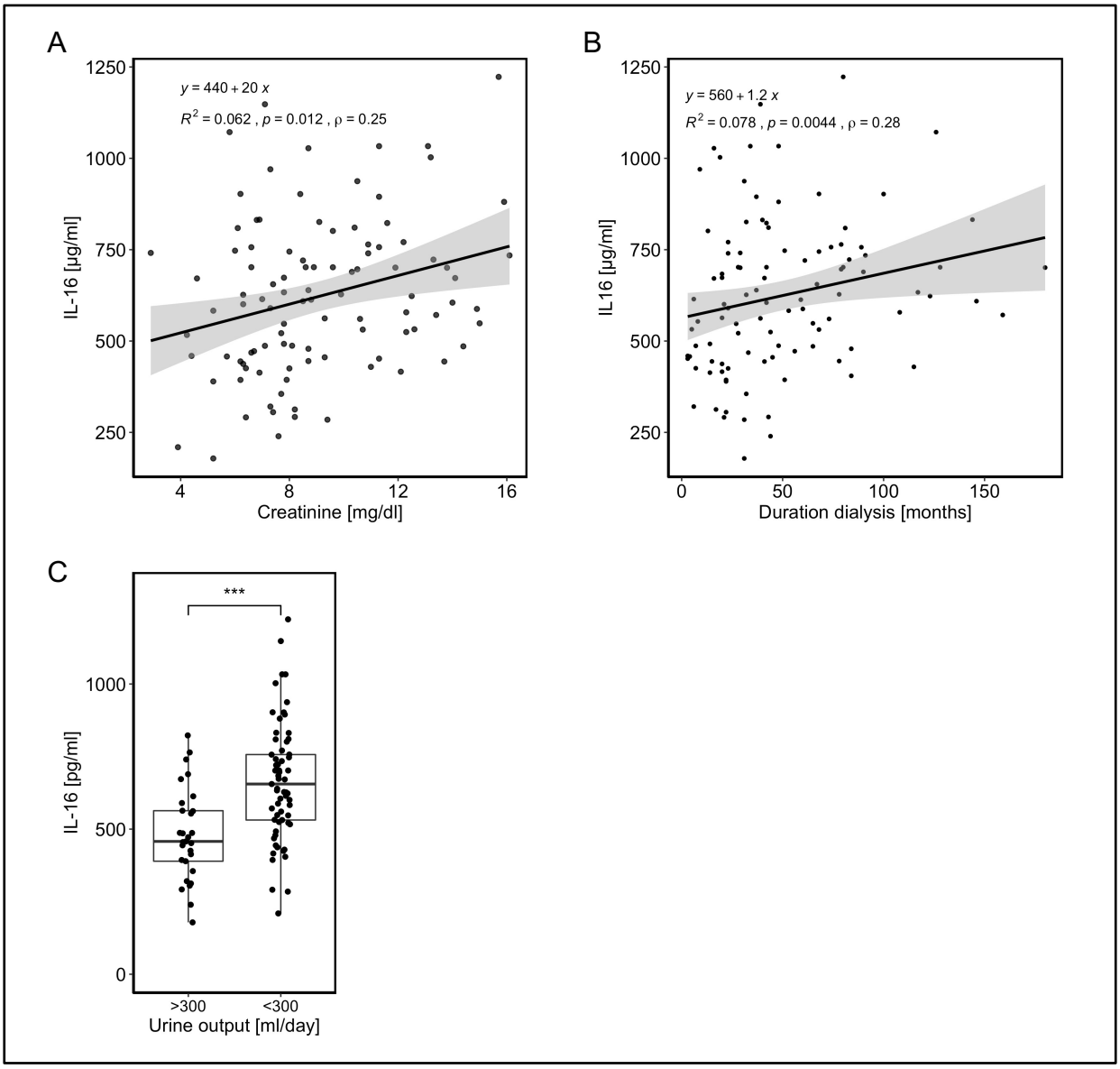

Figure 4: Oxalate study, New Haven, clinical and laboratory parameters

Association of IL-16 with clinical and laboratory parameters in the Oxalate study, New Haven, USA. (A) Correlation of creatinine and IL-16, n=100. (B) Correlation of duration of dialysis and IL-16, n=104. (C) Comparison of IL-16 levels in patients with (>300 ml/day) and without urine output (<300 ml/day), n=95.

Furthermore, clinical and laboratory parameters were investigated for a possible association with IL-16 (Figure 4). A positive correlation of creatinine and IL-16 was identified (ρ = 0.25, p = 0.012) (Figure 4A). The duration of dialysis was further found to correlate with IL-16 (ρ = 0.28, p = 0.004) (Figure 4B). Additionally, an association of residual kidney function, measured by urine output per day, with IL-16 was found. The median IL-16 level of patients without urine output (<300 ml/d), 655 pg/ml, was significantly higher than the IL-16 level median in patients with urine output (>300 ml/d) of 458 pg/ml (Wilcoxon-Mann-Whitney test, p = <0.001, effect size r = 0.42).

To replicate this finding of a correlation of IL-16 and pOx, a repetition of the study was performed by Sarah Burlein in Berlin. For this purpose, patients of the dialysis unit of the Charité – Universitätsmedizin Berlin who had been receiving regular HD for at least 3 months, were medically stable and had no acute infection, and healthy randomly selected control individuals were included. Plasma samples were collected from patients immediately before dialysis treatment and at a random time point from healthy controls. IL-16 was determined by Quantikine ELISA (R&D) and oxalate by enzymatic assay (Trinity Biotech).

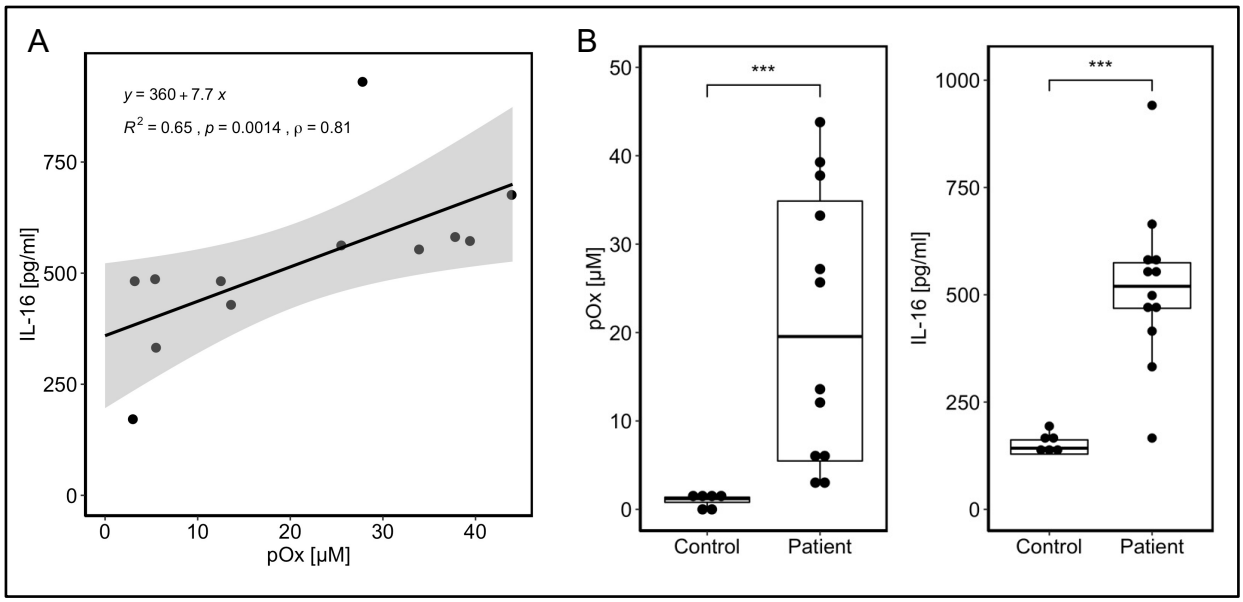

Figure 5: IL-16 study, Berlin, Germany, 2018

Study conducted by Sara Burlein. IL-16 study Berlin, Germany, 2018, with 12 CKD G5D patients and 6 healthy control subjects. (A) Correlation of pOx and IL-16. (B) Comparison of pOx and IL-16 levels between healthy control subjects and CKD G5D patients.

The correlation of pOx and IL-16 could again be identified in this small cohort of 12 patients ($\rho = 0.81$, $p = 0.001$) (Figure 5A). Moreover, when compared with healthy controls ($n = 6$), a significant difference was found in both pOx (Wilcoxon-Mann-Whitney test, $p<0.001$, effect size $r = 0.8$) and IL-16 (Wilcoxon-Mann-Whitney test, $p = 0.001$, $r = 0.77$), with higher values in the patient group (Figure 5B).

The increased levels of IL-16 may have resulted from reduced excretion of IL-16; therefore, with the suspicion that IL-16 may be some type of retention molecule, the effect of dialysis on the plasma IL-16 concentration was investigated. For this, Anja Pfau measured IL-16 with a DuoSet ELISA (R&D) post-hoc in patient samples which were collected by Theresa Ermer. In that study (Ermer et al., 2017), the influence of hemodialfiltration (HDF) and HD on pOx concentrations was investigated, and pOx measured just before, during, after, and 2 h after dialysis. A significant reduction in pOx was found with both procedures over the time course (Ermer et al., 2017). In contrast, no such reduction was seen with IL-16 (Figure 6), suggesting that IL-16 is not filtered during dialysis and therefore does not accumulate in patients for this reason. Nevertheless, limitations must be considered when evaluating this experiment, as IL-16 may be produced during dialysis, leading to a balance of filtration and secretion. Furthermore, no other cytokine measurement was performed to validate the assay and experiment.

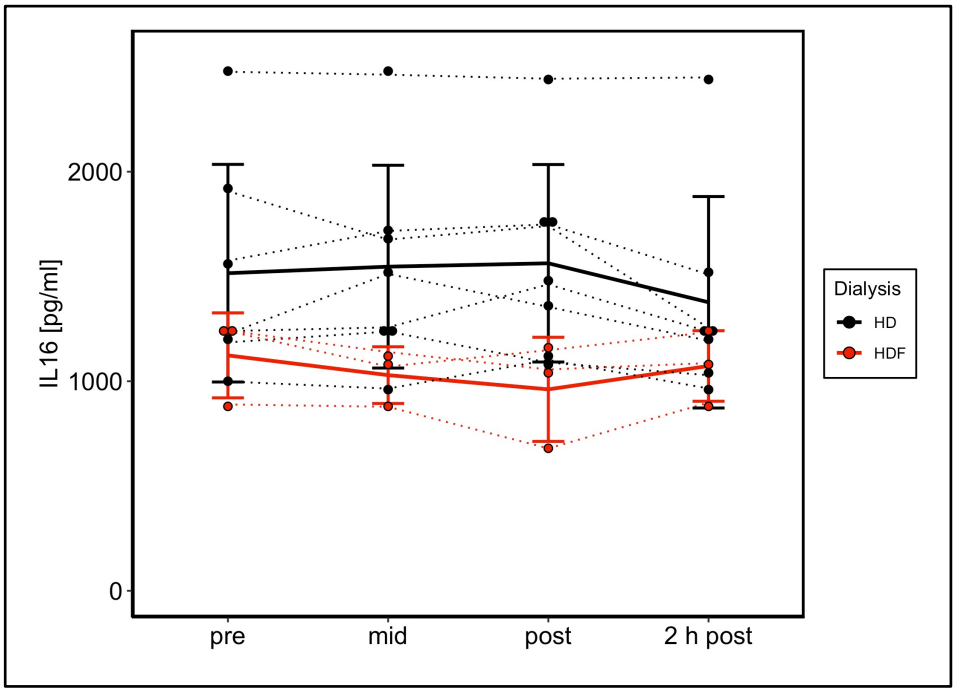

Figure 6: Impact of HD and HDF on IL-16 concentration in plasma of CKD G5D patients

Plasma samples collected before (pre), during (mid), directly after (post) or 2 h after dialysis (Ermer et al., 2017). IL-16 post-hoc analysis performed by Anja Pfau.

In search of the origin of IL-16, immune cells were suspected. As a first approach to get an impression of the secretion of IL-16 by PBMCs, Lisa Rubenbauer used a classical experimental setup, studying the potential involvement of the NLRP3 inflammasome. For this purpose, PBMC were obtained by density gradient centrifugation and cultured in the presence of stimulators. After 3 hours of pre-activation with LPS, 100 µg/ml CaOx was added to some of the cells and the supernatant collected after 6 more hours (Figure 7A).

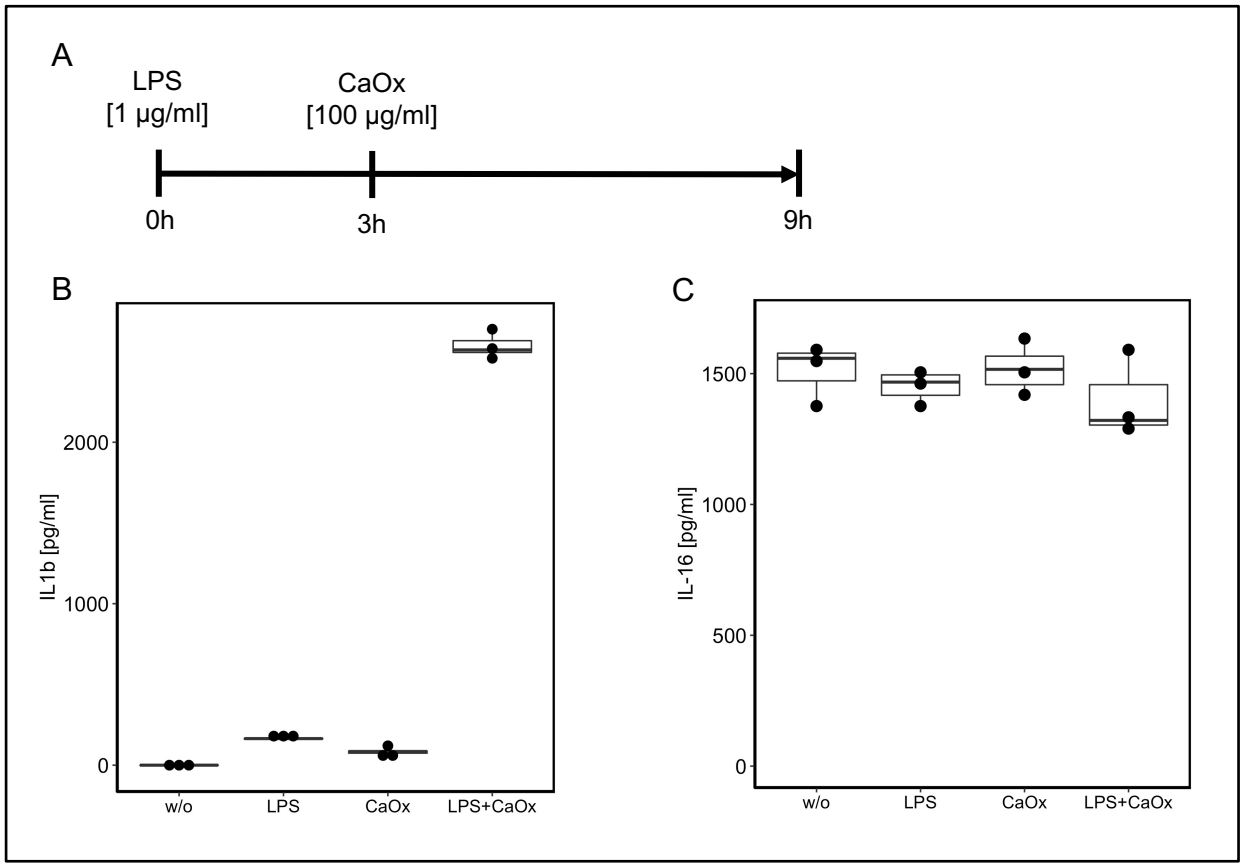

Figure 7: IL-16 secretion of PBMCs after inflammasome activation

Experiment conducted by Lisa Rubenbauer. (A) Experimental setup: PBMCs were isolated and pre-stimulated by 1 µg/ml LPS for 3 hours, followed by 6 hours stimulation with 100 µg/ml CaOx. (B+C) IL-1β and IL-16 were measured in the supernatant using DuoSet-ELISAs (R&D).

An increased release of IL-1β was measured when the PBMCs were stimulated with LPS and CaOx (Figure 7B). At the same time, IL-16 was found to be released into the supernatant independent of the stimulation (Figure 7C).

Lisa Rubenbauer also examined the relative expression of IL-16-GAPDH and IL-1β-GAPDH of human monocytes compared to human *in vitro* differentiated macrophages and found reciprocal behavior. While monocytes showed significantly higher expression

levels of IL-16-GAPDH compared to macrophages, macrophages showed significantly higher expression levels of IL-1β-GAPDH than monocytes (data not shown).

Based on the increased expression level of IL-16 in monocytes, Lisa Rubenbauer developed a new hypothesis, namely that there might be differences in the release of IL-16 between monocyte subtypes, with an increased release of non-classical monocytes compared to classical monocytes. The described monocyte shift in CKD patients could then lead to a higher abundance of cells which secrete more IL-16.

For this, Lisa Rubenbauer studied the basal secretion of the different monocyte subsets. After blood collection, PBMC isolation, and enrichment for monocytes, the cells were stained with the antibodies CD14-PC7 (Beckman Coulter, Brea, USA), CD16-PE (Beckman Coulter), CD3-FITC (Miltenyi Biotec, Bergisch Gladbach, Germany), and CD19-APC (Biolegend, San Diego, USA).

The monocyte subsets were sorted using fluorescence activated cell sorting (FACS) conducted by the BIH Cytometry Core Facility at the BCRT. The gating strategy used was based on gating out $DAPI^+$, $CD3^+$, and $CD19^+$ cells, which led to her readout plot of CD14 and CD16 (Figure 8). Classical monocytes were defined as $CD14^+$ $CD16^-$, intermediate monocytes as $CD14^+$ $CD16^+$, and non-classical monocytes as $CD14^-$ $CD16^+$.

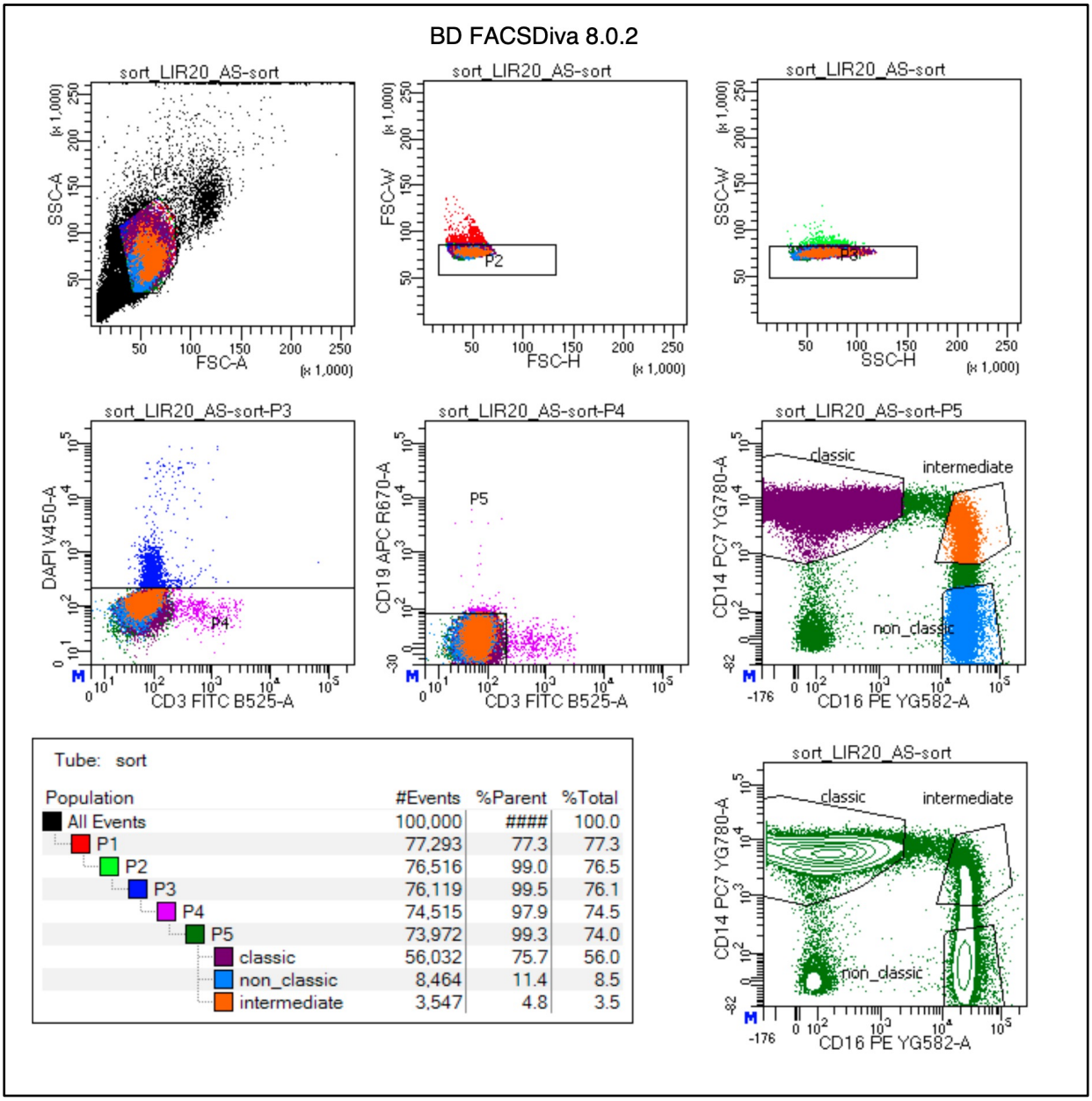

Figure 8: Gating strategy of monocyte subsets

Gating strategy for FACS-based isolation of monocytes subsets. One representative example of a healthy control subject shown. Experiment performed by Lisa Rubenbauer, 2019.

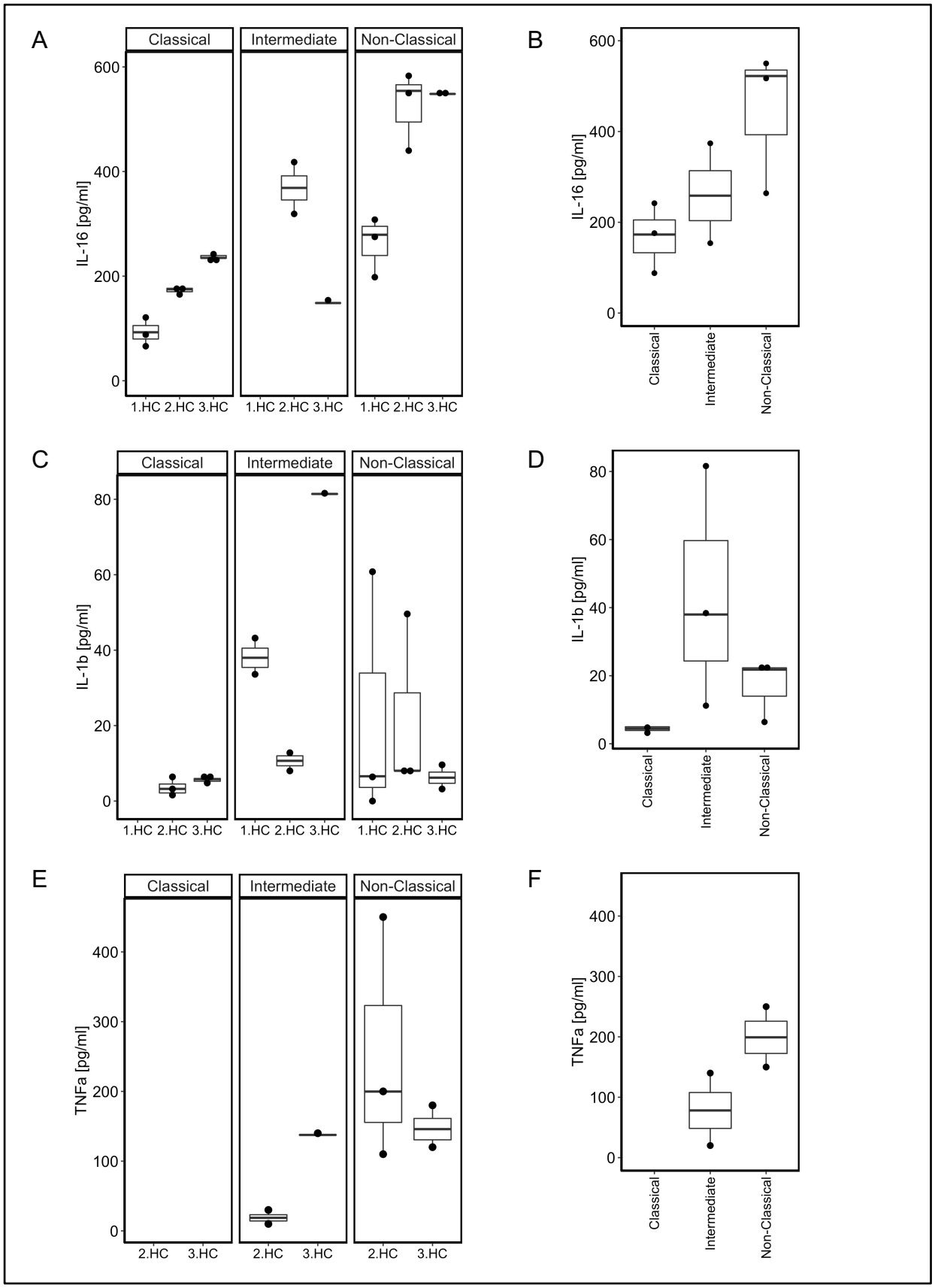

Figure 9: Cytokine secretion of monocyte subsets after basal culture

Measurements of IL-16, IL-1β and TNF-α were performed using DuoSet-ELISAs (R&D). Experiment conducted by Lisa Rubenbauer, 2019.

The cells were cultured in complete culture medium for 18 hours and the cytokines were measured in the supernatant by IL-16, IL-1β and TNF-α ELISAs (DuoSet, R&D). The experiment was performed twice and included three healthy controls (HCs). The mean IL-16 secretion of monocyte subtypes showed significant differences, with a mean secretion of 167.7 pg/ml (SD 64.2) by the classical monocytes, 295.3 pg/ml (SD 135.2) by the intermediate monocytes, and 431.7 pg/ml (SD 148.8) by the non-classical monocytes. IL-1β appears to be secreted by most monocyte subsets, with intermediate and non-classical monocytes having potentially higher levels of secretion. In the case of TNF-α, it is noticeable that no TNF-α could be detected in the supernatant of the classical monocytes.

In summary, Lisa Rubenbauer's preliminary results suggest that non-classical and intermediate monocytes secrete higher levels of IL-16 than classical monocytes.

1.5 Aims of the study, research questions and hypothesis

Generally, very little is known regarding IL-16 in CKD G5D patients; therefore, very fundamental questions must be addressed.

Origin

First, a crucial question concerns the origin of IL-16 and the responsible cell type in patients leading to the previously described elevated levels. As described before, IL-16 is synthesized by a variety of different cells and is expressed in different tissues. Two main sources were considered as the potential origin: kidney tissue and immune cells. As the IL-16 gene expression is remarkably higher in immune cells (Figure 2), these were in the focus of this work.

Since my group had found promising initial results regarding differences in the IL-16 secretion of monocyte subtypes (Figure 9), the basal IL-16 release of monocyte subtypes, especially non-classical monocytes, from healthy individuals was particularly interesting to investigate.

Because there is also little knowledge about the basal IL-16 secretion of different cell types of PBMCs in CKD patients especially, the secretion of T cells, B cells, NK cells, and

monocytes was interesting to be studied in comparison. In patients suffering from CKD, there might be a cell group that generally secretes more IL-16.

Additionally, intracellular levels of IL-16 when comparing between the cell types of PBMCs as well as between patients and control subjects appeared worthy of further investigation.

Secretion mechanism

Second, the secretion mechanism or stimulator in CKD G5D patients leading to IL-16 secretion is not yet known. The initial finding of the correlation of IL-16 and pOx suggests a direct effect of oxalate stimulation on a cell type, leading to the secretion of IL-16. The results of my work group after examining this potential connection by the stimulation of PBMCs with CaOx, as well as with a stimulation with LPS, however, could not detect any difference in secretion.

To further understand the secretion mechanism, to examine the role and importance of the caspase-3 cleavage, and to study the liberation or secretion of IL-16 in different forms of cell death, an *in vitro* model experiment with the use of murine BMDM was considered. As described earlier, the inflammasome complex of cells becomes activated by the appropriate stimulation, e.g., LPS and CaOx, which leads to pyroptosis pathways. If GSDMD is absent, however, caspase-3 is activated and leads to apoptotic cell death. Thus, it is therefore conceivable that IL-16 is only secreted and detectable if caspase-3 becomes activated, and therefore only from the cells where GSDMD is absent.

As described before, IL-16 secretion is often described in cell death-associated pathways. In CKD, several compounds and stimulators are imaginable that could be responsible for the induction of immune cell death. Even the dialysis membrane could be accountable for it. Since *in vitro* experiments show that PMNs undergo increased cell death when cultured with CaOx (Desai et al., 2017; Elferink & Riemersma, 1980), and PMNs secrete IL-16 in secondary necrosis (Roth et al., 2015), CaOx stimulation of PMNs came into focus in the search for a secretion mechanism. Potentially, the soluble form of oxalate, namely sodium oxalate (NaOx), could stimulate IL-16 secretion from PMNs, which should be investigated.

Importance of IL-16 in CKD

Third, nothing is known about the role or importance of IL-16 in CKD patients. Because IL-16 is often associated with the migration of Tregs and the induction of FoxP3 synthesis (McFadden et al., 2007), it became interesting to examine the relationship between Tregs and IL-16 as an initial starting point in the search for the role of IL-16 in CKD.

Hypothesis

In summary, several research questions and hypotheses need to be further investigated based on the results of my research group and the literature described above:

1. Hypothesis regarding the cellular source of IL-16 in CKD patients:
    A. Non-classical monocytes, which are more abundant in CKD patients, secrete more IL-16, resulting in higher levels of IL-16 in the plasma of patients.
    B. In CKD G5D patients, there is a general difference in PBMCs with a cell type that secretes higher IL-16 levels basally, resulting in higher plasma IL-16 levels.
    C. There is a difference in the basal intracellular level of IL-16 and the basal activity of caspase-3 in PBMCs of CKD-G5D patients compared with healthy control subjects.
2. Hypothesis regarding the mechanism of secretion:
    A. Upon stimulation with LPS and CaOx, the absence of GSDMD in BMDM leads to an activation of caspase-3 and therefore to a cleavage of IL-16 instead of pyroptotic cell integrity loss in GSDMD-wt BMDM and subsequently to higher IL-16 levels in the supernatant of GSDMD-ko BMDM.
    B. The stimulation of PMNs with soluble NaOx and/or CaOx crystals induces cell death-associated processes which liberate IL-16 into the supernatant.
3. Hypothesis regarding the importance of IL-16 in CKD:
    A. IL-16 correlates with the proportion of Tregs in patients' plasma, suggesting a Treg inducing function of IL-16.

2. Materials and Methods

2.1 Materials

2.1.1 Software

Microsoft Office for Mac	Version 16.3	Microsoft, Redmond, USA
Zotero	Version 5.0.97	Corporation for Digital Scholarship, George Mason University, USA
RStudio	Version 1.2.5001	RStudio Inc., Boston, USA
FCSExpress	Version 6	De Novo Software, Los Angeles, USA
Discovery Workbench MSD	Version 4.0	Meso Scale Diagnostics, Rockville, USA
LEGENDplex Data Analysis Software	Version 8.0	Biolegend, San Diego, USA
Microplate Manager 6 Software	Version 6.1	Bio-Rad Laboratories, Inc., Hercules, USA
Adobe Illustrator	Version 25.4.1	Adobe Inc., San José, USA

RStudio Packages:

- tidyverse
- knitr
- readxl
- foreign
- ggcorrplot
- rstatix

2.1.2 Laboratory equipment

Pipettes: Eppendorf Research plus (Eppendorf AG, Hamburg, Germany)

Table Centrifuges: Heraeus Fresco 21 Centrifuge, Thermo Scientific (Thermo Fisher); Eppendorf Centrifuge 5427R (Eppendorf)

Centrifuges: Eppendorf Centrifuge 5810 R (Eppendorf)

Incubator: Heraeus Kendro HeraCell 150 CO_2 Incubator (Thermo Fisher)

Table vacuum pump: neoLabLine 2-9345, (neoLab, Wayne, USA)

ELISA Plate Reader: Bio-Rad xMark Microplate Spectrometer (Bio-Rad Laboratories, Inc., Hercules, USA)

Flow Cytometer: MACSQuant Analyzer10 (Miltenyi Biotec, Bergisch Gladbach, Germany)

Table heater: Eppendorf ThermoMixer C (Eppendorf)

Electrophoresis Power Supply: EPS 200 (Pharmacia Biotech, Uppsala, Sweden)

Western Blot machine: Vilber Fusion FX (Vilber, Collégien, France)

Fine weight: KERN Alt 220-5DAM (KERN & Sohn GmbH, Balingen-Frommern, Germany)

Sterile Water: Mili-Q (Merck KGaA, Darmstadt, Germany)

2.1.3 Buffers

ACK Lyse Buffer

Ammonium chloride (NH4CL)	150 mM	5.145 g	Carl Roth	K298.1
Potassium hydrogen carbonate (KHCO3)	10 mM	0.5 g	Carl Roth	P748.1
Ethylenediaminetetraacetic acid Dipotassium Salt dihydrate (Na2EDTA)	0.1 mM	0.0186 g	Sigma-Aldrich	8043.1

Fill up to a volume of 500 ml with H2O, adjust pH to 7.28 with HCl.

Low FBS Medium (Used for Monocyte and PBMC Culture)

Roswell Park Memorial Institute (RPMI) 1640 Medium	500ml	Gibco	21875-034
Fetal bovine serum (FBS)	12.5 ml	Sigma-Aldrich or PAN Biotech	F7524 P30-3031
Penicillin-Streptomycin (Pen/Strep)	5 ml	Gibco	15140-122
L-Glutamine 200 mM	5 ml	Gibco	25030-024

High FBS Medium (Used for FACS Collection and PMN Culture)

RPMI 1640 Medium	500 ml	Gibco	21875-034
FBS	50 ml	Sigma-Aldrich PAN Biotech	F7524 P30-3031
Pen/Strep	5 ml	Gibco	15140-122
L-Glutamine 200 mM	5 ml	Gibco	25030-024

BMDM Differentiation Media

RPMI 1640 Medium	37.75 ml	Gibco	21875-034
FBS	5 ml	Sigma-Aldrich or PAN Biotech	F7524 P30-3031
L929 conditional media	7.5 ml		
Pen/Strep	0.5 ml	Gibco	15140-122

HEPES	1.25 ml	Gibco	15630-056

BMDM Washing Media

RPMI 1640 Medium	46.5 ml	Gibco	21875-034
FBS	2.5 ml	Sigma-Aldrich or PAN Biotech	F7524 P30-3031
Pen/Strep	0.5 ml	Gibco	15140-122
HEPES	0.5 ml	Gibco	15630-056

FACS Buffer

Dulbecco's Phosphate Buffered Saline (DPBS)	500 ml	Gibco	2205996
EDTA 1%	100 ml	Versen	
FBS	12 ml	Sigma-Aldrich or PAN Biotech	F7524 P30-3031

ELISA PBS 10X

Sodium chloride (NaCl)	80g	Sigma-Aldrich	S5886-1kg
Potassium chloride (KCl)	2.0 g	Chemsolute	1632.1000
Sodium Phosphate (H3PO4)	14.1 g	Carl Roth	4984.2
Potassium dihydrogen phosphate (KH2PO4)	2.7 g	Carl Roth	3904.2

Add 100 ml H2O

ELISA Wash Buffer

PBS 1X	500 ml		
Tween20	250 µl	Merck KGaA	8.22184.0500

ELISA Reagent Diluent 1

PBS 1X	50 ml		
Bovine Serum Albumin	0.5 g	Sigma-Aldrich	A7906-50G

ELISA Reagent Diluent 2

PBS 1X	12 ml		
Bovine Serum Albumin	3 ml	Sigma-Aldrich	A7030-10G

RIPA Buffer

1M Tris-HCl pH 7.2	5 ml	50 mM		

5M NaCl	3ml	150 mM	Sigma-Aldrich	S5886-1kg
0.5 M EDTA	2 ml	10 mM	Sigma-Aldrich	E5134-250G
10% SDS	1 ml	0.1% SDS	Carl Roth	2326.2
10% Sodium deoxycholate	10 ml	1% Sodium deoxycholate		
Triton X-100	1g	1%		

add up to 100 ml with dH2O

Cell Lysis Buffer

RIPA buffer	10 ml		
cOmplete ULTRA Tablets, glass vials Protease Inhibitor Cocktail	1 tablet	Roche	04 693 159 001
phosSTOP Phosphatse Inhibitor Cocktail Tablets	1 tablet	Roche	04906837001

Buffers used for Western Blot analysis

Resolving gel

	10%	12%		
dH2O	4.1 ml	3.35 ml		
1.5M Tris HCl pH 8.8	2.5 ml	2.5 ml	Carl Roth	0188.4
10% SDS stock solution	100 µl	100 µl	Carl Roth	2326.2
Acrylamid/Bis (30% stock)	3.3 ml	4 ml		
10% Ammonium peroxodisulfate	50 µl	50 µl	Carl Roth	2592.3
TEMED	5 µl	5 µl	Carl Roth	2367.3

Stacking gel

dH2O	3.05 ml		
0.5M Tris HCl	1.25 ml	Carl Roth	0188.4
10% SDS	50 µl	Carl Roth	2326.2
Acrylamid/Bis (30% stock)	650 µl		
10% Ammonium peroxodisulfate	50 µl	Carl Roth	2592.3
TEMED	6 µl	Carl Roth	2367.3

4X Loading Buffer

dH2O	5 ml		
0.5 M Tris pH 6.8	3 ml	Carl Roth	0188.4
Glycerol	4 ml		
20% SDS	4 ml	Carl Roth	2326.2
Bromophenol Blue	Pinch, by eye	Carl Roth	A512.1

Right before use: mix 400 ml 4X Loading Buffer with 100 µl Dithiothreitol (DTT).

10X Running Buffer

Tris-Base	30.3 g	Carl Roth	0188.4
Glycine	144.0 g	Carl Roth	3187.3
SDS	10.0 g	Carl Roth	2326.2

Add up to 1000 ml with H2O and prepare 1X working dilution prior to use.

10X Blotting Buffer

Tris-Base	30.3 g	Carl Roth	0188.4
Glycine	144 g	Carl Roth	3187.3

Add up to 1000 ml with dH2O.

1X Blotting Buffer

10X Blotting buffer	100 ml		
Methanol	200 ml	Merck	1.06009.2500

Add up to 1000 ml with dH2O.

Ponceau Red Staining

Ponceau S 0.1%	20 mg	Sigma-Aldrich	REF: P7170
dH2O	19.8 ml		
Acetic Acid	0.2 ml	Chemsolute	REF: 2234.1000

TBS 10X

Tris	60.55 g	Carl Roth	0188.4
NaCl	87.66 g	Sigma-Aldrich	S5886-1kg

Solve in 800 ml H2O, adjust pH to 7.2 using 25% HCl, add up to 1000 ml with H2O.

Wash Buffer

1X TBS	500 ml		
Tween20	250 µl	Merck KGaA	8.22184.0500

Blocking Buffer

TBS/0.05% Tween20	95 ml	95%		
Dry Milk	5 g	5%	Carl Roth	T145.3

2.2 Methods

2.2.1 Patients/Probands

The study protocol was approved by the local authorities (local Ethics Committee of Charité, Berlin Study No. EA2/242/17).

Patient recruitment was performed by randomly selecting CKD G5D patients (hereafter also referred to as patients) who were receiving their regular maintenance dialysis on the Charité – Universitätsmedizin Berlin, Charité Campus Mitte (CCM), dialysis ward, were willing to participate in the study, and had provided written informed consent. Patients had been on maintenance HD for at least 3 months, were not feeling acute sickness, and had no sign of an acute infection.

Healthy control subjects were randomly recruited among Charité students and Center for Cardiovascular Research (CCR) employees who were willing to participate in the study, had no known inflammatory disease, and reported no acute illness.

An additional plasma sample was collected from patients and healthy individuals to measure pOx and IL-16. If possible, further patient information was collected and an extended laboratory investigation of the blood count performed.

2.2.2 Animals

C57BL/6N GSDMD-deficient embryos were obtained from Genentech (Genentech, Inc, South San Francisco, USA) and transferred to female C57BL/6N mice. GSDMD-heterozygotic mice were subsequently paired to obtain GSDMD-wild-type and -deficient littermates.

Mice were kept under normal housing conditions, with a normal 12-hour dark cycle. Chow and drinking water were provided to them as much as desired. The animals were closely monitored, and their health was recorded. The animals were euthanized under “Tötungsanzeige” T0272/17.

2.2.3 Cell isolation and cell culture techniques

Before using the sterile workbench, the laminar flow cabinet was turned on early and disinfected thoroughly. A lab coat and gloves were always worn when working in the cell culture laboratory. Work with potentially infectious human material was always performed under the laminar flow cabinet or at a dedicated workstation. Potentially infectious waste was autoclaved before disposal.

Cell counting

Two different methods were used for cell counting. The same counting method was always used within an experiment. After preparation of the cell suspension using either culture medium, DPBS or HBSS (both Gibco, Thermo Fisher), the cells were counted and adjusted to an intended concentration.

Neubauer counting chamber: The cell suspension was thoroughly and carefully mixed by swaying the tube for few seconds. 10 µl of cells in fluid were transferred into an empty microcentrifuge tube. 10 or 90 µl of trypan blue suspension (Trypan Blue Stain (0.4%), Gibco, Thermo Fisher, REF: 15250-061) was added (1:2 ratio or 1:10). The hemocytometer, a Neubauer chamber, was prepared by thorough cleaning and attaching the cover slip using a few drops of water. Subsequently, 10 µl of cell suspension-trypan blue mix was pipetted onto the lower edge of the Neubauer chamber. Trypan blue stains cells that lost their cell integrity therefore indicated dead cells. Under the microscope, all white cells within all four quadrants were counted and the average calculated. The result was then multiplied by the dilution factor, e.g., 2 or 10, and by 10,000 to calculate the cell number per milliliter in the cell suspension.

Flow cytometer cell counting: After mixing, 10 µl of cell suspension was transferred into a new 5 ml FACS tube (Sarstedt AG & Co. KG, Nümbrecht, Germany, REF: 55.476.013) and 90 µl FACS buffer added. Without further staining or processing, 50 µl of cell suspension was taken up by the flow cytometer and the cell number counted. The beats within a defined live cell gate were determined and multiplied by 2 and 100 to determine the cell number per milliliter in the cell suspension.

Blood collection

For blood collection of healthy controls, the puncture site of the forearm was identified and thoroughly disinfected. The tourniquet was applied, and a butterfly needle (SAFETY Blood Collection/Infusion Set, Greiner Bio-One GmbH, Kremsmünster, Austria) inserted into the vein at an acute angle. The adapter (Vacuette Holdex, Greiner Bio-One GmbH) and the vacutainer 10 ml EDTA tube (Vacuette, Greiner Bio-One GmbH) or 10 ml Heparin Tube (Vacuette, Greiner Bio-One GmbH) were attached, and the appropriate amount of blood drawn. For the subsequent sorting for monocyte subtypes, approximately 120 ml of blood was required; for the sorting for PBMC, 40 ml was required, and for the isolation of PMNs, 20 - 40 ml of blood had to be drawn. The cannula was removed and a swab pressed onto the puncture site.

Blood from HD patients participating in my study was drawn by nurses and physicians in the dialysis unit after the port had been punctured and flushed immediately before dialysis began.

All blood samples were stored directly on ice and were further processed within one hour after collection.

For additional plasma collection for the measurement of oxalate and inflammatory parameters from the blood, another 6 or 10 ml EDTA tube was taken. It was centrifuged down at 2000 x g at 4 ° C. for 5 min. The plasma was now clearly separated from the erythrocytes. Using a polyethylene Pasteur pipette (Glaswarenfabriken Karl Hecht GmbH & Co KG, Sondheim, Germany, REF: 40569003), the plasma was transferred to several microcentrifuge tubes and centrifuged again on the tabletop centrifuge at 3000 x g at 4 ° C. for 5 min. After being transferred to new microcentrifuge tubes, the samples were frozen at -80 °C until further use.

PBMC Isolation

The EDTA blood was transferred to a 50 ml Falcon (Greiner Bio-One GmbH) and diluted in a 1:2 ratio, i.e., 10 ml blood and 10 ml DPBS (Gibco). 15 ml of Ficoll-Paque PLUS (GE Healthcare Bio-Sciences AB, Uppsala, Sweden, REF: 17-1440-02) with a density of 1.077 was now added to a fresh 50 ml Falcon tube. The 20 ml of diluted blood was subsequently carefully layered onto the Ficoll by pipetting slowly. To do this, the tube was held at an angle of approximately 45°. Two layers formed, which were not swirled.

The tube was centrifuged at 500 x g and 20° C. for 20 min without using the brake for stopping. After centrifugation, different layers were visible. On the bottom of the tube, there was an erythrocyte layer, on top of it a Ficoll/granulocyte layer, above it the buffy coat PBMC layer and at the very top plasma (Grievink et al., 2016). Some plasma was aspirated and the buffy coat with the PBMCs transferred to a new 50 ml Falcon Tube. This tube was filled with the required amount of DPBS until a volume of 50 ml was reached. The tube was centrifuged at 250 x g and 4°C for 10 min and the supernatant removed. The tube was filled with 10 ml ACK Lysis Buffer and the pellet detached from the bottom by careful pipetting. The cell suspension was allowed to stand for 5 min. The tube was filled with DPBS to achieve a volume of 50 ml and centrifuged at 400 x g and 4° C for 5 min, the supernatant was removed, and this washing step was repeated. Finally, the pellet was taken up in the desired amount of buffer and the cell number determined.

Instead of manually layering diluted blood on top of the Ficoll Paque, Leucosep tubes (Greiner Bio-One GmbH, REF: 227290) were used. These tubes consist of a porous barrier which separates the erythrocyte and granulocyte layer from the wanted PBMCs after centrifugation and simplifies the handling (Leucosep datasheet). It was observed, however, that PBMC samples isolated using the Leucosep tubes contained more cell debris in flow cytometry cell sorting and analysis and were not further used.

Monocyte Isolation

For the first monocyte experiment, the cells were magnetically isolated from PBMCs using a quadroMACS separator (Miltenyi Biotec) and a negative sorting Pan Monocyte Isolation Kit (Miltenyi Biotec) in accordance with the manufacturer's instructions. It is known that the negative sort alters the functionality of monocytes less than positive methods (Bhattacharjee et al., 2018)

The PBMC suspension was centrifuged down at 300 x g (1300 rpm) for 10 min at 4 ° C and the supernatant was removed. Based on the cell number of PBMCs, the cell suspension was now taken up in FACS buffer, i.e., 40 µl of FACS buffer per 10^7 cells. For the magnetic labelling of the cells, an appropriate amount of FcR Blocking and Biotin AB Cocktail was added. Per 10^7 PBMCs, 10 µl of FcR Blocking and Biotin AB Cocktail was necessary. The cell suspension was incubated for 5 min in the fridge (2-8° C). Then

30 µl per 10^7 cells of FACS buffer and 20 µl per 10^7 cells of Anti-Biotin-MicroBeads were added. The suspension was subsequently incubated in the fridge for 10 minutes.

For the magnetic separation, the cooled LS separation column (Miltenyi Biotec) of the quadroMACS separator was placed into the magnetic field. Beneath the column a 15 ml tube was placed in a bucket of ice. After flushing the column with 3 ml FACS buffer and discarding the fluid, the cell suspension was added and the cells that flowed through were collected. In negative sorting techniques, all cells except the cells of interest are labeled. In this case, the monocytes are therefore unlabeled and flow through the column first. The monocytes were collected, and the column was flushed three more times with 3 ml FACS buffer until no further fluid dripped out of the column.

If the remaining non-monocyte cells were supposed to be collected, the column was removed from the quadroMACS separator and 5 ml of FACS buffer added to the column. The cells were flushed out of the column by applying pressure to the piston.

The cell number of the isolated cells was then determined.

PMN Isolation

The PMN isolation was performed according to established protocols (Quinn & DeLeo, 2020). 40 ml of freshly taken heparin blood was taken up into a 50 ml syringe (Injectomat syringe, Fresenius Kabi AG, Bad Homburg, Germany, REF: 9000701) by using a large canula. The 4% Dextran solution (Dextran 500, Carl Roth, Karlsruhe, Germany, REF: 9219.1), dissolved in 0.9% NaCl, was added in a 1:4 ratio to the blood (12.5 ml). The syringe was carefully mixed by swaying for 30 sec and allowed to stand for 30 min at room temperature beneath the hood. Subsequently, the erythrocyte sedimentation became visible as well as the fluid above the erythrocytes consisting of plasma, dextran, sodium chloride and leukocytes. This fluid was transferred into a new 50 ml tube using a 19G winged canula (Butterfly). Carefully, the supernatant was underlaid with approx. 7 ml of Ficoll-Paque PLUS. The tube was spun down for 15 min at 290 x g (1300 rpm) at room temperature and the speed reduced to 222 x g (1100 rpm) after 15 min without brake.

From this point on, every step was performed on ice or in a cooled environment. After a total of 30 min centrifugation, the supernatant was removed and only the pellet kept. To lysate the remaining erythrocytes, 10 ml of cold autoclaved distilled water was added and

carefully pipetted up and down. After 30 seconds, 3.33 ml of 3.6% NaCl was added to make the cell suspension isotonic. Approximately 10 ml of HBSS (no calcium, no magnesium, no phenol red, Gibco, Thermo Fisher, REF: 14175-053) was added to the tube and spun down at 222 x g for 10 min at 4 °C. The supernatant was removed and the cell pellet taken up in 10 ml of high FBS media. The cell number was determined.

2.2.4 Flow cytometry

Flow cytometry cell sorting

The cell sorting was performed at the Flow Cytometry Core Facility of the BIH at the BCRT.

For cell sorting, PBMCs or isolated monocytes were used right after isolation and cell counting and always handled on ice. The cells were centrifuged down for 5 min and 300 x g at 4° C and taken up in 1 – 2 ml FACS buffer. The cell suspension was divided into different samples, as follows:

For the compensation, single-stained and unstained samples were prepared by pipetting approximately 5 µl of cell suspension into each well of a 96-well plate. For the sorted fully stained sample, the remaining majority of cells was transferred into a 1.5 ml microcentrifuge tube. The antibodies were added, and the volume was adjusted to 50 µl for the compensation samples by adding FACS buffer. The samples were incubated in the fridge for 15 min in the dark. The plate and the tube were centrifuged down, and the samples taken up in approximately 300 µl FACS buffer. The samples were then kept on ice and taken to the BCRT Flow Cytometry Core Facility within 1-2 hours. There, the samples were filtered using a 35 µm cell strainer (Falcon Round-Bottom Polystyrene Test Tubes with Cell Strainer Snap Cap, 5mL, Fisher Scientific, Thermo Fisher) to remove debris and cell clumps. Right before the actual cell sorting, propidium iodide (P.I.) was added. The sorting was performed using a BD FACSAria II (BD Bioscience, Franklin Lakes, USA) with a nozzle size of 70 µm and a sheath pressure of 70 psi. Cells were collected in tubes containing approximately 1 ml RPMI with 10% FBS. The purity of the cell populations was confirmed after sorting was completed.

Flow cytometry analysis

For the surface staining, the counted cells were distributed into different wells of a 96-well flat-bottom plate according to the experimental setup, with the minority of cells for the single-staining and the unstained sample and the most cells for the full-staining. If the panel contained a fixable viability dye, e.g., Zombie NIR, this staining was performed first. After centrifugation at 400 x g for 5 min at 4 ° C, removal of the liquid, washing with 200 µl PBS and repetition of centrifugation, cells were taken up in the fixable viability dye diluted in PBS or only PBS for unstained or single-stained samples. After 30 min of incubation at room temperature in the dark, the plate was centrifuged down and the liquids were removed. Subsequently, the cells were stained in the FACS-buffer-antibody mix according to the experimental setup and the panel design containing FcR-Blocker (FcR Blocking Reagent, Milteny Biotec, REF: 130-059-901). After 20 min of incubation at room temperature, the cells were washed twice by centrifugation, followed by the removal of liquids and addition of 200 µl FACS buffer. The cells were now ready for analysis on the flow cytometer or further processing if intracellular staining was desired.

The intracellular staining of transcription factor FoxP3 was performed using the eBioscience FOXP3/Transcription Factor Staining Buffer Set (Invitrogen, Thermo Fisher, Carlsbad, USA, REF: 00-5523-00). Following this, the buffers were prepared by mixing one-part fixation/permeabilization concentrate with three-part diluent and by preparing a 1X Permeabilization buffer by diluting the supplied 10X buffer 10-fold in distilled water. After the last washing step, the cells were taken up in 200 µl fixation/permeabilization buffer and pipetted up and down. The cells were incubated for 40 min at room temperature in the dark. For washing, the cells were centrifuged at 500 x g and room temperature for 5 min, and the liquids were removed and taken up in 200 µl permeabilization buffer. Washing was performed two times. Afterwards, the cells were taken up in 100 µl permeabilization buffer and 5 µl FoxP3-antibody was added. After 30 min of incubation in the dark, the cells were washed two more times. The cells were taken up in FACS buffer and run on the flow cytometer for analysis.

The intracellular staining of IL-16 and caspase-3 were performed using a Cyto-Fast Fix/Perm Buffer Set (Biolegend, REF: 97503). After the surface staining described above, the plate containing the cells was centrifuged down at 250 x g for 5 min at 4 °C, and the cells taken up in 100 µl Cyto-Fast Fix/Perm Buffer. To permeabilize the cells, the suspension was incubated for 20 min at room temperature. The cells were washed twice

by centrifugation, followed by removal of liquids and addition of 200 µl of Cyto-Fast Perm Wash solution. Afterwards, the cells were taken up in 100 µl of Cyto-Fast Perm Wash solution mix containing the desired antibodies. For the intracellular staining, the cells were incubated for 20 min at room temperature in the dark. After an additional washing step, the cells were taken up in 200 µl FACS buffer and analyzed on a flow cytometer.

Compensation was either performed with single staining controls of the respective antibody, or by using compensation beads. For the latter, two products were used:

MACS Comp Bead Kit anti-mouse Igk	Miltenyi Biotec	REF: 130-097-900	LOT: 5190404424
MACS Comp Bead Kit anti-REA	Miltenyi Biotec	REF: 130-104-693	LOT: 5190425341

Flow cytometry cell death experiment over time

The isolated PMNs were adjusted to a concentration of 2 x 10^6 cells/ml in culture medium and 100 µl cell suspension per well were seeded into a 96-well tissue culture treated plate (Costar, Corning Incorporated, New York, USA, REF: 3596). Then, 10 µl of the respective simulants were added. Either PBS as control, calcium oxalate (CaOx hydrate, Sigma-Aldrich, REF: 289841-250G) with a final concentration of 100 µg/ml, or sodium oxalate (NaOx, Sigma-Aldrich, REF: 71800-500G) with a final concentration of 100 µg/ml were added. The cell culture plate was put into the incubator.

At each time point, 100 µl of cell suspension was then carefully removed from the well, transferred into a 5 ml FACS tube, after which 11 µl (1:100 prediluted) P.I. suspension were added. Samples were immediately run on the flow cytometer. At each time point and for each preparation, triplicates were used.

Flow cytometry antibody panels

The indicated dilution refers to a staining volume of 100 µl. The dilution was always adjusted to the volume.

Human monocyte panel

Monocyte subsets were negatively defined using CD3, CD19 and CD56 and positively defined using HLA-DR, CD14 and CD16, which are commonly used for defining these cells (Abeles et al., 2012).

Antigen	Color	Clone	Company	Dilution
CD14	VioBlue	REA599	Miltenyi Biotec	1:50
CD16	APC	3G8	Biolegend	1:20
HLA-DR	PE	L243	Biolegend	1:20
CD3	FITC	REA613	Miltenyi Biotec	1:50
CD19	FITC	REA675	Miltenyi Biotec	1:50
CD56	FITC	REA196	Miltenyi Biotec	1:50
P.I. Solution			invitrogen	1:1000

Human PBMC panel

Antigen	Color	Clone	Company	Dilution
CD3	FITC	REA613	Miltenyi Biotec	1:50
CD14	VioBlue	REA599	Miltenyi Biotec	1:50
CD19	APCVio770	REA675	Miltenyi Biotec	1:50
CD56	BV510	5.1H11	Biolegend	1:20
HLA-DR	PE	L243	Biolegend	1:20
PI Solution			invitrogen	1:1000

Human IL16-Casp3-intracellular panel

A Fluorescence Minus One (FMO) control was used for the IL-16 antibody to identify the positive fluorescence signal. The fluorescence signal (mean fluorescence intensity, MFI) of IL-16-PE was quantified using the geometric mean.

Antigen	Color	Clone	Company	Dilution
CD3	PE-Vio770	REA613	Miltenyi Biotec	1:50
CD14	VioBlue	REA599	Miltenyi Biotec	1:50
CD16	APC	3G8	Biolegend	1:20
CD19	PerCP/Cy5.5	SJ25C1	Biolegend	1:20
CD56	BV510	5.1H11	Biolegend	1:20
Casp3	FITC	C92-605	BD	20 µl per test
IL-16	PE	14.1	Biolegend	1:20
Zombie NIR			Biolegend	1:1000

Human Treg panel

Antigen	Color	Clone	Company	Dilution
CD4	VioBlue	REA623	Miltenyi Biotec	1:50
CD8	APC	REA734	Miltenyi Biotec	1:50

CD25	PE	REA570	Miltenyi Biotec	1:50
CD45	BV510	2D1	Biolegend	1:20
CD127	PE-Cy7	A019D5	Biolegend	1:20
FoxP3	AF488	206D	Biolegend	1:20
Zombie NIR			Biolegend	1:1000

Murine GSDMD panel

Antigen	Color	Clone	Company	Dilution
CD11b	BV421	M1/70	Biolegend	1:100 – 1:300
CD45	PE-Cy7	30-F11	eBioscience	1:100
F4/80	PE	BM8	Biolegend	1:100
Zombie NIR			Biolegend	1:500

Human PMN panel

Antigen	Color	Clone	Company	Dilution
CD11b	BV421	M1/70	Biolegend	1:100 – 1:300
CD16	APC	3G8	Biolegend	1:100
Zombie NIR			Biolegend	1:500

Human PMN apoptosis assay

Antigen	Color	Clone	Company	Dilution
P.I. Solution			invitrogen	1:1000

2.2.5 Basal culture of sorted cells

After sorting, cell concentrations were adjusted and the cells cultured for 16 hours in culture medium. For harvesting, the cells were taken up with the pipette and transferred to previously labeled microcentrifuge tubes, centrifuged down at the pre-cooled table centrifuge for 5 min at 400 x g, and then the cell-free supernatant was transferred into additional microcentrifuge tubes. All samples were frozen till further use.

2.2.6 ELISA

Several different R&D DuoSet ELISA kits were used. These are sandwich ELISAs in which two specific antibodies sandwich the antigen. By adding a substrate, a proportional signal is generated that can then be measured (R&D, 2021).

DuoSet Human IL-1β /IL-1F2	R&D Systems	DY201-05	LOT P164641
DuoSet Human TNF- α	R&D Systems	DY210	LOT P171439
DuoSet Human IL-16	R&D Systems	DY316	LOT P105887
DuoSet Murine IL-16	R&D Systems	DY1727	LOT P105273

The manufacturer's protocol for the assay was followed. The required dilutions for capture antibody, standard, detection antibody, and streptavidin-HRP were thoroughly calculated based on the information provided on the LOT sheet. For the dilution of capture antibody, PBS was used, and for detection antibody and streptavidin, Reagent diluent 1 or 2. The DuoSet ELISA was primarily used to measure supernatant samples; if used for plasma samples, Reagent diluent 2 was used.

The day before the assay, the plate was coated by adding 100 µl diluted capture antibody to the plate, then sealed with a foil and stored at room temperature overnight. The following day, the plate was washed. For every washing step, 200 µl of washing buffer was added to every well using an 8-channel pipette (Eppendorf AG) and removed by either flipping it out at the sink or by using a table liquid remover. This washing was always repeated at least four times. Then, the plate was blocked using 250 µl of Reagent dilution 1. After 1 hour of incubation and an additional washing step, the diluted samples and the standard for calibration were applied, then the plate was covered with an adhesive strip and incubated for 2 hours at room temperature. After another washing, the detection antibody was added, and the plate was sealed and incubated for 1.5 hours at room temperature. After washing, the diluted streptavidin-HRP was added and incubated for 20 min at room temperature. Again, the plate was washed and the substrate solution (BD OptEIA, TMB Substrate Reagent Set, BD Biosciences, San Diego, USA) added. During the 20 min incubation, the samples became blue. Stop Solution (H2SO4) was added, and the blue color turned yellow. The plate was gently tapped so as to be mixed thoroughly, and the optical density was measured using a microplate reader at a wavelength of 450 nm. For optical correction, a second measurement was performed at 540 nm or 570 nm, respectively, and the value subtracted.

Using the software of the reader (Microplate Manager 6 Software), a standard curve was calculated and with the help of this, the concentrations determined. The measured values were multiplied by the dilution factor to calculate the final concentration of the samples.

Comparison of human IL-16 DuoSet ELISA and human IL-16 Quantikine ELISA

Plasma IL-16 measurement was performed using a human DuoSet IL-16-ELISA. As R&D's kit is not validated for the use of IL-16 measurement in plasma, however, the protocol was adapted with respect to the reagent diluent. The IL-16 Quantikine ELISA is intended to be used for human plasma.

In a previous experiment of my work group, the results of IL-16 measurements using the IL-16 DuoSet ELISA and the IL-16 Quantikine ELISA were compared. The IL-16 levels in plasma samples of 6 healthy controls and 20 CKD G5D patients were therefore measured by both assays. In the heathy control group, the mean IL-16 value for the IL-16 Quantikine ELISA was 150.1 pg/ml (SD 27) and it was 189.9 pg/ml (SD 18.3) for the IL-16 DuoSet-ELISA. The mean IL-16 Quantikine ELISA measurement in the patient group was 555.4 pg/ml (SD 256) and for the IL-16 DuoSet ELISA it was 714.4 pg/ml (SD 301).

Every sample in the control and patient group gave higher results in the DuoSet ELISA than in the Quantikine ELISA. Comparison of the relative difference for each sample showed that the DuoSet ELISA had higher values, with a mean of 28% (SD 16) in the control group and 29.8% (SD 14) in the patient group.

2.2.7 Oxalate Measurement

The measurement of oxalate in human plasma is associated with some difficulties since the concentration can be low, and oxalate is unstable if not acidified. Prolonged storage at room temperature can falsify the result (Pfau et al., 2020).

The exact protocol was described by my work group before (Pfau et al., 2020). In brief, 400 µl of plasma samples were deproteinized by centrifugation and filtration through Vivaspin 500 30,000 MWCO PES filter units (Sartorius, Göttingen, Germany, REF VS0122) and acidified using 16 µl 1N HCl.

The oxalate measurement was performed using a colorimetric enzymatic assay, commercially available from Trinity Biotech (Bray, Co. Wicklow, Ireland), that uses oxalate oxidase for the formation of indamine dye. The color produced is proportional to the oxalate concentration (Ladwig et al., 2005)

The 2-fold diluted samples were measured with a photometer.

2.2.8 LEGENDplex

For further analysis of the cytokine secretion of sorted cells, a LEGENDplex Macrophage/Microglia Panel (13-plex, REF: 740503, LOT: B292079, Biolegend, San Diego, USA) of the supernatant of cultured cells was performed. This bead-based immunoassay uses beads that differ in size and internal fluorescence intensities and which are conjugated with specific antibodies to serve in capturing the analyte of interest. The analytes measured by this kit include IL-12p70, TNF-a, IL-6, IL-4, IL-10, IL-1b, Arginase, TARC, IL-1RA, IL-12p40, IL-23, IFN-y, and IP-10. Using detection antibodies and streptavidin-phycoerythrin, a fluorescent signal provides the proportional amount of analyte and can be measured by flow cytometry (Biolegend, o. J.). The manufacturer's instructions regarding the protocol were followed.

For preparation, 20X Wash buffer was diluted with deionized water to have 1X Wash buffer. The Human Macrophage/Microglia Panel Standard Cocktail was reconstituted in 250 µl Assay buffer. 6 microcentrifuge tubes were labeled and 75 µl of Assay buffer pipetted in each. A standard solution series was prepared by transferring 25 µl of the top standard solution in the next tube and continued accordingly.

The plate was loaded with 12.5 µl of assay buffer into each well and 12.5 µl of standard or sample. After vortexing the mixed bead bottle, 12.5 µl of beads were pipetted into each well. The sealed plate was covered with aluminum foil and shaken at approximately 800 rpm for 2 hours. For washing, the plate was centrifuged at 250 x g for 5 min and the supernatant was removed. 200 µl of wash buffer was added and incubated for 1 min. Again, the plate was centrifuged, the supernatant was removed, and this washing step was repeated. Then 12.5 µl of detection antibody was added to each well, the plate was resealed, and it was protected from light and incubated on the shaker for 1 hour.

After incubation, 12.5 µl of SA-PE was added to each well and incubated again for 30 min on the shaker. After two more washing steps, samples were taken up in 150 µl wash buffer and measured by flow cytometry.

In the instrument settings on the MACSQuant Analyzer 10, FSC and SSC were set to display beads A and beads B. The voltages of the APC and FITC channels were set to distinguish 6 and 7 populations, respectively. The flow rate was set to low, the file name was named accordingly, and approximately 4500 beads were collected.

LEGENDplex data analysis software was used for analysis. The standard samples had to be identified, the standard curves for all analytes were generated, and the sample concentration of each analyte was calculated accordingly.

2.2.9 BMDM Isolation and Differentiation

In experimental settings, BMDM can be generated from bone marrow of mice after stimulation with growth factor for a defined time frame (Toda et al., 2021).

The bone marrow must be obtained starting from day 0. Therefore, the mouse was euthanized by isoflurane and cervical dislocation. The abdomen and the legs were sterilized using ethanol 70%. After opening the abdomen with sterile scissors and forceps, the legs were removed by cutting at the hip joint and transferred into a sterile petri dish. Using forceps, scissors, and paper towels, most of muscle and tissue was removed until the bones were visible.

This was stored in sterile DPBS in a 50 ml tube, and the work was continued under the sterile work bench. Subsequently, the knee was cut, and the femur and tibia were kept. A bone was transferred into an empty Petri dish and the proximal and distal epiphysis cut open. With a 5 ml syringe (BD Discardit II), washing media and a 21 G needle (Sterican, B. Braun Melsungen AG, Melsungen, Germany), the bone marrow was flushed out at one end of the bone. This was repeated with all bones. A sterile 70 µm cell strainer (FALCON, REF: 352350) was placed in a 50 ml Falcon tube and pre-wet with washing media. The bone marrow suspension was now passed through the sieve and the strainer washed with 1 ml washing media. The filtrate was centrifuged for 5 min at 1500 rpm at room temperature, the supernatant was discarded, and the cells were resuspended in 5 ml differentiation media. The cells were counted and adjusted to approximately 2-4 x 10^6 cells/ml seeded, with 5 ml in the smaller (Sarstedt, T25, REF: 83.3910.302) or 15 ml in

the medium sized (Sarstedt AG & Co. KG, T75, REF: 83.3911.302) tissue culture treated flasks. The flasks were cultured at 37 ° C and 5% CO2 in the incubator.

On days 3 and 5, the media was changed. For this purpose, the media was removed without disturbing the adherent cells. The flask was flushed with PBS and fresh differentiation media was added. The growth of the cells was monitored using a light microscope and flow cytometry.

By day 7, the cells were differentiated into BMDM. To loosen the cells, the medium was removed and trypsin-EDTA (Gibco, 15400-054) was added, with 4 ml for the large flasks and 0.5 ml for the smaller flasks. The plate was returned to the incubator for 5 min, the cells detached, and 10 ml of medium were added to stop the reaction. The cell suspension was transferred to a Falcon tube (Cellstar Tubes, Greiner Bio-One, REF: 227 261) and centrifuged at 1000 rpm for 5 min. After removing the supernatant, the cells were taken up in 5 ml of culture medium. Finally, the cells were counted and were ready to be seeded for stimulation experiments.

2.2.10 BMDM Stimulation Experiment

The differentiated BMDM were adjusted to a concentration of 1 x 10^6 cells per ml. A 24-well tissue culture treated plate (Sarstedt, REF: 83.3922.005) was used and 500 µl of cell suspension was pipetted into each well. In order for the cells to settle down on the new plate, they were not used until the following day.

To activate the inflammasome, two inflammasome activators are needed. 1 µg/ml LPS (InvivoGen, San Diego, USA) was used as the first danger signal, which must be applied in experimental settings about 3 hours earlier. Then, 100 µg/ml CaOx (Sigma-Aldrich) or 5 mM ATP (InvivoGen) were used as the second danger signal. To compare the actual effect of each compound of stimulation, several different samples are necessary: (1) no stimulation, (2) only LPS, (3/4) only ATP/CaOx, and (5/6) LPS and ATP/CaOx. At least four biological replicates were used.

The experiment started by adding 5 µl of the LPS working dilution or PBS to the wells, according to the experimental layout. After 3 hours of stimulation, 50 µl of ATP, CaOx or PBS was added to the wells. Again, the plate was incubated for 6 hours.

After a total of 9 hours of stimulation, the experiment was terminated. To stop the reaction, the plate was taken out of the incubator and directly put on ice, and the samples were further only handled on ice. First, the supernatant was transferred into individually labeled tubes without disturbing the attached cells. The supernatant was centrifuged down at 2000 x g for 5 min at 4 °C and the supernatant transferred into new tubes. For the protein isolation, 60 µl of cell lysate buffer was added to every well and pipetted up and down to loosen the sticky cells. To achieve the necessary amount of protein lysate, 4 to 6 biological replicates were pooled into one vial. The vials were incubated on ice for approx. 30 min and centrifuged down at 14,000 x g for 10 min at 4 °C. The lysate was transferred into new tubes and frozen at -80 ° C.

2.2.11 Protein Concentration Measurement

For the quantification of protein in the lysates, a Pierce BCA Protein Assay Kit (Thermo Fisher, REF: 23225) was used. This assay uses bicinchoninic acid (BCA), which leads to a purple-colored reaction that can be colorimetrically detected and is nearly linear to the protein concentration (Thermo Fisher Scientific, 2020)

The samples were always handled on ice and 5-fold diluted in PBS. For the standard curve, a dilution series with BSA was prepared. For this purpose, 60 µl of the 2000 µg/ml stock was transferred to a new tube and mixed with 60 µl PBS. Subsequently, 50 and 20 µl were transferred to the next smaller tubes and diluted with 12.5 and 13.3 µl PBS, respectively. From then on, starting with the 800 µg/ml tube, a twofold dilution series was prepared with 30 µl added from the higher concentrated tube into the lower concentrated tube and 30 µl PBS.

To prepare the BCA Working Reagent, 50 parts of BCA Reagent 1 were mixed with 1 part of BCA Reagent B. Subsequently, 10 µl of the sample, the standard dilution, or only PBS was pipetted into the wells of a 96-well flat-bottom plate (Greiner bio-one, REF 655101). All samples were run at least in duplicates. 200 µl of BCA Working Reagent was added to each well and the plate was incubated for 30 min at 37 ° C in the incubator. Then, the color reaction could be measured on a plate reader at a wavelength of 562 nm, and the protein concentration of the samples could be calculated using the standard curve.

2.2.12 Western Blot

To identify and quantify proteins in a protein lysate mixture, Western blots were performed. This assay is based on three basic working steps: First, the protein mixture is separated by gel electrophoresis according to the molecular mass; second, the proteins are transferred to a membrane; and third, the proteins are detected with antibodies against epitopes of the membrane-bound proteins and visualized by secondary antibodies and a color reaction (Luttmann et al., 2014).

For the discontinuous sodium dodecyl sulphate – polyacrylamide gel electrophoresis (SDS-PAGE), the gel is poured using two different gel compositions: a stacking gel with a low percentage of acrylamide and a resolving gel with a higher percentage of acrylamide. Due to the higher acrylamide content in the resolving gel, it is denser allowing separation of proteins by molecular weight.

First, the gel preparation device was set up, and the separating gel was prepared according to the recipe. This was then poured between two glass plates up to approximately 0.5 cm below the comb. To achieve a straight edge, approximately 1 ml of isopropanol was added to the surface of the gel. Once the gel was polymerized, the isopropanol could be removed. The surface of the gel was flushed with dH2O and dried using paper towels. Subsequently, the stacking gel was prepared and poured onto the hardened resolving gel. The comb was carefully placed in the stacking gel and the gel was left to polymerize.

The samples were prepared to contain the same amount of protein. The total volume that fits into a gel pocket depends on the width of the gel as well as the number of pockets. For example, into a 10 pocket 1.5 mm gel, 40 µl loading sample, and into a 15 pocket 1.5 mm gel, 20 µl loading sample was used, respectively.

The gels were loaded with 16-20 µg of protein. Loading samples were prepared with 2X Loading Buffer and the appropriate amount of protein lysate and cell lysis buffer.

The samples were heated up to 95 °C for 3 min and centrifuged at 13,000 x g for 5 min. The gel pockets were directly loaded with the appropriate amount of loading samples. Additionally, a molecular-weight size marker (PageRuler Plus, Prestained Protein Ladder, REF: 26619, Thermo Scientific) was loaded in one pocket. The gel was run at 100 V until it reached the separating gel and then the number was either increased to 120 V or reduced to 80 V until the sample reached the edge of the gel.

A PVDF-membrane (Immun-Blot, Bio-Rad Laboratories, Inc., USA) and 3MM Whatman blotting paper (Whatman Chromotography Paper) were cut to a similar size to the gel. The PVDF membrane was activated by placing it in methanol for a few seconds. The membrane was then washed in dH2O and left in transfer buffer until use. Care was taken to ensure that the membrane no longer dried out. The Whatman paper as well as the Scotch pads were also placed in blot buffer and pre-wetted in this manner. The gel was carefully released from the glass plates. Next, the actual Blot sandwich was prepared. This was done so that later the gel was placed on the cathode side and the PVDF-membrane on the anode side fixed between Whatman paper and Scotch pads in a plastic clamp. All air bubbles were carefully removed.

This sandwich was put into the blot chamber (Bio-Rad Laboratories, Inc., USA), a cooling pack was added and the chamber filled with blotting buffer. It was run at 29 V overnight in the cold room.

Using Ponceau dye solution (Ponceau S solution, BioReagent, Sigma-Aldrich, USA, REF: P7170), the membrane was stained for a few seconds and left to dry. By doing this, proteins can be detected on the membrane, thus verifying whether the blotting has worked. After washing the membrane with TBS/T, the membrane was incubated in blocking buffer for 2 hours on the shaker to block the membrane and reduce unspecific antibody binding. After three additional washing steps, the membrane was incubated in a 50 ml tube containing 5 ml of primary antibody diluted in TBS/T or blocking buffer in the cold room on a shaker overnight for approximately 16 hours.

Primary antibodies

Antigen and Source	Company		Dilution
Polyclonal Rabbit Anti-H/M/R/Mk-Caspase-3 Ab	Cell Signaling Technology	REF: 9662 LOT: 19	1:1000
Mouse monoclonal IL-16(A-1) Anti-Mouse/Rat/Human Ab	Santa Cruz	REF: sc-374606	1:200
Human IL-16 C-terminal Peptide Ab Antigen Affinity-purified Polyclonal Goat IgG	R&D Systems	REF: AF-316-SP	1:200
Polyclonal Goat Anti-IL-1beta/IL-1F2 Anti-Human IgG Ab	R&D Systems	REF: AF-201-NA, Lot: QM0817091	1:500
Monoclonal Mouse Anti-b-Tubulin	Sigma-Aldrich	clone D66, REF: T0198	1:1000
Mononuclear Rabbit Anti-H/M/R/Mk/B-GAPDH (14C10) Antibody	Cell Signaling Technology	REF: 2118	1:10000

The following day, the membrane was again washed three times and incubated for 2 hours with 10 ml of the secondary antibody diluted in TBS/T on the shaker at room temperature. The secondary antibody reacts specifically to the respective origin of the antibodies and is labeled with an enzyme.

Secondary antibodies

Antigen and Source	**Company**		**Dilution**
Peroxidase-conjugated AffiniPure Donkey Anti-**Mouse** IgG	Jackson ImmunoResearch Laboratories, Inc.; dianova GmbH	REF: 715-035-151 LOT: 144092	1:5000 – 1:10000
Peroxidase-conjugated AffiniPure Donkey Anti-**Rabbit** IgG	Jackson ImmunoResearch Laboratories, Inc.	REF: 711-035-152 LOT: 144356	1:5000 – 1:10000
Polyclonal Donkey Anti-**Goat** IgG	Invitrogen	REF: A32849	1:10000

After 3 washing steps with TBS/T, and 2 with TBS, the membrane was incubated for approximately 5 min with ECL substrate (Clarity Western ECL Substrate, Bio-Rad Laboratories, Inc., Hercules, USA). The membrane was put into plastic foil and a picture was taken with the Vilber Fusion FX.

To verify protein loading, a housekeeping protein was used that is uniformly present in the cells allowing confirmation of the loading of similar protein concentrations.

2.2.13 LDH Assay

Cell damage or cytotoxicity can be assessed by the measurement of cell membrane damage. If the cell integrity of a cell is lost, lactate dehydrogenase (LDH) is released into the supernatant, which can be measured and is proportional to cell membrane damage and cell death (PromoKine, 2021).

The PromoKine LDH Cytotoxicity Kit II (PromoCell GmbH, Heidelberg, Germany) was used, and the company's instructions were followed. Different controls were used: first, a background control with media and without cell supernatant; second, a negative control with the supernatant of cells without stimulation; and third, a positive control with the supernatant of cells that were treated with 10 µl Cell Lysis Solution prior to harvesting to measure the maximal possible released LDH.

For the assay, 10 µl of supernatant was pipetted into every well of a 96-well flat-bottom plate (Greiner Bio-One, REF: 655101). The LDH reaction mix was prepared by mixing 2 µl of WST substrate with 100 µl of LDH Assay Buffer per sample and well. 100 µl of LDH reaction mix was added to every well. The plate was incubated for 30 min at 37 °C in the incubator. The optical density was determined using the plate reader and with the wavelength 450 nm, and corrected with the wavelength 650 nm (450 - 650 nm).

To correct the measured optical density measurement for background noise, the media (1. control) was subtracted. To calculate the relative cytotoxicity, the value was divided by the positive control (3. control) and multiplied by 100 to get a proportion in percentage.

2.2.14 PMN Stimulation Experiment

After the PMN number was determined, the concentration was adjusted to 2 x 10^6/ml. To seed the cells, 500 µl of cell suspension in cell culture medium was seeded into each well of a 24-well cell culture treated plate. Each sample was seeded in three or four replicates. For stimulation, 50 µl of CaOx in PBS was added to the cells and equally distributed, resulting in a concentration of 100 µg/ml CaOx. For the control samples, 50 µl of PBS was added. After 5, 10 and 20 h, the experiment was terminated and samples were obtained. For this purpose, the plate was taken from the incubator and directly placed on ice. The supernatant of the culture and most of the cells were carefully rinsed from the plate and transferred to a microcentrifuge tube. 50 µl cell lysis buffer was added to the remaining cells on the plate. The tubes were centrifuged at 600 x g for 10 min and at 4 ° C, and the supernatant was transferred to a new tube. The cell pellet at the bottom of the tube was lysed using the protein lysate from the plates and the biological replicates were combined into one tube. All samples were frozen at -80°C until further use.

In the experiment aiming to investigate the influence of different stimulators on the release of LDH and IL-16, a concentration of 2 x 10^6 cells was again set, and 350 µl of cell suspension were seeded in a 48-well plate. Then, the respective simulators were added, each with an appropriate amount, so that the final concentration was achieved. After 20 h of culture in the incubator, the cells were frozen according to the protocol described above and the supernatant was collected. For each stimulator, biological triplicates were used.

Calcium oxalate hydrate (CaOx)	100 µg/ml	Sigma-Aldrich	REF: 289841-250G
MSU	200 µg/ml	InvivoGen, San Diego, USA	REF: tlrl-msu
CPPD Crystals	200 µg/ml	InvivoGen	REF: tlrl-cppd
Sodium oxalate (NaOx)	100 µg/ml	Sigma-Aldrich	REF: 71800-500G
ATP	5 mM	InvivoGen	REF: tlrl-atp
LPS-EB Ultrapure	1 µg/ml	InvivoGen	REF: tlrl-3pelps
PMA	1 µg/ml	Sigma-Aldrich	REF: P1585

2.2.15 Statistical analysis

Statistical analysis was performed using RStudio and the above-mentioned packages.

Given that this work mainly involves exploratory experiments and is intended for hypothesis generation, the p-value was not always corrected for multiple testing. Generally, a p-value of 0.05 was considered statistically significant. If not otherwise encoded, the p-value has been coded as: * <0.05, ** <0.01 and *** <0.001.

To compare group differences, non-parametric tests, including the Wilcoxon-Mann-Whitney tests, were performed. Correlations were assessed by calculating the Spearman's rank correlation coefficient. The influence of independent variables and their interaction on dependent variables were assessed using two-way ANOVAs, along with the Tukey post-hoc analysis (Tukey's HSD (honestly significant difference) test), to account for multiple comparisons.

3 Results

3.1 Characteristics of healthy controls and dialysis patients

In the following experiments, blood of 8 healthy individuals (control group) and 15 CKD G5D patients (patient group) was used.

Basic characteristics were compared between these two study groups (Table 1). The control group consisted of more women and was remarkably younger than the patient group. To get an impression of the cohort, the two parameters of main interest, namely plasma IL-16 and pOx, were determined using a human DuoSet-IL-16 ELISA and an oxalate oxidase assay. From some of the subjects, IL-16 values (controls: 3, patients: 0) and pOx values (controls: 4, patients: 3) were missing.

The control group showed a mean IL-16 level of 176.4 pg/ml (SD 40) and a pOx level of 4.46 µM (SD 1.2), while the patient group had an IL-16 level of 714.4 pg/ml (SD 179) and a pOx level of 25.2 µM (SD 11.8).

Table 1: Comparison of demographic data and IL-16 and pOx measurements between control group and patient group

Group	Number	Female (n)	Age [years] (SD)	IL-16 [pg/ml] (SD)	pOx [µM] (SD)
Control	8	62.5% (5)	30 (12.6)	176.4 (40)	4.46 (1.2)
Patient	15	20% (3)	69 (12.5)	714.4 (179)	25.2 (11.8)

Figure 10A graphically shows the differences in pOx and IL-16 levels between the control group and patient group. A Wilcoxon-Mann-Whitney test demonstrated a significant difference in pOx level ($p < 0.001$, effect size $r = 0.77$) and IL-16 level ($p < 0.001$, effect size $r = 0.72$).

Complete cases of patients with measurements of IL-16 as well as pOx were present in 12 patients. In these 12 patients, a linear correlation was investigated. The Spearman correlation did not reach significance but showed a trend towards a positive correlation ($\rho = 0.36$, $p = 0.25$) (Figure 10C).

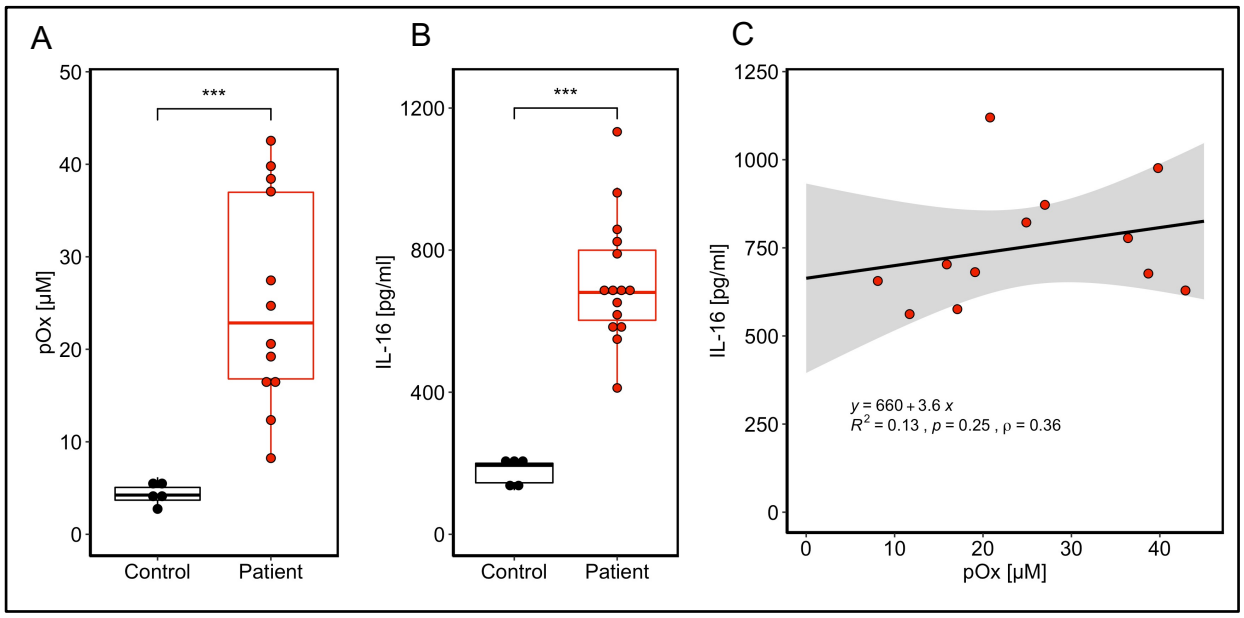

Figure 10: Oxalate and IL-16 concentrations in patients on dialysis and healthy volunteers with normal kidney function

Comparison of pOx (A) and IL-16 (B) levels in the plasma of patients and healthy control subjects. (C) Correlation of pOx and IL-16 in patients, n=12.

3.2 Basal Interleukin-16 secretion of monocyte subsets

For investigation of **hypothesis 1A,** it was necessary to examine whether the monocyte subsets of non-classical and intermediate monocytes secrete more IL-16 basally than classical monocytes. Three experiments were performed, each with one healthy subject.

In the first experiment, classical monocytes (defined as P.I.$^-$, CD3-CD19-CD56-FITC$^-$, HLA-DR-PE$^+$, CD14-VioBlue$^+$ and CD16-APC$^{low/-}$), intermediate monocytes (defined as P.I.$^-$, CD3-CD19-CD56-FITC$^-$, HLA-DR-PE$^+$, CD14-VioBlue$^+$ and CD16-APC$^+$) and non-classical monocytes (defined as P.I.$^-$, CD3-CD19-CD56-FITC$^-$, HLA-DR-PE$^+$, CD14-VioBlue^{low} and CD16-APC$^+$) were collected. In the second experiment, the above-mentioned cell populations were extended by an additional collection of P.I.$^-$, CD3-CD19-CD56-FITC$^-$, HLA-DR-PE$^+$, CD14-VioBlue$^-$ and CD16-APC$^+$ cells, which are suspected to be myeloid dendritic cells in peripheral blood. In the third experiment, the above-mentioned cell populations were extended by an additional collection of cells in the FITC channel (TBNK or dump channel), i.e., the P.I.$^-$, CD3-CD19-CD56-FITC$^+$ cells, to analyze the remaining T cells, B cells, and NK cells for their basal cytokine secretion.

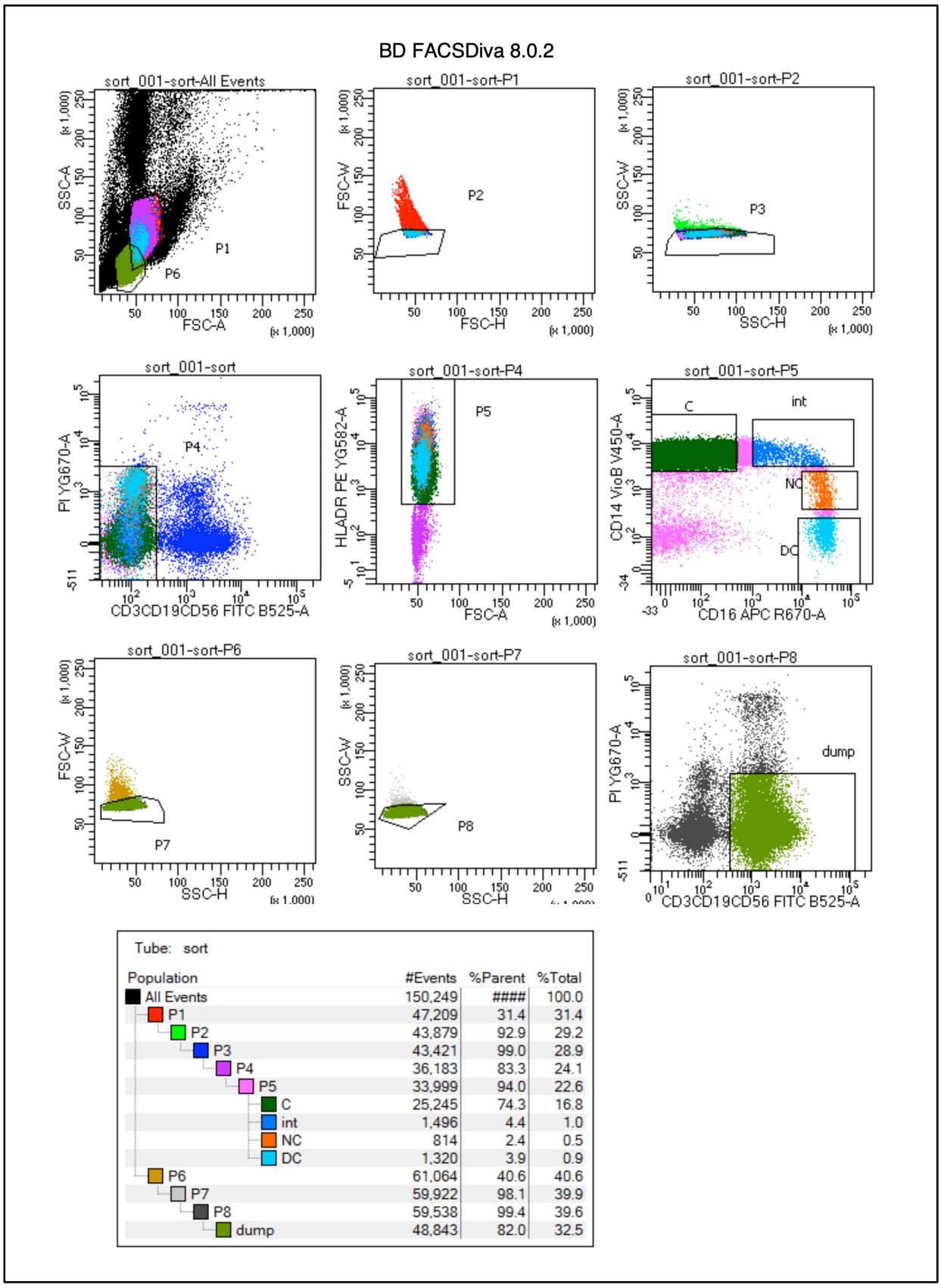

Figure 11: Revised FACS Gating strategy for monocyte subsets

FACS-based isolation of cells at the BCRT. C: Classical monocytes, int: Intermediate monocytes, NC: non-classical monocytes, DC: dendritic cells, dump: dump channel/TBNK.

The cell concentrations were adjusted to be the same for all samples of one experiment. 130,000 or 140,000 cells were cultured without any further added stimulator in 200 µl of monocyte culture medium per well in a 96-well plate.

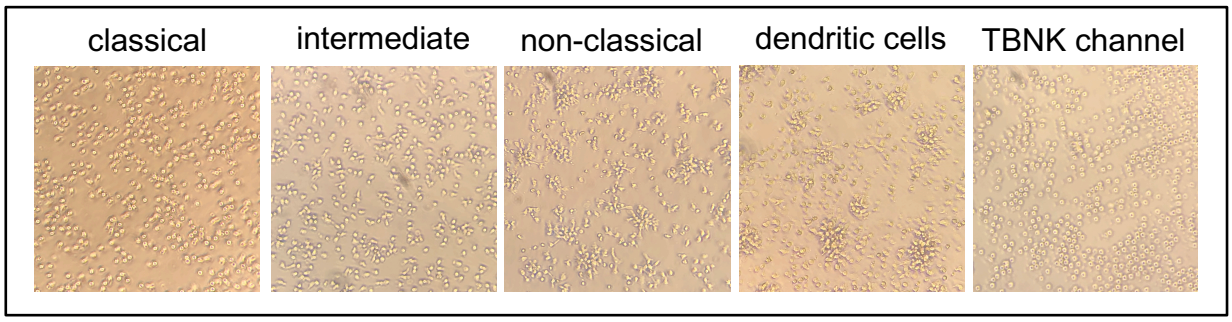

Figure 12: Morphological characteristics of cultured cells under the light microscope

After 16 hours of culture, differences in terms of cell shape as well as congregation of the populations were detected in the light microscope. The non-classical monocytes and the DCs shared some similarities seen through the microscope; these cells gathered closer together and exhibited a more irregular outer shape (Figure 12).

In total, the cell-free supernatants of the following samples were obtained: supernatant of the three monocyte subsets three times, supernatant of DCs twice, and supernatant of the cultured TBNK/dump channel cells once.

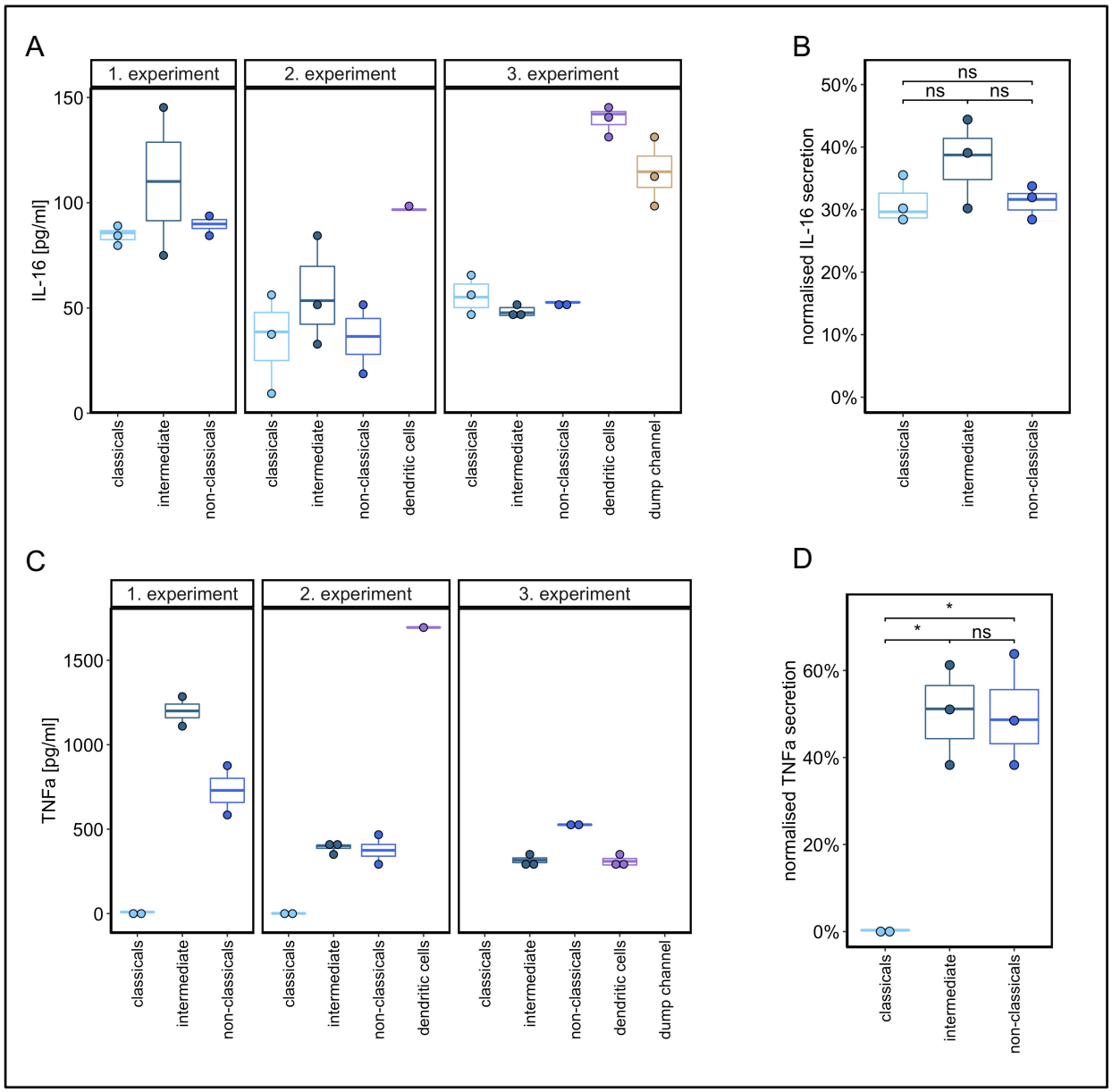

Figure 13: ELISA measurement of IL-16 and TNF-α in the supernatant after culture

IL-16 and TNF-α ELISA measurements in the supernatant after basal culture of sorted cells. Statistical analysis: Wilcoxon-Mann-Whitney test.

Secretion of IL-16 into the supernatant, measured by IL-16-DuoSet-ELISA, was detected in all samples. Figure 13A shows the absolute measured IL-16 concentrations, which ranged from an average of 45 pg/ml to 140 pg/ml. TNF-α secretion, measured by TNF-α-DuoSet-ELISA, was found to be highly variable, ranging from 2 pg/ml to 1700 pg/ml (Figure 13C).

As several confounding factors had to be considered, the absolute measured concentrations could not easily be compared; the cell number of the culture conditions varied between 130,000 and 140,000 cells per 200 µl culture media and inter-plate-differences between the ELISA assays were conceivable. Therefore, the cytokine secretion of the monocytes was normalized by the calculation of the relative secretion of a monocyte subset compared to the secretion of all monocytes combined.

When comparing the relative release of IL-16 between the three monocyte subtypes, the proportion ranged from 31 to 38% (Figure 13B). Thus, each of the three subtypes accounted for approximately one-third of the IL-16 release. Intermediate and non-classical monocytes each contributed to half of the monocyte TNF-α release, while almost no secretion was detected by classical monocytes (Figure 13D).

Furthermore, 13 cytokines were measured in the samples of the second and third experiments with the use of a LEGENDplex assay to obtain a basic impression of the cytokine release of the cell types (Figure 14). To better compare the secretion of the 13 cytokines between the monocyte subsets, the secretion rates were again normalized on the total secretion of monocytes (Figure 15).

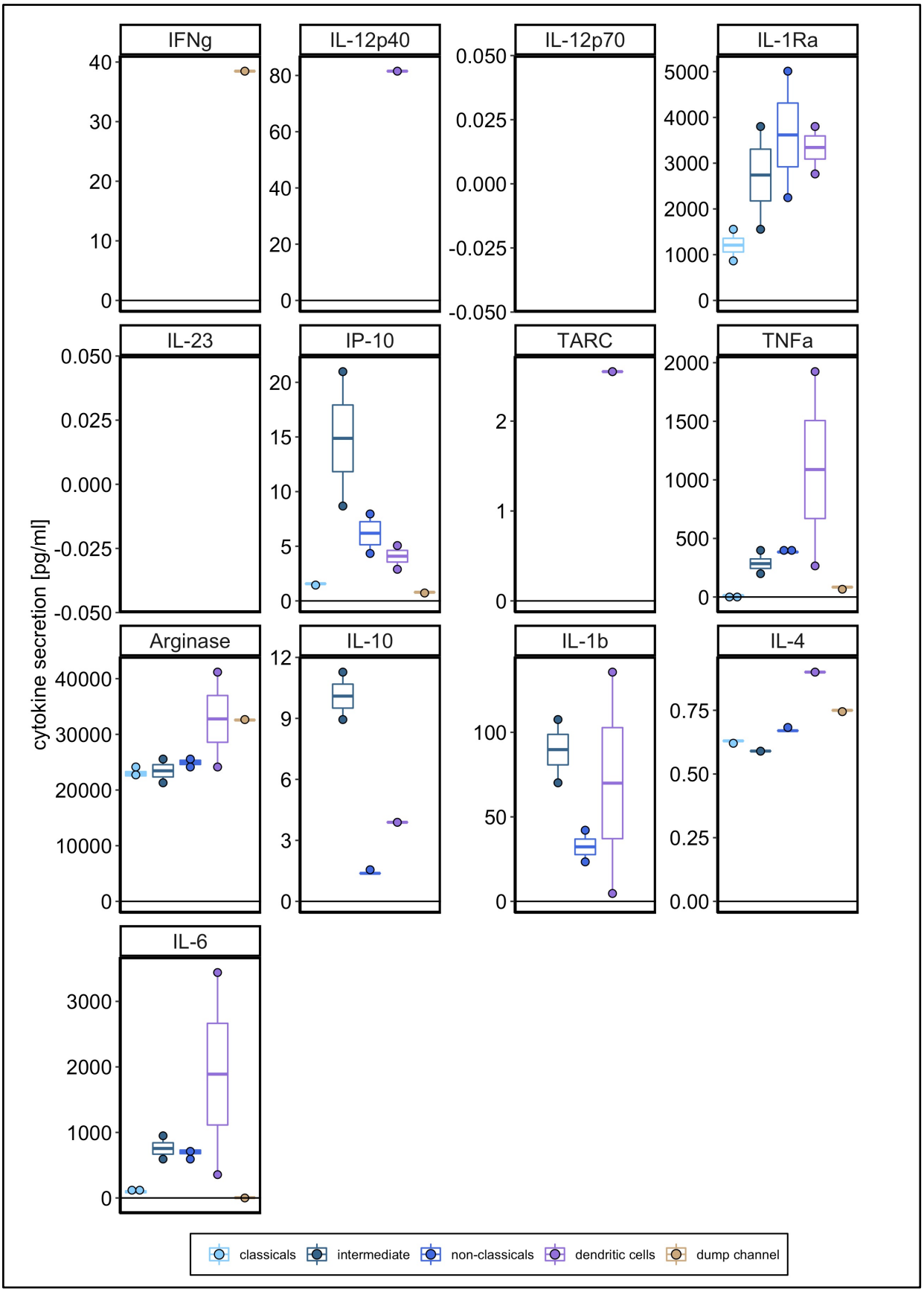

Figure 14: Cytokine secretion into the supernatant after culture, measured by LEGENDplex

LEGENDplex measurement of thirteen cytokines after cultivation. Two experiments were included.

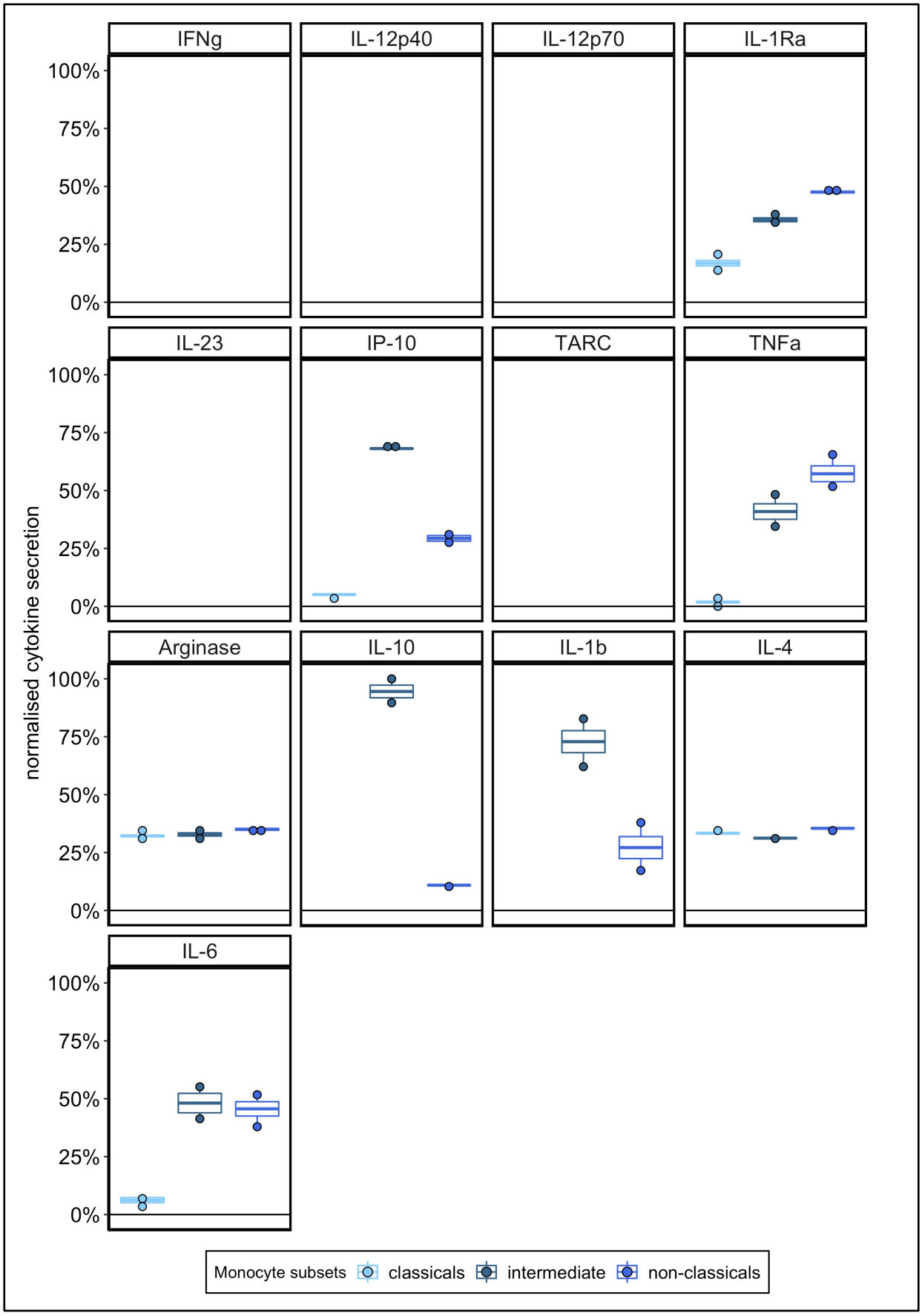

Figure 15: Relative cytokine secretion of every monocyte subset

None of the cell types showed secretion of IL-12p70 and IL-23 (Figure 14).

IL-12p40 secretion could not be detected in the monocyte samples. One DC sample, however, exhibited a secretion of 70 pg/ml (Figure 14).

The TNF-α secretion was again measured by the LEGENDplex assay, and again, a very low TNF-α secretion of the classical monocytes of approximately 12.6 pg/ml was detected. Intermediate and non-classical monocytes showed a similar secretion of 400 pg/ml. The DC samples showed a wide variation in secretion, i.e., between 250 and 1900 pg/ml (Figure 14). Intermediate monocytes were responsible for 41% and nonclassical monocytes for 58% of TNF-α secretion of monocytes, whereas classical monocytes accounted for only 1.8% (Figure 15).

A similar pattern as for TNF-α was also observed for the release of IL-6. While the lowest secretion was detected in the classical monocyte samples, with a mean secretion of 94.8 pg/ml, approximately similar levels of around 700-750 pg/ml were found in the supernatant of intermediate and non-classical monocytes. DCs showed a high variation of secretion, ranging from 340 pg/ml to 3440 pg/ml (Figure 14). With 48% secretion of IL-6 by intermediate and 45% by non-classical monocytes, these cell types secrete a similar relative amount, whereas classical monocytes account for only 6% of the secretion of monocytes (Figure 15).

Regarding the IL-4 concentration in the supernatant, only very low values of between 0.59 and 0.9 pg/ml, close to the limit of detection, were measured (Figure 14). Similarly, Arginase secretion was found in all cells, with no clear difference between cell types.

IL-10 secretion of classical monocytes could not be detected. The non-classical monocyte samples showed a secretion of 1.4 pg/ml, while the intermediate subset of monocytes exhibited a higher level of secretion of around 10 pg/ml (Figure 14), which accounted for 95% of the IL-10 secretion by monocytes (Figure 15).

Classical monocytes did not show any release of IL-1β. The intermediate monocytes, meanwhile, showed the highest release - around 90 pg/ml basally. Non-classical monocytes secreted around 40 pg/ml. A high variation of secretion was detected in the DCs, with a mean secretion of 70 pg/ml (Figure 14). Comparing the relative secretion of IL-1β of monocyte subsets, the majority, at approximately 73%, is secreted by intermediate monocytes (Figure 15).

TARC secretion could not be detected in the monocyte samples. Only one DC sample showed a positive signal of 2 pg/ml (Figure 14).

IL-1RA was found to be secreted by all cells, but not by TBNK cells. The secretion of the monocyte subsets seems to vary, with the lowest secretion of IL-1RA being by the classical monocyte subset, at around 1200 pg/ml, and the highest secretion by the non-classical monocyte subset, at around 3600 pg/ml. The DCs showed a secretion of 3300 pg/ml (Figure 14). Classical monocytes accounted for 17% of total monocyte IL-1RA secretion, intermediate monocytes for 36%, and nonclassical monocytes for 47% (Figure 15).

IFN-γ secretion was not detected in the monocyte subsets and dendritic cells. The TBNK cells, however, showed a secretion of around 40 pg/ml (Figure 14).

IP-10 release differed between the monocyte subtypes. Non-classical monocytes showed a secretion of 1.6 pg/ml, while intermediate monocytes secreted 14.9 pg/ml and non-classical monocytes 6.2 pg/ml (Figure 14). The majority of IP-10 from monocytes was secreted by intermediate monocytes, i.e., 68% (Figure 15).

3.3 Basal Interleukin-16 secretion of PBMCs of healthy control subjects and CKD G5D patients

Addressing **hypothesis 1B** and investigating the difference in IL-16 secretion of PBMCs both between cell types and between patients and controls, 40 mL of human blood was collected from healthy control subjects and CKD-G5D patients was collected. In total, the experiment was repeated three times, each time with cells from a healthy control and a patient. In total six probands were included in the analysis.

The PBMCs were sorted at the BCRT, and four cell populations were collected, namely T cells (P.I.$^-$, CD3-FITC$^+$), B cells (P.I.$^-$, CD3-FITC$^-$, CD56-BV510$^-$, CD19-APCVio770$^+$), NK cells (P.I.$^-$, CD3-FITC$^-$, CD19-APCVio770$^-$, CD56-BV510$^+$), and monocytes (P.I.$^-$, CD3-FITC$^-$, CD56-BV510$^-$, CD19-APCVio770$^-$, CD14-VioBlue$^+$, HLA-DR-PE$^+$). For the additional differentiation of the cells in size and granularity, different side scatter (SSC-A) and forward scatter (FSC-A) gates were used for defining lymphocytes and myeloid cells (Figure 16).

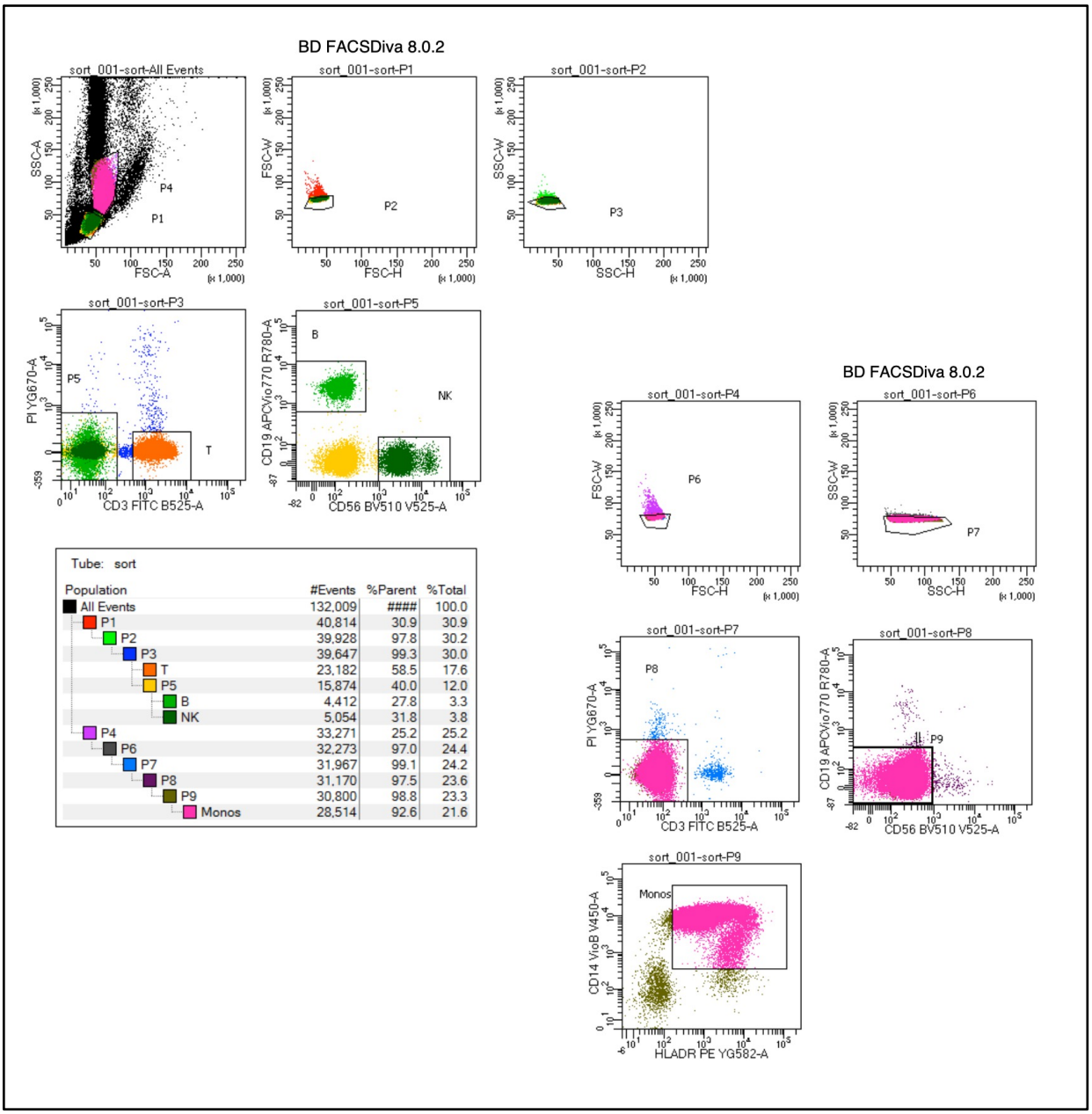

Figure 16: Gating strategy for FACS-based isolation of PBMCs

Representative example of the FACS gating strategy used to isolate T cells (T), B cells (B), NK cells (NK) and monocytes (Monos) of a healthy control subject.

The cell concentrations were adjusted to be equal in all samples. In the first experiment, a cell count of 130,000 cells per 200 µl culture medium was used for all approaches. Therefore, the cell concentration was 0.65 x 10^6 cells/ml. In the second and third experiment, for all samples 200,000 cells per 200 µl culture medium were added for all samples, i.e., a concentration of 1 x 10^6 cells/ml was achieved.

After 16 h of culture without additional stimulator, differences in cell shape were seen under the light microscope (Figure 17). Thereby, in particular, NK cells showed an irregular outer cell shape. The cell-free supernatants were frozen till further use.

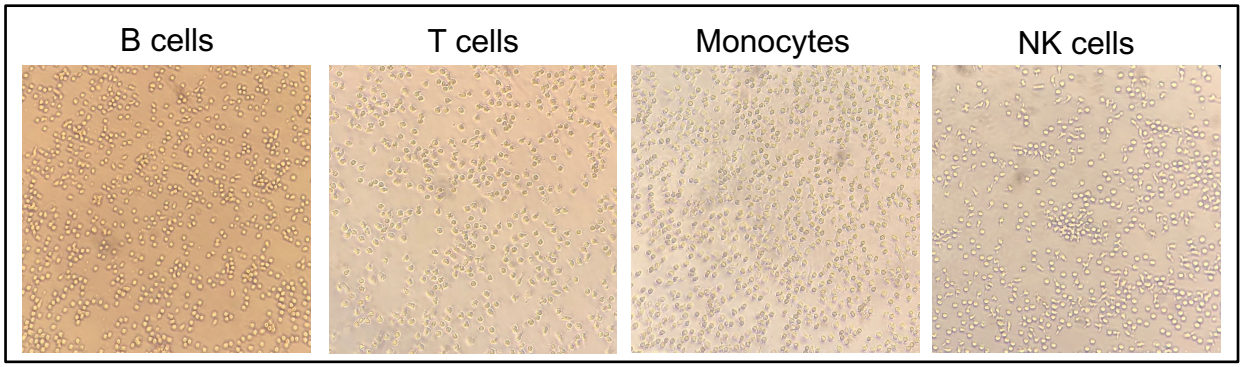

Figure 17: Morphological differences of PBMCs after 16 h culture

Assessment of morphological appearance of sorted and cultured PBMCs by light microscope.

In the IL-16 ELISA subsequently performed on the three patients and three healthy control subjects, IL-16 was found in the supernatant of all four cell types as well as in both the healthy control subjects and the CKD-G5D patients (Figure 18).

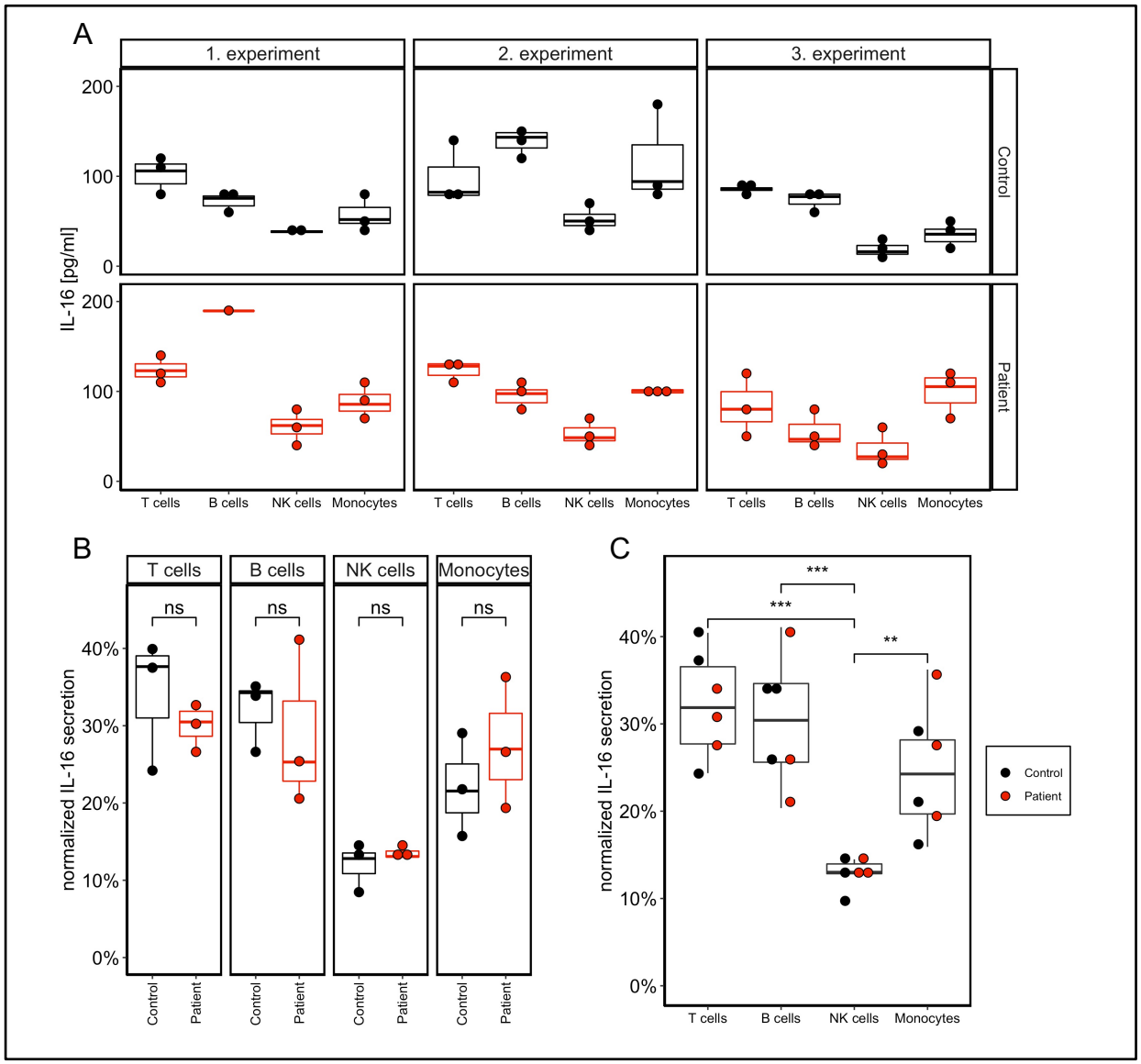

Figure 18: IL-16 secretion of PBMCs

IL-16 secretion of T cells, B cells, NK cells and monocytes after 16 hours of culture. (A) Absolute secretion of cells in three experiments, each with a healthy control subject and a CKD G5D patient. (B + C) Normalized IL-16 secretion, statistical analysis: two-way ANOVA and Tukey's HSD test.

When comparing the IL-16 secretion of PBMCs between healthy control subjects and patients, the absolute concentration ranges between 20 pg/ml and 190 pg/ml (Figure 18A). The absolute concentrations of the different cell types were compared between controls and patients, and no difference between the cell types was identified.

Although IL-16 secretion appears to be in a similar range in the three experiments, comparisons of absolute values of IL-16 concentration between experiments and assays may be problematic due to several reasons. First, the cultured cell concentration in the

first experiment was lower in all samples than in the second and third experiments. And second, as the samples were measured on different plates, there may be inter-plate differences in the IL-16-ELISA performed. Therefore, for each subject, the normalized concentration of IL-16 in the supernatant for one cell type was calculated relative to the total secretion of all PBMCs combined.

A two-way ANOVA was used to test the influence of two independent variables, namely cell type (T cells, B cells, NK cells, monocytes) and study group (control and patient group) as well as their interaction, on the dependent variable normalized IL-16 secretion.

While no significant role was found for the study group ($p = 1.0$), a significant difference was identified for the cell type ($p < 0.001$). The interaction of these two variables had no significant effect on the normalized IL-16 secretion ($p = 0.594$).

Figure 18B shows the normalized release of IL-16 divided by cell types as well as by patients and control subjects. The Tukey post-hoc analysis revealed no significant difference between cell types when the study groups were considered.

Additionally, the general secretion between the different cell types was compared (Figure 18C). The average IL-16 secretion of a cell type was determined independently of the study group of patients and controls. The relative secretion was found to differ between cell types, with T cells accounting for 32.2% (SD 6.2), B cells for 30.4% (SD 7.6), NK cells for 12.7% (SD 2.0) and monocytes for 24.71% (SD 7.4) of the total IL-16 secretion of PBMCs. Subsequently, a Tukey post-hoc analysis test was performed for multiple comparisons, showing significant differences between T cells and NK cells ($p = 0.0002$), B cells and NK cells ($p = 0.0007$), and monocytes and NK cells ($p = 0.02$). For a pictorial representation of the results in Figure 18C, the data points were color-coded according to the study group (control black, patient red).

3.4 Intracellular level of IL-16 and caspase-3 activity in patients and healthy control subjects

Subsequently, the question of differences in the basal intracellular concentration of IL-16 and basal activity of caspase-3 in PBMCs between healthy control subjects and patients was to be investigated (**hypothesis 1C**). In addition, general differences in intracellular

IL-16 levels without considering the study group were searched for between the four cell types.

In total, blood was drawn from four healthy control subjects and six CKD G5D patients (first experiment: only one healthy control subject, second to fourth experiments: one healthy control subject and two patients). The isolated and stained PBMCs were immediately run on the MACSQuant Analyzer 10 flow cytometer and analyzed in one batch using FCS Express 6.

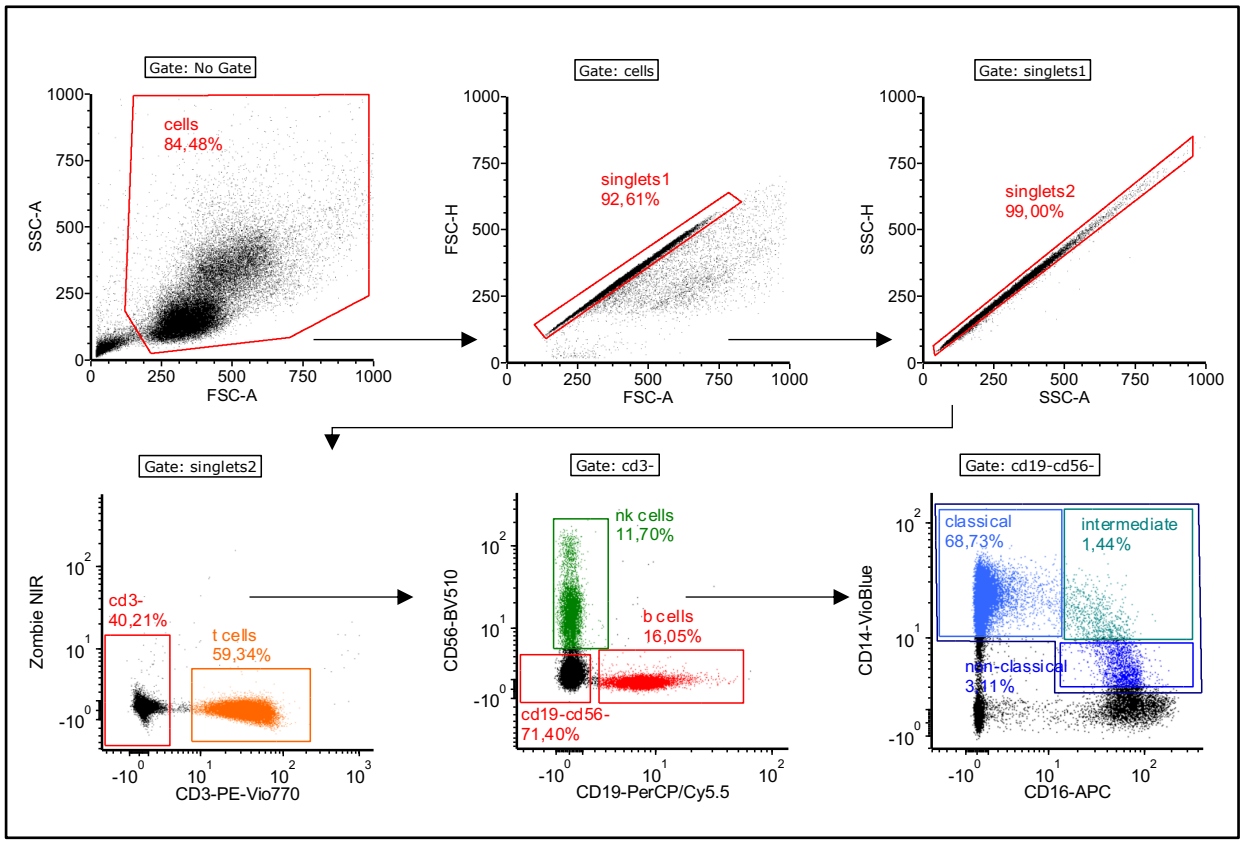

Figure 19: Gating strategy of PBMCs for intracellular IL-16 and caspase-3 panel

Flow cytometric gating strategy to define cell types of PBMCs in the intracellular IL-16 and capsase-3 panel. One representative example shown.

After defining cells by size and granularity as well as exclusion of cell doublets, four cell populations were gated on: T cells (Zombie NIR$^-$, CD3-PE-Vio770$^+$), B cells (Zombie NIR$^-$, CD3-PE-Vio770$^-$, CD19-PerCP/Cy5.5$^+$), NK cells (Zombie NIR$^-$, CD3-PE-Vio770$^-$, CD56-BV510$^+$) and monocytes (Zombie NIR$^-$, CD3-PE-Vio770$^-$, CD19-PerCP/Cy5.5$^-$, CD56-BV510$^-$, CD14-VioBlue$^{+/low}$, CD16-APC$^{-/+}$, Figure 19).

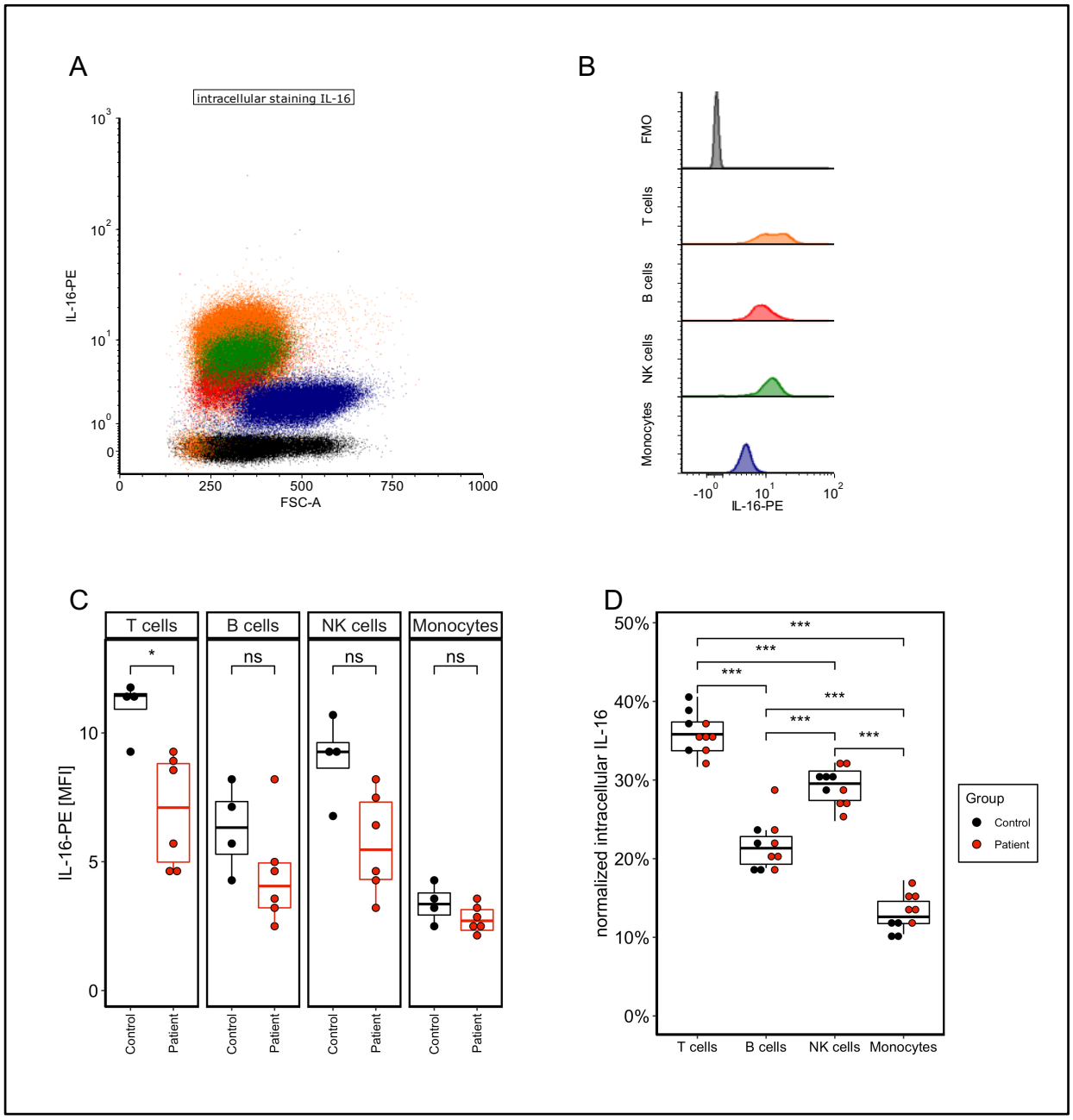

Figure 20: Intracellular level of IL-16 in PBMCs

Analysis of the intracellular IL-16 level in PBMCs. (A) Color Dot Plot of IL-16-PE on the y-axis with color-coded predefined cell types (orange = T cells, red = B cells, green = NK cells, blue = monocytes). (B) Histogram of IL-16-PE for different cell types. (C) Comparison of IL-16-PE MFI of four healthy control subjects and six patients. (D) Normalized intracellular IL-16 level compared between cell types, color-coded study group, statistical analysis: two-way ANOVA and Tukey's HSD test.

All cell populations, namely T cells, B cells, NK cells, and monocytes, showed a positive signal for IL-16-PE, indicating intracellular levels of IL-16 (Figure 20A). Differences in fluorescence signal were seen between the different cells (Figure 20B) and subsequently

quantified using the Geometric Mean (GM) of IL-16-PE as a measurement of MFI (Figure 20C).

Using a two-way ANOVA, the influence of two independent variables, namely cell type (T cells, B cells, NK cells, monocytes) and study group (control and patient group) as well as their interaction, on the dependent variable IL-16-MFI was tested.

This showed that both the study group ($p < 0.001$) and the cell type ($p < 0.001$), but not the interaction of those two variables ($p = 0.109$), however, had a significant effect on the MFI of IL-16.

In a multiple comparison of the IL-16-MFI mean of cell types between controls and patients using a Tukey's HSD test, only the T cells showed a significant difference ($p = 0.011$), with a lower level of IL-16-MFI in patients compared to controls. Although they did not reaching significance, the other cell types also showed a trend toward lower IL-16 MFI in patients compared with healthy controls.

In a further attempt to learn about PBMC biology regarding IL-16, an additional analysis was performed, and the intracellular IL-16 level of the four cell types was compared without taking the study population into account. As the IL-16-MFI was remarkably lower in the patient's group, the intracellular IL-16 content of one cell type was again normalized on the total level of intracellular IL-16 of PBMCs for each subject. This corrected the general trend towards lower IL-16 levels in patients and allowed all subjects to be compared.

T cells showed the highest normalized intracellular IL-16 level of 35.9% (SD 2.8), followed by NK cells with 29.2% (SD 2.5), B cells with 21.7% (SD 3.0) and monocytes with 13.2% (SD 2.3). Using one-way ANOVA, the mean normalized intracellular IL-16 levels were compared and a significant difference in the cell types found ($p < 2e-16$). A post-hoc Tukey's HSD test was performed to compare the cell types and all comparisons expressed a significant difference: B cells and T cells ($p < 0.001$), NK cells and T cells ($p < 0.001$), monocytes and T cells ($p < 0.001$), NK cells and B cells ($p < 0.001$), monocytes and B cells ($p < 0.001$), as well as monocytes and NK cells ($p < 0.001$). This finding is also visible in Figure 20D with the control group color-coded in black and the patient group coded in red.

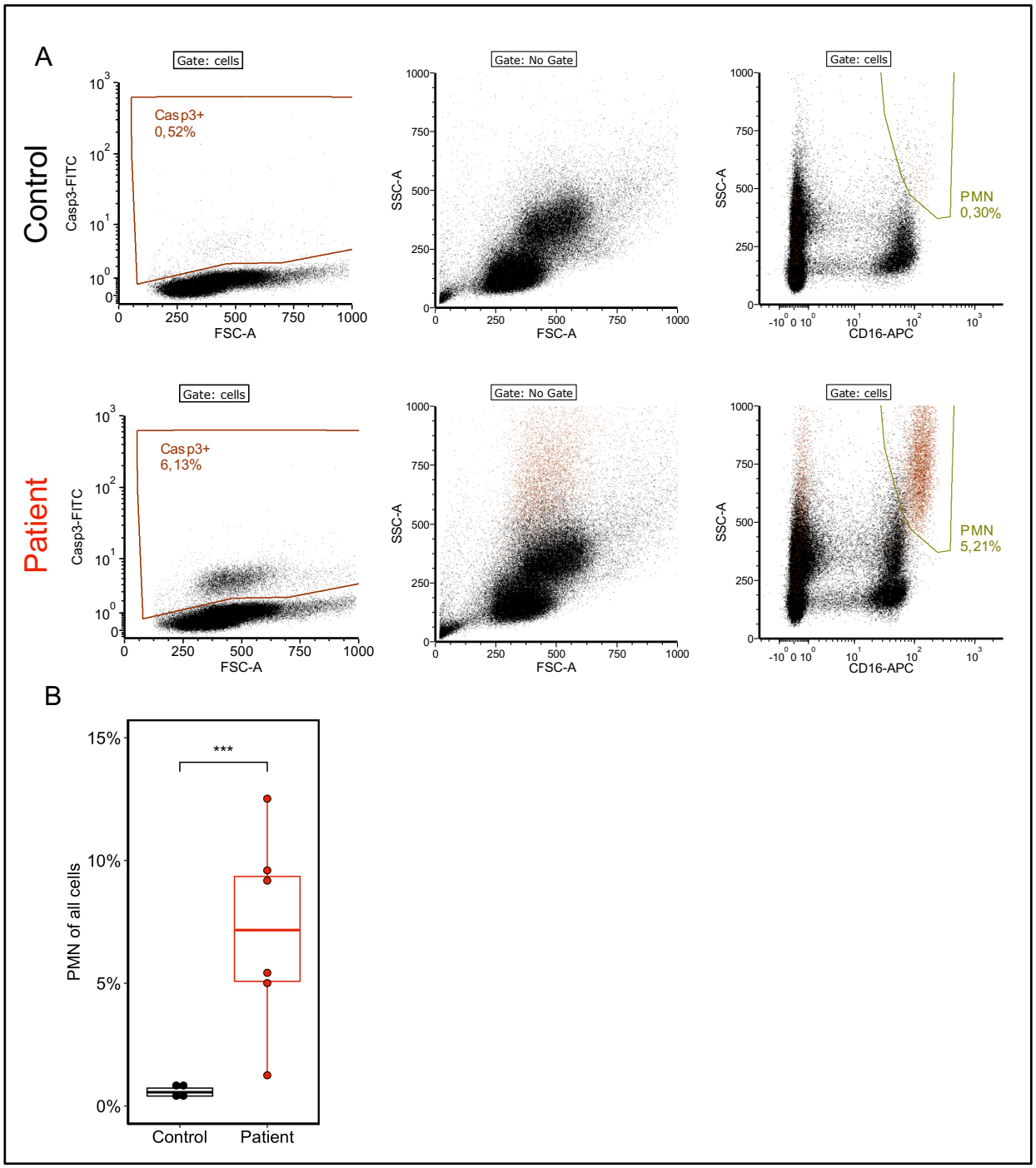

Figure 21: Caspase-3 positive cells

Analysis of caspase-3 positivity of all cells. (A) One representative example of the control and patient group. Backgating and identification of caspase-3 positive cell type. (B) Comparison of PMN proportion of all cells, statistical analysis: Wilcoxon-Mann-Whitney test.

Additionally, the percentage of cells with basal caspase-3 activity (Casp3+), meaning positive for Casp3-FITC in the flow cytometry experiment, was compared between patients and control subjects. Differences were found and a significantly higher

percentage of Casp3 positive cells was observed in patients. To examine the cell type positive for caspase-3, the Casp3+ gate was color-coded (brown color) and backgated (Figure 21A). The caspase-3-positive cells were found to be a population of PMNs (SSC^{high} $CD16^{+}$).

Since the peripheral blood leukocytes in this experiment were isolated on PBMCs, no PMNs were expected to be found in the analysis. Therefore, this chance observation was further analyzed and the proportion of PMNs compared between patients and control subjects. This showed that in the control group, 0.6% (SD 0.3) of all cells were PMNs, while in the patient group, 7.1% (SD 4.0) were PMNs (Figure 21B). A Wilcoxon-Mann-Whitney test showed a significant difference between the two study groups in the proportion of PMNs ($p = 0.001$).

3.5 Monocyte shift in CKD G5D patients

For the assessment of the monocyte shift, meaning a change in the composition of monocyte subtypes in CKD G5D patients towards more non-classical monocytes, a further analysis of the flow cytometric experiment with the human IL-16-Casp3-intracellular panel (see Methods section) was performed (**hypothesis 1B**). Again, four healthy controls and six patients were included in the analysis.

After defining cells in the forward and sideward scatter, the doublets were excluded and the monocytes generally defined as Zombie NIR^{-}, CD3-PE-$Vio770^{-}$, CD19-PerCP/$Cy5.5^{-}$, and CD56-$BV510^{-}$. For further differentiation into the different monocyte subtypes, CD14-VioBlue and CD16-APC were used, and the classical monocytes were defined as $CD14^{+}$ $CD16^{-}$, the intermediate monocytes as $CD14^{+}$ $CD16^{+}$, and the non-classical monocytes as $CD14^{low}$ $CD16^{+}$ (Figure 19). The relative amount of each monocyte subtype was calculated.

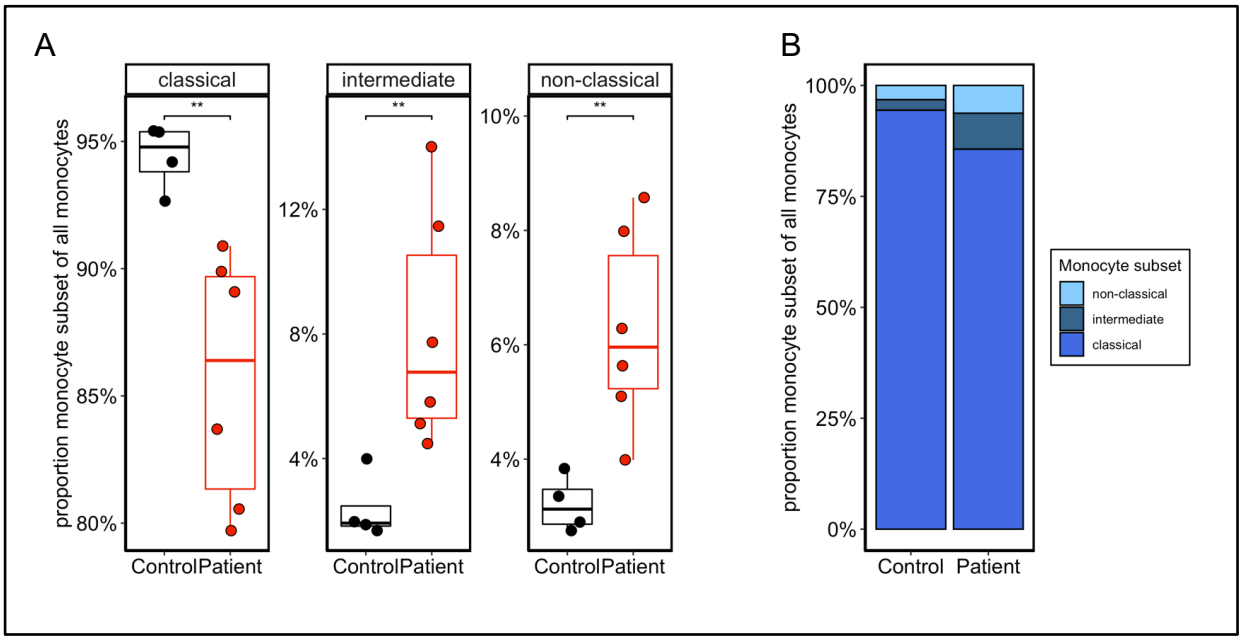

Figure 22: Monocyte subtype composition in patients and healthy control subjects

(A) Comparison of relative proportion of monocyte subsets of all monocytes between patients and control subjects, statistical analysis: Wilcoxon-Mann-Whitney test.

Figure 22 A displays boxplots for comparing the proportion of classical, intermediate, and non-classical monocytes between the control group and patients. Of all monocytes, classical monocytes accounted for 94.4% (SD 1.3%) in control subjects and 85.6% (SD 4.9%) in patients, intermediate monocytes for 2.4% (SD 1.1%) in control subjects and 8.1% (SD 3.8%) in patients, and non-classical monocytes for 3.2% (SD 0.5%) in control subjects and 6.2% (SD 1.7%) in patients.

The monocyte composition was analyzed with Wilcoxon-Mann-Whitney tests. For this purpose, the respective relative proportion of each monocyte subset was compared between patient and control groups. In patients, a significantly lower proportion of classical monocytes ($p < 0.01$) and a statistically significant higher proportion of intermediate ($p < 0.01$) and non-classical ($p < 0.01$) monocytes were found.

As an additional graphical representation of the monocyte subtype composition, the average proportion of the three different subsets of monocytes are colored in different shades of blue (Figure 22B).

3.6 Proportion of Tregs in healthy controls and patients

An additional panel was added to the previously described experiment to investigate **hypothesis 3A**, namely the possible importance of IL-16 in CKD through an induction of Tregs, resulting in higher level of Tregs in patients.

The obtained PBMCs of four control subjects and six CKD G5D patients were stained with surface and intracellular antibodies of the human Treg panel and directly run on the flow cytometer. Based on the panel, the regulatory T cells could be defined in two ways. Aiming to define Tregs as robustly as possible, both definitions were pursued and are presented separately here.

For gating, cells were first defined in the forward and sidewards scatter, and singlets were removed. Tregs were then defined as CD45-VioGreen^{+}, Zombie NIR^{-}, CD8-APC^{-}, and CD4-VioBlue^{+}. Subsequently, cells were either defined as CD25-PE^{+}, CD127- PE-Cy7^{-} (CD127-Tregs), or FoxP3-AF488 was used as an intracellular marker and cells were defined as FoxP3-AF488^{+}, CD25-PE^{+} (FoxP3+Tregs).

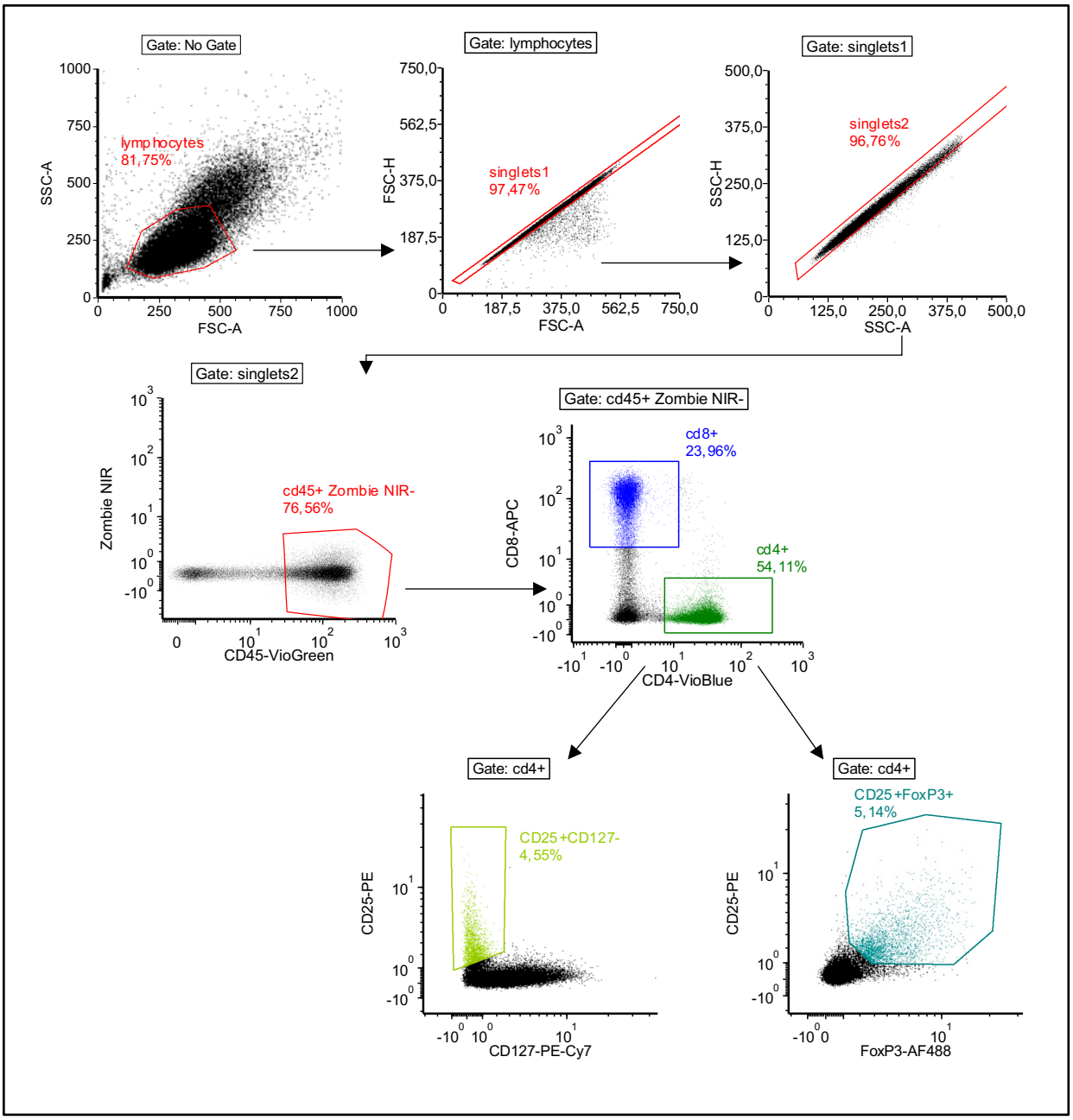

Figure 23: Gating strategy of regulatory T cells

Representative example of the gating strategy of a healthy control subject. After defining viable single cells that are $CD4^+$ $CD8^-$, Tregs were either defined as $CD127^-$ $CD25^+$ (CD127-Tregs) or as $FoxP3^+$ $CD25^-$ (FoxP3+Tregs).

The percentage of FoxP3+Tregs of CD4+ cells was 5.3% (SD 0.3%) in healthy controls and 8.9% (SD 3.1%) in patients. The proportion of CD127-Tregs of CD4+ cells was 4.7% (SD 0.4%) in healthy controls and 8.9% (SD 2.8%) in patients.

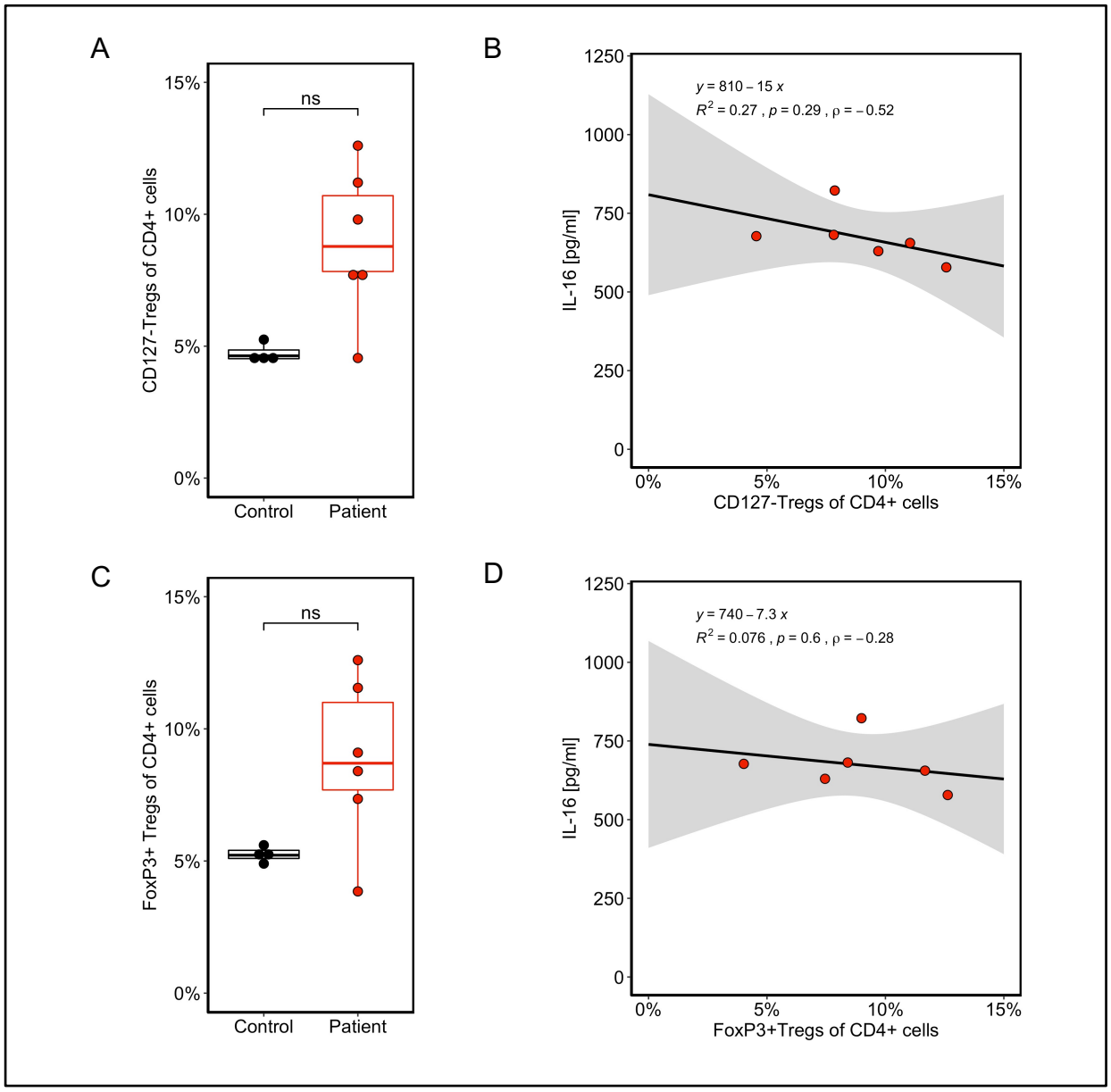

Figure 24: Comparison of Tregs between patients and control subjects and correlation with IL-16

(A+C) Comparison of the relative proportion of Tregs (CD127-Tregs or FoxP3-Tregs) between patients and control subjects, statistical analysis: Wilcoxon-Mann-Whitney test. (B+D) Correlation of Tregs and IL-16 in patients, statistical analysis: Spearman's rank correlation.

When comparing the proportion of CD127-Tregs and FoxP3+Tregs of CD4+ cells between healthy control subjects and patients, no significant difference was found (Wilcoxon-Mann-Whitney test, CD127-Tregs: p= 0.11, FoxP3+Tregs: p= 0.06, Figure 24 A and C).

A possible correlation between the percentage of Tregs in the peripheral blood of patients and their IL-16 plasma concentration was further investigated. A significant correlation was not identified for CD127-Tregs ($\rho = -0.52$, $p = 0.29$) or for FoxP3+Tregs ($\rho = -0.28$, $p = 0.6$) (Figure 24 B and D). The observed negative trend did not correspond to the expectation of a positive correlation.

In order to compare the two methods used to define Tregs (CD127-Tregs and FoxP3+Tregs), a correlation was performed of the two relative Treg proportions of CD4+ cells. A strong positive correlation was observed ($\rho = 0.92$, $p < 0.001$).

To investigate previously described pathological features of CKD patients, the CD4 to CD8 ratio was compared between the two study groups. The control group showed a CD4 to CD8 ratio of 1.87 (SD 0.6), while the patient group showed a CD4 to CD8 ratio of 1.62 (SD 0.6). The Wilcoxon-Mann-Whitney test revealed no significant difference between the two groups ($p=0.76$).

3.7 GSDMD-wt and -ko BMDM

Hypothesis 2A addresses the secretion mechanism of IL-16 and the importance of caspase-3 activation on the release of IL-16. Using a model based on murine BMDM with or without knockout of GSDMD, the secretion of IL-16 and the involvement of caspase-3 was sought to be investigated in murine macrophages.

For this purpose, bone marrow cells were obtained from the femur and tibia of GSDMD wild-type (wt) and knockout (ko) mice, and differentiated into macrophages using differentiation media and growth factors. Differences of the BMDM before, during and after the culture were determined by light microscope and by flow cytometry.

Pictures taken through the lenses of a light microscope on the day of seeding (day 0) and each time before the differentiation medium was changed (day 3 and day 5), as well as at the end of differentiation (day 7), showed a morphological change from relatively small round cells on day 0 to polymorphic cells with pseudopodia on day 7 (Figure 25).

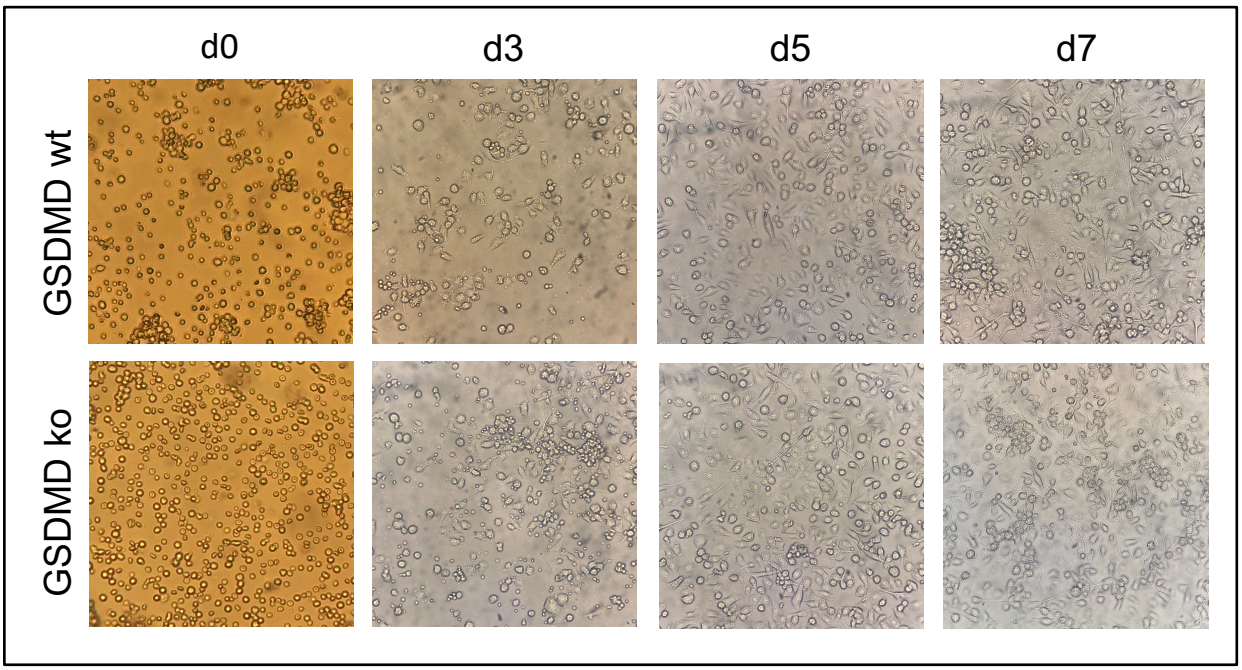

Figure 25: Morphological characteristics of BMDM over the culture period

Morphological difference in the course of differentiation over time (day (d) 0, d3, d5, d7). GSDMD-wt (wild-type) and -ko (knockout).

Additionally, the differentiation into BMDM was also monitored using flow cytometry. For this purpose, cells were stained with the Murine GSDMD panel (see Methods section) before seeding on day 0 and at the end of differentiation on day 7.

After gating on single cells, BMDM were defined as CD45-PE/Cy7^{+}, Zombie NIR^{-}, CD11b-BV421^{+}, and F4/80-PE^{+}. An increase of BMDM from day 0 to day 7 (Figure 26 d0, d7) became visible. At time 0, based on the definition described, 1.16% of wt- and 1.92% of ko-GSDMD bone marrow cells were positive for the markers defining macrophages. At day 7, after culture using differentiation media, 98.11% of wt- and 97.88% of ko-GSDMD BMDM cells were positive for macrophage markers. An increase in the size and granularity of cells in the forward and side scatter, as well as increased expression of CD45, was also found.

Based on the results in light microscopy, as well as flow cytometry, the differentiation of the bone marrow cells into macrophages can be considered successful and the cells to be BMDM.

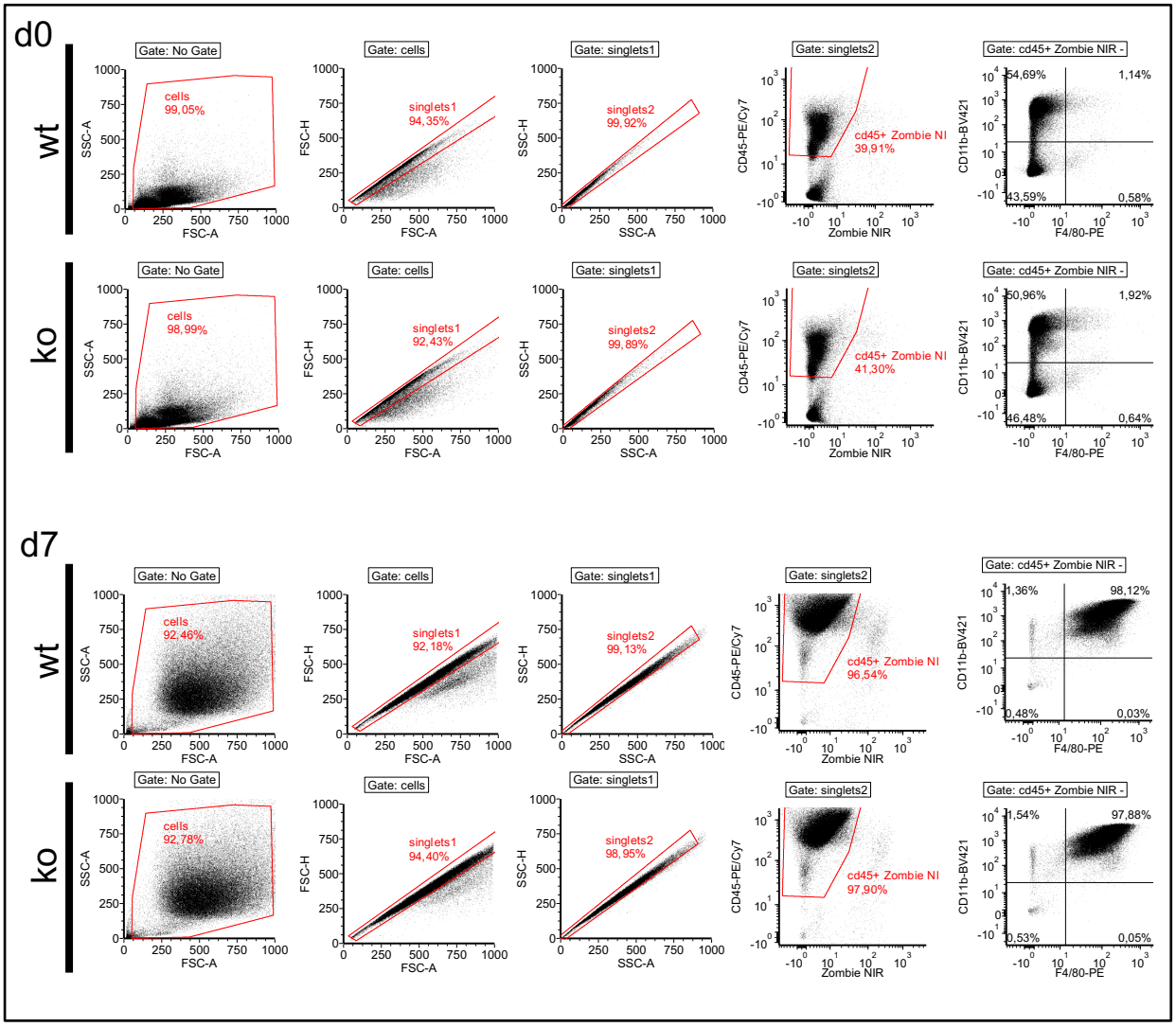

Figure 26: Flow cytometry characterization of BMDM at day 0 and day 7

Analysis of BMDM with macrophage marker on day 0 (d0) and day 7 (d7). ko: GSDMD-knockout, wt: GSMDM-wild-type.

For the actual experiment, cells seeded the previous day were pre-stimulated with or without LPS for 3 hours and then cultured with CaOx, ATP or without simulator. After a total of 9 hours of culture, the supernatant was obtained and the cells were lysed (Figure 27A).

For measuring the loss of cell integrity, which is the case in pyroptotic cell death, and which is expected to happen in the GSDMD-wt BMDM, LDH was determined in the supernatant.

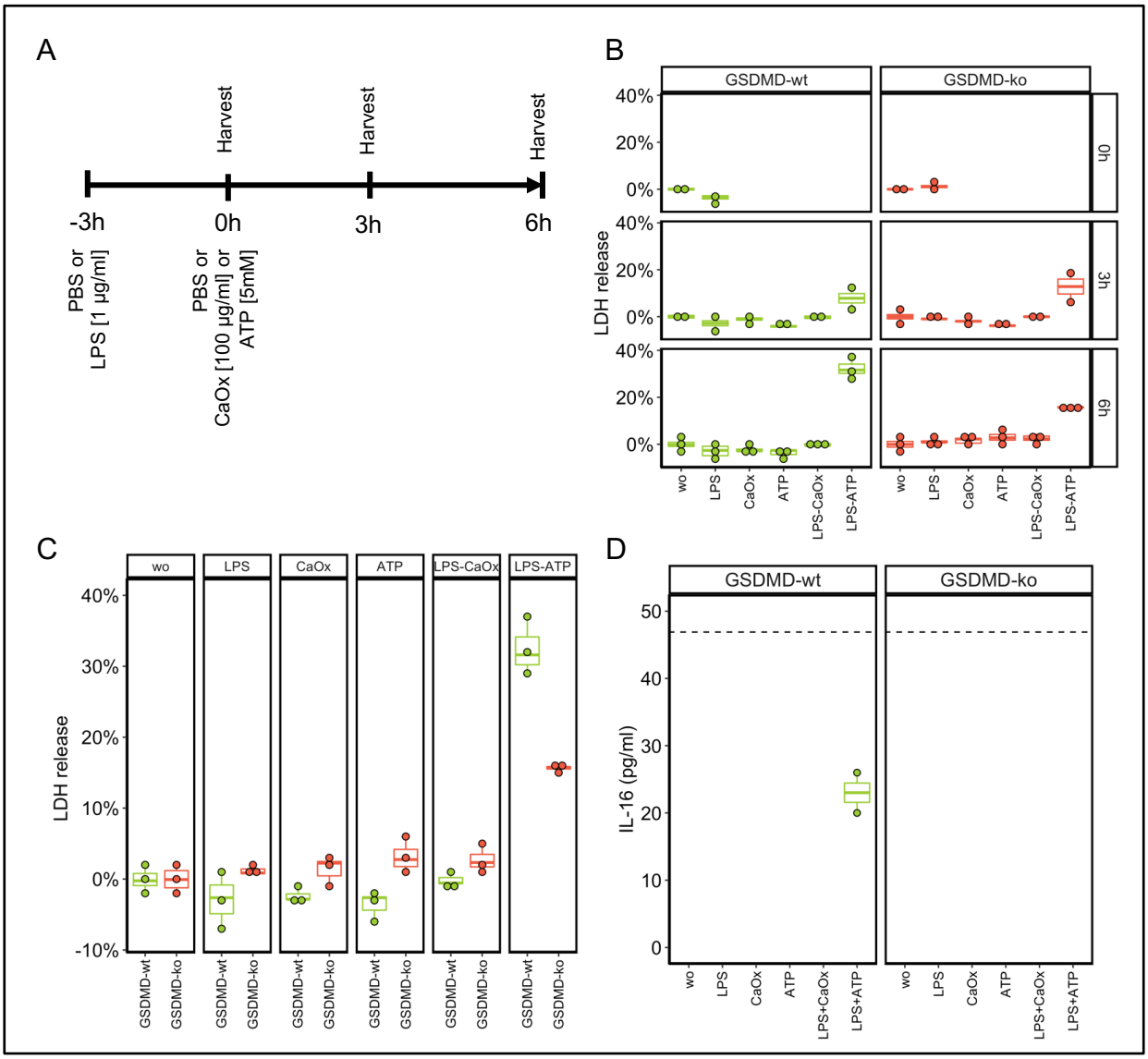

Figure 27: LDH release and IL-16 secretion of GSDMD-wt and -ko BMDM stimulated with LPS, CaOx and ATP

(A) Experimental design for BMDM stimulation. (B) Relative lactate dehydrogenase (LDH) release over time, compared between GSDMD-wt (wild-type) and -ko (knockout). (C) Relative LDH release after 6 hours, statistical analysis two-way ANOVA and Tukey's HSD test. (D) IL-16 measurement in the supernatant at time point 6 h (after 9 hours culture in total), dotted line: limit of detection.

The relative amount of LDH in the supernatant was compared between GSDMD-wt and -ko over the time course, namely 0 h, 3 h, and 6 h (Figure 27B). The time points refer to the time of addition of CaOx, ATP and PBS (wo), respectively. Most of the LDH measurements varied at around 0%. A clear positive LDH signal became apparent particulary in the LPS-ATP sample after 6 h of culture, or 9 h of culture in total.

Therefore, for better graphical representation, only the values at time point 6 h are presented in Figure 27C and compared between GSDMD-wt and GSDMD-ko.

Notably, there was a marked difference in LDH secretion upon stimulation with LPS+ATP between GSDMDM-wt and -ko BMDM. The GSDMDM-wt BMDM had a substantially greater secretion compared with the GSDMDM-ko BMDM (Figure 27C).

From the final samples, after 6 h of stimulation with the secondary stimulator, a murine DuoSet-IL-16 ELISA was performed. Since low concentrations were expected, the supernatant was not diluted. Nevertheless, only in the GSDMD-wt sample with LPS-CaOx stimulation was IL-16 detected. The measured 23 pg/ml (SD 4.1) was still below the detection limit of the ELISA (limit of detection: 46.9 pg/ml). In the other samples, no IL-16 could be measured.

In addition, a Western blot was prepared from the cell lysates and tested for IL-16, caspase-3, and IL-1β using primary and secondary antibodies (Figure 28).

The IL-16 bands on the Western blot did not differ between the GSDMDM-wt and GSDMD-ko. Several bands were visible, which made the clear assignment of the IL-16 band difficult.

Caspase-3 showed a regular band at 35 kDa, which is presumably the uncleaved caspase-3. In GSMDM-ko, this band was found to be weaker. In addition, a second band became visible at 15 kDa, which can be considered the active, cleaved form of caspase-3. The β-Tubulin second antibody confirmed equal protein loading.

Regarding IL-1β, a band of approximately 35 kDa size became visible in all samples with LPS stimulation, and in addition, a band at approximately 17 kDa was detected in GSDMDM-ko cell lysate after LPS+ATP stimulation, which again can be considered to be the cleaved intracellular IL-1b. β-Tubulin again confirmed uniform protein loading.

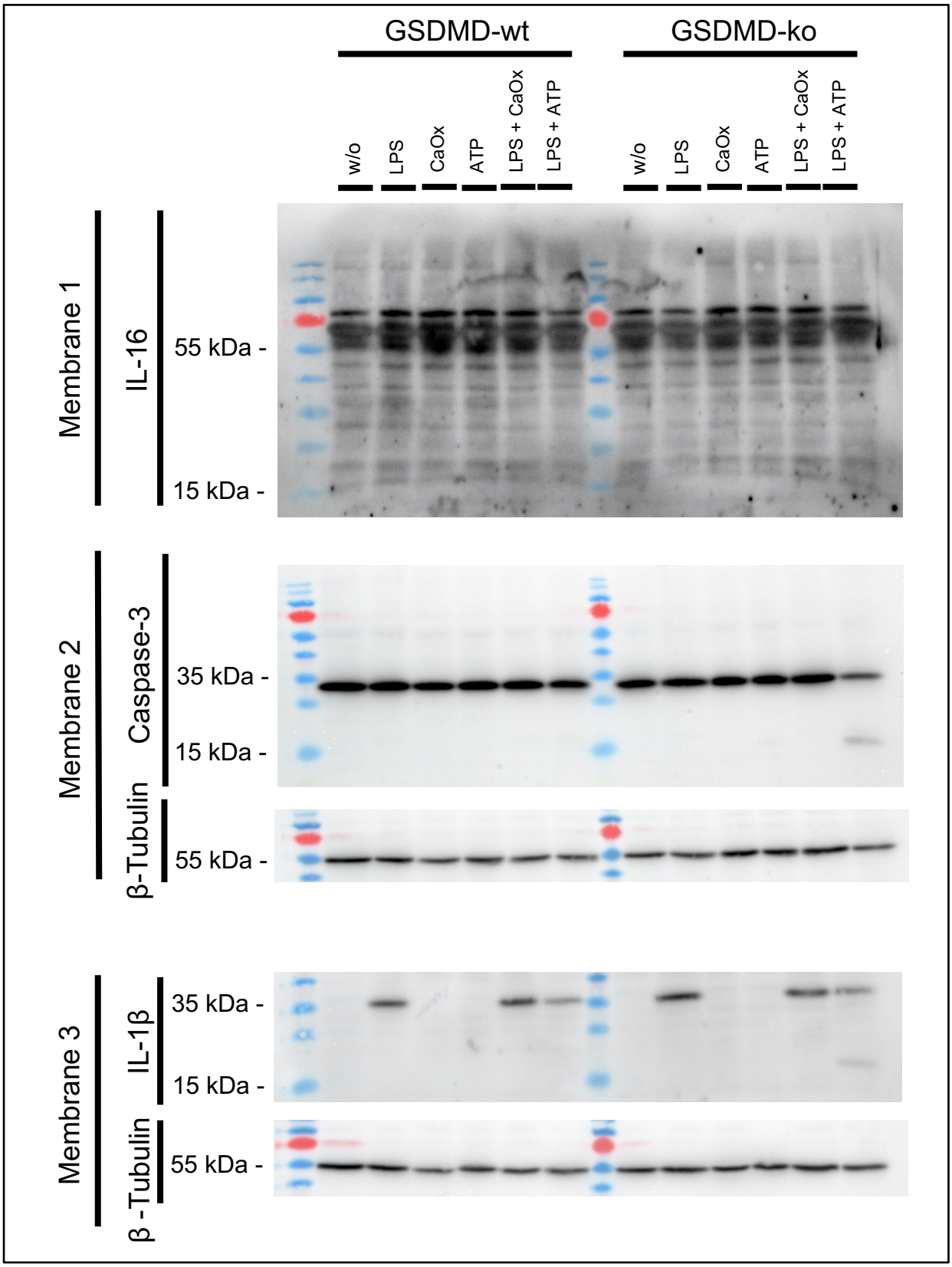

Figure 28: Western Blot of BMDM cell lysate after stimulation

IL-16, caspase-3 and IL-1β protein expression in cell lysate determined by Western blot. A protein ladder was used to assess the protein size and β-Tubulin was used as loading control.

3.8 PMN Stimulation

Hypothesis 2B assumes the possibility that PMNs are responsible for elevated IL-16 levels in patients' plasma and that the stimulation of PMN with soluble NaOx, or CaOx crystals may lead to increased release of IL-16 *in vitro*.

PMNs from healthy subjects were obtained by dextran solution, density gradient centrifugation, and hypertonic lysis. The purity was determined by flow cytometry using the human PMN panel (see Methods section). The relative proportion of granulocytes (SSC^{high}) of all cells was found to be 97.2%, and the proportion of neutrophils of all granulocytes, defined as FSC^{high}, SSC^{high}, Zombie NIR^{-}, CD11b-$BV421^{+}$, and CD11b-APC^{+} was around 94% (Figure 29).

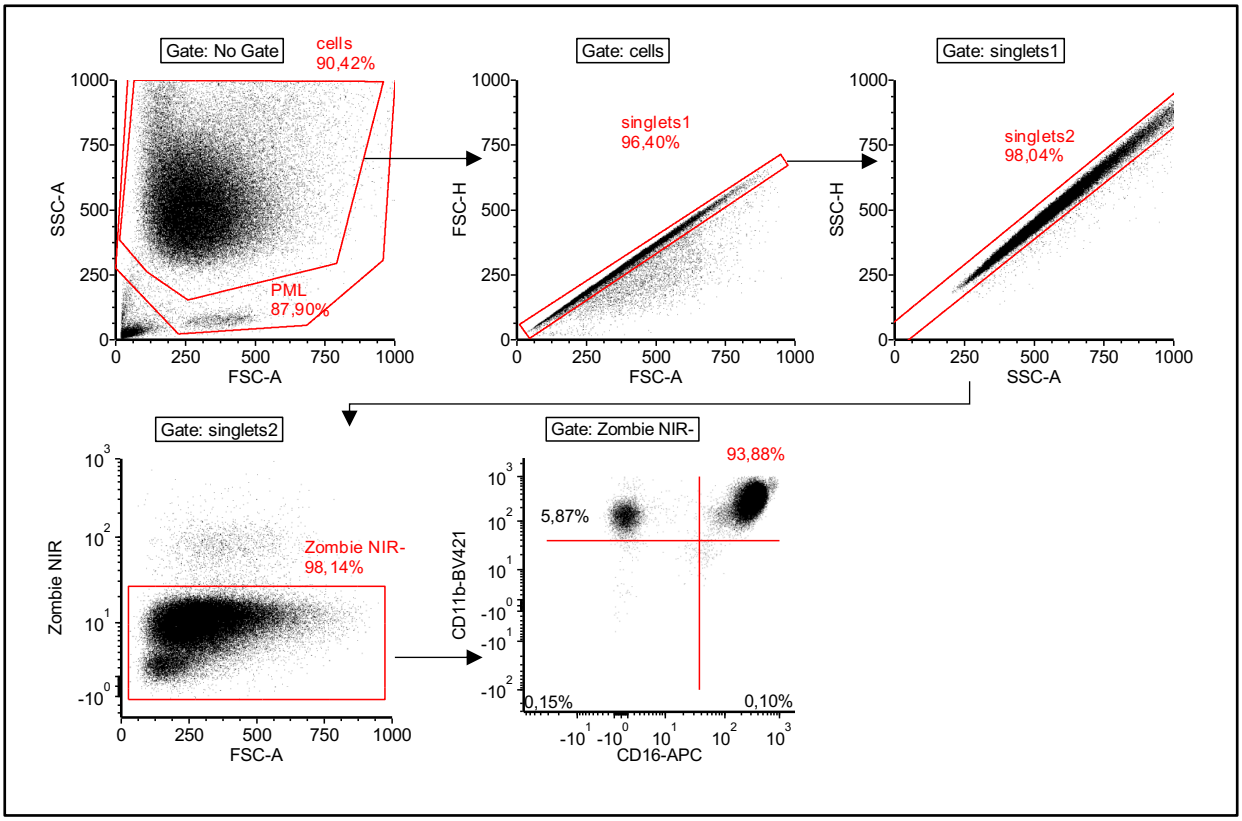

Figure 29: Assessment of neutrophil purity after PMN isolation

Analysis of neutrophil purity after isolation by flow cytometry using CD11b and CD16 as neutrophil surface markers, one representative result is presented.

Since it was assumed that the release of IL-16 is associated with cell death, a flow cytometry-based cell death experiment was performed. PMNs were cultured with 100 µg/ml CaOx, 100 µg/ml NaOx or without stimulator for a period of 63 h. At several time

points in between, the cells were stained with PI and run directly on a flow cytometer. The percentages of PI positive cells out of all cells were determined. The experiment was performed in triplicates.

Differences in the proportion of PI positive cells became visible (Figure 30). After the proportion of dead cells by hour 6 being similar at 10% in all three approaches, a difference in the proportion of dead cells became apparent in the experiment from hour 15 onwards. Hence, the percentage of dead cells after 24 h of culture was 18% without stimulator, 19.8% with NaOx, and 38% with CaOx. After 63 hours of culture without stimulation, 43% of PMNs were positive for PI, with NaOx stimulation it was 43% and with CaOx stimulation it was 66.3% (Figure 30).

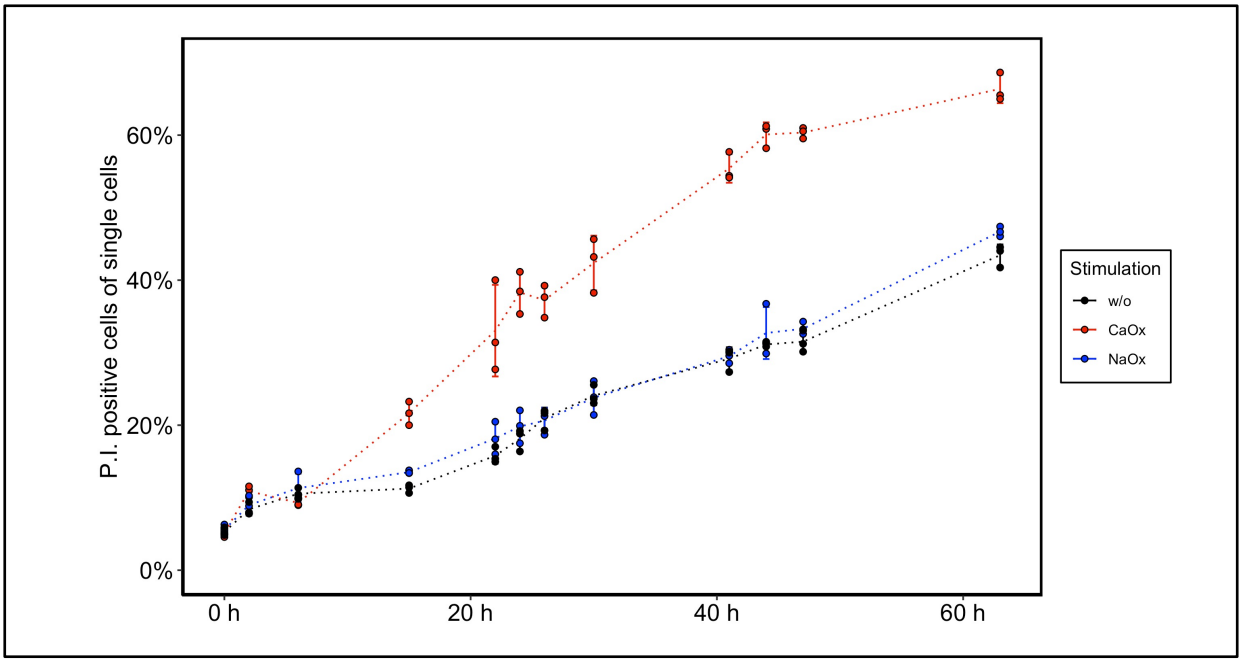

Figure 30: PMN culture with CaOx and NaOx and assessment of P.I. positive cells over time

Cell death, assessed by P.I. positivity in flow cytometry, of PMNs cultured with CaOx and NaOx or without (w/o) stimulation over the time course of 63 h.

Since no effect on cell death was found with NaOx stimulation, the further experiments on IL-16 release were conducted with CaOx first.

For studying IL-16 release, freshly isolated PMNs were cultured with CaOx. The cell-free supernatant was obtained, and the cells lysed for WB analysis. Three time points were defined at which the stimulation experiment was terminated, namely 5 h, 10 h, and 20 h. Based on the PI experiment (Figure 30), it was assumed that differences in cell death and

IL-16 release should become apparent at these time points. The stimulation of PMNs with CaOx was repeated four times, each time with one healthy subject.

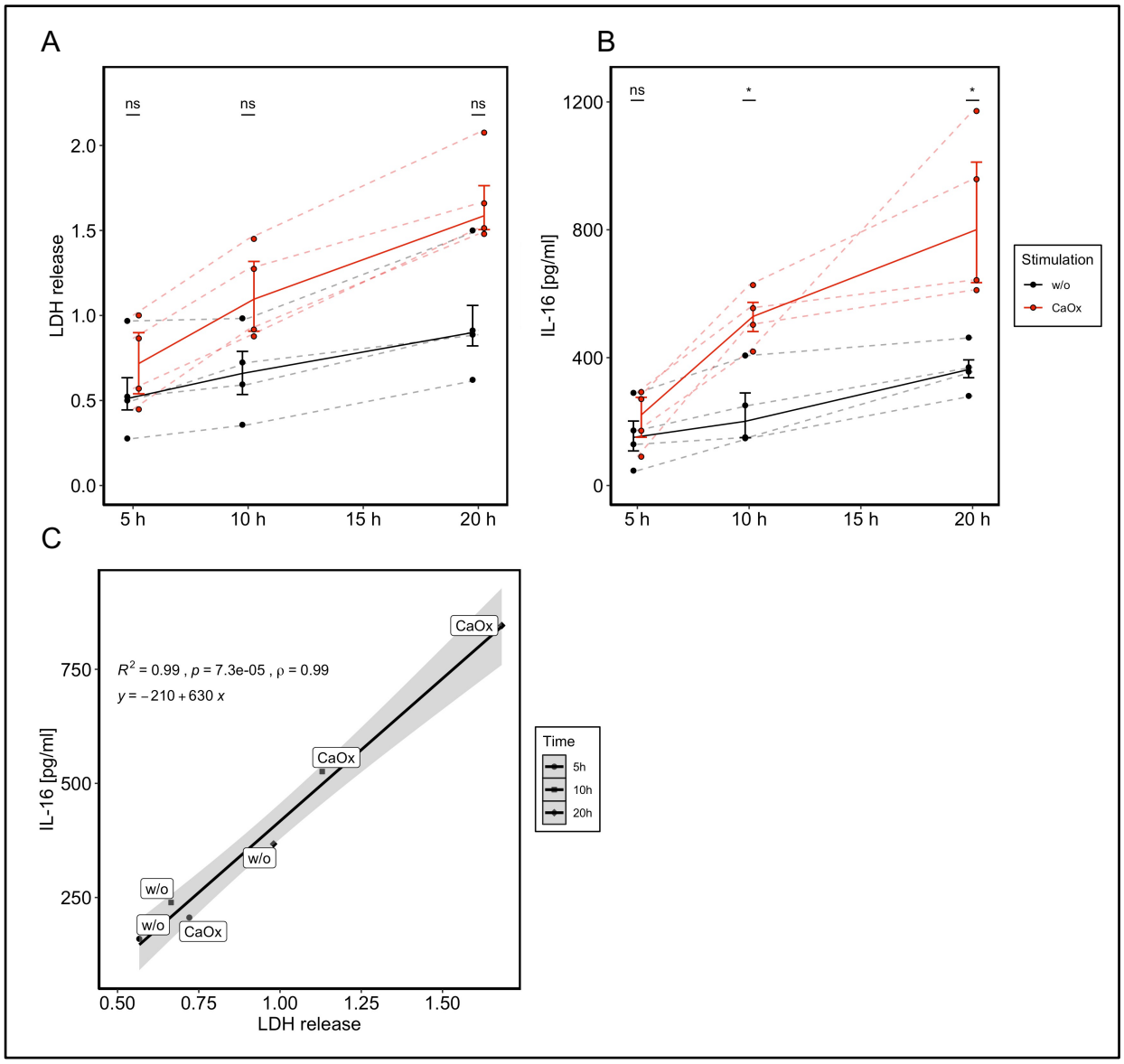

Figure 31: LDH and IL-16 secretion of PMN cultured with CaOx for 5 h, 10 h and 20 h

Stimulation of PMNs with 100 µg/ml CaOx for 5 h, 10 h, and 20 h. Results of four independent experiments. (A) Lactate dehydrogenase (LDH) release [Optical density (450-650 nm) - medium], and (B) IL-16 secretion, statistical analysis: Wilcoxon-Mann-Whitney test. Error bars: median and IQR.

After 5 h of culture, LDH and IL-16 were detected in the supernatant. In both experimental approaches, namely without (w/o) and with CaOx, the release of both LDH and IL-16 increased over time (Figure 31 A and B).

To compare the secretion of IL-16 and LDH between unstimulated PMNs and CaOx stimulated PMNs, a Wilcoxon-Mann-Whitney test was performed for each time point.

For LDH, no significant difference in the release into the supernatant was found after 5 h ($p = 0.49$), 10 h ($p = 0.11$) and 20 h ($p = 0.06$) of culture. Nevertheless, a trend became apparent with higher LDH release from PMNs stimulated with CaOx (Figure 31A).

The release of IL-16 was further compared between unstimulated and CaOx stimulated PMNs at the three time points. While no statistically significant difference was found after 5 h ($p = 0.68$), 10 h ($p = 0.03$) and 20 h ($p = 0.03$), a difference became apparent with a higher release of IL-16 into the supernatant by the PMNs stimulated with CaOx (Figure 31B).

To further determine a correlation of IL-16 release and LDH in the supernatant, a linear correlation of all 6 samples (3 time points, 2 stimulations) was calculated. In the Spearman analysis, a highly significant relationship was found ($\rho = 0.99$, $p < 0.001$) (Figure 31C).

In addition, a Western blot was prepared from the PMN lysates after culture with CaOx. The detection of caspase-3 revealed a uniform band at approximately 33 kDa, which can be interpreted as uncleaved caspase-3. In addition, a band was detected at 15 kDa, which was slightly more pronounced in the culture without stimulator after 10 h and 20 h. GAPDH confirmed uniform protein levels in all samples (Figure 32).

For IL-16 detection, many bands were visible. While the bands between 35 kDa to 55 kDa looked relatively uniform in all samples, a 15 kDa band was particularly evident in the two samples without stimulator after 10 h and 20 h, which is presumably the cleaved intracellular IL-16 (Figure 32).

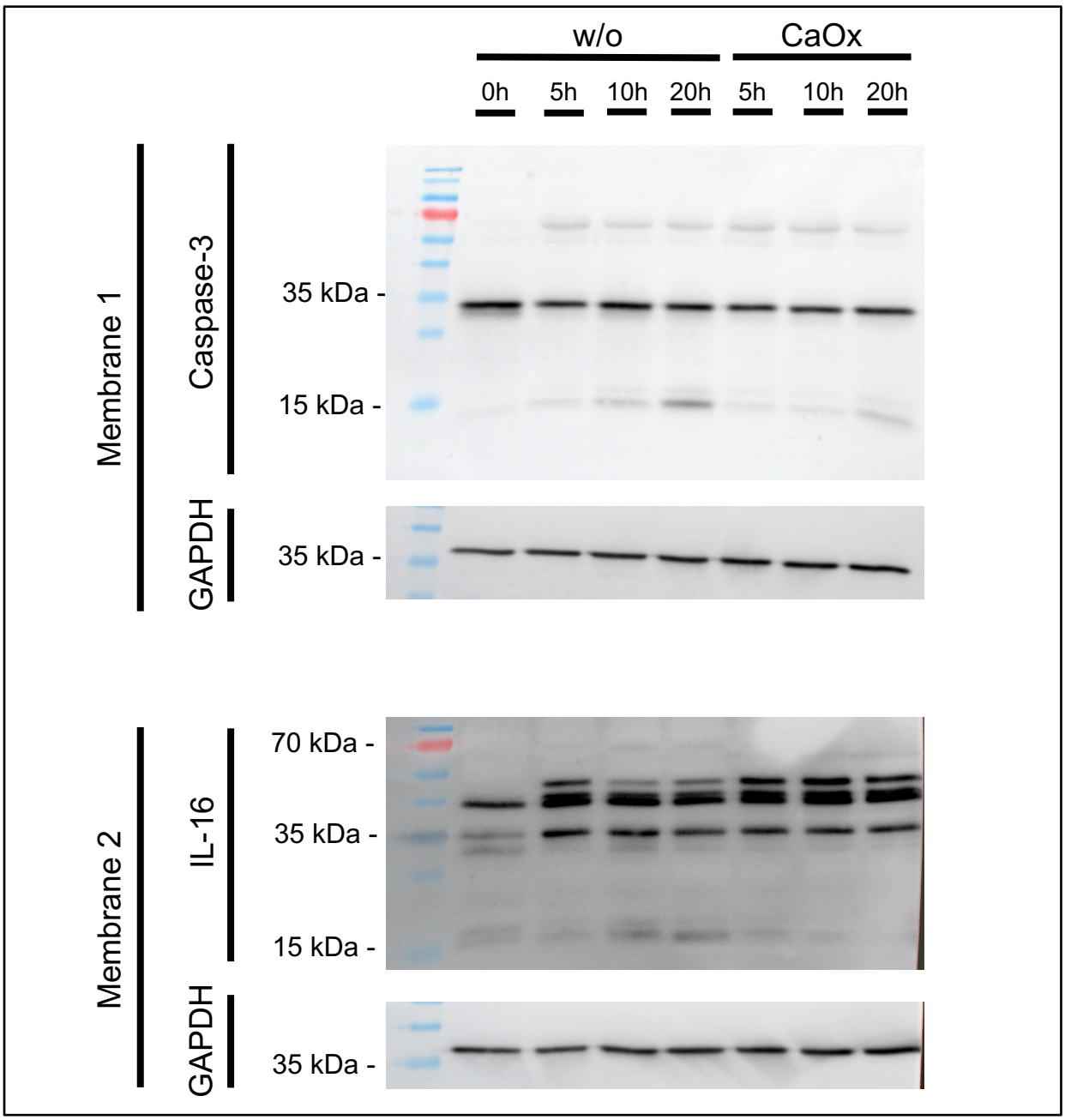

Figure 32: Western Blot analysis of PMN lysate after culture with CaOx or without stimulator

Caspase-3 and IL-16 protein expression in protein lysate after culture with CaOx or without stimulator (w/o) for 5 h, 10 h, or 20 h. GAPDH was used as loading control and a protein ladder was used to determine protein size. One representative experiment is shown.

Next, the intention was to investigate the specificity of the observed effect of IL-16 release after CaOx stimulation. Therefore, freshly isolated PMNs were incubated with several stimulators. For this purpose, crystals such as CaOx, monosodium urate (MSU) crystals,

calcium pyrophosphate dehydrate (CPPD) crystals, and also NaOx, ATP, LPS, and PMA were used, and the culture was carried out for 20 h.

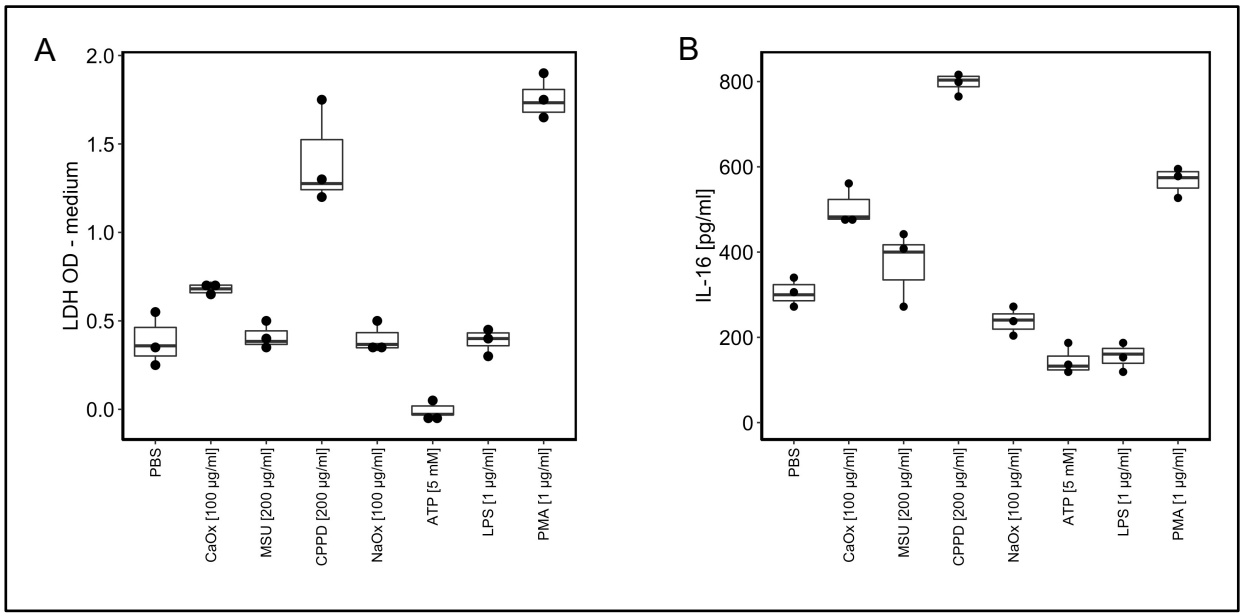

Figure 33: Stimulation of PMNs with different stimulators and assessment of LDH and IL-16 release

Stimulation of PMN with PBS (as control), CaOx [100µg/ml], MSU [200 µg/ml], CPPD [200 µg/ml], NaOx [100 µg/ml], ATP [5 mM], LPS [1 µg/ml], and PMA [1 µg/ml] for 20 h. One experiment performed.

Compared to the samples stimulated with PBS as a control, samples stimulated with CaOx, CPPD and PMA showed higher levels of LDH release. Samples stimulated with MSU, NaOx and LPS showed similar levels of LDH release, and samples stimulated with ATP exhibited a lower level of release (Figure 33A).

IL-16 secretion was detected in all samples at varying levels (Figure 33B). PMNs incubated with PBS secreted 306 pg/ml (SD 38), while higher levels were found when incubated with CaOx (506 pg/ml, SD50), CPPD (799 pg/ml, SD 24) and PMA (568 pg/ml, SD 39), and lower levels of secretion when incubated with ATP (142 pg/ml, SD 33) and LPS (155 pg/ml, SD 35). Similar levels of IL-16 in the supernatant were present when incubated with MSU (367 pg/ml, SD 86) and NaOx (235 pg/ml, SD 35).

4. Discussion

In an exploratory approach, my working group was able to find a correlation of pOx and IL-16 in an US cohort of 107 CKD G5D patients (Figure 3) and confirmed this finding in a second cohort of 12 CKD G5D patients in Germany (Figure 5). Furthermore, increased IL-16 concentrations in the plasma of patients were found compared to the plasma of healthy control subjects.

These findings were previously unknown and raise several questions, especially regarding first, the origin, second, the mechanism of release, and third, the significance of this cytokine in CKD. Based on previous findings of my work group and the published literature, several hypotheses were formulated to answer these three general questions.

4.1 Main findings and interpretation of results

4.1.1 IL-16 release of monocyte subsets and monocyte shift

To address **hypothesis 1A**, namely that the elevated IL-16 levels in CKD G5D patients can be explained by a difference in the monocyte subset composition leading to a higher proportion of monocytes which secrete more IL-16, two questions must be answered. First, whether the monocyte subsets of non-classical and intermediate monocytes generally secrete more IL-16 than classical monocytes, and second, whether the shift in the monocyte subtype composition (monocyte shift) in the population of CKD G5D patients with a higher proportion of non-classical monocytes can be found.

As a result of investigating the revised gating strategy, it seemed that the previous gating of the experiment performed by my work group did not account for two cell types. $CD56^{+}$ NK cells were not gated out by negative selection on the lineage marker, and a population of $CD14^{-}$ $CD16^{+}$ cells was still present after gating. These latter cells can be considered at least partly to be myeloid dendritic cells (Fromm et al., 2020). Although the cells of the previous sort experiments of my work group were enriched for monocytes by magnetic beads, myeloid dendritic cells may have been missed in the enrichment, as those cells share high similarities with monocytes.

Subsequently, in three independent experiments, no difference in the secretion of IL-16 was observed between the three monocyte subsets. Neither the absolute nor the relative amount of IL-16 in the supernatant was found to be different (Figure 13).

Therefore, my results contradict the previous results of my work group and experiments which found non-classical monocytes to secrete more IL-16 than intermediate and classical monocytes of three healthy individuals (Figure 9B).

Different conditions and explanations may have caused the discrepancy in results:

First, the non-classical monocyte population in the experiment of my work group before was defined differently and might have contained other cell types, such as myeloid dendritic cells and NK cells. Monocyte-derived dendritic cells (Reich et al., 2004) as well as Langerhans Cell-Like Dendritic Cells (Reich et al., 2001) were reported to express and secrete higher levels of IL-16 than monocytes. As analyzed in the PBMC sort experiment, however, NK cells seem to secrete less IL-16 than monocytes, which argues against a responsibility of these cells in the previous results of my work group (Figure 18). As my gating strategy excluded those cells, the higher level of IL-16 in the previous experiments could have originated from cells that were previously defined as non-classical monocytes.

Second, differences in the culture conditions regarding cell concentration or handling may have influenced the result. For example, the culture was performed for 18 h before while it was only lasted 16 hours in the experiments performed for this work.

To subsequently investigate further differences of the monocyte subsets, additional cytokines in the supernatant of the cultured cells were studied by LEGENDplex and TNF-α-ELISA.

Regarding the TNF-α measurement of the monocyte subsets, the LEGENDplex and the TNF-α DuoSet ELISA showed the same pattern as well as the same absolute values, namely that intermediate and non-classical monocytes secreted more TNF-α than classical monocytes. Moreover, these results match the results of the previous experiments of my work group. Published data also supports the results without stimulation (Champion et al., 2018; S.-M. Ong et al., 2018) and after LPS stimulation (Skrzeczyńska-Moncznik et al., 2008), although a contrasting pattern of basal secretion of TNF-α from the three monocyte subsets has also been reported by others (Boyette et al., 2017).

There also seems to be some controversy about the secretion of IL-6. While some report higher secretion of classical monocytes (Boyette et al., 2017), others report higher secretion of non-classical and intermediate monocytes (Champion et al., 2018; S.-M. Ong et al., 2018), which matches my results.

My results found higher secretion of IL-1β by intermediate monocytes, lower secretion by non-classical monocytes and no IL-1β secretion by classical monocytes, which is in line with some reports (Hadadi et al., 2016; S.-M. Ong et al., 2018). Others report that classical monocytes have the highest basal secretion of IL-1β (Boyette et al., 2017).

According to my results, intermediate monocytes secrete the most IL-10. Similar results have been described, i.e., that $CD14^{high}$ $CD16^{+}$ monocytes, which can be considered as intermediate monocytes, are the main secreters of IL-10 after LPS stimulation (Skrzeczyńska-Moncznik et al., 2008), while others report classical monocytes to secrete more IL-10 after LPS stimulation (Cros et al., 2010; Wong et al., 2011).

Some cytokines, including IL-23, IL-12p40, IL12p70, IL-23 and TARC, were not detected in my culture.

To study differences in monocyte composition, monocyte subtypes were analyzed by flow cytometry in comparison between 3 healthy controls and 6 CKD G5D patients, revealing a significantly lower proportion of classical monocytes and significantly increased amounts of intermediate and non-classical monocytes in patients. This is consistent with the literature (Nockher & Scherberich, 1998; Schepers et al., 2015; Wallquist et al., 2013), although some report a bigger difference. Even though the shift in the monocyte composition became apparent, it becomes clear that classical monocytes still account for most monocytes in the peripheral blood of CKD-G5D patients (Figure 22B).

In another experiment, the intracellular level of IL-16 was compared between different mononuclear cells of the peripheral blood, and monocytes were found to store the lowest level of IL-16 compared to T cells, NK cells and B cells (Figure 20D).

Since the difference in plasma IL-16 levels is increased 2-4-fold (Figure 5 and 10) in CKD G5D patients compared with healthy control subjects, a very strong difference in secretion would be required for a small cell population like non-classical and intermediate monocytes to be responsible for this increased IL-16 level in patients. At the same time,

no increased IL-16 secretion by non-classical and intermediate monocytes could be detected.

Taking all these considerations into account, **hypothesis 1A** must be considered refuted.

4.1.2 IL-16 secretion of PBMCs

Hypothesis 1B states that a difference in the release of IL-16 by PBMCs between control subjects and patients may be responsible for the increased IL-16 levels in patients.

To investigate whether there are differences in IL-16 secretion of PBMCs between healthy individuals and CKD G5D patients, a flow cytometry-based cell sorting of PBMCs, namely T cells, B cells, NK cells, and monocytes, was performed and the secretion after basal culture for 16 h determined by ELISA.

Consistent with the literature, IL-16 secretion of T cells (Andersson et al., 2011; Laberge et al., 1995), NK cells (Andersson et al., 2016), monocytes (Elssner et al., 2004) and B cells (Kaser et al., 2000) were detected in the supernatant after culture without stimulators, which is also referred to as basal culture.

When comparing the secretion of PBMCs between patients and control subjects, no difference in the absolute or normalized IL-16 secretion was found (Figure 18B). No cell type of patients' PBMCs appeared to secrete more IL-16 than those from healthy control subjects in the basal culture. To date, no data has been reported on the release of IL-16 from different cell types of PBMCs from CKD G5D patients compared with healthy individuals.

In type 1 diabetes, however, a lower secretion of IL-16 by PBMCs was detected after stimulation with PHA and culture for 72 h (Vendrame et al., 2012). This effect is explained by the authors, however, by a defect of caspase-3 which is characteristic for the disease and cannot be directly transferred to CKD.

In CKD, several cytokines are reported to be secreted to a greater or lesser extent by PBMCs *in vitro*. On the one hand, TNF-α secretion of PBMCs after 24 h culture without stimulator was found to be higher by PBMCs of CKD patients requiring long-term HD than by PBMCs of healthy control subjects (Sardenberg et al., 2004). On the other, leukocytes

of HD patients were found to secrete less IL-2, IL-10, and IL-15 after stimulation with Staphylococcus enterotoxin A for six days (Mansouri et al., 2013).

To investigate fundamental differences regarding IL-16 secretion between the cell types, a further analysis was performed to compare the basal normalized secretion of PBMCs without distinguishing between healthy control subjects and CKD G5D patients (Figure 18C). According to those results, T cells secrete the most IL-16, followed by B cells and monocytes, however, this did not reach significance. The significant lowest secretion, however, is by NK cells.

In line with my results, when comparing IL-16 release from different peripheral mononuclear cell types, others report that after stimulation with PMA and culture for 48 h, T cells to release the most IL-16, followed by B cells, followed by monocytes (J.-J. Li et al., 2011).

Because no difference was found in basal IL-16 release between any peripheral blood mononuclear cell type from healthy control subjects and CKD G5D patients, the **hypothesis 1B** that there is a basal difference in release must be refuted.

4.1.3 Intracellular IL-16 level of PBMCs

To compare intracellular IL-16 levels in PBMCs and to address **hypothesis 1C**, an analytical flow cytometry experiment was performed, and the MFI of IL-16-PE used to examine differences in the intracellular level of IL-16 between PBMCs of patients and healthy control subjects.

Overall, IL-16 MFI was detected in most cells of each cell type of PBMCs compared to the FMO control (Figure 20B).

According to the literature, intracellular IL-16 can be found by flow cytometry in most T cells (Blaschke et al., 2001; Krug et al., 2000; J.-J. Li et al., 2011) and monocytes (Elssner et al., 2004), which is in line with these results. Others report, however, only a proportion of each cell type of PBMCs to be intracellularly positive for IL-16 (Andersson et al., 2016).

The reported results show a trend towards lower IL-16 levels in B cells, NK cells, and monocytes as well as significantly lower IL-16 level in T cells of CKD G5D patients compared to healthy control subjects (Figure 20D). This is very different from what was

expected, as a cell type with an increased level of IL-16 was searched for in patients. Various explanatory approaches can be attempted. It is possible that due to the increased cell turnover, lower IL-16 is produced in PBMCs of patients, or that due to the increased release, which, however, could not be detected, lower levels are present intracellularly.

Interestingly, in other pathological conditions such as traumatic injury, increased plasma IL-16 levels and a reduction of T cells positive for intracellular IL-16 have been described (Shimonkevitz et al., 2005). In tobacco smokers, a significant lower proportion of NK+ IL-16+ cells were detected compared to healthy control subjects, despite no difference in the MFI of any PBMC type (Andersson et al., 2016). Furthermore, in CD8+ cells of the bronchoalveolar lavage (BAL), a reduction of IL-16 concentration was detected. (Andersson et al., 2011).

Although no results regarding the intracellular level of IL-16 in CKD are reported, the intracellular level of other cytokines were studied in CKD with partly contradictory results. For example, IL-6 and IL-1β were found reduced in monocytes, at least in CKD G1-4 (Zikou et al., 2015). Moreover, others report no difference in the intracellular level of IL-1β, IL-8, TNFα or IL-6 in monocytes between healthy controls or CKD G5D patients before or after stimulation with LPS (Himmelfarb et al., 2004). According to other results, a lower percentage of intracellular TNF-α^+ and IL-6^+ monocytes after LPS stimulation can be found in patients with CKD (Z. Liu et al., 2015). Furthermore, intracellular cytokine concentrations of T cells from HD patients compared to healthy control subjects were studied after 4 h culture with phorbol-12 myristate 13-acetate (PMA) plus Ionomycin, and higher levels of IL-2, IFN- γ and TNF-α were reported (Costa et al., 2008).

Regarding the fundamental biological difference of PBMCs with respect to the normalized intracellular level of IL-16 relative to total IL-16 level of PBMCs, characteristic differences were found, namely T cells were identified to have the highest amount of IL-16 intracellularly, followed by NK cells, B cells and monocytes.

These results fit perfectly with the IL-16 mRNA expression of blood cells described in the Human Protein Atlas for different tissues (Figure 2). They also note that T cells express more IL-16 than NK cells, which in turn would express more than B cells. Monocytes are also reported to have the lowest IL-16 mRNA expression (Figure 2).

In summary, the observed lower level of IL-16 in CKD G5D patients compared to healthy control subjects is noteworthy. However, no result was found that could explain the higher IL-16 level in patients' plasma and, therefore **hypothesis 1C** has to be rejected.

4.1.4 Low-density Neutrophils

When investigating differences in the caspase-3 activity of PBMCs, no cell type was detected that showed a higher caspase-3 activity level basally. It was described before that CD8+ T cells show a low basal activity of caspase-3 (Zhang et al., 1998), which could not be confirmed. The general understanding of caspase-3 attributes an executive function to this protease after it is cleaved by an initiator caspase (Ponder & Boise, 2019). As the PBMCs of the performed experiments were viable and freshly isolated, they should not have undergone an active process of apoptosis. Therefore, it is reasonable that no active caspase-3 in PBMCs could be found.

It was observed as a chance finding that a proportion of neutrophils with active caspase-3 were present in these experiments. As neutrophils are short-lived cells that undergo spontaneous apoptosis, it is comprehensible that caspase-3 activity of those cells was identified. It remains unclear, however, why almost all neutrophils are positive for active caspase-3. After HD, in fact an even lower caspase-3 activity was described (Korzeniewska-Dyl et al., 2010). It is conceivable, however, that when handling the cells, neutrophils apoptosis was induced, and as a result caspase-3 was activated. Neutrophils need to be handled more carefully as they are very sensitive cells, and as the experiment was not intended to study neutrophils, the handling could have falsified the caspase-3 activity of those cells.

Neutrophil contamination of PBMC samples is known to occur in cases of prolonged storage of whole blood at room temperature (Jerram et al., 2021). This effect is reported after at least 6 hours of storage. As the samples were handled immediately, however, and the handling of healthy control subjects' blood and patients' blood was the same, this effect must be considered as unlikely.

The isolation of PBMCs was performed by dense gradient centrifugation, therefore, the neutrophils found in the PBMC layer must be explained by a lower neutrophil density (Schenz et al., 2021). These low-density neutrophils (LDNs) have already been identified

in chronic and acute inflammatory diseases (Cloke et al., 2012; Deng et al., 2016; Hacbarth & Kajdacsy-Balla, 1986).

Some controversy exists about the origin of these LDNs and whether these cells must be viewed as an independent cell type or an immature precursor, or as degranulated neutrophils (Carmona-Rivera & Kaplan, 2013; Hassani et al., 2020).

The acute inflammatory diseases sepsis is characterized by an elevated recruitment of neutrophils into the circulation, which is also referred to as emergency granulopoiesis (Manz & Boettcher, 2014), and which leads to higher levels of immature LDNs in the blood stream (Drifte et al., 2013). These immature LDNs show a lower surface expression of CD16 and higher survival.

In CKD, a population of LDNs was found to exhibit surface markers which are associated with early stages of neutrophil differentiation, also suggesting an immature origin (Rodríguez-Carrio et al., 2019). Meanwhile, a second population of LDNs was described, which rather express a mature degranulated phenotype (Rodríguez-Carrio et al., 2019).

Since these LDNs were an incidental finding in my studies, these results should not be overinterpreted. It is noteworthy, however, that the LDNs were observed in three experiments and six patients and have also been described by others.

4.1.5 Regulatory T cells and IL-16

By addressing **hypothesis 3A** and investigating differences of the Treg proportion in the peripheral blood of CKD G5D patients compared to healthy individuals as well as by looking for an association with IL-16, a potential importance of IL-16 was to be studied.

The CKD G5D patients and healthy control subjects showed no significant difference in the proportion of Tregs in the peripheral blood. Furthermore, no correlation of the relative amount of Tregs with IL-16 in the plasma was detected (Figure 24).

Regarding the proportion of Tregs in CKD patients, some controversy exists. While most find a decrease of Tregs in patients treated by maintenance HD (Caprara et al., 2016; Mansouri et al., 2017), others report no difference (Lisowska et al., 2014), and some also report an increase (Libetta et al., 2010). Moreover, it was reported that the proportion of Tregs in the peripheral blood is age dependent, and healthy elderly individuals, as well

as elder patients with CKD G5D, express higher levels of Tregs than young control subjects and young CKD G5D patients (Freitas et al., 2019).

It must therefore be concluded that, based on these very preliminary results, IL-16 in the blood stream does not seem to have a direct effect on the proportion of Tregs and, therefore, **hypothesis 3A** must be rejected.

4.1.6 IL-16 release by BMDMs

As a model to investigate the role of caspase-3 in the release of IL-16, GSDMD-wild-type and -deficient BMDMs were differentiated and further stimulated, investigating **hypothesis 2A**.

The BMDM differentiation was proven successful by flow cytometry (Zajd et al., 2020). A small proportion of cells in the beginning of culture, however, already expressed macrophage surface markers. This small fraction may have occurred due to non-specific antibody binding. It is unclear whether macrophages are already present in the bone marrow cell mixture at the beginning of differentiation.

In the stimulation experiment using LPS, ATP and CaOx, the relative LDH release, as a measurement of cell integrity loss, showed an increase over time and a significant difference after 6h (9 h in total) in the culture with LPS and ATP. In line with the results of others (Tsuchiya et al., 2019), it was observed that stimulated BMDMs deficient of GSDMD liberate significantly less LDH (Figure 27 B and C). Furthermore, by Western blot, a higher concentration of cleaved caspase-3 and a higher intracellular level of IL-1β were found in the cell lysate of GSDMD-ko BMDMs. These observations prove the effectiveness of the model and the lower level of pyroptotic cell death in BMDMs deficient of GSDMD (Taabazuing et al., 2017; Tsuchiya et al., 2019).

IL-16 secretion was only detected in the supernatant of the LPS+ATP culture of GSDMD-wild-type BMDMs after 9 h of culture in total.

Overall, the IL-16 release of BMDMs was therefore significantly lower than expected. Fitting with the previous results of my work group, which showed a low IL-16 mRNA expression of macrophages, the secretion of IL-16 by macrophages has also been described by others as relatively low (Desnues et al., 2005). In the case of an infection

with Tropheryma whipplei, however, cell death associated pathways are induced and higher levels secreted (Gorvel et al., 2010).

Interestingly, secretion of IL-16 into the supernatant was only found in the pyroptotic samples, not in the BMDMs deficient of GSDMD, which showed elevated caspase-3 activity and were undergoing apoptosis. This suggests that cell integrity loss is necessary for detecting elevated IL-16 in the supernatant and thereby proposes a lytic cell death mechanism with loss of cell integrity (Frank & Vince, 2019); however, as the measurement was below the detection limit it should not be overinterpreted. No differences could be detected in the IL-16 Western blot of the BMDM GSDMD-wild-type and -knockout lysates.

Overall, the experiment must be considered successful, as the model was proved to work, but potentially ineffective for studying IL-16 release by cells in relation to caspase-3 activity, as the levels of secreted IL-16 were low.

4.1.7 PMNs and IL-16 release

With respect to **hypothesis 2B**, it was intended to study the influence of CaOx and NaOx stimulation on cell death and IL-16 release by PMNs of healthy control subjects i*n vitro*.

Over the time course of 63 h, increased cell death was found in all samples. A significantly higher proportion appeared if cultured in the presence of CaOx crystals. It was thereby demonstrated that CaOx stimulation, but not NaOx stimulation, results in increased cell death, measured by loss of cell integrity and by PI positivity.

It is known that neutrophils undergo spontaneous apoptosis if cultured *in vitro* (Alipour et al., 2020; Pongracz et al., 1999). Often, this is assessed by an additional staining with Annexin V which enables the differentiation into early and late cell death (Quinn & DeLeo, 2020); however, this has not yet been successfully established in the lab.

Different processes of neutrophil cell death are known. Generally, non-inflammatory pathways of cell death are distinguished from pro-inflammatory pathways, like necroptosis, pyroptosis and NETosis (Lawrence et al., 2020).

It was found that neutrophils cultured with CaOx crystals show increased secretion of LDH and IL-16 after 5 h and, 10 h, and a significant higher secretion of IL-16 after 20 h.

Even though IL-16 secretion of neutrophils after CaOx culture has not yet been described, these results fit well with the published work of others. First, it has been shown that neutrophils, cultured with crystals of various sizes including CaOx, undergo a pro-inflammatory form of cell death called necrosis, which is characterized by LDH release and NET formation (Desai et al., 2017). Second, it has been shown that secondary necrotic neutrophils secrete elevated levels of both LDH and IL-16 (Roth et al., 2015).

The clinical significance of these results has not yet been fully studied; however, in an animal model of CaOx nephropathy, mice showed a diffuse neutrophil infiltration into the kidneys (Mulay et al., 2013). As part of innate immunity, neutrophils are often viewed as the first line of defense and are therefore conceivable of being involved in phagocytosis of CaOx crystals.

Other stimulators were also tested for their effect on the release of LDH and IL-16 by neutrophils. It was observed that CaOx, CPPD, and PMA led to an increased release of IL-16, whereas MSU and NaOx had no effect, and ATP and LPS showed a reduced release of LDH and IL-16.

The influence of different stimulators on LDH release and cell death of neutrophils was studied by others before. It was reported that MSU crystals lead to a lower LDH secretion than CaOx (Desai et al., 2017), which fits with my results. CPPD was found to have an anti-apoptotic effect on neutrophils after 3 h of culture (Higo et al., 2010), which is very different from my experiments, as I found increased LDH release of PMNs if cultured with CPPD. The authors only used 30 µg/ml CPPD, while I used 200 µg/ml and a longer time of culture of 20 h, however. PMA was also shown to induce cell death measured by Sytox Green fluorescence (Remijsen et al., 2011) and P.I. staining (Takei et al., 1996), which is in line with my results. According to other studies, LPS (Glowacka et al., 2002) and ATP (Vaughan et al., 2007) inhibit neutrophil apoptosis. Although I did not observe a difference in LDH release when cultured with LPS, PMN culture in the presence of ATP showed decreased LDH release. Both stimulators decreased IL-16 release by PMNs.

Overall, the observed effect of increased IL-16 release from neutrophils when cultured with different stimulators, such as crystals, is thus not specific, as it was not only CaOx that led to increased IL-16 release in the supernatant.

Neutrophil apoptosis is known to be influenced by many factors. Other uremic retention molecules like indoxyl sulfate, which is protein bound (Cruz et al., 2014), and ADMA (von Leitner et al., 2011) directly act on neutrophils, at least *in vitro*. Indoxyl Sulfate induces apoptosis of neutrophils. It remains to be elucidated whether other uremic retention molecules can also induce the liberation of IL-16 by neutrophils, at least *in vitro*.

Lastly, a strong positive correlation of IL-16 and LDH was identified (Figure 31C). This correlation of IL-16 and LDH was also detected *in vitro* (Roth et al., 2015) and in patients suffering from hemophagocytic lymphohistiocytosis (Takada et al., 2004)

In summary, these results provide a promising link between the release of IL-16 by neutrophils and oxalate, although only the CaOx crystal, not the soluble NaOx, increased IL-16 release.

4.2 Limitations

4.2.1 Patients and Control Subjects

When comparing the characteristics of the two study groups, namely healthy control subjects and patients, clear differences become apparent. The groups differed in the gender distribution, as well as in the average age. Because control individuals and patients were not matched, these demographic factors should be considered as a potential influencing and confounding factor as well as a major limitation of the results, especially as age and gender are known to influence inflammatory profiles and cytokine levels (Kildey et al., 2014; Larsson et al., 2015; O'Mahony et al., 1998).

So far, no data on the influence of age or gender on IL-16 and pOx levels in humans has been published. It is known, however, that CaOx stones are more frequent in males (Lieske et al., 2014; Ye et al., 2020). In a cohort of 1200 children at the aged up to 18 years, no role of age or gender was found on plasma oxalate concentration (Porowski et al., 2008).

Because no consistent influence of gender or age on the analytes of interest was found in the previous cohorts, these limitations are considered acceptable, and the results are further interpreted with this caveat in mind.

Patients and control subjects included in this study were assumed to not have an acute infection. As it would not have been possible to wait for the current laboratory values due to the experimental design, inflammatory parameters were only assessed retrospectively. Some healthy control subjects and patients were included in different experiments, and therefore blood was drawn several times. IL-16 and pOx level, however, were determined only once.

It has been described that prolonged storage of plasma samples, especially at room temperature, has a major effect on IL-16 (Kofanova et al., 2018) and pOx (Pfau et al., 2020) measurements resulting in elevated results for both analytes. Therefore, special care was taken to always handle the samples on ice and freeze them quickly until further use.

As described above, IL-16 measurement with an IL-16 DuoSet ELISA for plasma samples yields approximately 28-29.8% higher values for both the control and patient group. Since all samples were measured with the same assay, however, generally higher values were expected, which should not have affected the group difference. Plasma oxalate was measured using an enzymatic assay that is commonly performed in our laboratory and is well validated.

When comparing the two groups regarding IL-16 and pOx levels, significant differences become noticeable. The patient group showed an approximately 4-fold increased concentration of IL-16 and approx. 5-fold increased concentration of pOx in the plasma. These differences are consistent with the previous findings of our working group.

Regarding the correlation of pOx and IL-16 in this small cohort of patients, no significant correlation was found. Nevertheless, a trend became obvious that fits the previously observed correlation with high plasma IL-16 concentrations in patients with high plasma oxalate.

Although the study groups in this work were not ideally matched, the similarity in observed IL-16 and pOx levels to previous data is considered to allow a valid conclusion. Whether the same results would be obtained in a better matched cohort would need to be the subject of further investigation.

4.2.2 IL-16 measurement of the supernatant after culture of human cells

The measured IL-16 concentrations in the supernatants of monocyte and PBMC cultures were at the lower end of the detection range, and for a few samples, even just below the limit of detection. This clearly reduces the reliability of the results. There are different aspects that could have caused this.

First, immune cell subsets, especially non-classical and intermediate monocytes, are rare populations in the peripheral blood, and therefore a high amount of blood is needed to collect reasonable cell numbers to further culture the cells. However, cell counts after sorting were low. As technical replicates were required to assure the validity of the results, the cultured cell numbers and the cell concentration were therefore lower than intended.

Second, as the basal IL-16 release was to be studied, the addition of substances was omitted. It might be argued that some properties of immune cells only become visible if the cells become activated and are cultured with a stimulator for a given time. Moreover, it is notable, that many authors use stimulators to study properties of immune cells. In particular, LPS is often used for monocyte cultures, which increases the secretion of some cytokines significantly compared to the basal secretion (Hadadi et al., 2016). This, however, is not the case for IL-16 (Figure 7). Other activators, however, were found to induce IL-16 secretion - for example, calcium ionophore and PMA in T cell cultures (Andersson et al., 2011) or PMA alone in B cell lines (Sharma et al., 2000). The culture without stimulator was intended to give a true impression of the general differences between cells. It must be noted that the absence of a stimulator probably resulted in lower concentrations of IL-16 in the supernatant, which might have led to the overlooking of a phenotypic difference between patients and control subjects.

Third, the culture was only performed for 16 hours, which must be seen as a rather short period of time for PBMCs. Since cell death has been described as a major influence on IL-16 release, a short culture period was preferred, however. Nevertheless, since the survival of different mononuclear cells in the culture conditions may have been different, it is possible that the differences in IL-16 release are due to differences in cell death between the cell types studied, especially, as additional cytokines are often used in different immune cell culture conditions, like anti-CD3/CD28 antibodies (Xu et al., 2018) and IL-2 (Ghaffari et al., 2019) in T cell cultures. This co-stimulation was also found to induce higher IL-16 protein production (D. M. Wu et al., 1999).

Because the measurement of biological duplicates gave similar results and the variance between cells was rather small, the performed ELISAs seem acceptable. It is also believed that a pronounced difference between monocyte subsets or PBMCs in terms of IL-16 secretion would have become visible.

4.2.3 Sorter-induced cellular stress

The culture of fluorescence-activated cell sorted PBMCs and monocytes was intended for investigating the basal secretion of cells without activation or stimulation by an added compound. The effect of cell sorting on cell properties, which is also referred to as sorter-induced cellular stress (SICS), is currently being discussed and high inter-experiment differences were found (Lopez & Hulspas, 2020; Pfister et al., 2020). Therefore, it must be considered that this might have confounded the survival and consequently the basal IL-16 secretion of cells. Although all cells were treated equally, it cannot be excluded that SICS affected the different cell types of monocytes or PBMCs differently, or that different experiments showed different levels of SICS.

4.2.4 Isotype controls and FMO

Isotype controls represent a widely used technique to account for unspecific background staining in flow cytometry (Maecker & Trotter, 2006). However, difficulties have also been reported when working with isotype controls, particularly when working with monocytes, and blockage of the Fc receptor has been suggested (Andersen et al., 2016).

In the performed flow cytometry experiments of this work, no isotype controls were used to distinguish between positive and negative populations. Fc blocking was, however, added if monocytes were stained. Regarding the intracellular staining for the IL-16 of PBMCs, an isotype control would have been very useful. Instead, FMO controls were used to define intracellularly IL-16-positive cells, which must be considered inferior, however.

4.2.5 BMDM

The *in vitro* differentiated BMDM must be considered as an artificial cell type differentiated by growth factors. They would have had limited predictive value for the release of IL-16 in humans. It remains uncertain what conclusions can be drawn from these results regarding the release of IL-16 in the clinical disease of CKD.

4.2.6 IL-16 Western Blot

The performed Western blots for IL-16 revealed several bands of different size ranging from 23 to 140 kDa, or 29 to 80 kDa, respectively. This made the interpretation of these Western blots very difficult or practically impossible. Interestingly, some other researchers also report a range of different IL-16 bands in Western blots (Chupp et al., 1998; Croq et al., 2010), which suggests general difficulties regarding the detection of this cytokine. Other investigators using the same antibody as in these experiments, however, obtained clear Western blot results (Roth et al., 2015). Therefore, the Western blot results of this study could also have been caused by technical difficulties or errors.

4.2.7 IL-16 secretion by PMNs

For the experiments on the release of IL-16 from PMNs, cells were isolated from healthy volunteers. This approach assumes that the triggering mechanism is an external stimulation and does not consider differences in PMNs of CKD G5D patients compared to healthy control subjects.

As mentioned earlier, most of the included probands were female. As gender differences were found regarding the cell death of neutrophils after culture *in vitro* (Molloy et al., 2003), it is conceivable that the study population might have influenced the results.

4.2.8 Measurement of pro-IL-16 or mature IL-16

In this work, it was assumed that the measured IL-16 corresponds to the cleaved/mature form of the cytokine. Regarding the measurement of IL-16 in the supernatant using the DuoSet-ELISA, the manufacturer does not specify that the measurement is of the mature

form. It is noticeable that in the results of this work, as well as in others, the measurement of IL-16 correlates very well with LDH. Therefore, it could also be argued that in the case of cell integrity loss, both LDH and pro-IL-16 are passively released and that subsequently the pro-IL-16 is determined by ELISA. It therefore becomes evident that protein detection by Western blot would be of great importance.

4.2.9 Causation does not imply causality

The original observation that formed the starting point for this work is the observed correlation between pOx and IL-16. It was also observed that IL-16, like pOx, was associated with the duration of dialysis and residual kidney excretion. Therefore, it must be considered that the correlation of pOx and IL-16 could be due to a common underlying variable, such as duration of dialysis or residual kidney function, and that there is no direct link between the two analytes pOx and IL-16.

4.2.10 IL-16 as a retention molecule

In this work, increased secretion of immune cells was investigated as a possible cause of the elevated IL-16 levels in CKD-G5D patients. It could also be argued that IL-16 is not elevated because of its higher secretion, but rather from a decreased kidney clearance. This argument cannot be disregarded. It is generally assumed that the glomerular filtration barrier functions with a size and charge selectivity (Jarad & Miner, 2009). Proteins smaller than 58 kDa can pass the glomerular filtration barrier (Vanholder et al., 2018). As IL-16 is described to have a molecular mass of approximate 60 kDa in the blood stream and no reduction of IL-16 has been found during dialysis (Figure 6), it is assumed that IL-16 cannot pass the glomerular filtration barrier. Again, however, it is apparent that the Western blot would be of high importance for determining the actual size present in the plasma.

4.3 Conclusion and future directions

The investigation of the source of IL-16 in CKD-G5D patients revealed that it is unlikely that a monocyte subset is responsible for the increased level of IL-16 in CKD-G5D patients. Furthermore, no single responsible cell type of PBMCs was identified that exhibited different characteristics in intracellular levels or secretion of IL-16 between patients and control subjects. It may be interesting, however, to pursue the overall lower level of IL-16 in PBMCs.

Several approaches to study the mechanism of secretion and the involvement of caspase-3 were attempted. The use of a murine model of BMDMs proved ineffective in examining the release of IL-16. The attempt to study the IL-16 release of PMNs, however, gave interesting results. These results are encouraging for further work on the possibility that PMNs are mainly responsible for the increased IL-16 levels in CKD-G5D patients. Several reasons support this:

1. The possible mechanism of IL-16 secretion by PMNs *in vitro* through an induction of cell death is a conclusive explanation for the origin of IL-16, as there are many triggers for cell death of PMNs in the plasma of CKD G5D patients. The identified mechanism of cell death by CaOx crystals proved to be nonspecific, as other stimulators also triggered IL-16 secretion. Multiple uremic retention molecules or pro-apoptotic triggers could be responsible for the increased cell death of PMNs.
2. The high abundance of PMNs can explain the high levels of IL-16 in patients. Compared to other cytokines, the absolute concentration of IL-16 in plasma is high (Figure 3A) and the four-time increase found in patients compared to healthy individuals is more likely to originate from a highly abundant cell type.
3. According to the expression of IL-16 by different cell types and tissues, granulocytes were found to express the highest level of IL-16 (Figure 2, Human Protein Atlas). Although this difference was not confirmed by intracellular staining by flow cytometry or Western blot in this work, it is worth comparing not only the expression but also the intracellular level and secretion of the different leukocytes including neutrophils in the future.
4. The caspase-3-active LDNs found serendipitously in PBMC samples from CKD G5D patients support the concept of immature or degranulated PMNs in CKD.

These may be explained by potentially higher cell turnover in CKD G5D patients, which could lead to increased IL-16 secretion due to the cell death of PMNs.

The most important question that needs further attention is the importance of IL-16 in CKD. An initial attempt was made to investigate the possible role of IL-16 in association with Tregs in the plasma of patients. It proved to be unsuccessful. Therefore, it is suggested to perform larger clinical studies focusing on clinical parameters or survival.

All in all, this work provides insight into IL-16 in CKD. The global disease burden of CKD is increasing, and the high mortality and morbidity of CKD is devastating. As the importance of specific immunotherapies against cytokines and the ability of cytokines as biomarkers are explored and used, the potential of IL-16 in CKD should be further investigated.

References

Abeles, (Robin) Daniel, McPhail, M. J., Sowter, D., Antoniades, C. G., Vergis, N., Vijay, G. K. M., Xystrakis, E., Khamri, W., Shawcross, D. L., Ma, Y., Wendon, J. A., & Vergani, D. (2012). CD14, CD16 and HLA-DR reliably identifies human monocytes and their subsets in the context of pathologically reduced HLA-DR expression by CD14hi/CD16neg monocytes: Expansion of CD14hi/CD16pos and contraction of CD14lo/CD16pos monocytes in acute liver failure. *Cytometry Part A*, *81A*(10), 823–834. https://doi.org/10.1002/cyto.a.22104

Alani, H., Tamimi, A., & Tamimi, N. (2014). Cardiovascular co-morbidity in chronic kidney disease: Current knowledge and future research needs. *World Journal of Nephrology*, *3*(4), 156–168. https://doi.org/10.5527/wjn.v3.i4.156

Alcover, A., Alarcón, B., & Di Bartolo, V. (2018). Cell Biology of T Cell Receptor Expression and Regulation. *Annual Review of Immunology*, *36*(1), 103–125. https://doi.org/10.1146/annurev-immunol-042617-053429

Alexandrakis, M. G., Passam, F. H., Kyriakou, D. S., Christophoridou, A. V., Perisinakis, K., Hatzivasili, A., Foudoulakis, A., & Castanas, E. (2004). Serum level of interleukin-16 in multiple myeloma patients and its relationship to disease activity. *American Journal of Hematology*, *75*(2), 101–106. https://doi.org/10.1002/ajh.10444

Alipour, R., Fatemi, A., Alsahebfosul, F., Andalib, A., & Pourazar, A. (2020). Autologous plasma versus fetal calf serum as a supplement for the culture of neutrophils. *BMC Research Notes*, *13*(1), 39. https://doi.org/10.1186/s13104-020-4902-z

Amdur, R. L., Feldman, H. I., Gupta, J., Yang, W., Kanetsky, P., Shlipak, M., Rahman, M., Lash, J. P., Townsend, R. R., Ojo, A., Roy-Chaudhury, A., Go, A. S., Joffe, M., He, J., Balakrishnan, V. S., Kimmel, P. L., Kusek, J. W., & Raj, D. S. (2016). Inflammation and Progression of CKD: The CRIC Study. *Clinical Journal of the American Society of Nephrology : CJASN*, *11*(9), 1546–1556. https://doi.org/10.2215/CJN.13121215

Andersen, M. N., Al-Karradi, S. N. H., Kragstrup, T. W., & Hokland, M. (2016). Elimination of erroneous results in flow cytometry caused by antibody binding to Fc receptors on human monocytes and macrophages: FcR-Blocking Eliminates Erroneous Results in Flow Cytometry. *Cytometry Part A*, *89*(11), 1001–1009. https://doi.org/10.1002/cyto.a.22995

Andersson, A., Bossios, A., Malmhäll, C., Sjöstrand, M., Eldh, M., Eldh, B.-M., Glader, P., Andersson, B., Qvarfordt, I., Riise, G. C., & Lindén, A. (2011). Effects of tobacco smoke on IL-16 in CD8+ cells from human airways and blood: A key role for oxygen free radicals? *American Journal of Physiology. Lung Cellular and Molecular Physiology*, *300*(1), L43-55. https://doi.org/10.1152/ajplung.00387.2009

Andersson, A., Malmhäll, C., Houltz, B., Tengvall, S., Sjöstrand, M., Qvarfordt, I., Lindén, A., & Bossios, A. (2016). Interleukin-16-producing NK cells and T-cells in the blood of tobacco smokers with and without COPD. *International Journal of Chronic Obstructive Pulmonary Disease*, *11*, 2245–2258. https://doi.org/10.2147/COPD.S103758

Arima, M., Plitt, J., Stellato, C., Bickel, C., Motojima, S., Makino, S., Fukuda, T., & Schleimer, R. P. (1999). Expression of interleukin-16 by human epithelial cells. Inhibition by dexamethasone. *American Journal of Respiratory Cell and Molecular Biology*, *21*(6), 684–692. https://doi.org/10.1165/ajrcmb.21.6.3671

Armbruster, C. E., Smith, S. N., Mody, L., & Mobley, H. L. T. (2018). Urine Cytokine and Chemokine Levels Predict Urinary Tract Infection Severity Independent of Uropathogen, Urine Bacterial Burden, Host Genetics, and Host Age. *Infection and Immunity*, *86*(9), e00327-18. https://doi.org/10.1128/IAI.00327-18

Assouvie, A., Daley-Bauer, L. P., & Rousselet, G. (2018). Growing Murine Bone Marrow-Derived Macrophages. In G. Rousselet (Hrsg.), *Macrophages: Methods and Protocols* (S. 29–33). Springer. https://doi.org/10.1007/978-1-4939-7837-3_3

Asumendi, A., Alvarez, A., Martinez, I., Smedsrød, B., & Vidal-Vanaclocha, F. (1996). Hepatic sinusoidal endothelium heterogeneity with respect to mannose receptor activity is interleukin-1 dependent. *Hepatology (Baltimore, Md.)*, *23*(6), 1521–1529. https://doi.org/10.1053/jhep.1996.v23.pm0008675173

Austyn, J. M., & Gordon, S. (1981). F4/80, a monoclonal antibody directed specifically against the mouse macrophage. *European Journal of Immunology*, *11*(10), 805–815. https://doi.org/10.1002/eji.1830111013

Baier, M., Bannert, N., Werner, A., Adler, H. S., Otteken, A., Beer, B., Norley, S., & Kurth, R. (1998). Chemoattractant Factors and the Control of Human Immunodeficiency Virus Replication. *Pathobiology*, *66*(3–4), 128–130. https://doi.org/10.1159/000028008

Betjes, M. G. H. (2013). Immune cell dysfunction and inflammation in end-stage renal disease. *Nature Reviews Nephrology*, *9*(5), 255–265. https://doi.org/10.1038/nrneph.2013.44

Bhattacharjee, J., Das, B., Mishra, A., Sahay, P., & Upadhyay, P. (2018). Monocytes isolated by positive and negative magnetic sorting techniques show different molecular characteristics and immunophenotypic behaviour. *F1000Research*, *6*, 2045. https://doi.org/10.12688/f1000research.12802.3

Bie, J. J. D., Jonker, E. H., Henricks, P. a. J., Hoevenaars, J., Little, F. F., Cruikshank, W. W., Nijkamp, F. P., & Oosterhout, A. J. M. V. (2002). Exogenous interleukin-16 inhibits antigen-induced airway hyper-reactivity, eosinophilia and Th2-type cytokine production in mice. *Clinical & Experimental Allergy*, *32*(11), 1651–1658. https://doi.org/10.1046/j.1365-2222.2002.01528.x

Biolegend. (o. J.). *LEGENDplex Macrophagen Panel*. Abgerufen 14. November 2021, von https://www.biolegend.com/Files/Images/media_assets/pro_detail/datasheets/75062_Hu_Macrophage-Microglia_Panel_V01.pdf

Blaschke, S., Schulz, H., Schwarz, G., Blaschke, V., Müller, G. A., & Reuss-Borst, M. (2001). Interleukin 16 expression in relation to disease activity in rheumatoid arthritis. *The Journal of Rheumatology*, *28*(1), 12–21.

Boltjes, A., & Van Wijk, F. (2014). Human Dendritic Cell Functional Specialization in Steady-State and Inflammation. *Frontiers in Immunology*, *5*, 131. https://doi.org/10.3389/fimmu.2014.00131

Boyette, L. B., Macedo, C., Hadi, K., Elinoff, B. D., Walters, J. T., Ramaswami, B., Chalasani, G., Taboas, J. M., Lakkis, F. G., & Metes, D. M. (2017). Phenotype, function, and differentiation potential of human monocyte subsets. *PLOS ONE*, *12*(4), e0176460. https://doi.org/10.1371/journal.pone.0176460

Brzica, H., Breljak, D., Burckhardt, B. C., Burckhardt, G., & Sabolić, I. (2013). Oxalate: From the Environment to Kidney Stones. *Archives of Industrial Hygiene and Toxicology*, *64*(4), 609–630. https://doi.org/10.2478/10004-1254-64-2013-2428

Caprara, C., Kinsey, G. R., Corradi, V., Xin, W., Ma, J. Z., Scalzotto, E., Martino, F. K., Okusa, M. D., Nalesso, F., Ferrari, F., Rosner, M., & Ronco, C. (2016). The Influence of Hemodialysis on T Regulatory Cells: A Meta-Analysis and Systematic Review. *Blood Purification*, *42*(4), 307–313. https://doi.org/10.1159/000449242

Carmona-Rivera, C., & Kaplan, M. J. (2013). Low-density granulocytes: A distinct class of neutrophils in systemic autoimmunity. *Seminars in Immunopathology*, *35*(4), 455–463. https://doi.org/10.1007/s00281-013-0375-7

Castanheira, F. V. S., & Kubes, P. (2019). Neutrophils and NETs in modulating acute and chronic inflammation. *Blood*, *133*(20), 2178–2185. https://doi.org/10.1182/blood-2018-11-844530

Castillo-Rodríguez, E., Pizarro-Sánchez, S., Sanz, A. B., Ramos, A. M., Sanchez-Niño, M. D., Martin-Cleary, C., Fernandez-Fernandez, B., & Ortiz, A. (2017). Inflammatory Cytokines as Uremic Toxins: "Ni Son Todos Los Que Estan, Ni Estan Todos Los Que Son". *Toxins*, *9*(4), 114. https://doi.org/10.3390/toxins9040114

Cendoroglo, M., Jaber, B. L., Balakrishnan, V. S., Perianayagam, M., King, A. J., & Pereira, B. J. G. (1999). Neutrophil Apoptosis and Dysfunction in Uremia. *Journal of the American Society of Nephrology*, *10*(1), 93–100. https://doi.org/10.1681/ASN.V10193

Champion, T. C., Partridge, L. J., Ong, S.-M., Malleret, B., Wong, S.-C., & Monk, P. N. (2018). Monocyte Subsets Have Distinct Patterns of Tetraspanin Expression and Different Capacities to Form Multinucleate Giant Cells. *Frontiers in Immunology*, *9*, 1247. https://doi.org/10.3389/fimmu.2018.01247

Chang, C.-H., Fan, P.-C., Lin, C.-Y., Yang, C.-H., Chen, Y.-T., Chang, S.-W., Yang, H.-Y., Jenq, C.-C., Hung, C.-C., Yang, C.-W., & Chen, Y.-C. (2015). Elevation of Interleukin-18 Correlates With Cardiovascular, Cerebrovascular, and Peripheral Vascular Events: A Cohort Study of Hemodialysis Patients. *Medicine*, *94*(42), e1836. https://doi.org/10.1097/MD.0000000000001836

Chen, M.-F., Chang, C.-H., Yang, L.-Y., Hsieh, P.-H., Shih, H.-N., Ueng, S. W. N., & Chang, Y. (2019). Synovial fluid interleukin-16, interleukin-18, and CRELD2 as novel biomarkers of prosthetic joint infections. *Bone & Joint Research*, *8*(4), 179–188. https://doi.org/10.1302/2046-3758.84.BJR-2018-0291.R1

Chonchol, M. (2006). HEMATOLOGY: ISSUES IN THE DIALYSIS PATIENT: Neutrophil Dysfunction and Infection Risk in End-Stage Renal Disease. *Seminars in Dialysis*, *19*(4), 291–296. https://doi.org/10.1111/j.1525-139X.2006.00175.x

Chupp, G. L., Wright, E. A., Wu, D., Vallen-Mashikian, M., Cruikshank, W. W., Center, D. M., Kornfeld, H., & Berman, J. S. (1998). Tissue and T Cell Distribution of Precursor and Mature IL-16. *The Journal of Immunology*, *161*(6), 3114–3119.

Cloke, T., Munder, M., Taylor, G., Müller, I., & Kropf, P. (2012). Characterization of a novel population of low-density granulocytes associated with disease severity in HIV-1 infection. *PloS One*, *7*(11), e48939. https://doi.org/10.1371/journal.pone.0048939

Cochat, P., Hulton, S.-A., Acquaviva, C., Danpure, C. J., Daudon, M., De Marchi, M., Fargue, S., Groothoff, J., Harambat, J., Hoppe, B., Jamieson, N. V., Kemper, M. J., Mandrile, G., Marangella, M., Picca, S., Rumsby, G., Salido, E., Straub, M., van Woerden, C. S., & on behalf of OxalEurope (). (2012). Primary hyperoxaluria Type 1: Indications for screening and guidance for diagnosis and treatment. *Nephrology Dialysis Transplantation*, *27*(5), 1729–1736. https://doi.org/10.1093/ndt/gfs078

Cohen, G. (2020). Immune Dysfunction in Uremia 2020. *Toxins*, *12*(7), 439. https://doi.org/10.3390/toxins12070439

Cohen, S. D., Phillips, T. M., Khetpal, P., & Kimmel, P. L. (2010). Cytokine patterns and survival in haemodialysis patients. *Nephrology, Dialysis, Transplantation: Official Publication of the European Dialysis and Transplant Association - European Renal Association*, *25*(4), 1239–1243. https://doi.org/10.1093/ndt/gfp625

Coillard, A., & Segura, E. (2019). In vivo Differentiation of Human Monocytes. *Frontiers in Immunology*, *10*, 1907. https://doi.org/10.3389/fimmu.2019.01907

Collin, M., & Bigley, V. (2018). Human dendritic cell subsets: An update. *Immunology*, *154*(1), 3–20. https://doi.org/10.1111/imm.12888

Collin, M., McGovern, N., & Haniffa, M. (2013). Human dendritic cell subsets. *Immunology*, *140*(1), 22–30. https://doi.org/10.1111/imm.12117

Collison, L. W., Workman, C. J., Kuo, T. T., Boyd, K., Wang, Y., Vignali, K. M., Cross, R., Sehy, D., Blumberg, R. S., & Vignali, D. A. A. (2007). The inhibitory cytokine IL-35 contributes to regulatory T-cell function. *Nature*, *450*(7169), 566–569. https://doi.org/10.1038/nature06306

Cooper, M. A., Fehniger, T. A., & Caligiuri, M. A. (2001). The biology of human natural killer-cell subsets. *Trends in Immunology*, *22*(11), 633–640. https://doi.org/10.1016/S1471-4906(01)02060-9

Costa, E., Lima, M., Alves, J. M., Rocha, S., Rocha-Pereira, P., Castro, E., Miranda, V., do, S. F. M., Loureiro, A., Quintanilha, A., Belo, L., & Santos-Silva, A. (2008). Inflammation, T-cell phenotype, and inflammatory cytokines in chronic kidney disease patients under hemodialysis and its relationship to resistance to recombinant human erythropoietin therapy. *Journal of Clinical Immunology*, *28*(3), 268–275. https://doi.org/10.1007/s10875-007-9168-x

Couser, W. G., Remuzzi, G., Mendis, S., & Tonelli, M. (2011). The contribution of chronic kidney disease to the global burden of major noncommunicable diseases. *Kidney International*, *80*(12), 1258–1270. https://doi.org/10.1038/ki.2011.368

Cozzolino, M., Mangano, M., Stucchi, A., Ciceri, P., Conte, F., & Galassi, A. (2018). Cardiovascular disease in dialysis patients. *Nephrology, Dialysis, Transplantation: Official Publication of the European Dialysis and Transplant Association - European Renal Association*, *33*(suppl_3), iii28–iii34. https://doi.org/10.1093/ndt/gfy174

Crivelli, J. J., Mitchell, T., Knight, J., Wood, K. D., Assimos, D. G., Holmes, R. P., & Fargue, S. (2021). Contribution of Dietary Oxalate and Oxalate Precursors to Urinary Oxalate Excretion. *Nutrients*, *13*(1), 62. https://doi.org/10.3390/nu13010062

Croq, F., Vizioli, J., Tuzova, M., Tahtouh, M., Sautiere, P.-E., Van Camp, C., Salzet, M., Cruikshank, W. W., Pestel, J., & Lefebvre, C. (2010). A homologous form of human interleukin 16 is implicated in microglia recruitment following nervous system injury in leech Hirudo medicinalis. *Glia*, *58*(14), 1649–1662. https://doi.org/10.1002/glia.21036

Cros, J., Cagnard, N., Woollard, K., Patey, N., Zhang, S.-Y., Senechal, B., Puel, A., Biswas, S. K., Moshous, D., Picard, C., Jais, J.-P., D'Cruz, D., Casanova, J.-L., Trouillet, C., & Geissmann, F. (2010). Human CD14dim Monocytes Patrol and Sense Nucleic Acids and Viruses via TLR7 and TLR8 Receptors. *Immunity*, *33*(3), 375–386. https://doi.org/10.1016/j.immuni.2010.08.012

Cruikshank, W., & Center, D. M. (1982). Modulation of lymphocyte migration by human lymphokines. II. Purification of a lymphotactic factor (LCF). *The Journal of Immunology*, *128*(6), 2569–2574.

Cruikshank, W. W., Kornfeld, H., & Center, D. M. (2000). Interleukin-16. *Journal of Leukocyte Biology*, *67*(6), 757–766. https://doi.org/10.1002/jlb.67.6.757

Cruikshank, W. W., Lim, K., Theodore, A. C., Cook, J., Fine, G., Weller, P. F., & Center, D. M. (1996). IL-16 inhibition of CD3-dependent lymphocyte activation and proliferation. *The Journal of Immunology*, *157*(12), 5240–5248.

Cruz, E. F. da, Cendoroglo, M., Manfredi, S. R., Eugênia Canziani, M., Quinto, B. M. R., Grabulosa, C. C., Guimarães-Souza, N. K., Peres, A. T., Carvalho, J. T. G. de, Batista, M. C., & Dalboni, M. A. (2014). Effect of Indoxyl Sulfate on Oxidative Stress, Apoptosis, and Monocyte Chemoattractant Protein-1 in Leukocytes. *ISRN Oxidative Medicine*, *2014*, 1–7. https://doi.org/10.1155/2014/412389

de Jager, D. J. (2009). Cardiovascular and Noncardiovascular Mortality Among Patients Starting Dialysis. *JAMA*, *302*(16), 1782. https://doi.org/10.1001/jama.2009.1488

Deng, Y., Ye, J., Luo, Q., Huang, Z., Peng, Y., Xiong, G., Guo, Y., Jiang, H., & Li, J. (2016). Low-Density Granulocytes Are Elevated in Mycobacterial Infection and Associated with the Severity of Tuberculosis. *PloS One*, *11*(4), e0153567. https://doi.org/10.1371/journal.pone.0153567

Desai, J., Foresto-Neto, O., Honarpisheh, M., Steiger, S., Nakazawa, D., Popper, B., Buhl, E. M., Boor, P., Mulay, S. R., & Anders, H.-J. (2017). Particles of different sizes and shapes induce neutrophil necroptosis followed by the release of neutrophil extracellular trap-like chromatin. *Scientific Reports*, *7*(1), 15003. https://doi.org/10.1038/s41598-017-15106-0

Desnues, B., Raoult, D., & Mege, J.-L. (2005). IL-16 is critical for Tropheryma whipplei replication in Whipple's disease. *Journal of Immunology (Baltimore, Md.: 1950)*, *175*(7), 4575–4582. https://doi.org/10.4049/jimmunol.175.7.4575

Dieter, B. P., McPherson, S. M., Afkarian, M., de Boer, I. H., Mehrotra, R., Short, R., Barbosa-Leiker, C., Alicic, R. Z., Meek, R. L., & Tuttle, K. R. (2016). Serum amyloid a and risk of death and end-stage renal disease in diabetic kidney disease. *Journal of Diabetes and Its Complications*, *30*(8), 1467–1472. https://doi.org/10.1016/j.jdiacomp.2016.07.018

do Sameiro-Faria, M., Ribeiro, S., Costa, E., Mendonça, D., Teixeira, L., Rocha-Pereira, P., Fernandes, J., Nascimento, H., Kohlova, M., Reis, F., Amado, L., Bronze-da-Rocha, E., Miranda, V., Quintanilha, A., Belo, L., & Santos-Silva, A. (2013). Risk Factors for Mortality in Hemodialysis Patients: Two-Year Follow-Up Study. *Disease Markers*, *35*(6), 791–798. https://doi.org/10.1155/2013/518945

Donate-Correa, J., Ferri, C. M., Sánchez-Quintana, F., Pérez-Castro, A., González-Luis, A., Martín-Núñez, E., Mora-Fernández, C., & Navarro-González, J. F. (2020). Inflammatory Cytokines in Diabetic Kidney Disease: Pathophysiologic and Therapeutic Implications. *Frontiers in Medicine*, *7*, 628289. https://doi.org/10.3389/fmed.2020.628289

Dounousi, E., Koliousi, E., Papagianni, A., Ioannou, K., Zikou, X., Katopodis, K., Kelesidis, A., Tsakiris, D., & Siamopoulos, K. C. (2012). Mononuclear leukocyte apoptosis and inflammatory markers in patients with chronic kidney disease. *American Journal of Nephrology*, *36*(6), 531–536. https://doi.org/10.1159/000345352

Drifte, G., Dunn-Siegrist, I., Tissières, P., & Pugin, J. (2013). Innate immune functions of immature neutrophils in patients with sepsis and severe systemic inflammatory response syndrome. *Critical Care Medicine*, *41*(3), 820–832. https://doi.org/10.1097/CCM.0b013e318274647d

Duranton, F., Cohen, G., De Smet, R., Rodriguez, M., Jankowski, J., Vanholder, R., Argiles, A., & European Uremic Toxin Work Group. (2012). Normal and pathologic concentrations of uremic toxins. *Journal of the American Society of Nephrology: JASN*, *23*(7), 1258–1270. https://doi.org/10.1681/ASN.2011121175

Ebert, T., Pawelzik, S.-C., Witasp, A., Arefin, S., Hobson, S., Kublickiene, K., Shiels, P. G., Bäck, M., & Stenvinkel, P. (2020). Inflammation and Premature Ageing in Chronic Kidney Disease. *Toxins*, *12*(4), 227. https://doi.org/10.3390/toxins12040227

Elferink, J. G., & Riemersma, R. C. (1980). Calcium oxalate crystal-induced cytolysis in polymorphonuclear leukocytes and erythrocytes. *Agents and Actions*, *10*(5), 439–444. https://doi.org/10.1007/BF01968044

Elssner, A., Doseff, A. I., Duncan, M., Kotur, M., & Wewers, M. D. (2004). IL-16 Is Constitutively Present in Peripheral Blood Monocytes and Spontaneously Released During Apoptosis. *The Journal of Immunology*, *172*(12), 7721–7725. https://doi.org/10.4049/jimmunol.172.12.7721

Ermer, T., Eckardt, K.-U., Aronson, P. S., & Knauf, F. (2016). Oxalate, inflammasome, and progression of kidney disease: *Current Opinion in Nephrology and Hypertension*, *25*(4), 363–371. https://doi.org/10.1097/MNH.0000000000000229

Ermer, T., Kopp, C., Asplin, J. R., Granja, I., Perazella, M. A., Reichel, M., Nolin, T. D., Eckardt, K.-U., Aronson, P. S., Finkelstein, F. O., & Knauf, F. (2017). Impact of Regular or Extended Hemodialysis and Hemodialfiltration on Plasma Oxalate Concentrations in Patients With End-Stage Renal Disease. *Kidney International Reports*, *2*(6), 1050–1058. https://doi.org/10.1016/j.ekir.2017.06.002

EUTox. (2021). *Eutox – European Uremic Toxin (EUTox) Work Group*. https://www.uremic-toxins.org/

Fajgenbaum, D. C., & June, C. H. (2020). Cytokine Storm. *New England Journal of Medicine*. https://doi.org/10.1056/NEJMra2026131

Fellström, B., Helmersson-Karlqvist, J., Lind, L., Soveri, I., Thulin, M., Ärnlöv, J., Kultima, K., & Larsson, A. (2021). Strong Associations Between Early Tubular Damage and Urinary Cytokine, Chemokine, and Growth Factor Levels in Elderly Males and Females. *Journal of Interferon & Cytokine Research: The Official Journal of the International Society for Interferon and Cytokine Research*, *41*(8), 283–290. https://doi.org/10.1089/jir.2021.0065

Fernández-Laso, V., Sastre, C., Valdivielso, J. M., Betriu, A., Fernández, E., Egido, J., Martín-Ventura, J. L., & Blanco-Colio, L. M. (2016). Soluble TWEAK and Major Adverse Cardiovascular Events in Patients with CKD. *Clinical Journal of the American Society of Nephrology*, *11*(3), 413–422. https://doi.org/10.2215/CJN.07900715

Frank, D., & Vince, J. E. (2019). Pyroptosis versus necroptosis: Similarities, differences, and crosstalk. *Cell Death & Differentiation*, *26*(1), 99–114. https://doi.org/10.1038/s41418-018-0212-6

Freitas, G. R. R., da Luz Fernandes, M., Agena, F., Jaluul, O., Silva, S. C., Lemos, F. B. C., Coelho, V., Elias, D.-N., & Galante, N. Z. (2019). Aging and End Stage Renal Disease Cause A Decrease in Absolute Circulating Lymphocyte Counts with A Shift to A Memory Profile and Diverge in Treg Population. *Aging and Disease*, *10*(1), 49–61. https://doi.org/10.14336/AD.2018.0318

Fromm, P. D., Silveira, P. A., Hsu, J. L., Papadimitrious, M. S., Lo, T.-H., Ju, X., Kupresanin, F., Romano, A., Hsu, W.-H., Bryant, C. E., Kong, B., Abadir, E., Mekkawy, A., M. McGuire, H., Groth, B. F. de St., Cunningham, I., Newman, E., Gibson, J., Hogarth, P. M., … Clark, G. J. (2020). Distinguishing human peripheral blood CD16+ myeloid cells based on phenotypic characteristics. *Journal of Leukocyte Biology*, *107*(2), 323–339. https://doi.org/10.1002/JLB.5A1119-362RRR

Fukushi, T., Yamamoto, T., Yoshida, M., Fujikura, E., Miyazaki, M., & Nakayama, M. (2020). Enhanced neutrophil apoptosis accompanying myeloperoxidase release during hemodialysis. *Scientific Reports*, *10*(1), 21747. https://doi.org/10.1038/s41598-020-78742-z

Gadaen, R. J. R., Kooman, J. P., Cornelis, T., Sande, F. M. van der, Winkens, B. J., & Broers, N. J. H. (2021). The Effects of Chronic Dialysis on Physical Status, Quality of Life, and Arterial Stiffness: A Longitudinal Study in Prevalent Dialysis Patients. *Nephron*, *145*(1), 44–54. https://doi.org/10.1159/000510624

Gandjour, A., Armsen, W., Wehmeyer, W., Multmeier, J., & Tschulena, U. (2020). Costs of patients with chronic kidney disease in Germany. *PLOS ONE*, *15*(4), e0231375. https://doi.org/10.1371/journal.pone.0231375

Gemeinsamer Bundesausschuss. (2020). *Qualitätssicherungs—Dialyse: Veröffentlichung des Jahresberichts 2019 zur Qualität in der Dialyse*. https://www.g-ba.de/beschluesse/4568/

Georgiev, P., Charbonnier, L.-M., & Chatila, T. A. (2019). Regulatory T Cells: The Many Faces of Foxp3. *Journal of Clinical Immunology*, *39*(7), 623–640. https://doi.org/10.1007/s10875-019-00684-7

Ghadiani, M. H., Besharati, S., Mousavinasab, N., & Jalalzadeh, M. (2012). Response rates to HB vaccine in CKD stages 3-4 and hemodialysis patients. *Journal of Research in Medical Sciences: The Official Journal of Isfahan University of Medical Sciences*, *17*(6), 527–533.

Ghaffari, S., Torabi-Rahvar, M., Omidkhoda, A., & Ahmadbeigi, N. (2019). Impact of various culture conditions on ex vivo expansion of polyclonal T cells for adoptive immunotherapy. *APMIS: Acta Pathologica, Microbiologica, et Immunologica Scandinavica*, *127*(12), 737–745. https://doi.org/10.1111/apm.12981

Gisterå, A., & Hansson, G. K. (2017). The immunology of atherosclerosis. *Nature Reviews Nephrology*, *13*(6), 368–380. https://doi.org/10.1038/nrneph.2017.51

Glas, J., Török, H. P., Unterhuber, H., Radlmayr, M., & Folwaczny, C. (2003). The -295T-to-C promoter polymorphism of the IL-16 gene is associated with Crohn's disease. *Clinical Immunology (Orlando, Fla.)*, *106*(3), 197–200. https://doi.org/10.1016/s1521-6616(03)00021-4

Glowacka, E., Banasik, M., Lewkowicz, P., & Tchorzewski, H. (2002). The effect of LPS on neutrophils from patients with high risk of type 1 diabetes mellitus in relation to IL-8, IL-10 and IL-12 production and apoptosis in vitro. *Scandinavian Journal of Immunology*, *55*(2), 210–217. https://doi.org/10.1046/j.1365-3083.2002.01046.x

Gohda, T., Maruyama, S., Kamei, N., Yamaguchi, S., Shibata, T., Murakoshi, M., Horikoshi, S., Tomino, Y., Ohsawa, I., Gotoh, H., Nojiri, S., & Suzuki, Y. (2017). Circulating TNF Receptors 1 and 2 Predict Mortality in Patients with End-stage Renal Disease Undergoing Dialysis. *Scientific Reports*, *7*(1), 43520. https://doi.org/10.1038/srep43520

Goicoechea, M., de Vinuesa, S. G., Gómez-Campderá, F., Aragoncillo, I., Verdalles, U., Mosse, A., & Luño, J. (2008). Serum fibrinogen levels are an independent predictor of mortality in patients with chronic kidney disease (CKD) stages 3 and 4. *Kidney International*, *74*, S67–S70. https://doi.org/10.1038/ki.2008.519

Gollapudi, P., Yoon, J.-W., Gollapudi, S., Pahl, M. V., & Vaziri, N. D. (2010). Leukocyte toll-like receptor expression in end-stage kidney disease. *American Journal of Nephrology*, *31*(3), 247–254. https://doi.org/10.1159/000276764

Gong, T., Liu, L., Jiang, W., & Zhou, R. (2020). DAMP-sensing receptors in sterile inflammation and inflammatory diseases. *Nature Reviews Immunology*, *20*(2), 95–112. https://doi.org/10.1038/s41577-019-0215-7

Gorvel, L., Al Moussawi, K., Ghigo, E., Capo, C., Mege, J.-L., & Desnues, B. (2010). Tropheryma whipplei, the Whipple's disease bacillus, induces macrophage apoptosis through the extrinsic pathway. *Cell Death & Disease*, *1*, e34. https://doi.org/10.1038/cddis.2010.11

Grabulosa, C. C., Manfredi, S. R., Canziani, M. E., Quinto, B. M. R., Barbosa, R. B., Rebello, J. F., Batista, M. C., Cendoroglo, M., & Dalboni, M. A. (2018). Chronic kidney disease induces inflammation by increasing Toll-like receptor-4, cytokine and cathelicidin expression in neutrophils and monocytes. *Experimental Cell Research*, *365*(2), 157–162. https://doi.org/10.1016/j.yexcr.2018.02.022

Gregg, L. P., Tio, M. C., Li, X., Adams-Huet, B., de Lemos, J. A., & Hedayati, S. S. (2018). Association of Monocyte Chemoattractant Protein-1 with Death and Atherosclerotic Events in Chronic Kidney Disease. *American Journal of Nephrology*, *47*(6), 395–405. https://doi.org/10.1159/000488806

Grégoire, C., Chasson, L., Luci, C., Tomasello, E., Geissmann, F., Vivier, E., & Walzer, T. (2007). The trafficking of natural killer cells. *Immunological Reviews*, *220*(1), 169–182. https://doi.org/10.1111/j.1600-065X.2007.00563.x

Grievink, H. W., Luisman, T., Kluft, C., Moerland, M., & Malone, K. E. (2016). Comparison of Three Isolation Techniques for Human Peripheral Blood Mononuclear Cells: Cell Recovery and Viability, Population Composition, and Cell Functionality. *Biopreservation and Biobanking*, *14*(5), 410–415. https://doi.org/10.1089/bio.2015.0104

Gu, X., Man, C., Zhang, H., & Fan, Y. (2019). High ankle-brachial index and risk of cardiovascular or all-cause mortality: A meta-analysis. *Atherosclerosis*, *282*, 29–36. https://doi.org/10.1016/j.atherosclerosis.2018.12.028

Guilliams, M., Mildner, A., & Yona, S. (2018). Developmental and Functional Heterogeneity of Monocytes. *Immunity*, *49*(4), 595–613. https://doi.org/10.1016/j.immuni.2018.10.005

Guo, H., & Ting, J. P.-Y. (2020). Inflammasome Assays In Vitro and in Mouse Models. *Current Protocols in Immunology*, *131*(1), e107. https://doi.org/10.1002/cpim.107

Guo, Q., Carrero, J. J., Yu, X., Barany, P., Qureshi, A. R., Eriksson, M., Anderstam, B., Chmielewski, M., Heimburger, O., Stenvinkel, P., Lindholm, B., & Axelsson, J. (2009). Associations of VEGF and its receptors sVEGFR-1 and -2 with cardiovascular disease and survival in prevalent haemodialysis patients. *Nephrology Dialysis Transplantation*, *24*(11), 3468–3473. https://doi.org/10.1093/ndt/gfp315

Gupta, J., Mitra, N., Kanetsky, P. A., Devaney, J., Wing, M. R., Reilly, M., Shah, V. O., Balakrishnan, V. S., Guzman, N. J., Girndt, M., Periera, B. G., Feldman, H. I., Kusek, J. W., Joffe, M. M., Raj, D. S., & Investigators, for the C. S. (2012). Association between Albuminuria, Kidney Function, and Inflammatory Biomarker Profile in CKD in CRIC. *Clinical Journal of the American Society of Nephrology*, *7*(12), 1938–1946. https://doi.org/10.2215/CJN.03500412

Hacbarth, E., & Kajdacsy-Balla, A. (1986). Low density neutrophils in patients with systemic lupus erythematosus, rheumatoid arthritis, and acute rheumatic fever. *Arthritis and Rheumatism*, *29*(11), 1334–1342. https://doi.org/10.1002/art.1780291105

Hadadi, E., Zhang, B., Baidžajevas, K., Yusof, N., Puan, K. J., Ong, S. M., Yeap, W. H., Rotzschke, O., Kiss-Toth, E., Wilson, H., & Wong, S. C. (2016). Differential IL-1β secretion by monocyte subsets is regulated by Hsp27 through modulating mRNA stability. *Scientific Reports*, *6*(1), 39035. https://doi.org/10.1038/srep39035

Hamed, S. A. (2019). Neurologic conditions and disorders of uremic syndrome of chronic kidney disease: Presentations, causes, and treatment strategies. *Expert Review of Clinical Pharmacology*, *12*(1), 61–90. https://doi.org/10.1080/17512433.2019.1555468

Har, R. L. H., Reich, H. N., Scholey, J. W., Daneman, D., Dunger, D. B., Moineddin, R., Dalton, R. N., Motran, L., Elia, Y., Deda, L., Ostrovsky, M., Sochett, E. B., Mahmud, F. H., & Cherney, D. Z. I. (2014). The urinary cytokine/chemokine signature of renal hyperfiltration in adolescents with type 1 diabetes. *PloS One*, *9*(11), e111131. https://doi.org/10.1371/journal.pone.0111131

Harm, S., Schildböck, C., & Hartmann, J. (2020). Cytokine Removal in Extracorporeal Blood Purification: An in vitro Study. *Blood Purification*, *49*(1–2), 33–43. https://doi.org/10.1159/000502680

Hassani, M., Hellebrekers, P., Chen, N., van Aalst, C., Bongers, S., Hietbrink, F., Koenderman, L., & Vrisekoop, N. (2020). On the origin of low-density neutrophils. *Journal of Leukocyte Biology*, *107*(5), 809–818. https://doi.org/10.1002/JLB.5HR0120-459R

Heine, G. H., Ortiz, A., Massy, Z. A., Lindholm, B., Wiecek, A., Martínez-Castelao, A., Covic, A., Goldsmith, D., Süleymanlar, G., London, G. M., Parati, G., Sicari, R., Zoccali, C., & Fliser, D. (2012). Monocyte subpopulations and cardiovascular risk in chronic kidney disease. *Nature Reviews Nephrology*, *8*(6), 362–369. https://doi.org/10.1038/nrneph.2012.41

Heine, G. H., Ulrich, C., Seibert, E., Seiler, S., Marell, J., Reichart, B., Krause, M., Schlitt, A., Köhler, H., & Girndt, M. (2008). CD14(++)CD16+ monocytes but not total monocyte numbers predict cardiovascular events in dialysis patients. *Kidney International*, *73*(5), 622–629. https://doi.org/10.1038/sj.ki.5002744

Heinrich, P. C., Müller, M., & Graeve, L. (Hrsg.). (2014). *Löffler/Petrides Biochemie und Pathobiochemie*. Springer Berlin Heidelberg. https://doi.org/10.1007/978-3-642-17972-3

Hénaut, L., Candellier, A., Boudot, C., Grissi, M., Mentaverri, R., Choukroun, G., Brazier, M., Kamel, S., & Massy, Z. A. (2019). New Insights into the Roles of Monocytes/Macrophages in Cardiovascular Calcification Associated with Chronic Kidney Disease. *Toxins*, *11*(9), 529. https://doi.org/10.3390/toxins11090529

Herberman, R. B., Nunn, M. E., & Lavrin, D. H. (1975). Natural cytotoxic reactivity of mouse lymphoid cells against syngeneic and allogeneic tumors. I. Distribution of reactivity and specificity. *International Journal of Cancer*, *16*(2), 216–229. https://doi.org/10.1002/ijc.2910160204

Higo, T., Duronio, V., Tudan, C., Burt, H. M., & Jackson, J. K. (2010). Calcium pyrophosphate dihydrate crystal-induced inhibition of neutrophil apoptosis: Involvement of Bcl-2 family members. *Inflammation Research: Official Journal of the European Histamine Research Society ... [et Al.]*, *59*(1), 71–81. https://doi.org/10.1007/s00011-009-0073-z

Hill, N. R., Fatoba, S. T., Oke, J. L., Hirst, J. A., O'Callaghan, C. A., Lasserson, D. S., & Hobbs, F. D. R. (2016). Global Prevalence of Chronic Kidney Disease – A Systematic Review and Meta-Analysis. *PLOS ONE*, *11*(7), e0158765. https://doi.org/10.1371/journal.pone.0158765

Himmelfarb, J., Le, P., Klenzak, J., Freedman, S., McMenamin, M. E., Ikizler, T. A., & PICARD Group. (2004). Impaired monocyte cytokine production in critically ill patients with acute renal failure. *Kidney International*, *66*(6), 2354–2360. https://doi.org/10.1111/j.1523-1755.2004.66023.x

Holmes, R. P., & Assimos, D. G. (1998). *GLYOXYLATE SYNTHESIS, AND ITS MODULATION AND INFLUENCE ON OXALATE SYNTHESIS*. 8.

Hori, S., Nomura, T., & Sakaguchi, S. (2003). Control of Regulatory T Cell Development by the Transcription Factor Foxp3. *Science*, *299*(5609), 1057–1061. https://doi.org/10.1126/science.1079490

Hung, S.-C., Hsu, T.-W., Lin, Y.-P., & Tarng, D.-C. (2012). Decoy Receptor 3, a Novel Inflammatory Marker, and Mortality in Hemodialysis Patients. *Clinical Journal of the American Society of Nephrology*, *7*(8), 1257–1265. https://doi.org/10.2215/CJN.08410811

Iseki, K., Tozawa, M., Yoshi, S., & Fukiyama, K. (1999). Serum C-reactive protein (CRP) and risk of death in chronic dialysis patients. *Nephrology Dialysis Transplantation*, *14*(8), 1956–1960. https://doi.org/10.1093/ndt/14.8.1956

Ishigami, J., & Matsushita, K. (2019). Clinical epidemiology of infectious disease among patients with chronic kidney disease. *Clinical and Experimental Nephrology*, *23*(4), 437–447. https://doi.org/10.1007/s10157-018-1641-8

Jaber, B. L., Balakrishnan, V. S., Cendoroglo, M. N., Perianayagam, M. C., King, A. J., & Pereira, B. J. G. (1998). Modulation of Neutrophil Apoptosis by Uremic Plasma during Hemodialysis. *Blood Purification*, *16*(6), 325–335. https://doi.org/10.1159/000014352

Jaber, B. L., Perianayagam, M. C., Balakrishnan, V. S., King, A. J., & Pereira, B. J. G. (2001). Mechanisms of neutrophil apoptosis in uremia and relevance of the Fas (APO-1, CD95)/Fas ligand system. *Journal of Leukocyte Biology*, *69*(6), 1006–1012. https://doi.org/10.1189/jlb.69.6.1006

Jankowski, J., Floege, J., Fliser, D., Böhm, M., & Marx, N. (2021). Cardiovascular Disease in Chronic Kidney Disease. *Circulation*, *143*(11), 1157–1172. https://doi.org/10.1161/CIRCULATIONAHA.120.050686

Jarad, G., & Miner, J. H. (2009). Update on the glomerular filtration barrier. *Current opinion in nephrology and hypertension*, *18*(3), 226–232.

Jerram, A., Guy, T. V., Beutler, L., Gunasegaran, B., Sluyter, R., Fazekas de St Groth, B., & McGuire, H. M. (2021). Effects of storage time and temperature on highly multiparametric flow analysis of peripheral blood samples; implications for clinical trial samples. *Bioscience Reports*, *41*(2), BSR20203827. https://doi.org/10.1042/BSR20203827

Jiang, Y.-H., Jhang, J.-F., Hsu, Y.-H., Ho, H.-C., Wu, Y.-H., & Kuo, H.-C. (2020). Urine cytokines as biomarkers for diagnosing interstitial cystitis/bladder pain syndrome and mapping its clinical characteristics. *American Journal of Physiology. Renal Physiology*, *318*(6), F1391–F1399. https://doi.org/10.1152/ajprenal.00051.2020

Justiz Vaillant, A. A., Jamal, Z., & Ramphul, K. (2021). Immunoglobulin. In *StatPearls*. StatPearls Publishing. http://www.ncbi.nlm.nih.gov/books/NBK513460/

Kalyan, S., & Kabelitz, D. (2013). Defining the nature of human γδ T cells: A biographical sketch of the highly empathetic. *Cellular & Molecular Immunology*, *10*(1), 21–29. https://doi.org/10.1038/cmi.2012.44

Kaser, A., Dunzendorfer, S., Offner, F. A., Ludwiczek, O., Enrich, B., Koch, R. O., Cruikshank, W. W., Wiedermann, C. J., & Tilg, H. (2000). B Lymphocyte-Derived IL-16 Attracts Dendritic Cells and Th Cells. *The Journal of Immunology*, *165*(5), 2474–2480. https://doi.org/10.4049/jimmunol.165.5.2474

Kaser, A., Dunzendorfer, S., Offner, F. A., Ryan, T., Schwabegger, A., Cruikshank, W. W., Wiedermann, C. J., & Tilg, H. (1999). A Role for IL-16 in the Cross-Talk Between Dendritic Cells and T Cells. *The Journal of Immunology*, *163*(6), 3232–3238.

Kashfi, S. M. H., Behboudi Farahbakhsh, F., Nazemalhosseini Mojarad, E., Mashayekhi, K., Azimzadeh, P., Romani, S., Derakhshani, S., Malekpour, H., Asadzadeh Aghdaei, H., & Zali, M. R. (2016). Interleukin-16 polymorphisms as new promising biomarkers for risk of gastric cancer. *Tumor Biology*, *37*(2), 2119–2126. https://doi.org/10.1007/s13277-015-4013-y

Kato, S., Chmielewski, M., Honda, H., Pecoits-Filho, R., Matsuo, S., Yuzawa, Y., Tranaeus, A., Stenvinkel, P., & Lindholm, B. (2008). Aspects of immune dysfunction in end-stage renal disease. *Clinical Journal of the American Society of Nephrology: CJASN*, *3*(5), 1526–1533. https://doi.org/10.2215/CJN.00950208

Kawabata, K., Makino, T., Makino, K., Kajihara, I., Fukushima, S., & Ihn, H. (2020). IL-16 expression is increased in the skin and sera of patients with systemic sclerosis. *Rheumatology*, *59*(3), 519–523. https://doi.org/10.1093/rheumatology/kez318

Keane, J., Nicoll, J., Kim, S., Wu, D. M. H., Cruikshank, W. W., Brazer, W., Natke, B., Zhang, Y., Center, D. M., & Kornfeld, H. (1998). Conservation of Structure and Function Between Human and Murine IL-16. *The Journal of Immunology*, *160*(12), 5945–5954.

Keates, A. C., Castagliuolo, I., Cruickshank, W. W., Qiu, B., Arseneau, K. O., Brazer, W., & Kelly, C. P. (2000). Interleukin 16 is up-regulated in Crohn's disease and participates in TNBS colitis in mice. *Gastroenterology*, *119*(4), 972–982. https://doi.org/10.1053/gast.2000.18164

Kelley, N., Jeltema, D., Duan, Y., & He, Y. (2019). The NLRP3 Inflammasome: An Overview of Mechanisms of Activation and Regulation. *International Journal of Molecular Sciences*, *20*(13), 3328. https://doi.org/10.3390/ijms20133328

Kildey, K., Rooks, K., Weier, S., Flower, R. L., & Dean, M. M. (2014). Effect of age, gender and mannose-binding lectin (MBL) status on the inflammatory profile in peripheral blood plasma of Australian blood donors. *Human Immunology*, *75*(9), 973–979. https://doi.org/10.1016/j.humimm.2014.08.200

Kim, J.-K., Hong, C.-W., Park, M. J., Song, Y. R., Kim, H. J., & Kim, S. G. (2017). Increased Neutrophil Extracellular Trap Formation in Uremia Is Associated with Chronic Inflammation and Prevalent Coronary Artery Disease. *Journal of Immunology Research*, *2017*, 8415179. https://doi.org/10.1155/2017/8415179

Kjekshus, J. (2015). Inflammation: Friend and Foe. *EBioMedicine*, *2*(7), 634–635. https://doi.org/10.1016/j.ebiom.2015.05.029

Knauf, F., Asplin, J. R., Granja, I., Schmidt, I. M., Moeckel, G. W., David, R. J., Flavell, R. A., & Aronson, P. S. (2013). NALP3-mediated inflammation is a principal cause of progressive renal failure in oxalate nephropathy. *Kidney International*, *84*(5), 895–901. https://doi.org/10.1038/ki.2013.207

Koc, M., Toprak, A., Arikan, H., Odabasi, Z., Elbir, Y., Tulunay, A., Asicioglu, E., Eksioglu-Demiralp, E., Glorieux, G., Vanholder, R., & Akoglu, E. (2011). Toll-like receptor expression in monocytes in patients with chronic kidney disease and haemodialysis: Relation with inflammation. *Nephrology, Dialysis, Transplantation: Official Publication of the European Dialysis and Transplant Association - European Renal Association*, *26*(3), 955–963. https://doi.org/10.1093/ndt/gfq500

Kofanova, O., Henry, E., Aguilar Quesada, R., Bulla, A., Navarro Linares, H., Lescuyer, P., Shea, K., Stone, M., Tybring, G., Bellora, C., & Betsou, F. (2018). IL8 and IL16 levels indicate serum and plasma quality. *Clinical Chemistry and Laboratory Medicine (CCLM)*, *56*(7), 1054–1062. https://doi.org/10.1515/cclm-2017-1047

Korzeniewska-Dyl, I., Wróblewski, K., Majewska, E., & Moczulski, D. (2010). The effect of uremia and hemodialysis on caspase-1 and caspase-3 activity in neutrophils. *Journal of Nephrology*, *23*(4), 425–430.

Kotas, M. E., & Medzhitov, R. (2015). Homeostasis, Inflammation, and Disease Susceptibility. *Cell*, *160*(5), 816–827. https://doi.org/10.1016/j.cell.2015.02.010

Krug, N., Cruikshank, W. W., Tschernig, T., Erpenbeck, V. J., Balke, K., Hohlfeld, J. M., Center, D. M., & Fabel, H. (2000). Interleukin 16 and T-cell chemoattractant activity in bronchoalveolar lavage 24 hours after allergen challenge in asthma. *American Journal of Respiratory and Critical Care Medicine*, *162*(1), 105–111. https://doi.org/10.1164/ajrccm.162.1.9908055

Krzanowski, M., Krzanowska, K., Gajda, M., Dumnicka, P., Dziewierz, A., Woziwodzka, K., Litwin, J. A., & Sułowicz, W. (2017). Pentraxin3 as a new indicator of cardiovascular-related death in patients with advanced chronic kidney disease? *Polish Archives of Internal Medicine*. https://doi.org/10.20452/pamw.3944

Kurschner, C., & Yuzaki, M. (1999). Neuronal Interleukin-16 (NIL-16): A Dual Function PDZ Domain Protein. *The Journal of Neuroscience*, *19*(18), 7770–7780. https://doi.org/10.1523/JNEUROSCI.19-18-07770.1999

Laberge, S., Cruikshank, W. W., Kornfeld, H., & Center, D. M. (1995). Histamine-induced secretion of lymphocyte chemoattractant factor from CD8+ T cells is independent of transcription and translation. Evidence for constitutive protein synthesis and storage. *Journal of Immunology (Baltimore, Md.: 1950)*, *155*(6), 2902–2910.

Ladwig, P. M., Liedtke, R. R., Larson, T. S., & Lieske, J. C. (2005). Sensitive spectrophotometric assay for plasma oxalate. *Clinical Chemistry*, *51*(12), 2377–2380. https://doi.org/10.1373/clinchem.2005.054353

Lahoz-Beneytez, J., Elemans, M., Zhang, Y., Ahmed, R., Salam, A., Block, M., Niederalt, C., Asquith, B., & Macallan, D. (2016). Human neutrophil kinetics: Modeling of stable isotope labeling data supports short blood neutrophil half-lives. *Blood*, *127*(26), 3431–3438. https://doi.org/10.1182/blood-2016-03-700336

Lai, L., Alaverdi, N., Maltais, L., & Morse, H. C. (1998). Mouse Cell Surface Antigens: Nomenclature and Immunophenotyping. *The Journal of Immunology*, *160*(8), 3861–3868.

Lakschevitz, F. S., Hassanpour, S., Rubin, A., Fine, N., Sun, C., & Glogauer, M. (2016). Identification of neutrophil surface marker changes in health and inflammation using high-throughput screening flow cytometry. *Experimental Cell Research*, *342*(2), 200–209. https://doi.org/10.1016/j.yexcr.2016.03.007

Lange, J. N., Wood, K. D., Knight, J., Assimos, D. G., & Holmes, R. P. (2012). Glyoxal Formation and Its Role in Endogenous Oxalate Synthesis. *Advances in Urology*, *2012*, e819202. https://doi.org/10.1155/2012/819202

Larsson, A., Carlsson, L., Gordh, T., Lind, A.-L., Thulin, M., & Kamali-Moghaddam, M. (2015). The effects of age and gender on plasma levels of 63 cytokines. *Journal of Immunological Methods*, *425*, 58–61. https://doi.org/10.1016/j.jim.2015.06.009

Lawrence, S. M., Corriden, R., & Nizet, V. (2020). How Neutrophils Meet Their End. *Trends in Immunology*, *41*(6), 531–544. https://doi.org/10.1016/j.it.2020.03.008

LeBien, T. W., & Tedder, T. F. (2008). B lymphocytes: How they develop and function. *Blood*, *112*(5), 1570–1580. https://doi.org/10.1182/blood-2008-02-078071

Lee, S., Kaneko, H., Sekigawa, I., Tokano, Y., Takasaki, Y., & Hashimoto, H. (1998). Circulating interleukin-16 in systemic lupus erythematosus. *Rheumatology*, *37*(12), 1334–1337. https://doi.org/10.1093/rheumatology/37.12.1334

Levey, A. S., & Coresh, J. (2012). Chronic kidney disease. *The Lancet*, *379*(9811), 165–180. https://doi.org/10.1016/S0140-6736(11)60178-5

Levey, A. S., Eckardt, K.-U., Dorman, N. M., Christiansen, S. L., Hoorn, E. J., Ingelfinger, J. R., Inker, L. A., Levin, A., Mehrotra, R., Palevsky, P. M., Perazella, M. A., Tong, A., Allison, S. J., Bockenhauer, D., Briggs, J. P., Bromberg, J. S., Davenport, A., Feldman, H. I., Fouque, D., … Winkelmayer, W. C. (2020). Nomenclature for kidney function and disease: Report of a Kidney Disease: Improving Global Outcomes (KDIGO) Consensus Conference. *Kidney International*, *97*(6), 1117–1129. https://doi.org/10.1016/j.kint.2020.02.010

Levey, A. S., Eckardt, K.-U., Tsukamoto, Y., Levin, A., Coresh, J., Rossert, J., Zeeuw, D. D. E., Hostetter, T. H., Lameire, N., & Eknoyan, G. (2005). Definition and classification of chronic kidney disease: A position statement from Kidney Disease: Improving Global Outcomes (KDIGO). *Kidney International*, *67*(6), 2089–2100. https://doi.org/10.1111/j.1523-1755.2005.00365.x

Li, C., Dai, J., Dong, G., Ma, Q., Li, Z., Zhang, H., Yan, F., Zhang, J., Wang, B., Shi, H., Zhu, Y., Yao, X., Si, C., & Xiong, H. (2019). Interleukin-16 aggravates ovalbumin-induced allergic inflammation by enhancing Th2 and Th17 cytokine production in a mouse model. *Immunology*, *157*(3), 257–267. https://doi.org/10.1111/imm.13068

Li, J.-J., Wei, W., Shi, H.-Z., Li, Y.-X., & Mo, W.-N. (2011). Cellular sources of interleukin 16 in benign and malignant pleural effusions. *Chinese Medical Journal*, *124*(24), 4160–4165.

Li, Y., Huang, H., Liu, B., Zhang, Y., Pan, X., Yu, X.-Y., Shen, Z., & Song, Y.-H. (2021). Inflammasomes as therapeutic targets in human diseases. *Signal Transduction and Targeted Therapy*, *6*(1), 1–14. https://doi.org/10.1038/s41392-021-00650-z

Libetta, C., Esposito, P., Sepe, V., Portalupi, V., Margiotta, E., Canevari, M., & Dal Canton, A. (2010). Dialysis treatment and regulatory T cells. *Nephrology Dialysis Transplantation*, *25*(5), 1723–1727. https://doi.org/10.1093/ndt/gfq055

Lichtenauer, M., Franz, M., Fritzenwanger, M., Figulla, H.-R., Gerdes, N., & Jung, C. (2015). Elevated Plasma Levels of Interleukin-12p40 and Interleukin-16 in Overweight Adolescents. *BioMed Research International*, *2015*. https://doi.org/10.1155/2015/940910

Lieske, J. C., Rule, A. D., Krambeck, A. E., Williams, J. C., Bergstralh, E. J., Mehta, R. A., & Moyer, T. P. (2014). Stone Composition as a Function of Age and Sex. *Clinical Journal of the American Society of Nephrology*, *9*(12), 2141–2146. https://doi.org/10.2215/CJN.05660614

Lim, K. G., Wan, H. C., Bozza, P. T., Resnick, M. B., Wong, D. T., Cruikshank, W. W., Kornfeld, H., Center, D. M., & Weller, P. F. (1996). Human eosinophils elaborate the lymphocyte chemoattractants. IL-16 (lymphocyte chemoattractant factor) and RANTES. *The Journal of Immunology*, *156*(7), 2566–2570.

Lindner, A., Charra, B., Sherrard, D. J., & Scribner, B. H. (1974, März 28). *Accelerated Atherosclerosis in Prolonged Maintenance Hemodialysis* (world) [Research-article]. Http://Dx.Doi.Org/10.1056/NEJM197403282901301; Massachusetts Medical Society. https://doi.org/10.1056/NEJM197403282901301

Lisowska, K. A., Dębska-Ślizień, A., Jasiulewicz, A., Bryl, E., & Witkowski, J. M. (2014). Influence of hemodialysis on circulating CD4(low)CD25 (high) regulatory T cells in end-stage renal disease patients. *Inflammation Research: Official Journal of the European Histamine Research Society ... [et Al.]*, *63*(2), 99–103. https://doi.org/10.1007/s00011-013-0679-z

Litjens, N. H. R., van Druningen, C. J., & Betjes, M. G. H. (2006). Progressive loss of renal function is associated with activation and depletion of naive T lymphocytes. *Clinical Immunology (Orlando, Fla.)*, *118*(1), 83–91. https://doi.org/10.1016/j.clim.2005.09.007

Liu, W., Putnam, A. L., Xu-yu, Z., Szot, G. L., Lee, M. R., Zhu, S., Gottlieb, P. A., Kapranov, P., Gingeras, T. R., de St. Groth, B. F., Clayberger, C., Soper, D. M., Ziegler, S. F., & Bluestone, J. A. (2006). CD127 expression inversely correlates with FoxP3 and suppressive function of human CD4+ T reg cells. *Journal of Experimental Medicine*, *203*(7), 1701–1711. https://doi.org/10.1084/jem.20060772

Liu, X., Du, J., Zhou, Y., Shu, Q., & Li, Y. (2013). Interleukin-16 polymorphism is associated with an increased risk of ischemic stroke. *Mediators of Inflammation*, *2013*, 564750. https://doi.org/10.1155/2013/564750

Liu, Z., Kan, Y.-H., Wei, Y.-D., Li, X.-J., Yang, F., Hou, Y., & Du, Y.-J. (2015). Decreased number of CD14+TLR4+ monocytes and their impaired cytokine responses to lipopolysaccharide in patients with chronic kidney disease. *Journal of Huazhong University of Science and Technology. Medical Sciences = Hua Zhong Ke Ji Da Xue Xue Bao. Yi Xue Ying De Wen Ban = Huazhong Keji Daxue Xuebao. Yixue Yingdewen Ban*, *35*(2), 206–211. https://doi.org/10.1007/s11596-015-1412-7

Long, S.-F., Chen, G.-A., & Fang, M.-S. (2015). Levels of interleukin-16 in peripheral blood of 52 patients with multiple myeloma and its clinical significance. *International Journal of Clinical and Experimental Medicine*, *8*(12), 22520–22524.

Lopez, P. A., & Hulspas, R. (2020). Special Issue on Enhancement of Reproducibility and Rigor. *Cytometry. Part A: The Journal of the International Society for Analytical Cytology*, *97*(2), 105–106. https://doi.org/10.1002/cyto.a.23972

Lorenzatti, A. J. (2021). Anti-inflammatory Treatment and Cardiovascular Outcomes: Results of Clinical Trials. *European Cardiology*, *16*, e15. https://doi.org/10.15420/ecr.2020.51

Luo, Q.-S., Wang, J.-L., Deng, Y.-Y., Huang, H.-D., Fu, H.-D., Li, C.-Y., & Huang, H.-N. (2014). Interleukin-16 Polymorphism Is Associated with an Increased Risk of Glioma. *Genetic Testing and Molecular Biomarkers*, *18*(10), 711–714. https://doi.org/10.1089/gtmb.2014.0170

Luo, S.-X., Li, S., Zhang, X.-H., Zhang, J.-J., Long, G.-H., Dong, G.-F., Su, W., Deng, Y., Liu, Y., Zhao, J.-M., & Qin, X. (2015). Genetic Polymorphisms of Interleukin-16 and Risk of Knee Osteoarthritis. *PLOS ONE*, *10*(5), e0123442. https://doi.org/10.1371/journal.pone.0123442

Luttmann, W., Bratke, K., Küpper, M., & Myrtek, D. (2014). *Der Experimentator: Immunologie*. Springer Berlin Heidelberg. https://doi.org/10.1007/978-3-642-41899-0

Maecker, H. T., & Trotter, J. (2006). Flow cytometry controls, instrument setup, and the determination of positivity. *Cytometry Part A*, *69A*(9), 1037–1042. https://doi.org/10.1002/cyto.a.20333

Mahajan, S., Kalra, O. P., Tripathi, A. K., Ahuja, G., & Kalra, V. (2005). Phagocytic Polymorphonuclear Function in Patients with Progressive Uremia and the Effect of Acute Hemodialysis. *Renal Failure*, *27*(4), 357–360. https://doi.org/10.1081/JDI-65223

Maisonneuve, P., Agodoa, L., Gellert, R., Stewart, J. H., Buccianti, G., Lowenfels, A. B., Wolfe, R. A., Jones, E., Disney, A. P., Briggs, D., McCredie, M., & Boyle, P. (1999). Cancer in patients on dialysis for end-stage renal disease: An international collaborative study. *Lancet (London, England)*, *354*(9173), 93–99. https://doi.org/10.1016/s0140-6736(99)06154-1

Majewska, E., Baj, Z., Sulowska, Z., Rysz, J., & Luciak, M. (2003). Effects of uraemia and haemodialysis on neutrophil apoptosis and expression of apoptosis-related proteins. *Nephrology Dialysis Transplantation*, *18*(12), 2582–2588. https://doi.org/10.1093/ndt/gfg441

Mallamaci, F., Benedetto, F. A., Tripepi, G., Cutrupi, S., Pizzini, P., Stancanelli, B., Seminara, G., Bonanno, G., Rapisarda, F., Fatuzzo, P., Malatino, L. S., & Zoccali, C. (2008). Vascular endothelial growth factor, left ventricular dysfunction and mortality in hemodialysis patients: *Journal of Hypertension*, *26*(9), 1875–1882. https://doi.org/10.1097/HJH.0b013e328307c3d2

Mandal, A., & Viswanathan, C. (2015). Natural killer cells: In health and disease. *Hematology/Oncology and Stem Cell Therapy*, *8*(2), 47–55. https://doi.org/10.1016/j.hemonc.2014.11.006

Mansouri, L., Nopp, A., Jacobson, S. H., Hylander, B., & Lundahl, J. (2017). Hemodialysis Patients Display a Declined Proportion of Th2 and Regulatory T Cells in Parallel with a High Interferon-γ Profile. *Nephron*, *136*(3), 254–260. https://doi.org/10.1159/000471814

Mansouri, L., Paulsson, J. M., Moshfegh, A., Jacobson, S. H., & Lundahl, J. (2013). Leukocyte proliferation and immune modulator production in patients with chronic kidney disease. *PloS One*, *8*(8), e73141. https://doi.org/10.1371/journal.pone.0073141

Manz, M. G., & Boettcher, S. (2014). Emergency granulopoiesis. *Nature Reviews. Immunology*, *14*(5), 302–314. https://doi.org/10.1038/nri3660

Marangella, M., Petrarulo, M., Mandolfo, S., Vitale, C., Cosseddu, D., & Linari, F. (1992). Plasma profiles and dialysis kinetics of oxalate in patients receiving hemodialysis. *Nephron*, *60*(1), 74–80. https://doi.org/10.1159/000186708

Mathew, R., Mason, D., & Kennedy, J. S. (2014). Vaccination issues in patients with chronic kidney disease. *Expert Review of Vaccines*, *13*(2), 285–298. https://doi.org/10.1586/14760584.2014.874950

Mathy, N. L., Scheuer, W., Lanzendörfer, M., Honold, K., Ambrosius, D., Norley, S., & Kurth, R. (2000). Interleukin-16 stimulates the expression and production of pro-inflammatory cytokines by human monocytes. *Immunology*, *100*(1), 63–69. https://doi.org/10.1046/j.1365-2567.2000.00997.x

Matsumoto, Y., Fujita, T., Hirai, I., Sahara, H., Torigoe, T., Ezoe, K., Saito, T., Cruikshank, W. W., Yotsuyanagi, T., & Sato, N. (2009). Immunosuppressive effect on T cell activation by interleukin-16- and interleukin-10-cDNA-double-transfected human squamous cell line. *Burns*, *35*(3), 383–389. https://doi.org/10.1016/j.burns.2008.06.017

McFadden, C., Morgan, R., Rahangdale, S., Green, D., Yamasaki, H., Center, D., & Cruikshank, W. (2007). Preferential Migration of T Regulatory Cells Induced by IL-16. *The Journal of Immunology*, *179*(10), 6439–6445. https://doi.org/10.4049/jimmunol.179.10.6439

Medzhitov, R. (2008). Origin and physiological roles of inflammation. *Nature*, *454*(7203), 428–435. https://doi.org/10.1038/nature07201

Meier, P., Dayer, E., Blanc, E., & Wauters, J.-P. (2002). Early T cell activation correlates with expression of apoptosis markers in patients with end-stage renal disease. *Journal of the American Society of Nephrology: JASN*, *13*(1), 204–212. https://doi.org/10.1681/ASN.V131204

Meijers, B., Glorieux, G., Poesen, R., & Bakker, S. J. L. (2014). Nonextracorporeal Methods for Decreasing Uremic Solute Concentration: A Future Way To Go? *Seminars in Nephrology*, *34*(2), 228–243. https://doi.org/10.1016/j.semnephrol.2014.02.012

Meuwese, C. L., Snaedal, S., Halbesma, N., Stenvinkel, P., Dekker, F. W., Qureshi, A. R., Barany, P., Heimburger, O., Lindholm, B., Krediet, R. T., Boeschoten, E. W., & Carrero, J. J. (2011). *Trimestral variations of C-reactive protein, interleukin-6 and tumour necrosis factor-α are similarly associated with survival in haemodialysis patients*. 6.

Milliner, D. S., Cochat, P., Hulton, S.-A., Harambat, J., Banos, A., Dehmel, B., & Lindner, E. (2021). Plasma oxalate and eGFR are correlated in primary hyperoxaluria patients with maintained kidney function—Data from three placebo-controlled studies. *Pediatric Nephrology*, *36*(7), 1785–1793. https://doi.org/10.1007/s00467-020-04894-9

Minervina, A., Pogorelyy, M., & Mamedov, I. (2019). T-cell receptor and B-cell receptor repertoire profiling in adaptive immunity. *Transplant International*, *32*(11), 1111–1123. https://doi.org/10.1111/tri.13475

Minihane, A. M., Vinoy, S., Russell, W. R., Baka, A., Roche, H. M., Tuohy, K. M., Teeling, J. L., Blaak, E. E., Fenech, M., Vauzour, D., McArdle, H. J., Kremer, B. H. A., Sterkman, L., Vafeiadou, K., Benedetti, M. M., Williams, C. M., & Calder, P. C. (2015). Low-grade inflammation, diet composition and health: Current research evidence and its translation. *British Journal of Nutrition*, *114*(7), 999–1012. https://doi.org/10.1017/S0007114515002093

Molloy, E. J., O'Neill, A. J., Grantham, J. J., Sheridan-Pereira, M., Fitzpatrick, J. M., Webb, D. W., & Watson, R. W. G. (2003). Sex-specific alterations in neutrophil apoptosis: The role of estradiol and progesterone. *Blood*, *102*(7), 2653–2659. https://doi.org/10.1182/blood-2003-02-0649

Monard, C., Rimmelé, T., & Ronco, C. (2019). Extracorporeal Blood Purification Therapies for Sepsis. *Blood Purification*, *47 Suppl 3*, 1–14. https://doi.org/10.1159/000499520

Moser, B., Roth, G., Brunner, M., Lilaj, T., Deicher, R., Wolner, E., Kovarik, J., Boltz-Nitulescu, G., Vychytil, A., & Ankersmit, H. J. (2003). Aberrant T cell activation and heightened apoptotic turnover in end-stage renal failure patients: A comparative evaluation between non-dialysis, haemodialysis, and peritoneal dialysis. *Biochemical and Biophysical Research Communications*, *308*(3), 581–585. https://doi.org/10.1016/s0006-291x(03)01389-5

Mousset, C. M., Hobo, W., Woestenenk, R., Preijers, F., Dolstra, H., & van der Waart, A. B. (2019). Comprehensive Phenotyping of T Cells Using Flow Cytometry. *Cytometry Part A*, *95*(6), 647–654. https://doi.org/10.1002/cyto.a.23724

Mühlhahn, P., Zweckstetter, M., Georgescu, J., Ciosto, C., Renner, C., Lanzendörfer, M., Lang, K., Ambrosius, D., Baier, M., Kurth, R., & Holak, T. A. (1998). Structure of interleukin 16 resembles a PDZ domain with an occluded peptide binding site. *Nature Structural Biology*, *5*(8), 682–686. https://doi.org/10.1038/1376

Mulay, S. R., Eberhard, J. N., Pfann, V., Marschner, J. A., Darisipudi, M. N., Daniel, C., Romoli, S., Desai, J., Grigorescu, M., Kumar, S. V., Rathkolb, B., Wolf, E., Hrabě de Angelis, M., Bäuerle, T., Dietel, B., Wagner, C. A., Amann, K., Eckardt, K.-U., Aronson, P. S., … Knauf, F. (2016). Oxalate-induced chronic kidney disease with its uremic and cardiovascular complications in C57BL/6 mice. *American Journal of Physiology-Renal Physiology*, *310*(8), F785–F795. https://doi.org/10.1152/ajprenal.00488.2015

Mulay, S. R., Kulkarni, O. P., Rupanagudi, K. V., Migliorini, A., Darisipudi, M. N., Vilaysane, A., Muruve, D., Shi, Y., Munro, F., Liapis, H., & Anders, H.-J. (2013). Calcium oxalate crystals induce renal inflammation by NLRP3-mediated IL-1β secretion. *Journal of Clinical Investigation*, *123*(1), 236–246. https://doi.org/10.1172/JCI63679

Murphy, K., & Weaver, C. (2016). *Janeway's immunobiology* (9th edition). Garland Science/Taylor & Francis Group, LLC.

Mydlík, M., & Derzsiová, K. (2008). Oxalic Acid as a uremic toxin. *Journal of Renal Nutrition: The Official Journal of the Council on Renal Nutrition of the National Kidney Foundation*, *18*(1), 33–39. https://doi.org/10.1053/j.jrn.2007.10.008

Naicker, S. D., Cormican, S., Griffin, T. P., Maretto, S., Martin, W. P., Ferguson, J. P., Cotter, D., Connaughton, E. P., Dennedy, M. C., & Griffin, M. D. (2018). Chronic Kidney Disease Severity Is Associated With Selective Expansion of a Distinctive Intermediate Monocyte Subpopulation. *Frontiers in Immunology*, *9*, 2845. https://doi.org/10.3389/fimmu.2018.02845

Navaneethan, S. D., Schold, J. D., Arrigain, S., Jolly, S. E., & Nally, J. V. (2015). Cause-Specific Deaths in Non–Dialysis-Dependent CKD. *Journal of the American Society of Nephrology*, *26*(10), 2512–2520. https://doi.org/10.1681/ASN.2014101034

Nobles, C., Bertone-Johnson, E. R., Ronnenberg, A. G., Faraj, J. M., Zagarins, S., Takashima-Uebelhoer, B. B., & Whitcomb, B. W. (2015). Correlation of urine and plasma cytokine levels among reproductive-aged women. *European Journal of Clinical Investigation*, *45*(5), 460–465. https://doi.org/10.1111/eci.12428

Nockher, W. A., & Scherberich, J. E. (1998). Expanded CD14 $^{+}$ CD16 $^{+}$ Monocyte Subpopulation in Patients with Acute and Chronic Infections Undergoing Hemodialysis. *Infection and Immunity*, *66*(6), 2782–2790. https://doi.org/10.1128/IAI.66.6.2782-2790.1998

Okuno, S., Ishimura, E., Kitatani, K., Fujino, Y., Kohno, K., Maeno, Y., Maekawa, K., Yamakawa, T., Imanishi, Y., Inaba, M., & Nishizawa, Y. (2007). Presence of abdominal aortic calcification is significantly associated with all-cause and cardiovascular mortality in maintenance hemodialysis patients. *American Journal of Kidney Diseases: The Official Journal of the National Kidney Foundation*, *49*(3), 417–425. https://doi.org/10.1053/j.ajkd.2006.12.017

O'Mahony, L., Holland, J., Jackson, J., Feighery, C., Hennessy, T. P., & Mealy, K. (1998). Quantitative intracellular cytokine measurement: Age-related changes in proinflammatory cytokine production. *Clinical and Experimental Immunology*, *113*(2), 213–219. https://doi.org/10.1046/j.1365-2249.1998.00641.x

Ong, S., Rose, N. R., & Čiháková, D. (2017). Natural killer cells in inflammatory heart disease. *Clinical Immunology*, *175*, 26–33. https://doi.org/10.1016/j.clim.2016.11.010

Ong, S.-M., Hadadi, E., Dang, T.-M., Yeap, W.-H., Tan, C. T.-Y., Ng, T.-P., Larbi, A., & Wong, S.-C. (2018). The pro-inflammatory phenotype of the human non-classical monocyte subset is attributed to senescence. *Cell Death & Disease*, *9*(3). https://doi.org/10.1038/s41419-018-0327-1

Osswald, H., & Hautmann, R. (1979). Renal Elimination Kinetics and Plasma Half-Life of Oxalate in Man. *Urologia Internationalis*, *34*(6), 440–450. https://doi.org/10.1159/000280294

Panichi, V., Maggiore, U., Taccola, D., Migliori, M., Rizza, G. M., Consani, C., Bertini, A., Sposini, S., Perez-Garcia, R., Rindi, P., Palla, R., & Tetta, C. (2004). Interleukin-6 is a stronger predictor of total and cardiovascular mortality than C-reactive protein in haemodialysis patients. *Nephrology Dialysis Transplantation*, *19*(5), 1154–1160. https://doi.org/10.1093/ndt/gfh052

Pape, H.-C., Kurtz, A., Silbernagl, S., Persson, A. B., & Brenner, B. (2014). *Physiologie* (7. Aufl.). Thieme.

Passlick, B., Flieger, D., & Ziegler-Heitbrock, H. (1989). Identification and characterization of a novel monocyte subpopulation in human peripheral blood. *Blood*, *74*(7), 2527–2534. https://doi.org/10.1182/blood.V74.7.2527.2527

Patente, T. A., Pinho, M. P., Oliveira, A. A., Evangelista, G. C. M., Bergami-Santos, P. C., & Barbuto, J. A. M. (2019). Human Dendritic Cells: Their Heterogeneity and Clinical Application Potential in Cancer Immunotherapy. *Frontiers in Immunology*, *9*, 3176. https://doi.org/10.3389/fimmu.2018.03176

Pergola, P. E., Devalaraja, M., Fishbane, S., Chonchol, M., Mathur, V. S., Smith, M. T., Lo, L., Herzog, K., Kakkar, R., & Davidson, M. H. (2021). Ziltivekimab for Treatment of Anemia of Inflammation in Patients on Hemodialysis: Results from a Phase 1/2 Multicenter, Randomized, Double-Blind, Placebo-Controlled Trial. *Journal of the American Society of Nephrology: JASN*, *32*(1), 211–222. https://doi.org/10.1681/ASN.2020050595

Pfau, A., Ermer, T., Coca, S. G., Tio, M. C., Genser, B., Reichel, M., Finkelstein, F. O., März, W., Wanner, C., Waikar, S. S., Eckardt, K.-U., Aronson, P. S., Drechsler, C., & Knauf, F. (2021). High Oxalate Concentrations Correlate with Increased Risk for Sudden Cardiac Death in Dialysis Patients. *Journal of the American Society of Nephrology: JASN*, *32*(9), 2375–2385. https://doi.org/10.1681/ASN.2020121793

Pfau, A., Wytopil, M., Chauhan, K., Reichel, M., Coca, S. G., Aronson, P. S., Eckardt, K.-U., & Knauf, F. (2020). Assessment of Plasma Oxalate Concentration in Patients With CKD. *Kidney International Reports*, *5*(11), 2013–2020. https://doi.org/10.1016/j.ekir.2020.08.029

Pfister, G., Toor, S. M., Sasidharan Nair, V., & Elkord, E. (2020). An evaluation of sorter induced cell stress (SICS) on peripheral blood mononuclear cells (PBMCs) after different sort conditions—Are your sorted cells getting SICS? *Journal of Immunological Methods*, *487*, 112902. https://doi.org/10.1016/j.jim.2020.112902

Pierre, C., & Gill, R. (2013). Primary Hyperoxaluria. *The New England Journal of Medicine*, 10.

Ponder, K. G., & Boise, L. H. (2019). The prodomain of caspase-3 regulates its own removal and caspase activation. *Cell Death Discovery*, *5*, 56. https://doi.org/10.1038/s41420-019-0142-1

Pongracz, J., Webb, P., Wang, K., Deacon, E., Lunn, O. J., & Lord, J. M. (1999). Spontaneous neutrophil apoptosis involves caspase 3-mediated activation of protein kinase C-delta. *The Journal of Biological Chemistry*, *274*(52), 37329–37334. https://doi.org/10.1074/jbc.274.52.37329

Poole, S., Bird, T. A., Selkirk, S., Gaines-Das, R. E., Choudry, Y., Stephenson, S. L., Kenny, A. J., & Saklatvaa, J. (1990). Fate of injected interleukin 1 in rats: Sequestration and degradation in the kidney. *Cytokine*, *2*(6), 416–422. https://doi.org/10.1016/1043-4666(90)90050-4

Porowski, T., Zoch-Zwierz, W., Konstantynowicz, J., Korzeniecka-Kozerska, A., Michaluk-Skutnik, J., & Porowska, H. (2008). Reference values of plasma oxalate in children and adolescents. *Pediatric Nephrology (Berlin, Germany)*, *23*(10), 1787–1794. https://doi.org/10.1007/s00467-008-0889-8

Prager, I., Liesche, C., van Ooijen, H., Urlaub, D., Verron, Q., Sandström, N., Fasbender, F., Claus, M., Eils, R., Beaudouin, J., Önfelt, B., & Watzl, C. (2019). NK cells switch from granzyme B to death receptor–mediated cytotoxicity during serial killing. *Journal of Experimental Medicine*, *216*(9), 2113–2127. https://doi.org/10.1084/jem.20181454

Prenen, J. a. C., Mees, E. J. D., & Boer, P. (1985). Plasma oxalate concentration and oxalate distribution volume in patients with normal and decreased renal function. *European Journal of Clinical Investigation*, *15*(1), 45–49. https://doi.org/10.1111/j.1365-2362.1985.tb00142.x

PromoKine. (2021). *LDH Cytotoxicity Kit II*. https://www.promocell.com/app/uploads/product-information/manual/PK-CA577-K313.pdf

Purzycka-Bohdan, D., Szczerkowska-Dobosz, A., Zablotna, M., Wierzbicka, J., Piotrowska, A., Zmijewski, M. A., Nedoszytko, B., & Nowicki, R. (2016). Assessment of Interleukin 16 Serum Levels and Skin Expression in Psoriasis Patients in Correlation with Clinical Severity of the Disease. *PLOS ONE*, *11*(10), e0165577. https://doi.org/10.1371/journal.pone.0165577

Quinn, M. T., & DeLeo, F. R. (Hrsg.). (2020). *Neutrophil: Methods and Protocols* (Bd. 2087). Springer US. https://doi.org/10.1007/978-1-0716-0154-9

Qureshi, O. S., Zheng, Y., Nakamura, K., Attridge, K., Manzotti, C., Schmidt, E. M., Baker, J., Jeffery, L. E., Kaur, S., Briggs, Z., Hou, T. Z., Futter, C. E., Anderson, G., Walker, L. S. K., & Sansom, D. M. (2011). Trans-Endocytosis of CD80 and CD86: A Molecular Basis for the Cell-Extrinsic Function of CTLA-4. *Science*, *332*(6029), 600–603. https://doi.org/10.1126/science.1202947

Rachmawati, H., Beljaars, L., Reker-Smit, C., Van Loenen-Weemaes, A. M., Hagens, W. I., Meijer, D. K. F., & Poelstra, K. (2004). Pharmacokinetic and biodistribution profile of recombinant human interleukin-10 following intravenous administration in rats with extensive liver fibrosis. *Pharmaceutical Research*, *21*(11), 2072–2078. https://doi.org/10.1023/b:pham.0000048199.94510.b0

Ragab, D., Salah Eldin, H., Taeimah, M., Khattab, R., & Salem, R. (2020). The COVID-19 Cytokine Storm; What We Know So Far. *Frontiers in Immunology*, *11*, 1446. https://doi.org/10.3389/fimmu.2020.01446

Rapp, N., Evenepoel, P., Stenvinkel, P., & Schurgers, L. (2020). Uremic Toxins and Vascular Calcification-Missing the Forest for All the Trees. *Toxins*, *12*(10), E624. https://doi.org/10.3390/toxins12100624

R&D. (2021). *R&D Systems ELISA Guide*. https://resources.rndsystems.com/images/site/rnd-systems-elisa-guide-br3.pdf

Reich, K., Heine, A., Hugo, S., Blaschke, V., Middel, P., Kaser, A., Tilg, H., Blaschke, S., Gutgesell, C., & Neumann, C. (2001). Engagement of the Fc epsilon RI stimulates the production of IL-16 in Langerhans cell-like dendritic cells. *Journal of Immunology (Baltimore, Md.: 1950)*, *167*(11), 6321–6329. https://doi.org/10.4049/jimmunol.167.11.6321

Reich, K., S, H., P, M., V, B., A, H., & C, N. (2004). The maturation-dependent production of interleukin-16 is impaired in monocyte-derived dendritic cells from atopic dermatitis patients but is restored by inflammatory cytokines TNF-alpha and IL-1beta. *Experimental Dermatology*, *13*(12). https://doi.org/10.1111/j.0906-6705.2004.00251.x

Remijsen, Q., Vanden Berghe, T., Wirawan, E., Asselbergh, B., Parthoens, E., De Rycke, R., Noppen, S., Delforge, M., Willems, J., & Vandenabeele, P. (2011). Neutrophil extracellular trap cell death requires both autophagy and superoxide generation. *Cell Research*, *21*(2), 290–304. https://doi.org/10.1038/cr.2010.150

Rhodes, J. W., Tong, O., Harman, A. N., & Turville, S. G. (2019). Human Dendritic Cell Subsets, Ontogeny, and Impact on HIV Infection. *Frontiers in Immunology*, *10*, 1088. https://doi.org/10.3389/fimmu.2019.01088

Richmond, J., Tuzova, M., Cruikshank, W., & Center, D. (2014). Regulation of Cellular Processes by Interleukin-16 in Homeostasis and Cancer. *Journal of Cellular Physiology*, *229*(2), 139–147. https://doi.org/10.1002/jcp.24441

Rider, P., Voronov, E., Dinarello, C. A., & Cohen, I. (2017). Alarmins: Feel the Stress. *The Journal of Immunology*, 9.

Ridker, P. M., MacFadyen, J. G., Glynn, R. J., Koenig, W., Libby, P., Everett, B. M., Lefkowitz, M., Thuren, T., & Cornel, J. H. (2018). Inhibition of Interleukin-1β by Canakinumab and Cardiovascular Outcomes in Patients With Chronic Kidney Disease. *Journal of the American College of Cardiology*, *71*(21), 2405–2414. https://doi.org/10.1016/j.jacc.2018.03.490

Riley, L. K., & Rupert, J. (2015). Evaluation of Patients with Leukocytosis. *American Family Physician*, *92*(11), 1004–1011.

Rios, F. J., Touyz, R. M., & Montezano, A. C. (2017). Isolation and Differentiation of Murine Macrophages. In R. M. Touyz & E. L. Schiffrin (Hrsg.), *Hypertension: Methods and Protocols* (S. 297–309). Springer. https://doi.org/10.1007/978-1-4939-6625-7_23

Robinson, M. D., & Oshlack, A. (2010). A scaling normalization method for differential expression analysis of RNA-seq data. *Genome Biology*, *11*(3), R25. https://doi.org/10.1186/gb-2010-11-3-r25

Rodríguez-Carrio, J., Carrillo-López, N., Ulloa, C., Seijo, M., Rodríguez-García, M., Rodríguez-Suárez, C., Díaz-Corte, C., Cannata-Andía, J. B., Suárez, A., & Dusso, A. S. (2019). A subset of low density granulocytes is associated with vascular calcification in chronic kidney disease patients. *Scientific Reports*, *9*(1), 13230. https://doi.org/10.1038/s41598-019-49429-x

Rogacev, K. S., Seiler, S., Zawada, A. M., Reichart, B., Herath, E., Roth, D., Ulrich, C., Fliser, D., & Heine, G. H. (2011). CD14++CD16+ monocytes and cardiovascular outcome in patients with chronic kidney disease. *European Heart Journal*, *32*(1), 84–92. https://doi.org/10.1093/eurheartj/ehq371

Rose-John, S. (2018). Interleukin-6 Family Cytokines. *Cold Spring Harbor Perspectives in Biology*, *10*(2). https://doi.org/10.1101/cshperspect.a028415

Rossaint, J., Unruh, M., & Zarbock, A. (2016). Fibroblast growth factor 23 actions in inflammation: A key factor in CKD outcomes. *Nephrology Dialysis Transplantation*, gfw331. https://doi.org/10.1093/ndt/gfw331

Roth, S., Agthe, M., Eickhoff, S., Möller, S., Karsten, C. M., Borregaard, N., Solbach, W., & Laskay, T. (2015). Secondary necrotic neutrophils release interleukin-16C and macrophage migration inhibitory factor from stores in the cytosol. *Cell Death Discovery*, *1*, 15056. https://doi.org/10.1038/cddiscovery.2015.56

Rule, A. D., Krambeck, A. E., & Lieske, J. C. (2011). Chronic Kidney Disease in Kidney Stone Formers. *Clinical Journal of the American Society of Nephrology*, *6*(8), 2069–2075. https://doi.org/10.2215/CJN.10651110

Rumsaeng, V., Cruikshank, W. W., Foster, B., Prussin, C., Kirshenbaum, A. S., Davis, T. A., Kornfeld, H., Center, D. M., & Metcalfe, D. D. (1997). Human mast cells produce the CD4+ T lymphocyte chemoattractant factor, IL-16. *The Journal of Immunology*, *159*(6), 2904–2910.

Saad, K., Elsayh, K. I., Zahran, A. M., & Sobhy, K. M. (2014). Lymphocyte populations and apoptosis of peripheral blood B and T lymphocytes in children with end stage renal disease. *Renal Failure*, *36*(4), 502–507. https://doi.org/10.3109/0886022X.2013.875833

Saran, R., Robinson, B., Abbott, K. C., Bragg-Gresham, J., Chen, X., Gipson, D., Gu, H., Hirth, R. A., Hutton, D., Jin, Y., Kapke, A., Kurtz, V., Li, Y., McCullough, K., Modi, Z., Morgenstern, H., Mukhopadhyay, P., Pearson, J., Pisoni, R., … Shahinian, V. (2020). US Renal Data System 2019 Annual Data Report: Epidemiology of Kidney Disease in the United States. *American Journal of Kidney Diseases*, *75*(1), A6–A7. https://doi.org/10.1053/j.ajkd.2019.09.003

Sardenberg, C., Suassuna, P., Watanabe, R., Cruz Andreoli, M. C., Aparecida Dalboni, M., Faria Seabra, V., Draibe, S. A., Cendoroglo Neto, M., & Jaber, B. (2004). Balance between cytokine production by peripheral blood mononuclear cells and reactive oxygen species production by monocytes in patients with chronic kidney disease. *Renal Failure*, *26*(6), 673–681. https://doi.org/10.1081/jdi-200037122

Sarnak, M. J., & Jaber, B. L. (2000). Mortality caused by sepsis in patients with end-stage renal disease compared with the general population. *Kidney International*, *58*(4), 1758–1764. https://doi.org/10.1111/j.1523-1755.2000.00337.x

Scales, C. D., Smith, A. C., Hanley, J. M., & Saigal, C. S. (2012). Prevalence of Kidney Stones in the United States. *European Urology*, *62*(1), 160–165. https://doi.org/10.1016/j.eururo.2012.03.052

Schädler, D., Pausch, C., Heise, D., Meier-Hellmann, A., Brederlau, J., Weiler, N., Marx, G., Putensen, C., Spies, C., Jörres, A., Quintel, M., Engel, C., Kellum, J. A., & Kuhlmann, M. K. (2017). The effect of a novel extracorporeal cytokine hemoadsorption device on IL-6 elimination in septic patients: A randomized controlled trial. *PloS One*, *12*(10), e0187015. https://doi.org/10.1371/journal.pone.0187015

Schenz, J., Obermaier, M., Uhle, S., Weigand, M. A., & Uhle, F. (2021). Low-Density Granulocyte Contamination From Peripheral Blood Mononuclear Cells of Patients With Sepsis and How to Remove It—A Technical Report. *Frontiers in Immunology*, *12*, 684119. https://doi.org/10.3389/fimmu.2021.684119

Schepers, E., Houthuys, E., Dhondt, A., De Meyer, G., Neirynck, N., Bernaert, P., Van den Bergh, R., Brouckaert, P., Vanholder, R., & Glorieux, G. (2015). Transcriptome Analysis in Patients with Chronic Kidney Disease on Hemodialysis Disclosing a Key Role for CD16+CX3CR1+ Monocytes. *PLOS ONE*, *10*(4), e0121750. https://doi.org/10.1371/journal.pone.0121750

Schindler, R. (2004). Causes and therapy of microinflammation in renal failure. *Nephrology, Dialysis, Transplantation: Official Publication of the European Dialysis and Transplant Association - European Renal Association*, *19 Suppl 5*, V34-40. https://doi.org/10.1093/ndt/gfh1054

Sciaky, D., Brazer, W., Center, D. M., Cruikshank, W. W., & Smith, T. J. (2000). Cultured Human Fibroblasts Express Constitutive IL-16 mRNA: Cytokine Induction of Active IL-16 Protein Synthesis Through a Caspase-3-Dependent Mechanism. *The Journal of Immunology*, *164*(7), 3806–3814. https://doi.org/10.4049/jimmunol.164.7.3806

Seeliger, B., Stahl, K., & David, S. (2020). [Extracorporeal techniques for blood purification in sepsis: An update]. *Der Internist*, *61*(10), 1010–1016. https://doi.org/10.1007/s00108-020-00862-5

Sela, S., Shurtz-Swirski, R., Cohen-Mazor, M., Mazor, R., Chezar, J., Shapiro, G., Hassan, K., Shkolnik, G., Geron, R., & Kristal, B. (2005). Primed Peripheral Polymorphonuclear Leukocyte: A Culprit Underlying Chronic Low-Grade Inflammation and Systemic Oxidative Stress in Chronic Kidney Disease. *Journal of the American Society of Nephrology*, *16*(8), 2431–2438. https://doi.org/10.1681/ASN.2004110929

Sharma, V., Sparks, J. L., & Vail, J. D. (2000). Human B-cell lines constitutively express and secrete interleukin-16. *Immunology*, *99*(2), 266–271. https://doi.org/10.1046/j.1365-2567.2000.00959.x

Shevach, E. M., & Thornton, A. M. (2014). tTregs, pTregs, and iTregs: Similarities and differences. *Immunological Reviews*, *259*(1), 88–102. https://doi.org/10.1111/imr.12160

Shi, J., Gao, W., & Shao, F. (2017). Pyroptosis: Gasdermin-Mediated Programmed Necrotic Cell Death. *Trends in Biochemical Sciences*, *42*(4), 245–254. https://doi.org/10.1016/j.tibs.2016.10.004

Shimonkevitz, R., Northrop, J., Harris, L., Craun, M., & Bar-Or, D. (2005). Interleukin-16 expression in the peripheral blood and CD8 T lymphocytes after traumatic injury. *The Journal of Trauma*, *58*(2), 252–258. https://doi.org/10.1097/01.ta.0000141884.49076.53

Sjöberg, B., Qureshi, A. R., Heimbürger, O., Stenvinkel, P., Lind, L., Larsson, A., Bárány, P., & Ärnlöv, J. (2016). Association between levels of pentraxin 3 and incidence of chronic kidney disease in the elderly. *Journal of Internal Medicine*, *279*(2), 173–179. https://doi.org/10.1111/joim.12411

Skrzeczyńska-Moncznik, J., Bzowska, M., Lo˝seke, S., Grage-Griebenow, E., Zembala, M., & Pryjma, J. (2008). Peripheral Blood CD14 ^{high} CD16 $^{+}$ Monocytes are Main Producers of IL-10. *Scandinavian Journal of Immunology*, *67*(2), 152–159. https://doi.org/10.1111/j.1365-3083.2007.02051.x

Skundric, D. S., Dai, R., Zakarian, V. L., Bessert, D., Skoff, R. P., Cruikshank, W. W., & Kurjakovic, Z. (2005). Anti-IL-16 therapy reduces CD4+ T-cell infiltration and improves paralysis and histopathology of relapsing EAE. *Journal of Neuroscience Research*, *79*(5), 680–693. https://doi.org/10.1002/jnr.20377

Snow, T. A. C., Littlewood, S., Corredor, C., Singer, M., & Arulkumaran, N. (2021). Effect of Extracorporeal Blood Purification on Mortality in Sepsis: A Meta-Analysis and Trial Sequential Analysis. *Blood Purification*, *50*(4–5), 462–472. https://doi.org/10.1159/000510982

Spits, H., Artis, D., Colonna, M., Diefenbach, A., Di Santo, J. P., Eberl, G., Koyasu, S., Locksley, R. M., McKenzie, A. N. J., Mebius, R. E., Powrie, F., & Vivier, E. (2013). Innate lymphoid cells—A proposal for uniform nomenclature. *Nature Reviews Immunology*, *13*(2), 145–149. https://doi.org/10.1038/nri3365

Steinbrink, K., Wölfl, M., Jonuleit, H., Knop, J., & Enk, A. H. (1997). Induction of tolerance by IL-10-treated dendritic cells. *The Journal of Immunology*, *159*(10), 4772–4780.

Stelzhammer, V., Haenisch, F., Chan, M. K., Cooper, J. D., Steiner, J., Steeb, H., Martins-de-Souza, D., Rahmoune, H., Guest, P. C., & Bahn, S. (2014). Proteomic changes in serum of first onset, antidepressant drug-naïve major depression patients. *The International Journal of Neuropsychopharmacology*, *17*(10), 1599–1608. https://doi.org/10.1017/S1461145714000819

Stewart, J. H., Vajdic, C. M., van Leeuwen, M. T., Amin, J., Webster, A. C., Chapman, J. R., McDonald, S. P., Grulich, A. E., & McCredie, M. R. E. (2009). The pattern of excess cancer in dialysis and transplantation. *Nephrology, Dialysis, Transplantation: Official Publication of the European Dialysis and Transplant Association - European Renal Association*, *24*(10), 3225–3231. https://doi.org/10.1093/ndt/gfp331

Suliman, M. E., Qureshi, A. R., Carrero, J. J., Barany, P., Yilmaz, M. I., Snaedal-Jonsdottir, S., Alvestrand, A., Heimburger, O., Lindholm, B., & Stenvinkel, P. (2008). The long pentraxin PTX-3 in prevalent hemodialysis patients: Associations with comorbidities and mortality. *QJM*, *101*(5), 397–405. https://doi.org/10.1093/qjmed/hcn019

Summers, C., Rankin, S. M., Condliffe, A. M., Singh, N., Peters, A. M., & Chilvers, E. R. (2010). Neutrophil kinetics in health and disease. *Trends in Immunology*, *31*(8), 318–324. https://doi.org/10.1016/j.it.2010.05.006

Taabazuing, C. Y., Okondo, M. C., & Bachovchin, D. A. (2017). Pyroptosis and Apoptosis Pathways Engage in Bidirectional Crosstalk in Monocytes and Macrophages. *Cell Chemical Biology*, *24*(4), 507-514.e4. https://doi.org/10.1016/j.chembiol.2017.03.009

Takada, H., Ohga, S., Mizuno, Y., Nomura, A., & Hara, T. (2004). Increased IL-16 levels in hemophagocytic lymphohistiocytosis. *Journal of Pediatric Hematology/Oncology*, *26*(9), 567–573. https://doi.org/10.1097/01.mph.0000134465.86671.2e

Takei, H., Araki, A., Watanabe, H., Ichinose, A., & Sendo, F. (1996). Rapid killing of human neutrophils by the potent activator phorbol 12-myristate 13-acetate (PMA) accompanied by changes different from typical apoptosis or necrosis. *Journal of Leukocyte Biology*, *59*(2), 229–240. https://doi.org/10.1002/jlb.59.2.229

Tang, Y.-J., Wang, J.-L., Xie, K.-G., & Lan, C.-G. (2016). Association of interleukin 16 gene polymorphisms and plasma IL16 level with osteosarcoma risk. *Scientific Reports*, *6*(1), 34607. https://doi.org/10.1038/srep34607

The Human Protein Atlas. (2021). *Tissue expression of IL16*. https://www.proteinatlas.org/ENSG00000172349-IL16/tissue

Thermo Fisher scientific. (2020). *Protocol Pierce BCA Protein Assay*. https://assets.thermofisher.com/TFS-Assets/LSG/manuals/MAN0011430_Pierce_BCA_Protein_Asy_UG.pdf

Thompson, S., James, M., Wiebe, N., Hemmelgarn, B., Manns, B., Klarenbach, S., Tonelli, M., & Alberta Kidney Disease Network. (2015). Cause of Death in Patients with Reduced Kidney Function. *Journal of the American Society of Nephrology: JASN*, *26*(10), 2504–2511. https://doi.org/10.1681/ASN.2014070714

Thongprayoon, C., Krambeck, A. E., & Rule, A. D. (2020). Determining the true burden of kidney stone disease. *Nature Reviews Nephrology*, *16*(12), 736–746. https://doi.org/10.1038/s41581-020-0320-7

Thornton, A. M., & Shevach, E. M. (1998). CD4+CD25+ Immunoregulatory T Cells Suppress Polyclonal T Cell Activation In Vitro by Inhibiting Interleukin 2 Production. *Journal of Experimental Medicine*, *188*(2), 287–296. https://doi.org/10.1084/jem.188.2.287

Toda, G., Yamauchi, T., Kadowaki, T., & Ueki, K. (2021). Preparation and culture of bone marrow-derived macrophages from mice for functional analysis. *STAR Protocols*, *2*(1), 100246. https://doi.org/10.1016/j.xpro.2020.100246

Togashi, Y., Shitara, K., & Nishikawa, H. (2019). Regulatory T cells in cancer immunosuppression—Implications for anticancer therapy. *Nature Reviews Clinical Oncology*, *16*(6), 356–371. https://doi.org/10.1038/s41571-019-0175-7

Tong, M., Carrero, J. J., Qureshi, A. R., Anderstam, B., Heimbürger, O., Bárány, P., Axelsson, J., Alvestrand, A., Stenvinkel, P., Lindholm, B., & Suliman, M. E. (2007). Plasma Pentraxin 3 in Patients with Chronic Kidney Disease: Associations with Renal Function, Protein-Energy Wasting, Cardiovascular Disease, and Mortality. *Clinical Journal of the American Society of Nephrology*, *2*(5), 889–897. https://doi.org/10.2215/CJN.00870207

Tsuchiya, K., Nakajima, S., Hosojima, S., Thi Nguyen, D., Hattori, T., Manh Le, T., Hori, O., Mahib, M. R., Yamaguchi, Y., Miura, M., Kinoshita, T., Kushiyama, H., Sakurai, M., Shiroishi, T., & Suda, T. (2019). Caspase-1 initiates apoptosis in the absence of gasdermin D. *Nature Communications*, *10*(1), 2091. https://doi.org/10.1038/s41467-019-09753-2

Tuegel, C., Katz, R., Alam, M., Bhat, Z., Bellovich, K., de Boer, I., Brosius, F., Gadegbeku, C., Gipson, D., Hawkins, J., Himmelfarb, J., Ju, W., Kestenbaum, B., Kretzler, M., Robinson-Cohen, C., Steigerwalt, S., & Bansal, N. (2018). GDF-15, Galectin 3, Soluble ST2, and Risk of Mortality and Cardiovascular Events in CKD. *American Journal of Kidney Diseases*, *72*(4), 519–528. https://doi.org/10.1053/j.ajkd.2018.03.025

USRDS. (2019). *USRDS Annual Data Report 2019, Mortality*. USRDS. https://adr.usrds.org/

Valipour, B., Velaei, K., Abedelahi, A., Karimipour, M., Darabi, M., & Charoudeh, H. N. (2019). NK cells: An attractive candidate for cancer therapy. *Journal of Cellular Physiology*, *234*(11), 19352–19365. https://doi.org/10.1002/jcp.28657

Vanholder, R., Pletinck, A., Schepers, E., & Glorieux, G. (2018). Biochemical and Clinical Impact of Organic Uremic Retention Solutes: A Comprehensive Update. *Toxins*, *10*(1). https://doi.org/10.3390/toxins10010033

Vanholder, R., Smet, R. D., Glorieux, G., Argilés, A., Baurmeister, U., Brunet, P., Clark, W., Cohen, G., Deyn, P. P. D., Deppisch, R., Descamps-Latscha, B., Henle, T., Jörres, A., Lemke, H. D., Massy, Z. A., Passlick-Deetjen, J., Rodriguez, M., Stegmayr, B., Stenvinkel, P., … Group (EUTox), F. the E. U. T. W. (2003). Review on uremic toxins: Classification, concentration, and interindividual variability. *Kidney International*, *63*(5), 1934–1943. https://doi.org/10.1046/j.1523-1755.2003.00924.x

Vaughan, K. R., Stokes, L., Prince, L. R., Marriott, H. M., Meis, S., Kassack, M. U., Bingle, C. D., Sabroe, I., Surprenant, A., & Whyte, M. K. B. (2007). Inhibition of neutrophil apoptosis by ATP is mediated by the P2Y11 receptor. *Journal of Immunology (Baltimore, Md.: 1950)*, *179*(12), 8544–8553. https://doi.org/10.4049/jimmunol.179.12.8544

Vazquez, M. I., Catalan-Dibene, J., & Zlotnik, A. (2015). B cells responses and cytokine production are regulated by their immune microenvironment. *Cytokine*, *74*(2), 318–326. https://doi.org/10.1016/j.cyto.2015.02.007

Vendrame, F., Cataldo, D., Ciarlo, L., Umland, O., Misasi, R., & Dotta, F. (2012). In type 1 diabetes immunocompetent cells are defective in IL-16 secretion. *Scandinavian Journal of Immunology*, *75*(1), 127–128. https://doi.org/10.1111/j.1365-3083.2011.02630.x

Villani, A.-C., Satija, R., Reynolds, G., Sarkizova, S., Shekhar, K., Fletcher, J., Griesbeck, M., Butler, A., Zheng, S., Lazo, S., Jardine, L., Dixon, D., Stephenson, E., Nilsson, E., Grundberg, I., McDonald, D., Filby, A., Li, W., Jager, P. L. D., … Hacohen, N. (2017). Single-cell RNA-seq reveals new types of human blood dendritic cells, monocytes, and progenitors. *Science*, *356*(6335), eaah4573. https://doi.org/10.1126/science.aah4573

von Leitner, E.-C., Klinke, A., Atzler, D., Slocum, J. L., Lund, N., Kielstein, J. T., Maas, R., Schmidt-Haupt, R., Pekarova, M., Hellwinkel, O., Tsikas, D., D'Alecy, L. G., Lau, D., Willems, S., Kubala, L., Ehmke, H., Meinertz, T., Blankenberg, S., Schwedhelm, E., … Sydow, K. (2011). Pathogenic cycle between the endogenous nitric oxide synthase inhibitor asymmetrical dimethylarginine and the leukocyte-derived hemoprotein myeloperoxidase. *Circulation*, *124*(24), 2735–2745. https://doi.org/10.1161/CIRCULATIONAHA.111.060541

Wallquist, C., Paulson, J. M., Hylander, B., Lundahl, J., & Jacobson, S. H. (2013). Increased accumulation of CD16+ monocytes at local sites of inflammation in patients with chronic kidney disease. *Scandinavian Journal of Immunology*, *78*(6), 538–544. https://doi.org/10.1111/sji.12115

Wang, J. (2018). Neutrophils in tissue injury and repair. *Cell and Tissue Research*, *371*(3), 531–539. https://doi.org/10.1007/s00441-017-2785-7

Wang, P., Lu, Y., Wen, Y., Yu, D., Ge, L., Dong, W., Xiang, L., & Shao, J. (2013). IL-16 Induces Intestinal Inflammation via PepT1 Upregulation in a Pufferfish Model: New Insights into the Molecular Mechanism of Inflammatory Bowel Disease. *The Journal of Immunology*, *191*(3), 1413–1427. https://doi.org/10.4049/jimmunol.1202598

Wang, X., Li, L., Wang, Y., Li, X., Feng, Q., Hou, Y., Ma, C., Gao, C., Hou, M., & Peng, J. (2019). High-Dose Dexamethasone Alters the Increase in Interleukin-16 Level in Adult Immune Thrombocytopenia. *Frontiers in Immunology*, *10*. https://doi.org/10.3389/fimmu.2019.00451

Wang, X.-R., Zhang, J.-J., Xu, X.-X., & Wu, Y.-G. (2019). Prevalence of coronary artery calcification and its association with mortality, cardiovascular events in patients with chronic kidney disease: A systematic review and meta-analysis. *Renal Failure*, *41*(1), 244–256. https://doi.org/10.1080/0886022X.2019.1595646

Weiner, D. E., Tighiouart, H., Elsayed, E. F., Griffith, J. L., Salem, D. N., Levey, A. S., & Sarnak, M. J. (2008). The Relationship Between Nontraditional Risk Factors and Outcomes in Individuals With Stage 3 to 4 CKD. *American Journal of Kidney Diseases*, *51*(2), 212–223. https://doi.org/10.1053/j.ajkd.2007.10.035

Wong, K. L., Tai, J. J.-Y., Wong, W.-C., Han, H., Sem, X., Yeap, W.-H., Kourilsky, P., & Wong, S.-C. (2011). Gene expression profiling reveals the defining features of the classical, intermediate, and nonclassical human monocyte subsets. *Blood*, *118*(5), e16–e31. https://doi.org/10.1182/blood-2010-12-326355

Wu, D. M., Zhang, Y., Parada, N. A., Kornfeld, H., Nicoll, J., Center, D. M., & Cruikshank, W. W. (1999). Processing and release of IL-16 from CD4+ but not CD8+ T cells is activation dependent. *Journal of Immunology (Baltimore, Md.: 1950)*, *162*(3), 1287–1293.

Wu, J., Wang, Y., Zhang, Y., & Li, L. (2011). Association Between Interleukin-16 Polymorphisms and Risk of Coronary Artery Disease. *DNA and Cell Biology*, *30*(5), 305–308. https://doi.org/10.1089/dna.2010.1145

Wu, M.-F., Wang, Y.-C., Shen, T.-C., Chang, W.-S., Li, H.-T., Liao, C.-H., Gong, C.-L., Wang, Z.-H., Tsai, C.-W., Hsia, T.-C., & Bau, D.-T. (2020). Significant Association of Interleukin-16 Genetic Variations to Taiwanese Lung Cancer. *In Vivo*, *34*(3), 1117–1123. https://doi.org/10.21873/invivo.11883

Wynn, T. A., & Vannella, K. M. (2016). Macrophages in Tissue Repair, Regeneration, and Fibrosis. *Immunity*, *44*(3), 450–462. https://doi.org/10.1016/j.immuni.2016.02.015

Xiang, F., Zhu, J., Cao, X., Shen, B., Zou, J., Liu, Z., Zhang, H., Teng, J., Liu, H., & Ding, X. (2016). Lymphocyte depletion and subset alteration correlate to renal function in chronic kidney disease patients. *Renal Failure*, *38*(1), 7–14. https://doi.org/10.3109/0886022X.2015.1106871

Xiong, J., Qiao, Y., Yu, Z., Huang, Y., Yang, K., He, T., & Zhao, J. (2021). T-Lymphocyte Subsets Alteration, Infection and Renal Outcome in Advanced Chronic Kidney Disease. *Frontiers in Medicine*, *8*, 1539. https://doi.org/10.3389/fmed.2021.742419

Xu, H., Wang, N., Cao, W., Huang, L., Zhou, J., & Sheng, L. (2018). Influence of various medium environment to in vitro human T cell culture. *In Vitro Cellular & Developmental Biology. Animal*, *54*(8), 559–566. https://doi.org/10.1007/s11626-018-0273-3

Xue, H., Gao, L., Wu, Y., Fang, W., Wang, L., Li, C., Li, Y., Liang, W., & Zhang, L. (2009). The IL-16 gene polymorphisms and the risk of the systemic lupus erythematosus. *Clinica Chimica Acta; International Journal of Clinical Chemistry*, *403*(1–2), 223–225. https://doi.org/10.1016/j.cca.2009.03.016

Yang, H., Han, Y., Wu, L., & Wu, C. (2017). Diagnostic and prognostic value of serum interleukin-16 in patients with gastric cancer. *Molecular Medicine Reports*, *16*(6), 9143–9148. https://doi.org/10.3892/mmr.2017.7688

Yang, Y., Ning, Y., Shang, W., Luo, R., Li, L., Guo, S., Xu, G., He, X., & Ge, S. (2016). Association of peripheral arterial disease with all-cause and cardiovascular mortality in hemodialysis patients: A meta-analysis. *BMC Nephrology*, *17*(1), 195. https://doi.org/10.1186/s12882-016-0397-1

Ye, Z., Zeng, G., Yang, H., Li, J., Tang, K., Wang, G., Wang, S., Yu, Y., Wang, Y., Zhang, T., Long, Y., Li, W., Wang, C., Wang, W., Gao, S., Shan, Y., Huang, X., Bai, Z., Lin, X., … Xu, H. (2020). The status and characteristics of urinary stone composition in China. *BJU International*, *125*(6), 801–809. https://doi.org/10.1111/bju.14765

Yilmaz, M. I., Solak, Y., Saglam, M., Cayci, T., Acikel, C., Unal, H. U., Eyileten, T., Oguz, Y., Sari, S., Carrero, J. J., Stenvinkel, P., Covic, A., & Kanbay, M. (2014). The Relationship between IL-10 Levels and Cardiovascular Events in Patients with CKD. *Clinical Journal of the American Society of Nephrology*, *9*(7), 1207–1216. https://doi.org/10.2215/CJN.08660813

Yoon, J. W., Pahl, M. V., & Vaziri, N. D. (2007). Spontaneous leukocyte activation and oxygen-free radical generation in end-stage renal disease. *Kidney International*, *71*(2), 167–172. https://doi.org/10.1038/sj.ki.5002019

Yoon, J.-W., Gollapudi, S., Pahl, M. V., & Vaziri, N. D. (2006). Naïve and central memory T-cell lymphopenia in end-stage renal disease. *Kidney International*, *70*(2), 371–376. https://doi.org/10.1038/sj.ki.5001550

Yoshimoto, T., Wang, C.-R., Yoneto, T., Matsuzawa, A., Cruikshank, W. W., & Nariuchi, H. (2000). Role of IL-16 in delayed-type hypersensitivity reaction. *Blood*, *95*(9), 2869–2874. https://doi.org/10.1182/blood.V95.9.2869.009k18_2869_2874

Yunna, C., Mengru, H., Lei, W., & Weidong, C. (2020). Macrophage M1/M2 polarization. *European Journal of Pharmacology*, *877*, 173090. https://doi.org/10.1016/j.ejphar.2020.173090

Zajd, C. M., Ziemba, A. M., Miralles, G. M., Nguyen, T., Feustel, P. J., Dunn, S. M., Gilbert, R. J., & Lennartz, M. R. (2020). Bone Marrow-Derived and Elicited Peritoneal Macrophages Are Not Created Equal: The Questions Asked Dictate the Cell Type Used. *Frontiers in Immunology*, *11*, 269. https://doi.org/10.3389/fimmu.2020.00269

Zeidler, C., Germeshausen, M., Klein, C., & Welte, K. (2009). Clinical implications of ELA2-, HAX1-, and G-CSF-receptor (CSF3R) mutations in severe congenital neutropenia. *British Journal of Haematology*, *144*(4), 459–467. https://doi.org/10.1111/j.1365-2141.2008.07425.x

Zhang, Y., Center, D. M., Wu, D., M. H., Cruikshank, W. W., Yuan, J., Andrews, D. W., & Kornfeld, H. (1998). Processing and Activation of Pro-Interleukin-16 by Caspase-3. *Journal of Biological Chemistry*, *273*(2), 1144–1149. https://doi.org/10.1074/jbc.273.2.1144

Zheng, D., Liwinski, T., & Elinav, E. (2020). Inflammasome activation and regulation: Toward a better understanding of complex mechanisms. *Cell Discovery*, *6*(1), 1–22. https://doi.org/10.1038/s41421-020-0167-x

Zhong, J., & Shi, G. (2019). Editorial: Regulation of Inflammation in Chronic Disease. *Frontiers in Immunology*, *10*, 737. https://doi.org/10.3389/fimmu.2019.00737

Zhu, J. (2018). T Helper Cell Differentiation, Heterogeneity, and Plasticity. *Cold Spring Harbor Perspectives in Biology*, *10*(10), a030338. https://doi.org/10.1101/cshperspect.a030338

Zikou, X., Tellis, C. C., Rousouli, K., Dounousi, E., Siamopoulos, K. C., & Tselepis, A. D. (2015). Differential Membrane Expression of Toll-Like Receptors and Intracellular Cytokine Induction in Peripheral Blood Monocytes of Patients with Chronic Kidney Disease and Diabetic Nephropathy. *Nephron Clinical Practice*, *128*(3–4), 399–406. https://doi.org/10.1159/000369815

Zimmermann, J., Herrlinger, S., Pruy, A., Metzger, T., & Wanner, C. (1999). Inflammation enhances cardiovascular risk and mortality in hemodialysis patients. *Kidney International*, *55*(2), 648–658. https://doi.org/10.1046/j.1523-1755.1999.00273.x

Zindel, J., & Kubes, P. (2020). DAMPs, PAMPs, and LAMPs in Immunity and Sterile Inflammation. *Annual Review of Pathology: Mechanisms of Disease*, *15*(1), 493–518. https://doi.org/10.1146/annurev-pathmechdis-012419-032847

Zoccali, C., Mallamaci, F., Tripepi, G., Cutrupi, S., Parlongo, S., Malatino, L. S., Bonanno, G., Rapisarda, F., Fatuzzo, P., Seminara, G., Stancanelli, B., Nicocia, G., & Buemi, M. (2003). Fibrinogen, mortality and incident cardiovascular complications in end-stage renal failure. *Journal of Internal Medicine*, *254*(2), 132–139. https://doi.org/10.1046/j.1365-2796.2003.01180.x

Zoccali, C., Vanholder, R., Massy, Z. A., Ortiz, A., Sarafidis, P., Dekker, F. W., Fliser, D., Fouque, D., Heine, G. H., Jager, K. J., Kanbay, M., Mallamaci, F., Parati, G., Rossignol, P., Wiecek, A., & London, G. (2017). The systemic nature of CKD. *Nature Reviews Nephrology*, *13*(6), 344–358. https://doi.org/10.1038/nrneph.2017.52

Eidesstattliche Versicherung

„Ich, Frederic Brösecke, versichere an Eides statt durch meine eigenhändige Unterschrift, dass ich die vorgelegte Dissertation mit dem Thema: „Interleukin-16 in Chronic Kidney Disease – On the Origin, Secretion and Importance“/ „Interleukin-16 in Chronischer Nierenerkrankung – Über Ursprung, Ausschüttung und Bedeutung“ selbstständig und ohne nicht offengelegte Hilfe Dritter verfasst und keine anderen als die angegebenen Quellen und Hilfsmittel genutzt habe.

Alle Stellen, die wörtlich oder dem Sinne nach auf Publikationen oder Vorträgen anderer Autoren/innen beruhen, sind als solche in korrekter Zitierung kenntlich gemacht. Die Abschnitte zu Methodik (insbesondere praktische Arbeiten, Laborbestimmungen, statistische Aufarbeitung) und Resultaten (insbesondere Abbildungen, Graphiken und Tabellen) werden von mir verantwortet.

Ich versichere ferner, dass ich die in Zusammenarbeit mit anderen Personen generierten Daten, Datenauswertungen und Schlussfolgerungen korrekt gekennzeichnet und meinen eigenen Beitrag sowie die Beiträge anderer Personen korrekt kenntlich gemacht habe (siehe Anteilserklärung). Texte oder Textteile, die gemeinsam mit anderen erstellt oder verwendet wurden, habe ich korrekt kenntlich gemacht.

Meine Anteile an etwaigen Publikationen zu dieser Dissertation entsprechen denen, die in der untenstehenden gemeinsamen Erklärung mit dem/der Erstbetreuer/in, angegeben sind. Für sämtliche im Rahmen der Dissertation entstandenen Publikationen wurden die Richtlinien des ICMJE (International Committee of Medical Journal Editors; www.icmje.og) zur Autorenschaft eingehalten. Ich erkläre ferner, dass ich mich zur Einhaltung der Satzung der Charité – Universitätsmedizin Berlin zur Sicherung Guter Wissenschaftlicher Praxis verpflichte.

Weiterhin versichere ich, dass ich diese Dissertation weder in gleicher noch in ähnlicher Form bereits an einer anderen Fakultät eingereicht habe.

Die Bedeutung dieser eidesstattlichen Versicherung und die strafrechtlichen Folgen einer unwahren eidesstattlichen Versicherung (§§156, 161 des Strafgesetzbuches) sind mir bekannt und bewusst.“

_____ _____

Datum Unterschrift

Anteilserklärung an erfolgten Publikationen

Frederic Brösecke hatte folgenden Anteil an folgender Publikation:

Abstrakt und Poster: **F. Brösecke**, A. Pfau, L. Rubenbauer, T. Ermer, A. B. Dein Terra Mota Ribeiro, S. Burlein, K.-U. Eckardt, M. Reichel, F. Knauf; *Interleukin-16 ist stark erhöht bei Dialysepatient*innen und korreliert mit der Plasmaoxalat Konzentration,* 13. Jahrestagung der Deutschen Gesellschaft für Nephrologie, Rostock, Deutschland, 2021

Beitrag im Einzelnen: Durchführung der Versuche zu Abbildung 4 und 5, erneute Auswertung der Daten zu den Abbildungen 1-3, Erstellung aller Abbildungen 1-5 sowie der Abbildung im Methodenteil, Schreiben des Textes (Abstrakt, Einleitung, Methoden, Bildunterschriften, Zusammenfassung), Gestaltung des Posters mit Zusammenstellen der Versuche und Auswahl der Grafiken

_____

Unterschrift, Datum und Stempel des/der erstbetreuenden Hochschullehrers/in

_____

Unterschrift des Doktoranden/der Doktorandin

Lebenslauf Frederic Emanuel Brösecke

Mein Lebenslauf wird aus datenschutzrechtlichen Gründen in der elektronischen Version meiner Arbeit nicht veröffentlicht.

Danksagung

Mein besonderer Dank gilt Felix Knauf, der mit seiner außergewöhnlichen Offenheit und seinem großen Vertrauen eine besondere Zusammenarbeit ermöglicht hat. Seine große Freude an der Forschung in sehr unterschiedlichen Bereichen, sein besonderes Engagement in der Lehre, seine soziale Tätigkeit im Bereich Global Health und seine herzliche Art werden mich in meinem zukünftigen Leben prägen.

Außerdem ist Michael Chiorazzi und Richard A. Flavell mein großer Dank geschuldet. Die Möglichkeit im Rahmen meiner Doktorarbeit Einblicke in ihre Arbeit zu erlangen und mit ihnen zusammen wissenschaftliche Fragestellungen zu bearbeiten war für mich außerordentlich beeindruckend.

Außerdem habe ich Martin Reichel zu danken, der mir bei jeglichen Herausforderungen im Labor immer eine große Unterstützung war und bei dem ich auch in verzweifelten Stunden nach Hilfe fragen konnte. Gemeinsame Diskussionen bei der Formulierung von Hypothesen, bei der Planung von Versuchen und beim kritischem Hinterfragen von Ergebnissen haben mich in wissenschaftlichem Denken viel gelehrt.

Mein Dank gilt des Weiteren Andrea, Ana, Vanessa, Madeleine, Ádám, Saskia, Ricky, Jack, Frauke, Bia und Lisa.

Darüber hinaus habe ich für dieses Projekt TRENAL, dem BIH und dem DAAD zu danken, ohne deren finanzielle Unterstützung diese Doktorarbeit vielleicht nicht möglich gewesen wäre.

Abschließend habe ich meinen Eltern, meinem Bruder, meinen Großeltern, meinen Freunden und allen wichtigen Menschen in meinem Leben zu danken. Ohne eure offenen Ohren und emotionale Unterstützung hätte ich diese manchmal etwas frustrierende aber meist sehr bereichernde Arbeit nicht geschafft.

Bescheinigung Statistik

CHARITÉ

CharitéCentrum für Human- und Gesundheitswissenschaften

Charité | Campus Charité Mitte | 10117 Berlin

Name, Vorname: Brösecke, Frederic

Emailadresse: frederic.broesecke@charite.de

Matrikelnummer: 223674

PromotionsbetreuerIn: Prof. Dr. Felix Knauf

Promotionsinstitution / Klinik: Medizinische Klinik m.S. Nephrologie und Internistische Intensivmedizin

Institut für Biometrie und klinische Epidemiologie (iBikE)

Direktor: Prof. Dr. Frank Konietschke

Postantschrift:
Charitéplatz 1 | 10117 Berlin
Besucheranschrift:
Sauerbruchweg 3 | 10117 Berlin

Tel. +49 (0)30 450 562171
https://biometrie.charite.de/

Bescheinigung

Hiermit bescheinige ich, dass Herr Frederic Brösecke innerhalb der Service Unit Biometrie des Instituts für Biometrie und klinische Epidemiologie (iBikE) bei mir eine statistische Beratung zu einem Promotionsvorhaben wahrgenommen hat. Folgende Beratungstermine wurden wahrgenommen:

- Termin 1: 05.02.2021
- Termin 2: 30.11.2021

Folgende wesentliche Ratschläge hinsichtlich einer sinnvollen Auswertung und Interpretation der Daten wurden während der Beratung erteilt:

- Confounder Adjustierung für den Einfluss von pOx auf das Outcome IL-16 mit Hilfe eines linearen multiplen Regressionsmodells. Dabei sollte die Selektion der Variablen über eine Rückwärtselektion mit AIC als Kriterium durchgeführt werden.
- Angabe der Konfidenzintervalle zu den entsprechenden Schätzern
- Bei den Markophagen sollte auf Grund des explorativen Charakters der Studie auf statistische Tests verzichten werden.
- Multiple Imputation zur Ersetzung von fehlenden Werten für die Regression.

Diese Bescheinigung garantiert nicht die richtige Umsetzung der in der Beratung gemachten Vorschläge, die korrekte Durchführung der empfohlenen statistischen Verfahren und die richtige Darstellung und Interpretation der Ergebnisse. Die Verantwortung hierfür obliegt allein dem Promovierenden. Das Institut für Biometrie und klinische Epidemiologie übernimmt hierfür keine Haftung.

Datum: 02.06.2022

Name des Beraters/ der Beraterin: Lorena Hafermann

[redacted]

CHARITÉ
UNIVERSITÄTSMEDIZIN BERLIN
Institut für Biometrie und
Klinische Epidemiologie
Campus Charité Mitte
Charitéplatz 1 | D-10117 Berlin
Sitz: Reinhardtstr. 58